MECHANISMS OF TRIGEMINAL ACTIVATION AND SENSITISATION: IMPLICATIONS FOR MIGRAINE PATHOPHYSIOLOGY

DOCTORAL (PhD) THESIS

Timea Aczél PharmD

Science of Pharmacology Doctoral School
Neuropharmacology Program

Program Director: Erika Pintér MD, PhD, DSc

Supervisor: Kata Bölcskei MD, PhD

UNIVERSITY OF PÉCS, MEDICAL SCHOOL
DEPARTMENT OF PHARMACOLOGY AND PHARMACOTHERAPY

PÉCS
2022

Table of Contents

Table of Contents 1
Abbreviations 4
Introduction 5
Orofacial pain disorders 5
Headache disorders, migraine 6
Trigeminovascular system 10
Overview of the trigeminal sensory neurons 11
Sensitisation, trigeminovascular activation 13
Role of glial cells in sensitisation 14
The importance of the tachykinin family 17
Hemokinin-1 18
Animal models in trigeminal sensitisation 19
Aims 21
Materials and Methods 22
Animal studies 22
Orofacial inflammatory pain model 22
Microarray analysis 23
Sample collection and handling 25
Peripheral blood mononuclear cell (PBMC) isolation 25
Quantitative real-time PCR (RT-qPCR) 26
RNAscope in situ hybridization (ISH) 26
NanoString nCounter technology 27
Mixed Glial Cell Culture (MGC) 28
Radioactive $^{45}Ca^{2+}$-uptake technique 28
Luminex Multiplex Immunoassay 28
Human study 29
Study subjects 29
Protocol for sample collection 29
RNA extraction procedure and quality control 30
Illumina library preparation and sequencing 30
Statistical analysis and bioinformatics 31

Chapter 1. Transcriptional alterations in the trigeminal ganglia, nucleus and peripheral blood mononuclear cells in a rat orofacial pain model 33
Results 33
CFA induced gene expression changes between ipsi- and contralateral sides in TG on day seven 33
Several biological processes and pathways were shown to be involved in CFA-induced inflammation 34
Inflammation caused decreased orofacial mechanonociceptive threshold in rats 34
Inflammation induced alterations in the expression of various genes in rat tissues 35
Discussion 39
Chapter 2. Identification of disease- and headache-specific mediators and pathways in migraine using blood transcriptomic analysis 42
Results 42
Clinical characteristics 42
DE genes derived from interictal vs healthy comparison 42
DE genes derived from ictal vs interictal comparison 42
DE genes derived from ictal vs healthy comparison 42
Mitochondrial dysfunction was suggested by analysis of migraineurs' samples 43
Discussion 47
Chapter 3. Hemokinin-1 gene expression is upregulated in trigeminal ganglia in an inflammatory orofacial pain model: potential role in peripheral sensitisation 50
Results 50
Tac4 mRNA levels changed in parallel with orofacial allodynia after CFA-induced inflammation in rat TG 50
CFA induced upregulation Tac4 mRNA in both primary sensory neurons and SGCs of the rat TG 51
Behavioural tests suggested anxiety-like behaviour in Tac4$^{-/-}$ gene-deficient mice 52
CFA induced upregulation Tac4 mRNA in both primary sensory neurons and SGCs of the mice TG 54
CFA-induced changes in neuronal and glial activation marker levels in the TG of Tac4 gene-deficient mice 55
Neuroinflammation-related genes were differently altered in TG of saline-or CFA-treated Tac4$^{-/-}$ and WT mice 56
Discussion 61
Chapter 4. Hemokinin-1 expression and effect on a mixed glial cell culture 64
Results 64

Tac4 transcripts were co-localised with Aif1 (Iba1), Gfap, Olig2-expressing cells of mouse MGCs 64
Hemokinin-1 treatment induced radioactive $^{45}Ca^{2+}$ uptake in mouse MGCs 66
Hemokinin-1 treatment increased the inflammatory cytokine production in mouse MGCs 66
Discussion 68
Novelty and relevance of our findings 70
Future perspectives 71
Acknowledgements 72
References 73
Appendix 97
List of Publications 110
Articles related to the thesis 110
Articles not related to the thesis 111
Oral presentations related to the thesis 112
Oral presentations not related to the thesis 112
Poster presentations related to the thesis 113
Poster presentations not related to the thesis 113
Other contribution to oral presentations 114
Other contribution to poster presentations 115

Abbreviations

5-HT – Serotonin (5-hydroxytryptamine)
AIF1 – Allograft inflammatory factor 1
BDNF – Brain-derived growth factor
CFA – Complete Freund's Adjuvant
CGRP – Calcitonin gene-related peptide
CNS – Central nervous system
COX2 – cyclooxygenase 2
CSD – Cortical spreading depression
DRG – Dorsal root ganglia
DE – Differentially expressed
ECS – Extracellular solution
GFAP – Glial fibrillary acid protein
Grp39 – G-protein coupled receptor 39
HK-1 – Hemokinin-1
IASP – International Association for the Study of Pain
Iba1 – Ionized calcium-binding adaptor molecule 1
ICHD – International Classification of Headache Disorders
IL-1β – Interleukin 1-beta
IL-6 – Interleukin 6
Kiss1 – Kisspeptin 1
Kiss1r – Kisspeptin-1 receptor
Lkaaear1 – LKAAEAR Motif Containing 1
MCP-1/CCL2 – Monocyte chemoattractant protein-1
MGC – Mixed glial cell culture
NK – Neurokinin
OFP – Orofacial pain
OFT – Open field test
PACAP – Pituitary adenylate cyclase-activating peptide
PBMCs – Peripheral blood mononuclear cells
PBS – Phosphate buffered saline
PCR – Polymerase chain reaction
PNS – Peripheral nervous system
SGC – Satellite Glial cells
SP – Substance P
SST – Somatostatin
TACs – Trigeminal autonomic cephalalgias
TCC – Trigeminocervical complex
TNC – Trigeminal nucleus caudalis
TNFα – Tumour necrosis factor-alpha
TG – Trigeminal ganglion
TRPA1 – Transient receptor potential ankyrin 1
TRPV1 – Transient receptor potential vanilloid 1
TVS – Trigeminovascular system
RT-qPCR – Quantitative reverse transcription PCR

Introduction

Orofacial pain (OFP) and headache conditions are among the most common pain diseases afflicting a significant portion of society. Orofacial pain is a frequent pain perceived in the face and oral cavity. Migraine is a primary headache with a characteristically recurrent unilateral, throbbing, convulsive pain sensation, with the intensity ranging from moderate to very severe. Migraine headaches present various symptoms: most often associated with nausea, vomiting, and increased sensitivity to sound and light, sometimes smell and touch. The pathophysiological background of these illnesses might be diverse; however, according to the most accepted theory, an essential part of the pathomechanism is activation and sensitisation of the extra- and intracranial trigeminal primary afferents. Altered functioning of the trigeminovascular system stands behind the arising pain. However, the underlying pathophysiology is still unclear.

The present thesis aims to get a better insight into understanding the process of trigeminal sensitisation and migraine pathomechanism describing transcriptomic alterations in inflammatory orofacial pain animal models, in a human migraine study and cell culture experiments.

Orofacial pain disorders

International Association for the Study of Pain (IASP) terminology defines pain as “an unpleasant sensory and emotional experience associated with actual or potential tissue damage” [1]. Meanwhile, orofacial pain may be described as pain “localized to the region above the neck, in front of the ears and below the orbitomeatal line, as well as pain within the oral cavity” [2]. Focusing on the OFP, Lipton and his colleagues declare that an estimated 22% of the American adult population suffers from chronic OFP and approximately 7% in the UK with a high degree of prevalence rates in women [3,4]. This estimation was confirmed by other studies showing a commonness around 17–26% in the general population, of which 7–11% can be considered chronic [5], therefore causing reduced quality of life [6]. Despite its relatively widespread presence, proper diagnosis and treatment of orofacial pain conditions display a complex and essential health care problem. OFP can be derived from several target tissues (meninges, cornea, tooth pulp, mucosa and the temporomandibular joint, etc.); thus, it can have a distinct pathophysiological background [7]. Therefore, it is difficult to categorize the various types of pain [8]. Several pain societies disclosed classifications of orofacial pain conditions (Appendix Table 1.), which present overlaps and dissimilarities, reflecting the complexity of the disorders.

Despite the complexity of their pathophysiology, neuroplastic alterations in the trigeminal system, involving anatomical structures like the trigeminal ganglion (TG), trigeminal nucleus caudalis (TNC), and upper cervical spinal cord (C1-2), are considered to be the common phenomenon underlying OFP conditions [9]. Aspects of pain transduction, peripheral and central mechanisms, neuronal and glial interactions, neuronal transmitters involved in processes are in the focus of ongoing studies regarding OFP and trigeminal system to elucidate unique properties of different OFP conditions [7,9–11]. Inflammation of the temporomandibular joint, temporal artery, sinuses, or orbit can cause headache, which could have the same characteristics as the primary disorders. A positive association between painful temporomandibular conditions and primary headaches have also been reported [12,13].

Headache disorders, migraine

Although activation of the trigeminal system is at the pathophysiological basis of all orofacial and headache disorders, location, attack frequency, duration, accompanying symptoms, and treatment response can be a guide to classify craniofacial pains [14]. Migraine–associated phenomena might include moderate-to-severe unilateral pain of pulsating or throbbing quality and accompanying symptoms such as nausea/emesis or photo-/phonophobia and allodynia [15–17]. It is a complex spectrum disorder caused by various genetic and environmental aetiological factors occurring in several clinical manifestations with or without aura [18]. As a primary headache disorder, migraine is a common disabling brain disorder affecting up to 15–20% of the general population, and it constitutes a significant health problem. According to the *Global Burden of Disease (GBD)* study, migraine took second place in 2017 in the world ranking, contributing to 5.6% of all years lived with disability [19–21] and third place in 2019 below low back pain and depressive disorders [22]. In addition, headache disorders were enlisted second among females aged 15–49 years [22].

The origin and precise pathological mechanisms of migraine are still being debated, particularly concerning peripheral and central sensitisation processes [23–27].

The pharmacological therapy is not a resolved issue since the frequent use of combined analgesics or the specific antimigraine drugs, triptans, can paradoxically exacerbate the condition (medication overuse headache), and treatment used as prophylaxis (e.g. certain antiepileptics and antidepressants – Table 1.) may only offer partial relief at the cost of potentially unpleasant adverse effects [27–30]. Therefore, it is evident that identifying potential novel drug targets is needed to advance antimigraine drug development.

Table 1. Preventive drugs for migraine therapy and side effects [31–33].

Preventive therapy for migraine	
Drug	**Side effects**
β-Adrenergic–receptor antagonists	
Propranolol	fatigue, postural symptoms; contraindicated in patients with asthma
Metoprolol	
Antidepressants	
Amitriptyline	drowsiness
Antiepileptics	
Valproate	sleepiness, weight gain, tremor, hair loss, fetal disorders, hematologic, liver abnormalities
Gabapentin	tiredness, dizziness
Topiramate	confusion, paresthesia, weight loss
Calcium channel blockers	
Verapamil	constipation, leg swelling, atrioventricular conduction disturbances
Flunarizine	tiredness, weight gain, depression, parkinsonism
Serotonin antagonists	
Pizotyline	drowsiness, weight gain
Methysergide	drowsiness, leg cramps, hair loss, retroperitoneal fibrosis

Since the 1990s, the trigeminovascular system (TVS) activation theory has been in the focus of migraine research [34,35]. The TVS provides an important pain-transmission link between the vascular and neuronal elements because this is the major afferent pain pathway between the cranial vessels and the nuclei in the brainstem [36]. A wide variety of triggers initiates migraine, and there is a vast variation between the aetiological factors, clinical manifestations, and severity. Therefore, for decades, there has been a great debate on the predominant importance of the vascular and neurogenic inflammatory mechanisms and peripheral versus central sensitisation processes. Furthermore, the interactions between genetic predisposal and environmental factors also seem critical [37–39]. Among the mechanisms of migraine neuro-vascular alterations, sensory neuropeptide (e.g. calcitonin gene-related peptide – CGRP and substance P – SP) and serotonin (5-hydroxytryptamine- 5-HT) release, neurogenic inflammation, plasma protein extravasation, peripheral and central sensitisation are enlisted, but the precise pathophysiological mechanisms are still unclear [40–42]. Based on several data lines, it is now evident that a significant contributor to headache development is the

neuropeptide CGRP contained in both primary and secondary trigeminal sensory neurons. CGRP plasma levels were shown to be elevated during attacks. The administration of exogenous CGRP can trigger headaches and monoclonal antibodies blocking the peptide or its receptors as well as receptor antagonists have been proven to have clinical efficacy and are currently approved medications [43]. The presently used first-line drugs in migraine attacks are serotonin 5-$HT_{1B/1D}$ receptor agonists, which contract the pathologically dilated meningeal vessels and inhibit neuronal hyperexcitability in the TVS. However, due to several therapy-resistant patients, as well as severe cardiovascular and gastrointestinal side effects, treatment optimization is still required [44]. More recently, the CGRP receptor antagonists, 5-HT_{1F} receptor agonists and anti-CGRP monoclonal antibodies have been developed. Fortunately, several of these have been approved for use (Table 2.), pinning great hope for their efficiency [45–51]. Although the newly developed monoclonal antibodies against CGRP or its receptor seem to be effective and safe, the risks of long-term CGRP blockade in migraine patients still needs to be elucidated. Also, little is known about the efficacy and safety during pregnancy or in adolescents [46]. Therefore, understanding the pathophysiological mechanisms through precise clinical and translational research approaches is crucial to identify key mediators and determine novel therapeutic targets.

Table 2. Triptans and recently approved drugs in migraine therapy [46,52–54].

Triptans and recently approved drugs				
Classification	***Drugs***	***Side effects***	***Indication***	***Date of approval***
Stimulation of 5-HT$_{1B}$, 5-HT$_{1D(1F)}$ receptor				
Triptans	Almotriptan	cardiovascular	acute treatment of migraine	class of drugs first introduced in the 1990s.
	Eletriptan			
	Frovatriptan			
	Naratriptan			
	Rizatriptan			
	Sumatriptan			
	Zolmitriptan			
Stimulation of 5-HT$_{1F}$ receptor				
Ditans	Lasmiditan	dizziness, paresthesia, somnolence		FDA - October 2019
Blockade of CGRP receptors				
Monoclonal antibody	Erenumab	constipation, pruritus, muscle spasms, transient reactions at the injection site	migraine prophylaxis	FDA - May 2018 EMA - July 2018
Gepants	Atogepant	constipation, nausea	episodic migraine prophylaxis	FDA - September 2021
	Rimegepant	dizziness, nausea, urinary tract infection	acute treatment of migraine	FDA - February 2020
	Ubrogepant	dizziness, nausea, excessive sleepiness	acute treatment of migraine	FDA - December 2019
Blockade of CGRP				
Monoclonal antibody	Eptinezumab	reactions at the injection site	migraine prophylaxis (first intravenous)	FDA - February 2020
	Fremanezumab		migraine prophylaxis	FDA - September 2018 EMA - March 2019
	Galcanezumab		migraine prophylaxis	FDA- September 2018 EMA - November 2018

Trigeminovascular system

Cell bodies of the pseudounipolar primary afferents lie in the TG, the first centre of the pain processing course, through which stimuli from extra and intracranial structures are transmitted further to the trigeminocervical complex (TCC). TNC and C1-C2 regions of the cervical spinal cord together form the TCC. The trigeminal nerve enters the brainstem at the pontine level, from where orofacial nociceptive stimuli are transmitted to second-order neurons. Afterwards, information is transferred to the third-order thalamocortical neurons [55,56]. Sensitisation of this system may be responsible for developing various orofacial pains and headaches and is also responsible for the development of facial allodynia. Three divisions of the trigeminal sensory nerve exist, which consists of the ophthalmic (V1), maxillary (V2), and mandibular (V3) branches (Figure 1.). Location of these nerve innervations might be at the basis of distinct localizations of primary headaches and facial pain: ophthalmic branch (V1) is considered the most important in primary headache disorders, like migraine, given the characteristic periorbital pain. Small meningeal branches of V1 richly innervate the cerebral dura mater. Activation of primary trigeminal afferents causes the release of vasoactive neuropeptides (e.g., CGRP and SP), thus causing vasodilatation, protein extravasation, and neurogenic inflammation. V2 and V3 might also innervate the dura mater, not only the maxillary and mandibular regions of the head, indicating an overlap between regions [14,57]. TCC also receives inputs from the posterior dura and cervical dermatomes, synapsing in the C2-C4 regions, and explaining occipital head and neck pain in migraine [58]. Apart from the sensory cortex, thalamic nuclei, the cingulate cortex, and insulae participate in a network of neuronal structures that can mediate pain processing [16].

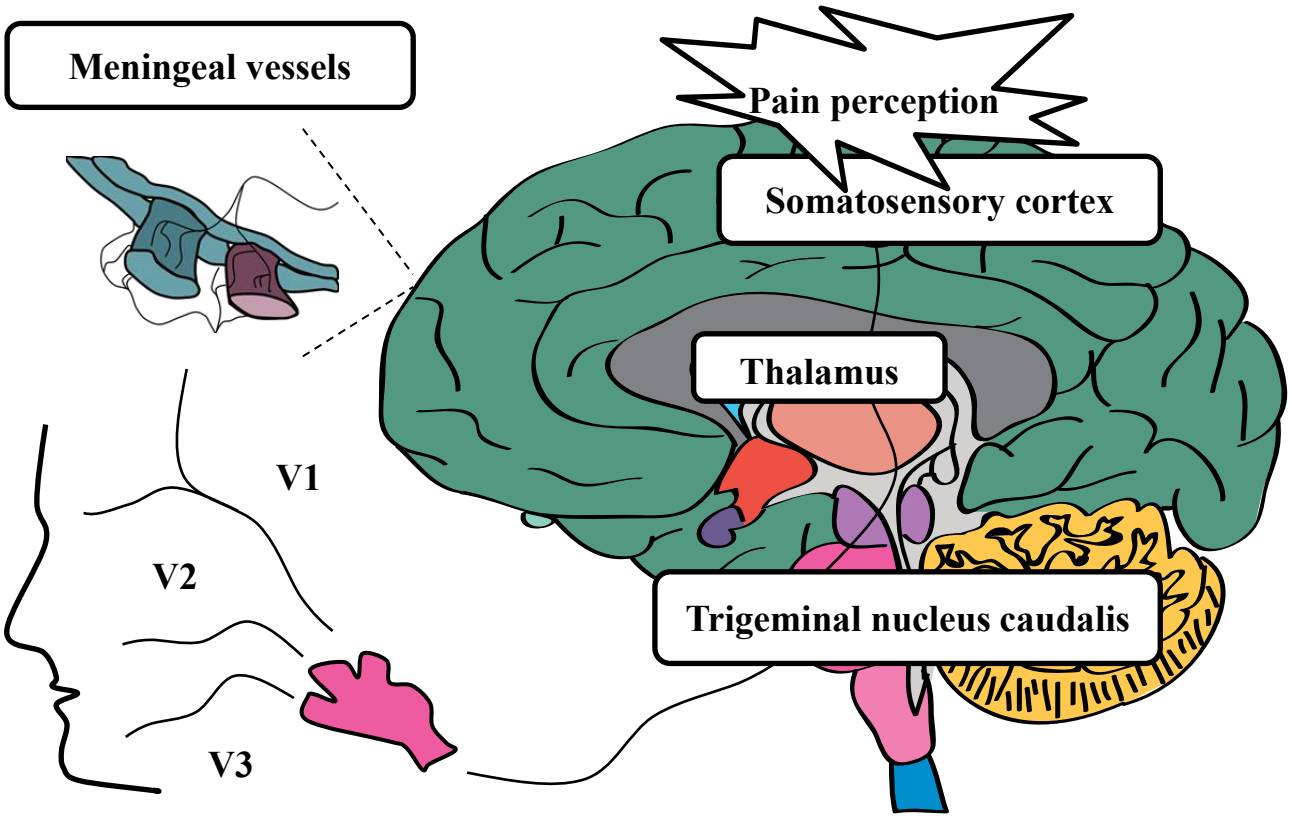

Figure 1. Outlines of the trigeminovascular system. Trigeminal primary afferents (ophthalmic (V1), maxillary (V2), and mandibular (V3) branches of the trigeminal nerve), whose cell bodies are located in the trigeminal ganglion (TG), innervating the dura mater and meningeal vasculature from which stimuli are transmitted to second-order neurons in the trigeminal-cervical complex (TCC), which includes the trigeminal nucleus caudalis (TNC) and first and second cervical dorsal horn (C1, C2). From here, information passes into the thalamus and then into the somatosensory cortex. The trigeminal nerve also innervates the face, the eye, and the nasal and oral cavities [33,58–60].

Overview of the trigeminal sensory neurons

Sensory or afferent neurons are specific types capable of sensory transduction and transmission by conveying various sensory stimuli to the central nervous system. Nociceptive afferents mainly include thinly myelinated and unmyelinated A and C fibres [61]. Sensory ganglia contain the cell bodies of primary afferents that transmit sensory information from the periphery into the central nervous system (CNS). The cell bodies of sensory afferents are situated in the dorsal root ganglia (DRG) or in the case of the orofacial complex in the TG. Sensory neurons are classified as pseudounipolar cells, consisting of an axon with two branches—one projects to the periphery, the other to the CNS. DRG and TG present several functional similarities and the capability to detect and respond to various stimuli (pain, touch,

temperature, and proprioception). Besides functional homogeneity, their location, embryological origin, transcription pattern, and responsiveness to multiple medications differ [62–64]. TG is localized at the base of the skull, outside the blood-brain barrier and their sensory neurons innervate the facial region, while DRG innervates the rest of the body [65]. Both can detect several chemical, mechanical, and thermal stimuli. Interestingly, TG presents unique features regarding the chemosensitive perception of olfactory and taste detection [66].

The TG mainly includes soma and axons of primary afferent neurons and glial cells. Neurons present as small- and medium-sized pseudounipolar cells, with bodies of primarily round, oval, elongated shape, in which a particularly round and centrally located nucleus and nucleoli might be observed. Cell bodies of the trigeminal neuron are enveloped by satellite glial cells (SGC) [67].

A significant percentage of trigeminal and dorsal root ganglia nociceptive sensory neurons are peptidergic, thus expressing various neuropeptides like tachykinins (SP and neurokinins) and CGRP in response to activation [68–70]. These neuropeptides constitute the main focus of primary headaches, like migraine research. Neuropeptides can be released from primary sensory neurons' peripheral and central endings, contributing to inflammatory processes and pain transmission [71,72]. CGRP is a potent vasodilator neuropeptide released during migraine attacks, thus seems to have an essential role in the pathophysiology of migraine. The peptide can bind to the CGRP receptor, widely present on smooth muscle cells in cranial vasculature and the TG, which consists of calcitonin receptor-like receptor (CLR), receptor activity modifying protein 1 (RAMP1), and receptor component protein (RCP) subunits [36,41]. Beyond the well-studied CGRP, SP, and pituitary adenylate cyclase-activating peptide (PACAP), others like cholecystokinin, galanin, somatostatin are present in the ganglia, with their receptors declared on the neurons [73,74]. In addition, receptors for other neurotransmitters also are localized on trigeminal ganglion neurons. Glutamate receptors seem to be present on the neuron, among which metabotropic glutamate receptors (mGluR) is located in SGCs. N-methyl-D-aspartate (NMDA) receptor activation is proved to contribute to mechanical hyperalgesia via sensitisation of the transient receptor potential vanilloid 1 (TRPV1) [75]. Transient receptor potential (TRP) receptors are mostly Ca^{2+}-permeable, non-selective cation channels, typically expressed in nociceptors [76], thus being involved in sensitizing mechanisms. TRP channels are essential pain transducers as they sense low pH media, oxidative stress, heat, protons, proinflammatory cytokines, and other mediators associated with pain and inflammation. Besides TRPV1, transient receptor potential ankyrin 1 (TRPA1) and transient receptor potential melastatin 8 (TRPM8) receptors are also expressed,

partly co-expressed in TG neurons. Their implication in trigeminal nociception and headache disorders is widely discussed [77–79]. P2X3 receptors also might be involved in nociception in inflammatory pain [80].

Sensitisation, trigeminovascular activation

The terminology of sensitisation is described by IASP as follows: “Increased responsiveness of nociceptive neurons to their normal input, and/or recruitment of a response to normally subthreshold inputs”. Clinically, this may stand behind hyperalgesia, when increased pain might be felt due to a painful stimulus, and allodynia, when pain is given rise by a stimulus that does not normally provoke pain. Peripheral and central sensitisation exists depending on which type of neuron is involved [81].

Studies report changes in pain sensitivity in patients with fibromyalgia, osteoarthritis, musculoskeletal disorders with headache, temporomandibular joint disorders, dental pain, neuropathic pain disorders [81]. When sensitisation occurs, nociceptor inputs can trigger a prolonged hyper-excitability of neurons in nociceptive pathways, bringing forth eventual spontaneous action potential firing [82]. Cutaneous allodynia reported in chronic migraineurs, orofacial inflammation, or nerve injury manifests due to trigeminal sensitisation. In this process, the sensitisation of primary afferents and the second-order or third-order thalamic neurons develop. As a background for central sensitisation in chronic pain, synaptic plasticity, an imbalance between excitatory and inhibitory neurotransmitters, and lately glia–neuron interaction have been enlisted [10,83]. Thereby nerve injury inflammation causes gliosis. The glial cells in the CNS undergo a massive change with a similar phenomenon in sensory ganglia [82]. Description of detailed mechanisms that alter pain sensitivity and released mediators that regulate neuronal excitability are presented in the following chapters, focusing mainly on trigeminal ganglia.

Role of glial cells in sensitisation

Several studies focused on the involvement and critical role of glial cells in pathological conditions, such as dysfunction of the nervous system, including the generation and/or maintenance of pain [11,55,82,84–88]. Due to inflammatory processes, the hyperactivation of TG neurons occurs, followed by activation of non-neuronal glial cells and macrophages and cytokine production (Figure 2.). Glial mediators further promote neuronal sensitisation. Thus, understanding neuron-glia interaction and crosstalk is relevant in orofacial pain and headache development [10,89].

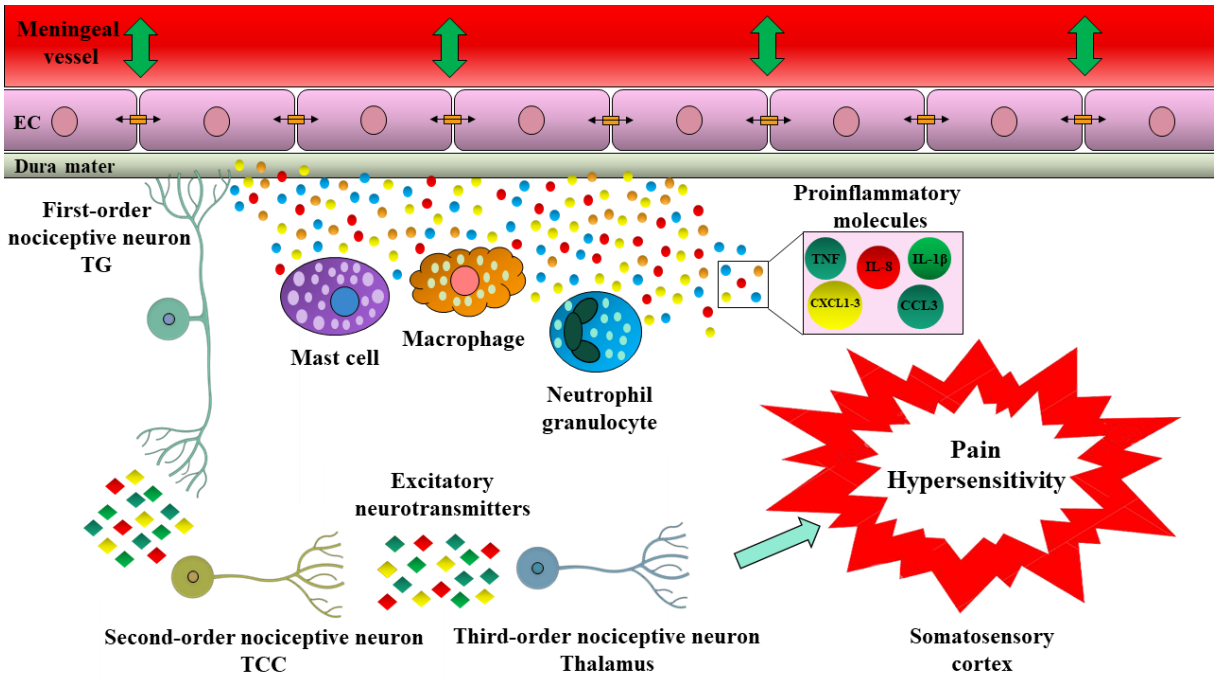

Figure 2. Sketch of hypersensitivity and headache development in the trigeminovascular microenvironment. Activation of immune cells inflicts the release of inflammatory molecules, such as cytokines and chemokines, causing vasodilation of dural vasculature and influencing tight junction between endothelial cells. Activated trigeminal neurons send signals to cortical brain regions for further processing. C-C motif ligand 3 (CCL3); C-X-C motif chemokine ligand 1 (CXCL1); C-X-C motif chemokine ligand 2 (CXCL2); C-X-C motif chemokine ligand 3 (CXCL3); endothelial cell (EC); interleukin-1β (IL-1β); interleukin-8 (IL-8); trigeminocervical complex (TCC); tumor necrosis factor (TNF); trigeminal ganglion (TG) [89].

Glial cells are non-neuronal cells of the peripheral and central nervous system (PNS, CNS) that regulate the neuronal microenvironment, taking part in the nutrition, structural maintenance of neuronal networks, and modulation of neuronal excitability. The extracellular gap between glial and neuronal surfaces is small (around 20 nm), neuronal microvilli/gap junctions helping the vast exchange of chemical neurotransmitters between them. Inflammation in facial skin might also cause the augmented formation of gap junctions (connexin 26) in TG neurons and glial cells. Although glial cells play a similar role in PNS and CNS, different glial subtypes are distinguished. Oligodendrocytes, astrocytes, ependymal cells, and microglia are part of the CNS, while peripheral ganglions contain Schwann cells, SGCs and resident microglia-like macrophages [10,64,82,90,91].

Although certain differences can be detected, SGCs and astrocytes present similar characteristics. Astrocytes express specific proteins of the S100 family (found in oligodendrocytes and Schwann cells as well), glutamine synthetase (GS) and glial fibrillary acidic protein (GFAP). SGCs share most of the characteristics of astrocytes, for example, contributing to neuronal nutrition and functioning and maintaining the environment around neurons. Similar to astrocytes under a normal state, SGCs contains low levels of GFAP. Still, inflammation and nerve injury cause massive expression of GFAP, observed in various orofacial pain models [55,82]: dental injury [92], temporomandibular joint (TMJ) inflammation [93], whisker pad inflammation [94], chronic constriction injury of the infraorbital nerve [95], migraine [96]. Among various mediators, CGRP has been suggested to have a role in the crosstalk between neurons and glial cells. Its receptors have been confirmed not only on neurons but both Schwann and satellite cells. It is believed that neuropeptides like SP and CGRP, due to various noxious stimuli, are synthesized and released from the neuronal soma of the TG. Apart from autocrine functions, it can activate SGCs, thus increasing GFAP expression and activating purinergic pathways [97,98]. An increment in the sensitivity of SGCs to ATP was observed when orofacial inflammation caused adenosine triphosphate (ATP) release from the soma of the trigeminal neuron [99]. Enhanced P2X7 signalling in SGCs and elevated intracellular Ca^{2+} concentration may be in the background of orofacial allodynia following peripheral nerve injury and inflammation. The increased intracellular calcium concentration led to the synthesis and release of proinflammatory cytokines: tumour necrosis factor-alpha (TNFα) or interleukin 1-beta (IL-1β) from SGCs in the trigeminal nerve injury model. Further, IL-1β binds to its receptor in small-diameter TG neurons, increasing neuronal excitability. Similarly, in vitro, SP, or CGRP application to trigeminal SGC cultures results in cytokine (IL-1β, TNFα, or IL-6) release [11,100] (Figure 3.).

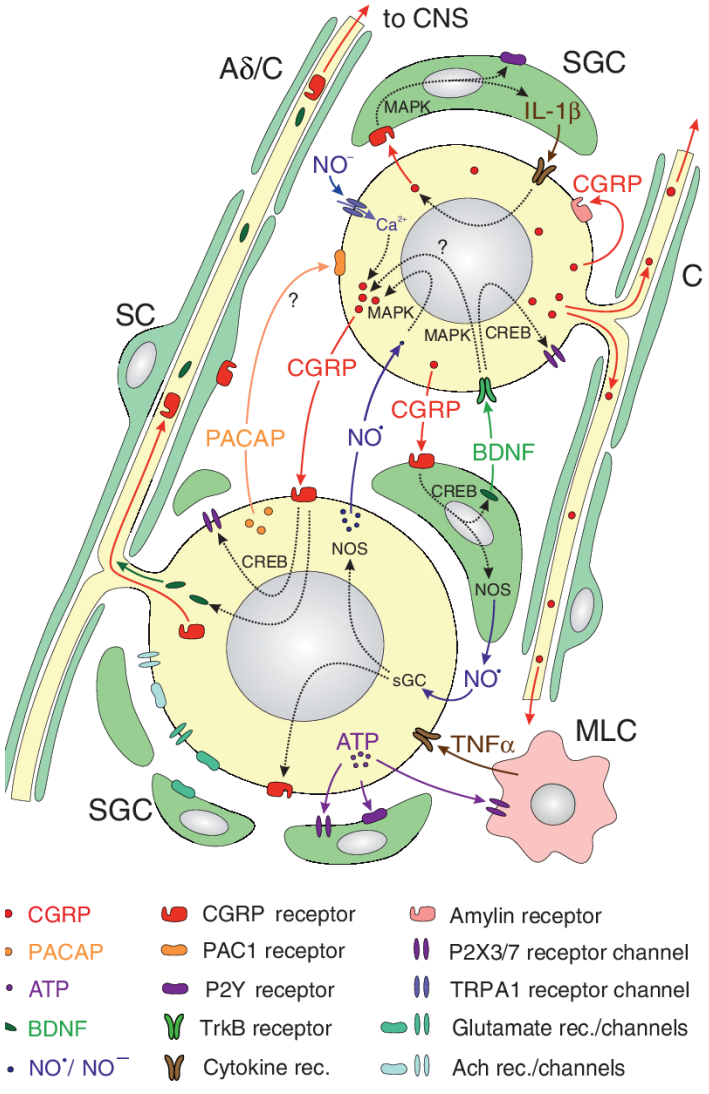

Figure 3. Representation of signalling processes between trigeminal ganglion and satellite cells; nitric oxide (NO); cAMP response-element binding protein (CREB); mitogen-activated protein kinase (MAPK); nitric oxide synthase (NOS); interleukin 1β (IL-1β); brain-derived neurotrophic factor (BDNF); macrophage-like cells (MLC); tumour necrosis factor α (TNFα) [101].

Microglia represents the principal resident immunocompetent cells in the brain sharing monocytes and macrophages' phenotypic markers and features [102]. Immune cells seem to contribute to pain hypersensitivity [103]; therefore, activation of microglial cells also occurs during orofacial inflammation. Activated microglia can release various reactive molecules and regulate neuronal excitability, such as pronociceptive cytokines: TNFα, interleukins (IL-1β and IL-18), and brain-derived growth factor (BDNF), thereby modulating pain processes [104]. Proteins, like ionized calcium-binding protein (Iba1) and CD11b, are typically used as markers of proliferation and morphologic activation of microglial cells/macrophages [102,105].

Extensive macrophage infiltration in the TG beside resident microglia-like macrophage might occur due to trigeminal nerve injury and inflammation [10,64].

Communication between neurons and microglia/macrophages seems important in migraine-related sensitisation, acting through purinergic pathways [106]. CGRP inflicts neurotrophin release from SGCs, BDNF and CGRP being both elevated in migraine [107]. TNFα or SP released from proliferating macrophages, involving ERK 1/2 and p38 MAPK signalling pathways, redounds to trigeminal hyperexcitability [9]. Various neuropeptide receptors have been detected in different microglial cell systems like PACAP (VPAC1, PAC1), somatostatin (sst2, sst3, sst4), CGRP, tachykinin (NK-1, NK-2, NK-3) receptors [103,108]. Overall, PNS and CNS glia might have a substantial effect in the context of pain and inflammatory processes.

The importance of the tachykinin family

As previously mentioned, tachykinins are among the neuropeptides contained in peptidergic primary afferent neurons with relevant roles in neurogenic inflammation and nociceptive transmission [71,72]. Important tachykinin members are SP and neurokinin A (NKA), derived from *Tac1*, neurokinin B (NKB), coded by *Tac3*, and hemokinin-1 (HK-1) by *Tac4*. The three tachykinin proteins act through the G-protein coupled neurokinin NK-1, NK- 2, and NK-3 receptors [109,110]. NK-1 receptor antagonists were proved to reduce neuropathic mechanical hyperalgesia and inflammatory pain in animal models [111–113]. Since SP and its NK-1 receptor play an essential role in pain transmission, and given their presence in trigeminal sensory neurons [114], it has also become the focus of migraine studies. SP released from the trigeminal neurons induces plasma extravasation and vasodilatation in the dura mater [35]. It has been shown that the SP/NK-1 system participates in the orofacial heat hyperalgesia in animal models of orofacial inflammation and nerve injury [115]. Preclinical data were promising regarding NK-1 receptor antagonists in several pain conditions and inflammatory disease models [115–117]. Nevertheless, human clinical studies could not prove the analgesic effect of these compounds, either in migraine [118–120] or other conditions like post-operative dental pain [121] or neuropathic pain [122]. The possible explanation for the failure of NK-1 receptor antagonists as analgesics and anti-migraine drugs remains unclear [123,124].

Hemokinin-1

The discovery of HK-1 encoded by the *Tac4* gene [125] raised new questions in tachykinin research. HK-1 might be a novel essential molecule in pain and inflammatory processes [126]. There is a growing amount of information regarding the mRNA expression of the *Tac4* gene both in the PNS and CNS. In contrast with other tachykinin members, relatively high expression of the *Tac4* gene can be found in peripheral non-nervous tissues, such as the lung, spleen, adrenal gland and immune cells like B and T lymphocytes, macrophages, and dendritic cells [125,127–129]. *Tac4* gene predicts one homologous transcript in mice and rats, but several peptide isoforms can be found in humans. HK-1 binds to all tachykinin receptors, presenting the highest affinity to the NK-1 receptor [129,130]. However, HK-1 also has distinct, NK-1-independent actions [131,132]. The structural similarity of the family members makes further exploration of HK-1 detection difficult. Although a few studies focus on antibody development [133], trying to avoid cross-reactivity between antibodies with an in-house developed antibody [134], the validity of existing antibodies against HK-1 on the market is questionable. Despite the structural similarities and joint receptors of HK-1 and SP, some of their functions appear to be different, even opposing each other [131,135–138]. This could be explained by the activation of different signalling pathways by HK-1 compared to SP or by the suspected existence of a specific receptor for HK-1 [131]. Therefore, since the receptor affinities of HK-1 are not precisely known, antagonists cannot be used to validate the target.

Studies investigating the pain modulatory task of the HK-1 provided evidence for the complex functioning of the peptide. HK-1 produced a pronociceptive effect after intrathecal or intracerebroventricular administration in rat/mice, causing pain and scratching behaviour without influencing the withdrawal latency to a noxious heat stimulus [129,136,139]. However, an analgesic effect was shown in other studies using similar concentrations upon intracerebroventricular injection in mice [140–142]. Upregulation of *Tac4* mRNA expression in microglia upon lipopolysaccharide stimulation [143] and in the dorsal spinal cord of rats after complete Freund's adjuvant (CFA)-induced paw inflammation [144] has been described, suggesting a possible role in neurodegenerative and neuroinflammatory disorders. A recent study of our research group suggests its role in mediating arthritic pain and cellular, but not vascular inflammatory mechanisms. Using HK-1, NK1-deficient mice and TG cell cultures from NMRI mice, the authors also propose an NK-1 receptor-independent activation [145] and provide further evidence for the pronociceptive role of HK-1 [138]. However, little is known about the *Tac4* gene / HK-1 in the trigeminovascular system.

Animal models in trigeminal sensitisation

Various gene expression studies on migraine patients have provided consistent evidence for the involvement of inflammatory pathways [146,147], supporting the validity of animal models of inflammation. Central sensitisation of secondary nociceptive neurons of the TNC in migraine patients was postulated by the presence of cutaneous allodynia during the headache phase [148]. Experimental demonstration of sensitized cornea reflex of migraineurs supported this hypothesis [149]. The phenomenon was also shown in animal models. Inflammatory soup induced sensitisation of peripheral and central trigeminovascular neurons, resulting in increased mechanical hypersensitivity of the dura and the face [150,151]. Also, experimental data confirm that inflammation or nerve lesion on the face can induce meningeal vasodilation or neurogenic inflammation [152,153].

Animal models are frequently used to validate drug targets, however, modelling the complex mechanisms and symptoms accompanying primary headache disorders like migraine continues to be challenging. All models have limitations since pain cannot be objectively measured in animals, and we have an incomplete understanding of the pathophysiological processes involved in migraine. Complete translation of the human disorder to rodents is not possible. As discussed before, there is convincing evidence that activation of the trigeminovascular system, resulting from peripheral and central sensitisation, is responsible for the headache phase of the migraine, furthermore hyperalgesia and allodynia [154–157].

Several reviews describe validated animal models of pain relevant for headache. Direct electrical stimulation of trigeminal neurons, administration of inflammatory, algogenic substances (“inflammatory soup”: bradykinin, serotonin, histamine and prostaglandin) to the meninges, exogenous administration (e.g. nitroglycerin, PACAP) chemicals, cortical spreading depression induction, medication overuse of headache models present a wide range of animal models to choose from. Behavioural assays are performed besides electrophysiology, flowmetry, and various marker detection using immunohistochemistry. These reflect migraine-like phenomena such as mechanical allodynia (e.g. von Frey filaments applied to whisker pad or periorbital regions to determine withdrawal response), sensitivity to light (e.g. place or light avoidance tests), and altered overall spontaneous response activity [158–160].

A frequently used inflammatory animal model applies CFA [94,161–163]. CFA injected in the whisker pad of rodents results in inflammation and mechanical hyperalgesia/allodynia on the orofacial region [164]. Although it is not considered a typical migraine model, it can be used as a trigeminal activation model, having the advantage of being reliable and highly

reproducible. Besides the enlisted methodologies, transcriptomic analysis allows an unbiased approach to reveal critical pathways responsible for the pathophysiological changes [165]. Microarray analysis after CFA injection in the whisker pad [166] or masseter muscle [167] had been performed.

Peripheral blood mononuclear cells (PBMCs) isolated from peripheral blood consist of lymphocytes (T cells, B cells, natural killer cells) and monocytes. Due to minimally invasive sampling and relatively simple isolation, PBMCs became attractive biological marker candidates in clinical practice. They are considered biological materials capable of reflecting pathophysiological changes in the CNS in various diseases. Neuroinflammatory processes can be characterized in a specific way using PBMCs. Thus, it has provided new opportunities for biomarker research [168–170].

Aims

1. We aimed to follow the temporal changes of facial mechanonociceptive thresholds and gene expression in TG, TNC, and PBMCs in parallel after CFA inflammation in rats using microarray and RT-qPCR analysis to get a better insight into the pathomechanism of trigeminal pain disorders.
2. To identify disease- and headache-specific pathophysiological pathways and possible therapeutic targets, we aimed to analyse the transcriptome of PBMCs of migraineurs in a self-controlled manner during and between attacks.
3. Since the role of HK-1/*Tac4* in the trigeminovascular system and facial pain have been poorly investigated, we aimed to explore the potential role of HK-1 in the trigeminal environment. We aimed to detect the changes of expression of *Tac4* in the TG in a rat inflammatory orofacial pain model and investigate behavioural alterations and gene-expression variations of selected markers of neuronal sensitisation and neuroinflammation in the same model in mice, comparing wild-type and *Tac4*-deficient (*Tac4*$^{-/-}$) mice.
4. We aimed to describe the expression of the *Tac4* gene on glial cells in an in vitro set-up and the effect of HK-1 in mixed glial cell culture to get a better insight into the potential impact of HK-1 on neuron-glia communication and its molecular pathways.

Materials and Methods

Animal studies

Experiments were performed on male Wistar rats (Toxicoop, Hungary) weighing 200–300 g and on male, C57Bl/6 and *Tac4* gene-deleted (*Tac4*$^{-/-}$) mice weighing 20–25 g (8-12 weeks old). The original breeding pairs of the *Tac4*$^{-/-}$ mice were obtained from Alexandra Berger's lab (University Health Network, Toronto, Canada) [171]. Transgenic mice were obtained on a C57Bl/6 background and backcrossed to homozygosity for > 5 generations before using C57Bl/6 mice as controls (Charles River, Sulzfeld, Germany).

Animals were kept under standard conditions: light-dark cycle (12h light/dark cycle) and temperature (24-25ºC). Standard diet and water were provided *ad libitum* in the animal house of the University of Pécs Department of Pharmacology and Pharmacotherapy. All rats were habituated to handling and light restraint used for the orofacial von Frey test for three days, mice one day before the start of the experiments.

All experiments were approved by the National Ethics Committee on Animal Research (license No.: BA02/2000-9/2011 and BA02/2000-7/2018) and were carried out according to the European legislation (Directive 2010/63/EU) and Hungarian Government regulation (40/2013., II. 14.) on the protection of animals used for scientific purposes.

Orofacial inflammatory pain model

Induction of the local inflammatory state was achieved by unilateral s.c. injection of 50 µl complete Freund's adjuvant (CFA; Sigma-Aldrich, Saint Louis, USA; killed Mycobacteria suspended in paraffin oil; 1 mg/ml) into the whisker pad of rats and bilateral s.c. injection of 10-10 µl CFA into the whisker pad of the mice under ketamine (rats: 72 mg/kg, mice: 100 mg/kg) and xylazine (rats: 8 mg/kg, mice: 5 mg/kg) anaesthesia. The same volume of saline injection was given in the case of control groups, both mice and rats.

Microarray analysis

Gene expression was analysed using Agilent microarray platforms. TG tissue samples were collected from rats seven days after receiving s.c. CFA injection. TGs were immediately snap-frozen in liquid nitrogen after excision. Contralateral sides of CFA-injected rats were the controls. Total RNA was isolated from snap-frozen samples using the RNeasy Mini Kit (Qiagen, Carlsbad, CA), and high-quality samples (RIN>8.0) were further used for expression analysis. Sample labelling, array hybridization and primary data analysis were performed by ArrayStar Inc. (Rockville, MD, USA). Total RNA samples were amplified and labelled with Cy3-dCTP. Labelled amplicons were purified, fragmented and hybridized to rat LncRNA Array v1.0 (4 x 44K, Arraystar Inc.) slides. One-colour microarray-based gene expression analysis was used. After hybridization, slides were washed, fixed and scanned. Data files were deposited to NCBI's Gene Expression Omnibus [172] and are accessible through GEO Series accession number GSE111160.

Mechanonociception measurement

A set of von Frey nylon monofilaments (Stoelting, Wood Dale, Illinois, U.S.A) was used to perform mechanical pain thresholds measurements on the orofacial region on days zero (control day) and one, three, seven days after CFA or saline administration. Rodents were lightly restrained using a soft cotton glove to allow easier habituation. The series of von Frey filaments were used with increasing strengths (rats: 0.8-12 g, mice: 0.0075-1 g) to measure facial mechanosensitivity (Figure 4.). Based on previous experience and literature data, a protocol previously used on the paw was adapted to the orofacial region [173]. Out of five stimulations, the mechanonociceptive threshold was determined as the lowest force evoking at least two withdrawal responses (face stroking with the forepaw or head shaking).

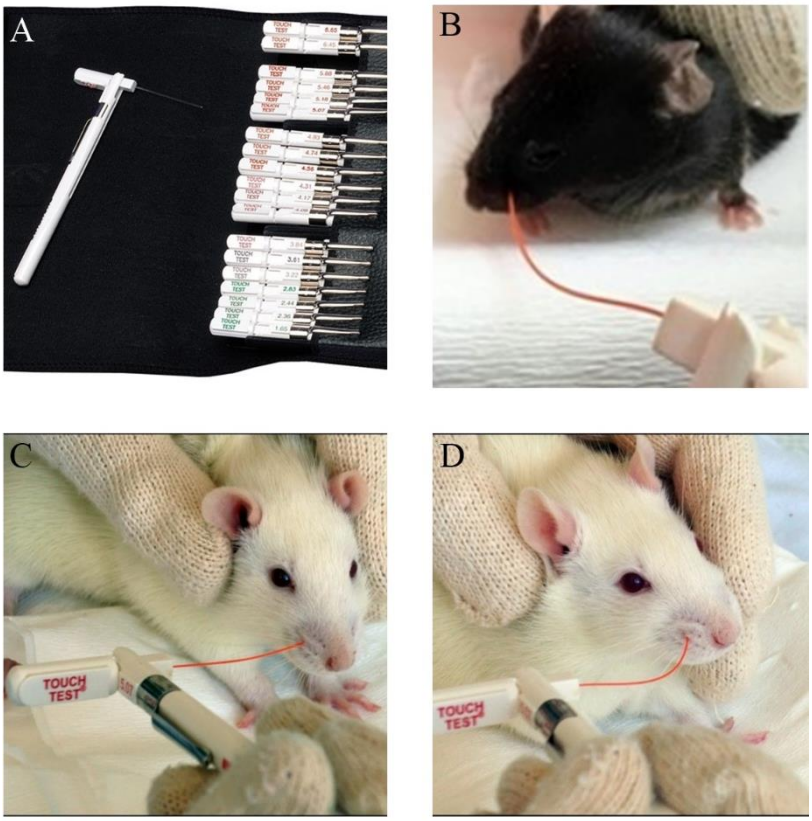

Figure 4. Orofacial mechanical pain threshold measurements with von Frey filaments **(A)** in mice **(B)** and rats **(C, D)**.

Spontaneous motor activity measurement

The open field test (OFT) was used to assay mice's spontaneous activity and anxiety levels. The mice were placed into the same area of a brightly lit observation box (60 cm x 40 cm), then the behaviour of mice was recorded for 10 min. Recorded videos were evaluated using Ethovision software (Noldus Information Technology, Wageningen, Netherlands).

Sample collection and handling

For RT-qPCR analysis, TG and TNC tissue samples were collected from animals one, three, seven days after receiving s.c. CFA injection, following behavioural experiments. Animals were anaesthetized using pentobarbital (rats: 50 mg/kg and mice 70 mg/kg: i.p.). Blood was drawn by cardiac puncture and further processed as follows in the *Isolation of peripheral blood mononuclear cells* section. After exsanguination, animals were decapitated, and TGs and TNCs were excised, immediately snap-frozen in liquid nitrogen, and stored at -80°C until real-time PCR processing.

For the RNAscope method, animals were transcardially perfused with 0.01 M phosphate-buffered saline (PBS; pH 7.6) followed by 4% paraformaldehyde on day three after CFA or saline injections. TGs were postfixed for 24 hours at room temperature, rinsed in PBS, dehydrated, and embedded in paraffin. 5 µm sections were cut using a sliding microtome (HM 430 Thermo Fisher Scientific, USA).

Mice TG samples for NanoString analysis were snap-frozen on day three and stored at −80°C until use. RNAscope and NanoString analysis were performed on tissues from animals not involved in behavioural studies.

Peripheral blood mononuclear cell (PBMC) isolation

PBMCs were purified from fresh peripheral blood according to the Ficoll-PaquePREMIUM manufacturer's instructions (GE Healthcare, Budapest, Hungary). Anticoagulant-treated blood and an equal volume of salt solution were transferred to sterile centrifuge tubes. The mixture was carefully overlaid on Ficoll-PaquePREMIUM and centrifuged 40 min at 400×g, 20 °C. The white coat layer was transferred into a new centrifuge tube, suspended with salt solution and centrifuged 10 min at 400×g, 20 °C. The supernatant was removed, the pellet was resuspended in a salt solution, followed by another centrifugation (10 min at 400×g, 20 °C). After removing the supernatant, the obtained cells were resuspended with 1 ml of TRI Reagent (Molecular Research Center, Inc., Cincinnati, OH, USA) and stored at −80°C until further process. In the case of mice, for technical reasons (small blood volume), a sample was pooled from 3 individual animals.

Quantitative real-time PCR (RT-qPCR)

According to the TRI Reagent manufacturer's protocol, total RNA isolation was carried out. Briefly, tissues were homogenized in 1 ml of TRI Reagent, and 200 µl of bromo-chloro-propane (Sigma-Aldrich, Saint Louis, USA) was added. After corresponding incubation times and centrifugations, RNA was purified using the Direct-zol RNA MiniPrep kit (Zymo Research, Irvine, CA, USA) as follows. An equal volume of the aqueous phase and absolute ethanol were mixed. The mixture was loaded onto the column, washed, and the RNA was eluted in RNase-free water. The quantity and quality of the RNA samples were checked on Nanodrop ND-1000 Spectrophotometer V3.5 (Nano-Drop Technologies, Inc., Wilmington, DE, USA). According to the manufacturer's instructions, total RNA was reverse transcribed using Maxima First Strand cDNA Synthesis Kit (ThermoScientific, Santa Clara, CA, USA). RT-qPCR was done using a Stratagene Mx3000P qPCR System (Agilent Technologies, Santa Clara, USA). PCR amplification was performed with SensiFast SYBR Lo-ROX Kit (Bioline, Taunton, USA). Transcripts of the housekeeping genes glyceraldehyde 3-phosphate dehydrogenase (*Gapdh*), hypoxanthine phosphoribosyltransferase 1 (*Hprt1*), beta-2-microglobulin (*β2m*) and peptidyl-prolyl cis-trans isomerase (*Ppia*) were measured in all tissue samples. The best-suited reference genes or combinations for normalization were selected using geNorm: *Ppia* and *Hprt1* for PBMCs and *β2m*, *Hprt1* for TG and TNC rat; *Ppia* for TG and *Ppia, Gapdh* for PBMCs and TNC mice samples. The geometric mean of their Cq values was calculated. Primers of similar efficiencies were used, and $2^{-\Delta\Delta Cq}$ fold change values were calculated. Appendix Table 2. contains the sequences of primers used for RT-qPCR.

RNAscope in situ hybridization (ISH)

RNAscope technique was performed on 5 µm thick longitudinal rat and mice TG sections processing with RNAscope Multiplex Fluorescent Reagent Kit v2 (ACD, Hayward, CA, USA). Briefly, tissue sections were baked, deparaffinized, H_2O_2-blocked, boiled, pretreated with Protease Plus and hybridized with mouse *Tac4*, mouse 3-plex positive and negative control probes. Signal amplification and channel development were applied sequentially. Sections were counterstained with 4′,6-diamidino-2-phenylindole (DAPI) and mounted with ProLong Glass Antifade Mountant for confocal imaging. Probes applied dilutions of fluorophores are listed in Appendix Table 3. Fluorescent images were acquired using an Olympus Fluoview FV-1000 laser scanning confocal microscope (Olympus, Tokyo, Japan) and Fluo-View FV-1000S-IX81 image acquisition software system. The confocal aperture was set

to 80 µm. The analogue sequential scanning was performed using a 40x objective lens (NA: 0.75). The optical thickness was set to 1 µm, and the resolution was 1024x1024 pixels. The excitation time was set to 4 µs per pixel. Virtual colours were selected to depict fluorescent signals: blue for DAPI, green for fluorescein (*Polr2a, Kcnn3* and *Aif1*), red for Cyanine 3 (*Tac4* and *Ppib*) and white for Cyanine 5 (*Ubc, Gfap, Rbfox3* and *Olig2*). Images of the respective four channels were stored both individually and superimposed to evaluate the co-localization of fluorescent signals. Basal and elevated *Tac4* expression levels were analysed semi-quantitatively using ImageJ software according to the manufacturer's guideline in a blinded manner.

RNAscope was also performed on air-dried cytospins prepared from Mixed Glial Cell Cultures (MGCs), according to the previously described method, with minor differences. Air-dried cytospin MGC samples were fixed in 10% neutral buffered formalin (Merck KGaA, Darmstadt, Germany), treated with Protease III (1:10 diluted from RNAscope Pretreatment Reagents) according to the manufacturer's protocol (320538 Tech Note). Probe hybridization and signal amplification steps have been described above.

NanoString nCounter technology

Mouse neuroinflammation panel of 770 genes included for research of immunity and inflammation, neurobiology and neuropathology were described using NanoString nCounter technology (NanoString Technologies, Seattle, WA), according to the manufacturer's instructions. Total RNA isolation and purification from mouse TG tissues were made using TRI Reagent and Direct-zol RNA MiniPrep kit as previously described, including an additional on-column DNase treatment. The RNA quality and quantity were measured with Bioanalyzer 2100 (Agilent, Santa Clara, CA, USA), Qubit Fluorometer Fluorescence Qubit 4.0 (ThermoFisher Scientific, Waltham, MA, USA), and Nanodrop ND-1000 Spectrophotometer V3.5 (Nano-Drop Technologies, Inc., Wilmington, DE, USA). Only samples with high quality (RIN > 8.1 and 260/280 ratios of ~2.0) were used for NanoString analysis.

The RNA samples (25 ng of each) were processed using Mus musculus Neuroinflammation panel v1.0 according to the manufacturer's instructions (manual MAN-10023-11) on the NanoString SPRINT Profiler instrument. Data analysis was performed using nCounter® Advanced Analysis plugin v2.0.115 for the nSolver Analysis Software v4.0.70 with the ProbeAnnotations_NS_Mm_NeuroInflam_v1.0 file provided by NanoString. Default settings were used. Briefly, raw data with gene counts lower than 50 were removed, suitable reference genes were evaluated using geNorm pairwise variation statistic, gene count data were

normalized, differentially expressed (DE) genes were determined and cell type profiling was performed for each comparison.

Mixed Glial Cell Culture (MGC)

Primary cell cultures composed of astrocytes, oligodendrocytes, and microglia, free of neurons, meningeal cells, and fibroblasts, were prepared using neonatal mice cortical tissue. After removal of bulbus olfactorius and cerebellum, the whole brains of one-three-day old C57Bl6 mice pups were enzymatically dissociated using Neural Tissue Dissociation Kit (P), following the manufacturer's instructions (Miltenyi Biotec Inc, Auburn, USA). Single-cell suspensions were seeded on poly-L-lysine coated Petri dishes and were kept at standard culturing conditions (37 °C, 5% CO_2) through 3 weeks of differentiation. Mixed glial cell cultures (MGC) were treated as follows. In situ hybridization by Advanced Cell Diagnostics RNAscope was performed on air-dried cytospins prepared from MGCs. Cultures were treated with mouse HK-1 (500 nM, 1 µM, 5 µM) for the radioactive $^{45}Ca^{2+}$-uptake technique. Inflammatory cytokine measurement was also performed using Luminex Multiplex Immunoassay from the supernatants of HK-1 (500 nM, 1 µM, 5 µM) treated glial cells.

Radioactive $^{45}Ca^{2+}$-uptake technique

Radioactive $^{45}Ca^{2+}$-uptake experiments were performed as previously described [174]. Briefly, mixed glial cell cultures were washed 5 times with calcium-free Hank's solution (pH 7.4), then incubated in 15 µl of the same buffer containing the appropriate hemokinin-1 concentrations (500 nM, 1 µM, 5 µM) at 37°C. The procedure was followed by washing steps with an extracellular solution (ECS) to eliminate the residual buffer. The retained isotope was collected in 15 µl 0.1% SDS, and Packard Tri-Carb 2800 TR scintillation counter was used to measure radioactivity, presented in Counts Per Minute (CPM), where CPM represented the total radiation read from each sample.

Luminex Multiplex Immunoassay

Supernatants of MGCs treated for 24 hours with HK-1 (500 nM, 1 µM, 5 µM) were stored at −80°C before running the assay. Luminex xMAP was used to determine the protein concentrations of 5 distinct cytokines/chemokines: CCL5 (RANTES), CXCL1 (KC), interleukin 1 beta (IL-1β), interleukin 6 (IL-6), monocyte chemoattractant protein-1 (MCP- 1/CCL2), tumour necrosis factor-alpha (TNFα). MILLIPLEX®MAP Kit (Merck KGaA, Darmstadt, Germany) was used according to the manufacturer's instructions. Briefly,

all samples were thawed and were tested in a blind fashion and duplicate. 25 µl volume of each sample, standard, universal assay buffer and ECS, as the matrix solution was added to a 96- well plate. The same volume of detection antibodies was added at the end of overnight incubation, followed by streptavidin-PE. After the last washing step, 150 µl drive fluid was added to the wells, and reading was performed using the Luminex MAGPIX® and Luminex xPonent 4.2 software. The Five Parameter Logistic regression curve was generated by the Analyst 5.1 (Merck Millipore, Darmstadt, Germany) software calculating with bead median fluorescence intensity values. Results are shown in pg/ml.

Human study

The protocol of the human study was authorized by the National Public Health Center, Ministry of Human Capacities of Hungary (28324–5/2019/EÜIG). All subjects gave their written informed consent according to the Declaration of Helsinki.

Study subjects

Episodic migraineurs with (n=3) or without aura (n=21) between 20 and 65 years were recruited. Migraine patients were included according to the criteria of the third edition of the International Classification of Headache Disorders [175]. Recurrent attacks last 4–72 hours and are characterized by pain with unilateral, pulsating quality, moderate-severe intensity, aggravation by routine physical activity and association with nausea and/or photophobia and phonophobia. Patients with chronic inflammatory diseases and depression were not included in the study. In the control group, healthy volunteers were recruited, matching all demographic characteristics. Thirty-six female and 1 male subject were included in the study: 24 episodic migraine patients with or without aura and 13 healthy controls.

Protocol for sample collection

Blood samples were collected from migraine sufferers in an attack-free (interictal) period and during an attack (ictal). The attack-free (interictal) sample was drawn if the patient had no headache for at least 24 hours. For ictal samples, no painkiller was taken by patients until the blood sampling. There were no restrictions on fluids and food intake. Features of migraine were assessed using a detailed questionnaire filled out by participants.

Blood was collected from cubital veins of participants into glass tubes containing ethylenediaminetetraacetic acid (EDTA). The PBMCs were isolated using Ficoll-Paque PREMIUM (GE Healthcare, Budapest, Hungary), as previously described, using 4 ml of

anticoagulant-treated blood. At the end of the procedure, cells were resuspended with 1 ml of TRI Reagent (Molecular Research Center, Cincinnati, OH, USA) and stored at −80°C until further investigations.

RNA extraction procedure and quality control

Extraction and purification of total RNA were performed as previously described (Quantitative Real-Time PCR), adding on-column DNase digestion during purification. RNA concentrations were determined using Qubit 3.0 (Invitrogen, Carlsbad, CA, USA), and quality control of RNA was carried out on TapeStation 4200, using RNA ScreenTape (Agilent Technologies, Santa Clara, CA, USA). We proceeded with high-quality (RIN > 8) RNA samples for library preparation.

Illumina library preparation and sequencing

The library for Illumina sequencing was prepared using NEBNext Ultra II Directional RNA Library Prep Kit for Illumina (NEB, Ipswitch, MA, USA). Briefly, mRNA was isolated from 500 ng total RNA using NEBNext Poly(A) mRNA MAgnetic Isolation Module (NEB, Ipswitch, MA, USA). The mRNA was fragmented, end prepped and adapter-ligated. Finally, the library was amplified according to the manufacturer's instructions. The quality of the libraries was checked on the 4200 TapeSation System using D1000 Screen Tape. The quantity was measured on Qubit 3.0. Illumina sequencing was performed on the NextSeq550 instrument (Illumina, San Diego, CA, USA) with a 1x76 run configuration.

Statistical analysis and bioinformatics

The raw microarray data were analysed using R and Bioconductor [176,177]. The data were quantile normalised to reduce technical noise with the Limma package [178]. The statistical testing for differential expression was also performed using Limma, which applies linear modelling with a modified t-test to calculate the p-values and fold change values. The functional enrichment analysis against Gene Ontology (GO) [179], KEGG [180] and Reactome [181] databases were performed using the topGO [182] and gage [183] packages in R.

GraphPad Prism software (GraphPad Software, Inc., La Jolla, CA, USA) was used to analyse behavioural data, RT-qPCR, radioactive $^{45}Ca^{2}$+-uptake experiments, Luminex Multiplex Immunoassay and RNAScope quantification. Two-way analysis of variance (ANOVA) with repeated measures followed by Tuckey's multiple comparison tests were performed for time-matching samples (behavioural studies), one-way or two-way ANOVA followed by Tukey's multiple comparison tests for RT-qPCR data and Student's t-test for unpaired samples for RNAScope analysis to compare saline- and CFA-treated tissues. Results are plotted as the mean ± standard error of the mean (SEM). Probability values $p \leq 0.05$ were accepted as significant in all tests.

Analysis of NanoString data was performed using nCounter® Advanced Analysis Software v2.0.115. Differentially expressed genes were determined by applying log-linear model (linear regression) with a p-value threshold of 0.05. The correlation of cell-type marker genes was determined with a threshold of $p<0.05$ for each comparison.

Twenty interictal samples were included in the transcriptomic analysis of the human study. The sequencing reads were aligned against the Homo sapiens reference genome (GRCh37 Ensembl release) with STAR v2.5.3a. After alignment, the reads were associated with known protein-coding genes, and the number of reads aligned within each gene was counted using Rsubread package v2.0.0. Gene count data were normalized using the trimmed mean of M values (TMM) normalization method of the edgeR R/Bioconductor package (v3.28, R v3.6.0, Bioconductor v3.9). The data were further log-transformed for statistical testing using the voom approach in the limma package. Normalized counts were represented as transcripts per million (TPM) values. Fold change (FC) values between the compared groups resulting from the linear modelling process and modified t-test p-values were produced by the limma package. The Benjamini–Hochberg method was used to control the False Discovery Rate (FDR), and adjusted p-values were calculated by limma. In the case of paired ictal and interictal samples, the correlation between samples originating from the same patient was taken into

account using the duplicateCorrelation function of limma. Functional analysis was performed to consider the annotations of genes using the Gene Ontology (GO), Kyoto Encyclopedia of Genes and Genomes (KEGG), and Reactome databases. Detection of functional enrichment was performed in the differentially expressed gene list (DE list enrichment: Fisher's exact test for GO, hypergeometric test for KEGG and Reactome) and towards the top of the list when all genes have been ranked according to the evidence for being differentially expressed (ranked list enrichment: non-parametric Kolmogorov-Smirnov test for GO and KEGG, hypergeometric test for Reactome) applying the topGO v2.37.0, ReactomePA v1.30.0, gage v2.36.0 packages. The pathview package v1.26.0 was used to visualize mapping data to KEGG pathways [89].

Chapter 1. Transcriptional alterations in the trigeminal ganglia, nucleus and peripheral blood mononuclear cells in a rat orofacial pain model

Results

CFA induced gene expression changes between ipsi- and contralateral sides in TG on day seven

512 DE (319 up- and 191 downregulated) transcripts were identified between the control (contralateral) and CFA (ipsilateral) TG samples ($p \leq 0.05$; $|FC| > 2$), using microarray analysis. The top up-and downregulated transcripts are provided in Appendix Table 4. At the top of the list, a lncRNA (MRAK049104; FC 5.20) takes place; however, its function is unknown. *Neurod2*, involved in neurogenic differentiation, was the most downregulated (FC -9.20). Figure 5. shows the 44 differentially expressed genes at a significance level $p \leq 0.001$ and $|FC| > 2$, including some olfactory, taste and pheromone receptors, as well as the chemokine receptor (*Ccr7*) and the estrogen receptor 1 (*Esr1*). The treatment effect was reflected in the clustering of the samples (Figure 5.). Microarray analysis was performed on TG samples from day seven.

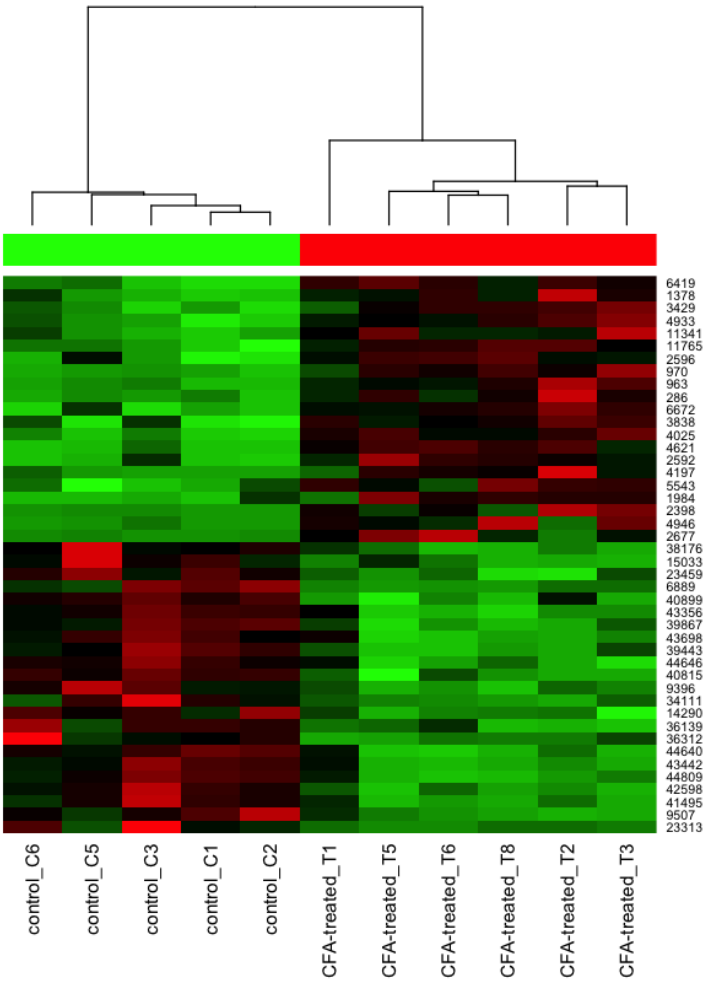

Figure 5. Heat map clustering of the top 25 DE genes, as results of CFA-treated and contralateral side TG comparison (n=5-6). Pearson's metrics have been used in the hierarchical clustering. Red: high expression; green: low expression; rows: one differentially expressed (DE) feature; columns: one sample.

Several biological processes and pathways were shown to be involved in CFA-induced inflammation

Functional enrichment analysis was performed, including the DE genes (|FC|>2, p-value ≤0.001) found in contralateral and ipsilateral comparisons, to gain information regarding the biological processes and pathways involved (Appendix Table 5.). Steroid and carbohydrate metabolic processes, sensory perception and olfactory transduction were enlisted among terms.

Inflammation caused decreased orofacial mechanonociceptive threshold in rats

The facial mechanonociceptive threshold of the CFA-injected side of rats was significantly decreased compared to the contralateral side starting from day one after injection. The threshold reached its minimum on day three and reversed on day seven (Figure 6.).

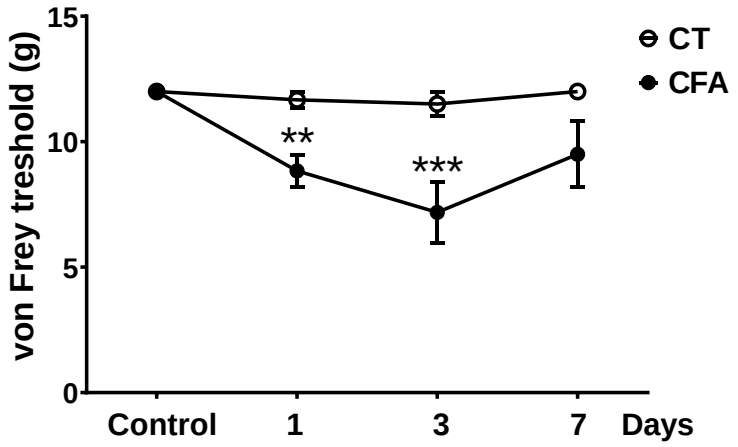

Figure 6. Changes in orofacial mechanical threshold in responses to mechanical stimuli during the von Frey test before (control) and one, three, seven days after 50 µl s.c. complete Freund's adjuvant injection. Data: mean ± SEM; n=3-9; asterisks: significant differences between contralateral (CT) and ipsilateral (CFA) sides (** p≤0.01, ***p≤0.001); two-way ANOVA followed by Tukey's multiple comparison test.

Inflammation induced alterations in the expression of various genes in rat tissues

Validation of differentially expressed mRNAs in TG

Using quantitative real-time RT-qPCR, the transcription levels of four differentially expressed genes were further determined to validate microarray results. *Lkaaear1*, G-protein coupled receptor 39 (*Gpr39*) (FC 3.04 and 4.01), kisspeptin (*Kiss1*) and kisspeptin-1 receptor (*Kiss1r*), *Neurod2* (FC -1.74, -2.63 and -9.2), were chosen for validation (Appendix Table 4. and Supplementary Material of the original article). On day seven, *Gpr39* and *Kiss1r* expression changes were similar to the microarray data (Figure 7.). However, PCR results could not confirm microarray data on *Lkaaear1, Neurod2* and *Kiss1*. Besides, we could detect *Neurod2* in TNC but not in TG using our RT-qPCR protocol. Although *FosB*, Allograft Inflammatory Factor 1 (*Aif1*, encoding Iba1 protein*)*, Glial Fibrillary Acidic Protein *(Gfap)* and Calcitonin Related Polypeptide Alpha (*Calca*, encoding CGRP*)* were not enlisted among DE genes, we also analysed the variation of these mRNA levels. On day seven, no significant differences were detected with the PCR method related to these markers, results being in line with microarray data.

Gene expression alterations reached their maximum on day three in TG samples

Using the RT-qPCR method, we measured temporal changes of mRNA levels of eight genes in TG tissues after CFA injection. CFA caused a significant elevation in mRNA levels of *Kiss1r*, neuronal (*FosB*), glial (*Aif1*), and astrocyte/satellite (*Gfap*) activation markers compared to the saline treatment on day one. By day three, *Gpr39* (9.18), *Lkaaear1 (*9.97), *Kiss1 (*9.51), *Kiss1r* (14.31), *Calca* (117.82), *FosB* (7.40) and *Gfap* (27.80) reached their maximum. *Aif1* reached a 3.6-fold peak on day one. mRNA levels of *Lkaaear1*, *Kiss1r*, *Aif1* gradually decreased at the last time point until reaching a non-significant level compared to the saline-treated control side (Figure 7.).

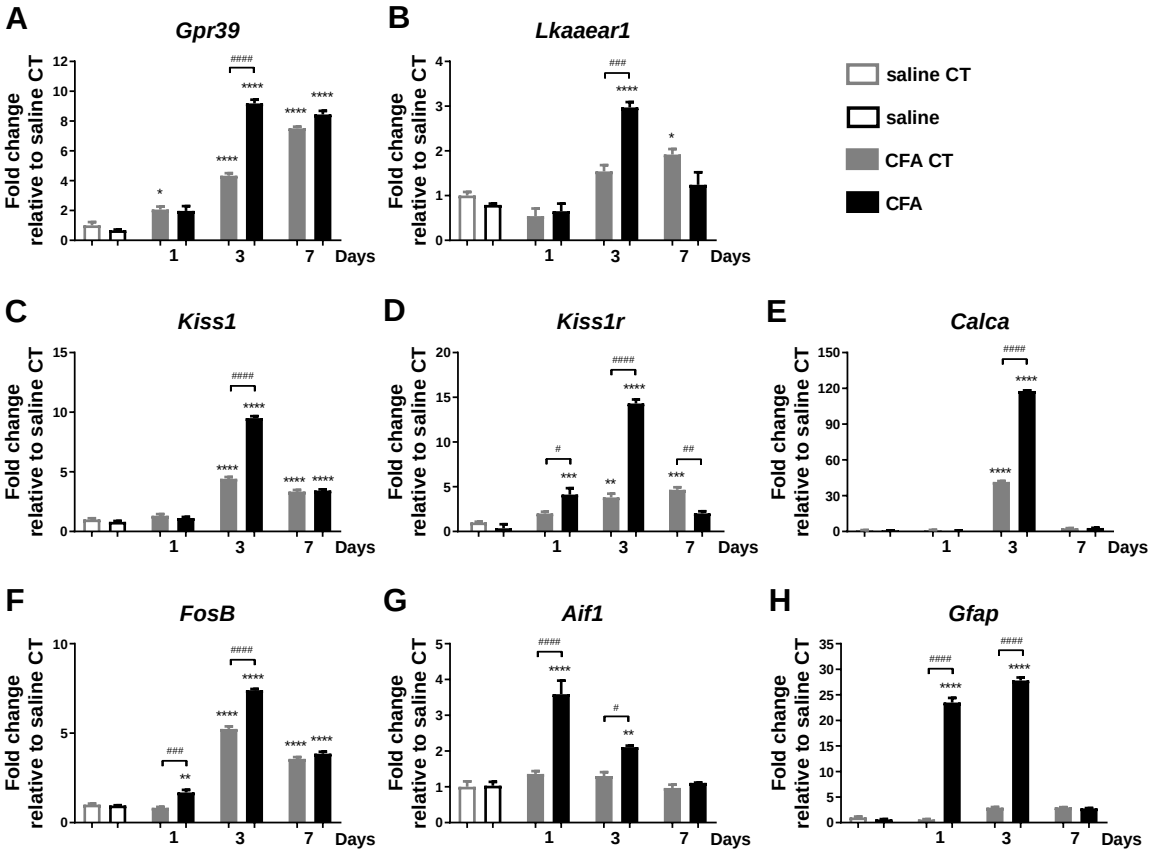

Figure 7. Time course of fold changes relative to saline control in the trigeminal ganglia. *Gpr39* (A), *Lkaaear1* (B), *Kiss1* (C), *Kiss1r* (D), *Calca* (E), *FosB* (F), *Aif1* (G) and *Gfap* (H) mRNA expressions are provided one, three and seven days after CFA injection. Housekeeping genes: *β2m* and *Hprt1;* data: mean ± SEM; n=3-3; asterisks: significant differences saline vs CT/CFA samples (*p≤0.05, **p≤0.01, ***p≤0.001, ****p≤0.0001); hash mark: significant differences between CT and CFA samples (#p≤0.05, ##p≤0.01, ###p≤0.001, ####p≤0.0001); one-way ANOVA followed Tukey's multiple comparison test.

Some of the genes presented alterations in TNC

Similar trends were seen in TNC samples. Almost all genes showed significantly altered temporal change due to CFA compared to CFA control and saline control groups, presenting a maximum at day three. There was no significant difference case of *Kiss1r* at different time points (Figure 8.).

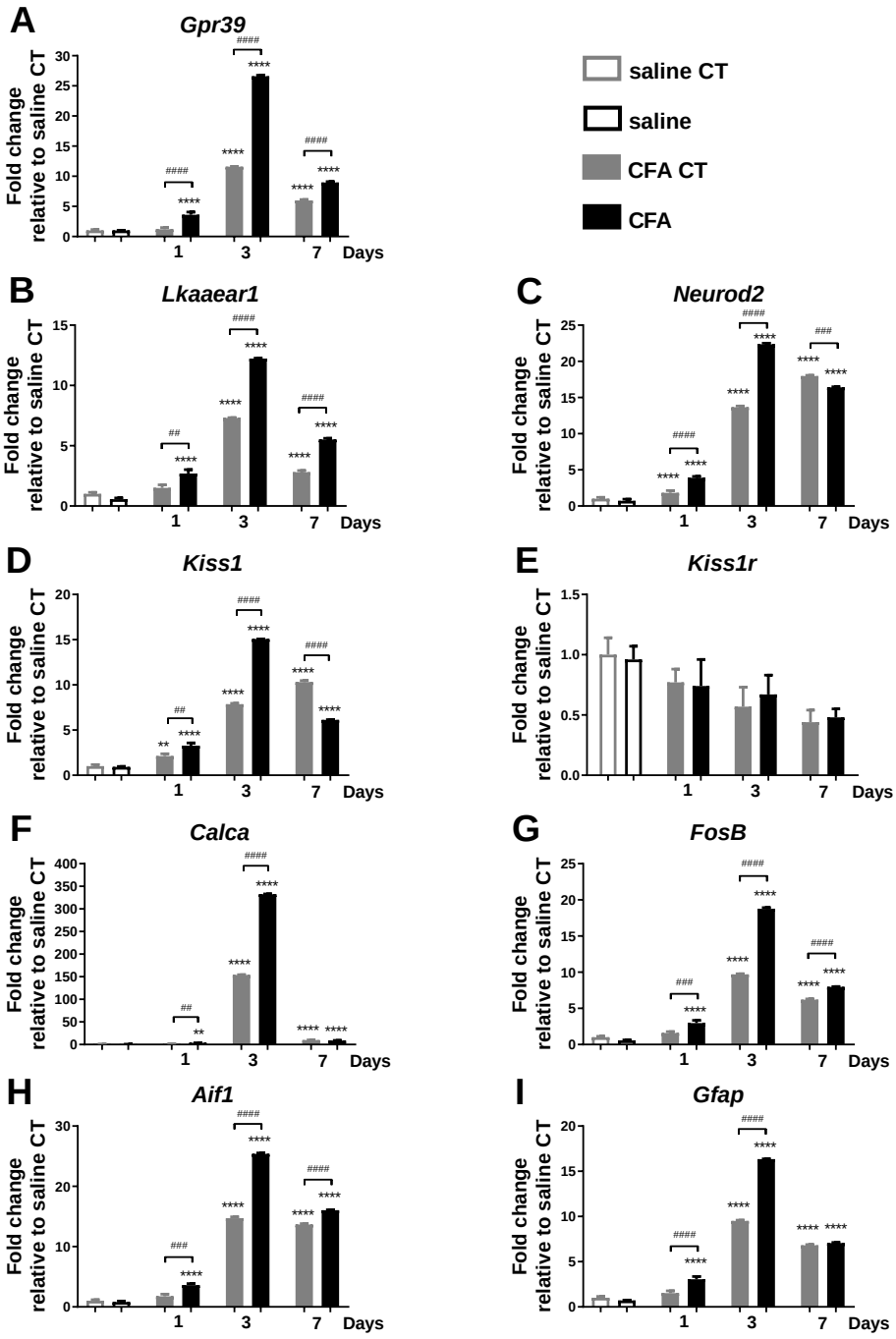

Figure 8. Time course of fold changes relative to saline control in the TNC. *Gpr39* (A), *Lkaaear1* (B), *Neurod2* (C), *Kiss1* (D), *Kiss1r* (E), *Calca* (F), *FosB* (G), *Aif1* (H) and *Gfap* (I) mRNA expressions are provided one, three and seven days after CFA injection. Housekeeping genes: *β2m* and *Hprt1*.; data: mean ± SEM; n=3-3; asterisks: significant differences between saline and CT/CFA samples (*p≤0.05, **p≤0.01, ***p≤0.001, ****p≤0.0001); hash marks: significant differences between CT and CFA samples (#p≤0.05, ##p≤0.01, ###p≤0.001, ####p≤0.0001); one-way ANOVA followed by Tukey's multiple comparison test.

Gene expression alterations were reflected in PBMC samples

Alterations of *Lkaaear1* and *Kiss1r* gene mRNA levels in PBMC were low but significant when CFA was compared to saline. *Lkaaear1* showed a similar pattern to *Kiss1r*, where *Lkaaear1* presented a maximum of 2.33 and *Kiss1r* a 3.86-fold change at day one. There were no significant differences in *Gpr39* expression changes. Interestingly, *FosB* and *Aif1* showed significantly increased levels at each time point due to CFA treatment, while *Gfap* only on day seven (Figure 9.).

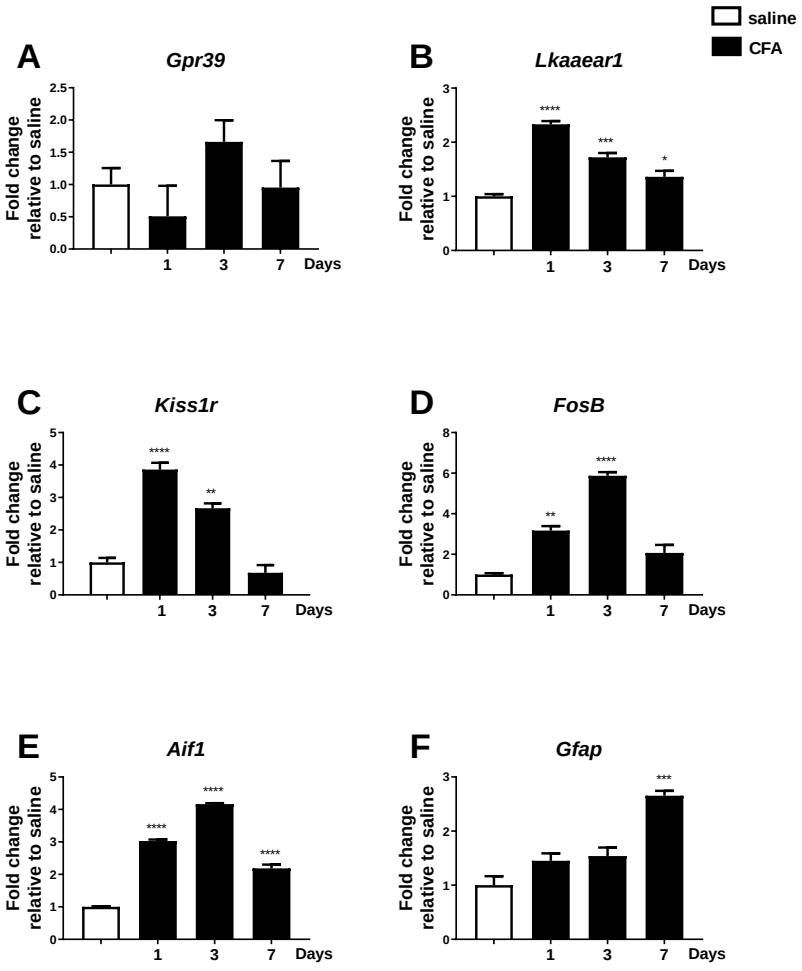

Figure 7. Time course of fold changes relative to saline control in PBMC. *Gpr39* (A), *Lkaaear1* (B), *Kiss1r* (C), *FosB* (D), *Aif1* (E) and *Gfap* (F) mRNA expression are provided one, three and seven days after CFA injection Housekeeping genes: *Ppia* and *Hprt1*; data: mean ± SEM; n=3-3; asterisks: significant differences between saline and CT/CFA samples (*p≤0.05, **p≤0.01, ***p≤0.001, ****p≤0.0001); hash marks: significant differences between CT and CFA samples (#p≤0.05, ##p≤0.01, ###p≤0.001, ####p≤0.0001); one-way ANOVA followed by Tukey's multiple comparison test.

Discussion

To our knowledge, these data represent the first comprehensive study on the CFA-induced orofacial inflammatory rat model that includes transcriptional changes in the TG, TNC and peripheral blood mononuclear cells in correlation with behavioural observations. We detected up- and downregulation of several genes, with possible involvement in sensitisation of both primary and secondary trigeminal nerves.

The nociceptor sensitisation in rodents after inflammation has been in the focus of various experiments, using electrophysiological, histological and molecular biological approaches [61,73,185–188]. Yet, there have only been a few rodent studies investigating gene expression changes in the TGs after CFA-induced orofacial inflammation [166,167].

Our microarray analysis revealed many DE olfactory, taste and pheromone receptor genes between the ipsi- and contralateral sides seven days after CFA treatment. Interestingly, besides chemoreceptors, TG-specific genes linked to olfactory signal transduction in mice and humans [189,190] had been revealed. Odorants stimulate both olfactory and trigeminal systems [191]; however, their degree of interaction and involvement in trigeminal sensitisation is unknown. Olfactory hypersensitivity can be associated with migraine, as the phenomenon was linked with a unique cortical response even outside of attacks [192]. In addition to perfume-triggered migraine, osmophobia, odour hallucination, and taste abnormalities are associated with migraine [16,193,194]. The microarray analysis showed the transcript of thyroid hormone receptor beta (*Thrb*) significantly altered. Literature data suggest that migraine is more frequent in patients with subclinical hypothyroidism [195]. In addition, chemokine signalling (*Ccr7*), among many others, and long non-coding RNAs (lncRNA) are putatively involved in the process of sensitisation.

We further determined the time-dependent changes of one of the most upregulated genes (*Lkaaear1*) from microarray data. *Lkaaear1* (*C20orf201*) encodes an LKAAEAR motive containing protein with little information in the literature regarding its function. The expression of *Lkaaear1* mRNA in various cancer cell lines has been described; thus, its role in cancer development has been studied lately [196]. *Neurod2* might be implicated in neuronal differentiation and synaptic plasticity [197,198]. Studies suggest that Neurod2, among others, can control distinct peptidergic functioning of inhibitory neurons in the dorsal spinal cord [199]. Two G-protein-coupled receptors (*Gpr39* and *Kiss1r*) and kisspeptin (*Kiss1*), genes with possible roles in nociception, were also chosen for further investigation. *Gpr39*, being a member of the ghrelin receptor subfamily, has zinc as a natural ligand. Its expression was shown in brain

regions associated with mood disorders and has become part of the antiepileptic drug development strategy [200]. Recently it has been proposed that Gpr39 might play an active role in reducing inflammation [201,202]. Kisspeptin, encoded by the *Kiss1* gene, has an emerging role in the neuroendocrine regulation of reproduction and puberty [203–206]. In addition, elevation in both mRNA and protein levels of *Kiss1*/kisspeptin was seen due to intra-articular CFA injection [207]. Both intraplantar and intrathecal kisspeptin administration caused hyperalgesia in mice [208]. Moreover, i.c.v. injection of kisspeptin-10 produces hyperalgesia and opioid antagonistic activity [209], suggesting its possible involvement in regulating pain sensitivity. Interestingly, different experimental data suggest the role of different tachykinins in puberty modulation through interaction with kisspeptin signalling [210].

CFA induced significant orofacial mechanical allodynia with a maximum on day three. This is in accordance with previous literature findings [211] and in correlation with patterns of the previously mentioned genes in TG and, interestingly, some of them in TNC. *Lkaaear1* and *Kiss1r* expression were also notably increased in PBMCs.

It is essential to highlight a delayed but considerable increase of mRNA levels on the contralateral side of CFA-treated rats. This result underlines previous findings regarding the existence of a contralateral effect more minor in magnitude after inflammatory and neural injury in animal models and humans [212,213]. Thus, we also included a saline-injected group as a control in PCR measurements. We aimed to keep the animal number at a minimum level while considering the possible trauma caused by only the injection itself. However, there was no significant functional alteration on the contralateral side; thus, the comparison to the opposite side remains functionally valid.

We chose to investigate CGRP encoding *Calca* since it is a valid mediator and novel pharmacological target of migraine and was associated with inflammatory pain [41,214–218]. Its expression was shown to be up-regulated in TGs in rodent models of orofacial inflammation [219–222]. Accordingly, transcripts of *Calca* were significantly increased in the TG at day three after CFA injection. Transcriptional changes of *Calca* in the TNC showed a similar expression pattern, reflecting mechanisms involved in central sensitisation. Presenting only transcriptional alterations in our work represents a limitation of the study. However, lately, the elevation of CGRP protein in TNC was proved in the same model [223].

Markers of activated neuronal and glial cells were selected for gene expression profiling. Therefore, we chose *FosB* as a neuronal activation marker, *Gfap* for astrocyte/SGC and *Aif1* for microglia/macrophage activation [224–226]. GFAP has been proved to be an important marker in astrocyte proliferation, blood-brain barrier functioning, signal transduction

pathways and neuron-glia interactions and is known to be induced due to brain damage and CNS degeneration. Although initially it was described as an astrocyte-specific marker, later several studies described its presence in peripheral glial cells and non-CNS cells, including lymphocytes [227]. Iba1, encoded by *Aif1*, expressed in various cells such as monocyte/macrophages and activated T lymphocytes, is mainly used as a microglia/macrophage-specific marker [228,229]. All mentioned activation markers were significantly increased at day one of the inflammation in both TGs and TNCs, peaked on day three and decreased by day seven when allodynia was declining. Remarkably, a more minor but significant increase of expression was also detectable in PBMCs, highlighting the importance of blood transcriptomics data in CNS diseases. To the best of our knowledge, these findings are the first to describe these transcripts in the PBMCs of animals in this setup. However, various human data suggests GFAP as a blood biomarker in diseases like acute stroke diagnosis [230], head trauma [231], intracerebral haemorrhage with symptoms of acute stroke [232–234], traumatic brain injury [235,236], being predictive of a neurological outcome. Recently, elevated GFAP protein expression in TG after CFA injection in the rat's whisker pad was confirmed [237]. Elevation in the density of Iba1 immunopositive cells in TNC after CFA injection in the facial skin of rats [238] was already presented. *Aif1* was identified in human PBMCs, and extracellular *Aif1* treatment of PBMCs potentiates Th1 response [239]. In addition, human data suggest that *Aif1* driven from peripheral blood monocytes/serum might serve as a diagnostic biomarker to detect allograft rejection [240] and endometrial cancer [241]. Although more studies focus on Fos gene/protein expression in CNS, some recent data describe slight modulation of *FosB* mRNA in peripheral blood lymphocytes of addict patients [242].

The advantage of PBMCs, as an easily accessible material of immune cells, is increasingly recognized in recent literature [170]. Yet, no study has evaluated TG gene expression changes by combining data with peripheral blood mononuclear cell sample measurement and behavioural studies. It is clear that the measurement of *FosB, Aif-1, Gfap, Lkaaear1* changes in the PBMCs does not have a diagnostic value at this stage, and it is too early to conclude. Although, it would be interesting to perform further studies to see whether it could have a predictive value regarding orofacial pain and headache disorders. In addition, it would be worth considering using peripheral blood mononuclear cell isolation in animal models as a translational tool for human studies.

Chapter 2. Identification of disease- and headache-specific mediators and pathways in migraine using blood transcriptomic analysis

Results

Clinical characteristics

The demographic and clinical data of study participants are provided in Table 3. The presented groups were without any between-group differences in any enlisted characteristics. Interictal blood samples were collected from all twenty-four migraineurs, while during the attack, eight samples were gathered in a self-control manner.

DE genes derived from interictal vs healthy comparison

When interictal was compared to the healthy group, 163 DE genes were found (fold change threshold of 1.5, p-value threshold of 0.05): 135 were upregulated, and 28 were downregulated. The interleukin *IL-1β* gene (*IL1B*), cyclooxygenase 2 (*COX2/ PTGS2*), tumor necrosis factor (*TNF*), and numerous chemokines, such as IL-8 (*IL8*), were enlisted in the top DE gene list (Appendix Table 6.).

DE genes derived from ictal vs interictal comparison

In ictal - interictal comparison, 144 DE genes were detected (fold change: 1.3, p-value: 0.05): 64 were upregulated, 80 were downregulated. Heterogeneous nuclear ribonucleoprotein C like 1 (*HNRNPCL1*), olfactory receptor family 10 subfamily G member 2 (*OR10G2*) and interleukin 20 receptor subunit alpha (*IL20RA*) can be found among the top DE gene list (Appendix Table 7.). After false discovery rate (FDR) correction, two genes remained on the list, with the adjusted p-values below 0.25: the heterogeneous nuclear ribonucleoprotein C like 1 (*HNRNPCL1*) and the cornichon family AMPA receptor auxiliary protein 3 (*CNIH3*).

DE genes derived from ictal vs healthy comparison

In ictal samples compared to healthy ones, 131 genes were differentially expressed (fold change: 1.5, p-value: 0.05), 118 were upregulated, 13 were downregulated. The *IL1B* gene was also implicated in this comparison, among others, like *PTGS2*, *TNF*, and *IL8* (Appendix Table 8.). DE genes are visualized on heat maps (Figures 8-10.).

Table 3. Demographic and clinical characteristics of study participants. Values are provided as mean±SD.

Group	Migraineurs with (n=3) and without aura (n=21)	Healthy control subjects (n=13)
Gender	female n=23 male n= 1	female n=13
Age (years)	35 ± 12.25	35 ± 4.96
Body mass index (BMI)	22.21 ± 4.57	24 ± 3.47
Last meal (hours ago)	6.59 ± 6.29	3.69 ± 5.32
Co-morbidities and therapy		
Known other diseases	n=10	
Regular medication (except for attack therapy)	n=7	
Hormonal contraceptives	n=8	n=4
Antimigraine prophylactic therapy	n=24	
Clinical features of the headache		
Disease duration (years)	15 ± 12	
Attack frequency (attack/year)	32 ± 37.37	
Visual analogue scale (VAS)	7 ± 1.44	
Allodynia	n=9	
Menstruation-headache relationship (sensitive)	n=10	
Migraineurs in the family	n=15	
Regular sport activity	n=13	
Features of attacks before samplings		
Number of attacks in the previous month	3 ± 3.31	
Last attack before interictal blood sampling (days ago)	16.58 ± 28.35	
Beginning of attack before ictal blood sampling (hours)	17.91 ± 29.47	

Mitochondrial dysfunction was suggested by analysis of migraineurs' samples

Functional enrichment analysis of DE genes (DE list enrichment) and ranked list enrichment of all genes was performed to better insight into functions, networks and biological processes involved in migraine. Significant GO, KEGG and Reactome terms are provided in

Appendix Table 9. When interictal was compared to the healthy group, cytokine and chemokine receptor binding, interleukin-10 (IL-10) signalling, and oxidative phosphorylation in the mitochondria were significantly altered. When the ictal group was compared to interictal, hormone and cytokine activity, oxidative phosphorylation and chemosensory receptors were implicated. Furthermore, the ictal-healthy comparison included IL-4, IL-10 and IL-13, and chemokine, growth factor and neuroactive ligand-receptor interactions. The ranked list enrichment analysis of all genes statistically significantly implicated the metabolic pathway of oxidative phosphorylation (Appendix Table 9.) in interictal-healthy and ictal-interictal comparison of the PBMC samples. Mitochondrial functioning was affected in both comparisons.

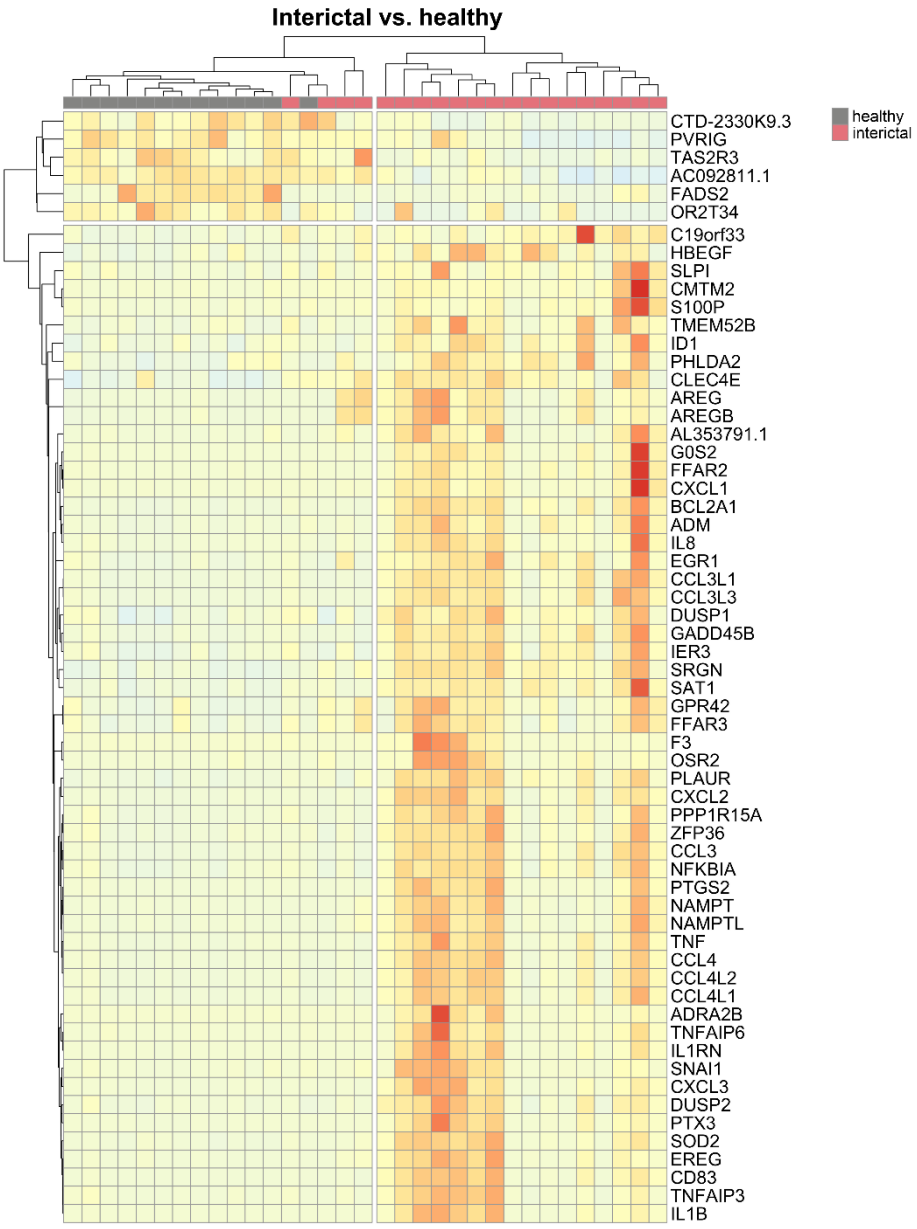

Figure 8. Heat map representation of DE genes in the interictal - healthy comparison. Columns indicate samples; rows indicate genes.

Pearson correlation was respectively calculated between samples and genes, visualized by dendrograms.

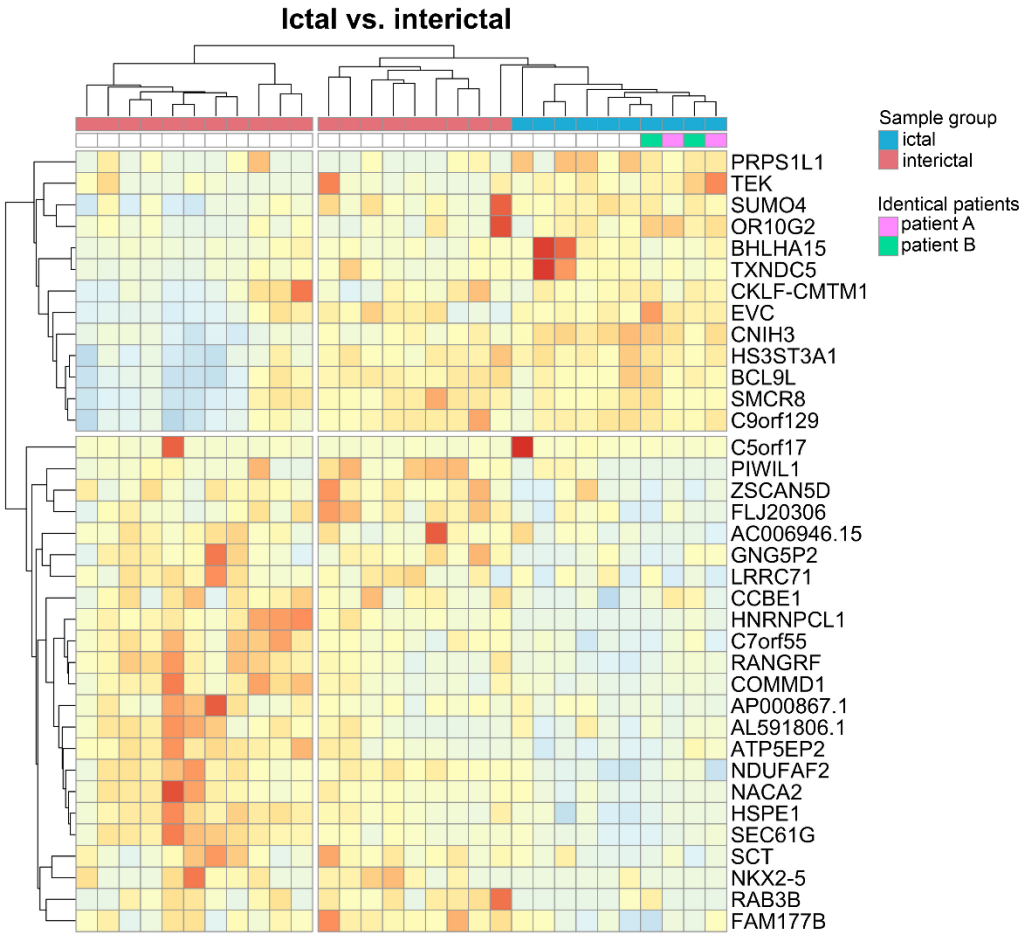

Figure 9. Heat map representation of DE genes in the ictal - interictal comparison. Columns indicate samples; rows indicate genes. Pearson correlation was respectively calculated between samples and genes, visualized by dendrograms. Patients A and B have two samples from different time points.

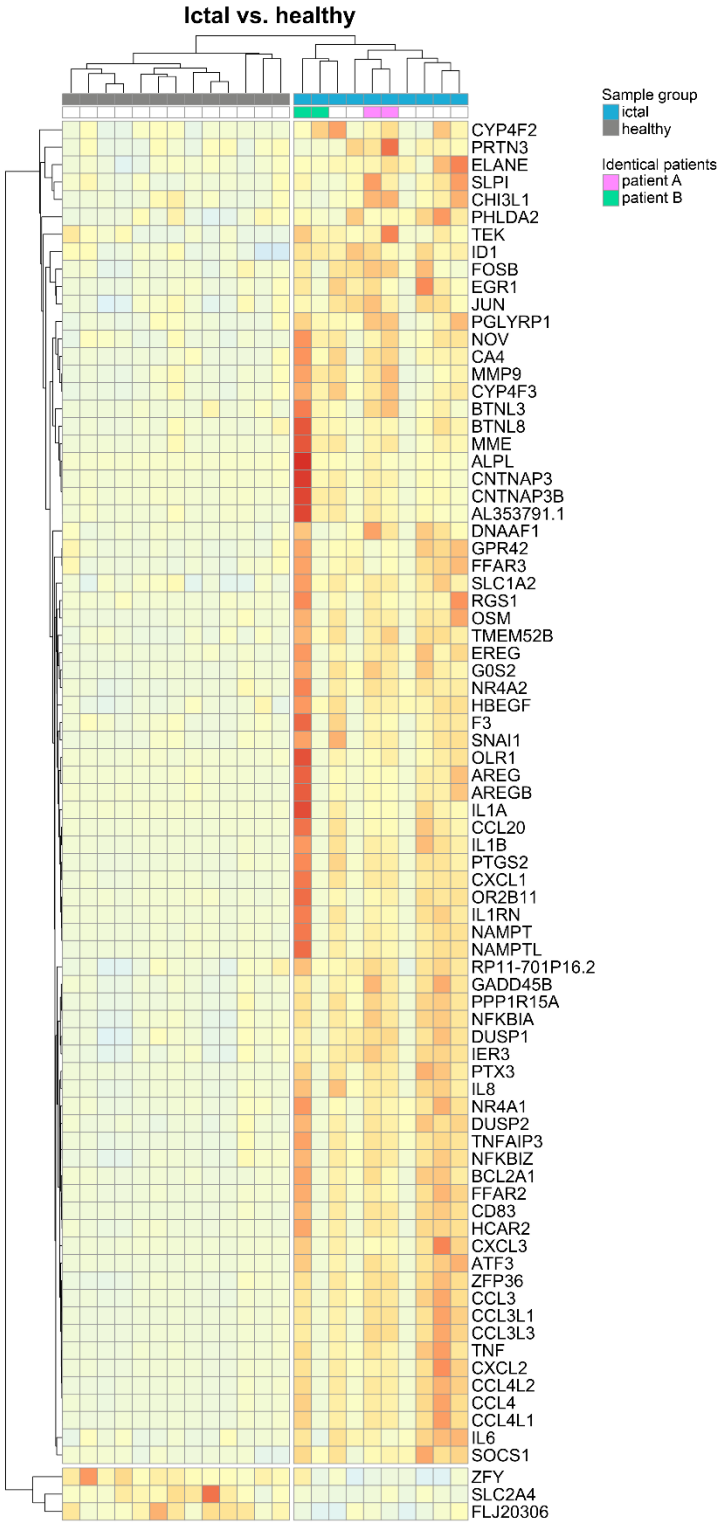

Figure 10. Heat map representation of DE genes in the ictal - healthy comparison. Columns indicate samples; rows indicate genes. Pearson correlation was respectively calculated between samples and genes, visualized by dendrograms. Patients A and B have two samples from different time points.

Discussion

Animal models provide powerful tools of human disease pathophysiology mapping; however, adapting human disease phenomena to animal models is challenging (reverse translation). Forward translation (from animals to humans) is also crucial for the appropriate interpretation of the experimental findings. One of our target scopes was to build a database that might work both ways regarding migraine and headache disorders. Thus, our next step was to initiate a human migraine study, where PBMC samples would represent the key element, making possible the comparison of animal and human data. To our knowledge, this is the first study to perform transcriptome analysis of PBMCs isolated from migraine patients, including samples taken in an attack-free period and during headaches. Comparing these groups with healthy controls made possible the identification of both disease-specific and headache-specific alterations and revealed the importance of inflammatory pathways and the potential contribution of various cytokines to migraine susceptibility. Furthermore, our results suggest the possible implication of mitochondrial dysfunction in migraine.

As previously described in the introductory section, there has been an ongoing debate about the precise pathophysiological mechanism of migraine. However, the headache is a prevalent neurovascular brain disorder, possibly generated by activating the trigeminovascular system, causing neurogenic vasodilation and inflammation of the meninges [16,26]. Although there is positive feedback regarding the recently approved anti-CGRP monoclonal antibodies used in therapy, most preventive treatment is still based on empirical observations. Thus, a better understanding of the pathophysiological mechanisms is essential for identifying the key mediators and new therapeutic targets.

It is also now accepted that migraine susceptibility has a vital genetic component. Novel methodologies, such as next-generation sequencing can be implemented to discover critical genes in migraine research. Few genomic next-generation sequencing studies exist on this topic, focusing on specific genes associated with glutamatergic neurotransmission, neuron and synaptic development, pain-sensing, brain vasculature function [243]. Although recently several genetic discoveries were made by genome-wide association studies (GWASs), for the time being, none of the harvested genes could be compelling as genetic biomarkers of migraine [244]. DE genes have been described in the whole peripheral blood of migraineurs by microarray or bead array [168,245]. Next-generation RNA sequencing was also performed in a late study, where healthy individuals were compared to migraineurs. This study provided significant changes in immune function and cytokine signalling [146]. As mentioned before,

the PBMC transcriptome had been reported to correlate better with the alterations in the brain [168], thus instead of whole blood, we analysed PBMCs, which makes a unique component of the study.

Significant gene expression could be detected independently of headache episodes compared to the control group, which could be markers of migraine susceptibility but not necessarily attack-specific.

It is known that inflammatory processes are also crucial in headache generation. Meningeal mast cell, glial cell activation, subsequent proinflammatory cytokines (IL-1β, IL-6, TNF-α), and chemokine release play significant roles in the progression of migraine headache (Figure 2.). Moreover, cortical spreading depolarization induces neuroinflammatory signalling in the brain parenchyma due to inflammasome activation [246–248]. Our study detected upregulation of several cytokines and chemokines (*ILB, TNF, IL6, CXCL1, 2* or *3*) and *COX-2* in PBMCs samples of migraineurs interictal and ictal samples compared to healthy controls, thus suggesting a systemic change of immune functions. Elevated plasma levels of several proinflammatory cytokines like IL-1, IL-6 [249], TNFα [250], IL-8, CCL3 and CCL5 [251,252] and C-reactive proteins (CRP) [253,254] have been shown in migraine reports. According to the literature, during attacks, the concentration of IL-1β, IL-6, IL-8, IL-10, and TNF-α were further increased [255,256]. Cytokines are essential regulators of inflammatory and immune signalling. Several of them, such as IL-1β or TNFα, have been directly implicated in pain sensitisation by acting on peripheral nociceptive nerve terminals and sensory ganglia and causing central sensitisation. [257–260]. Data supported their potential contribution to headache-related mechanisms in various animal studies. [261,262]. The pronociceptive nature of *CXCL1, 2* or *3* (ligands of the CXCR2 receptor) have been reported [263], their intrathecal administration initiated hyperalgesia in mice [264]. These chemokines might have implications in neuropathic pain [264–266] and traumatic brain injury [267,268]. CXCL1 in the synovial fluid correlated with osteoarthritis severity [269]. Amphiregulin and epiregulin (*AREG/EREG*), both ligands of epidermal growth factor receptor (EGFR), have been involved in tumour growth and inflammation [270,271]. Epiregulin seems to be pronociceptive in mice, and EGFR inhibitors were analgesic in various animal models of chronic pain [272]. Elevated levels of *AREG*/amphiregulin in PBMCs isolated from bone marrow and synovial fluid of patients with rheumatoid arthritis has been detected. [273]. An interesting finding among the DE genes is the upregulation of CD83, which is mainly expressed on dendritic cells and acts as an activator of regulatory T cells and thus has a major role in the suppression of the inflammatory reaction. It has been implicated in various autoimmune diseases such as rheumatoid arthritis or

inflammatory bowel disease [274]. The importance of elevated expression in PBMCs of migraine patients is not clear at this point. Not surprisingly, our functional enrichment results highlighted the importance of a cytokine, chemokine, inflammatory, and immune activity alteration found in all comparisons.

Abnormalities in energy metabolism, mitochondrial function and oxidative stress in migraine have focused on recent comprehensive reviews [275,276] and a meta-analysis [277] indicating its emerging importance relating to the topic. It has been suggested that the headache attack can be regarded as an adaptive response to restore energy homeostasis. Impaired mitochondrial functioning has been detected in the brain and skeletal muscle of migraine patients during attacks, but also even interictally [278–281]. Moreover, migraine triggers have also been raised to act as promoters of oxidative stress [282,283]. Various studies have consistently reported elevated oxidative stress markers or a deficit of antioxidant mechanisms [275,277]. Our functional enrichment analysis revealed functions and biological processes that confirms and supplements this literature data. Our findings might highlight mitochondrial functioning, oxidative stress in migraine research and offer valuable targets for further drug therapy development.

This study has two considerable limitations. Briefly, RNA-based results are not confirmed by measuring the concentrations of the affected cytokines. Still, the transcriptome analysis results are in line with previous literature data [284]. The second limitation is that only the ictal-interictal comparison yielded results after controlling for the false discovery rate. Heterogeneity of the patient pool might indicate an increased number of patients. Critical results remain to be confirmed in a later study with a more significant number of participants.

Chapter 3. Hemokinin-1 gene expression is upregulated in trigeminal ganglia in an inflammatory orofacial pain model: potential role in peripheral sensitisation

Results

Tac4 mRNA levels changed in parallel with orofacial allodynia after CFA-induced inflammation in rat TG

The mechanonociceptive threshold of the whisker pad area of CFA-injected rats was significantly decreased compared to the saline-injected rats in all three days, reaching its minimum on day three (Figure 11. A), as described in the previous chapter. *Tac4* gene expression was also measured in PBMCs, TG and TNC samples. *Tac4* mRNA expression levels in TG (Figure 11. B) correlated with the shift in von Frey thresholds, reaching its maximum on day three. Unfortunately, in TNC and PBMC samples, the *Tac4* expression could not be detected with sufficient reliability using this method.

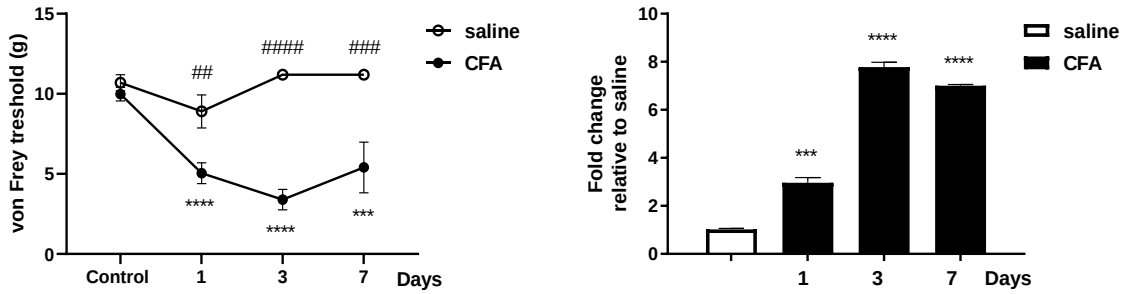

Figure 11. Changes in orofacial mechanical threshold in responses to mechanical stimuli during the von Frey test before (control) and one, three, seven days after 50 µl s.c. complete Freund's adjuvant/saline injection. Data: mean ± SEM; n= 5-16; asterisks: significant differences control day vs days after CFA treatment (***p≤0.001 ***p≤0.001); hash marks: significant differences between saline and CFA samples (##p≤0.05, ###p≤0.0001, ####p≤0.0001); two-way ANOVA followed by Tukey's multiple comparison test **(A)**; Time course of *Tac4* mRNA fold changes relative to saline control in rat TG on day one, three and seven after CFA/saline injection. Housekeeping genes: *β2m* and *Hprt1*; Data: mean ± SEM; n=3 at each time point; asterisks: significant differences between saline and CFA samples (***p≤0.001, ****p≤0.0001), one-way ANOVA followed by Tukey's multiple comparison test **(B)**.

CFA induced upregulation Tac4 mRNA in both primary sensory neurons and SGCs of the rat TG

To investigate the basal and altered level of *Tac4* mRNA expression in rat TG after saline or CFA injection, we performed fluorescent RNAscope *in situ* hybridization that provides cellular resolution and tissue context. *Tac4* transcripts were localized primarily on SGCs and sensory neurons in saline-treated samples (Figure 12. left panel). CFA treatment caused significant upregulation in both cell types (Figure 13.). *Tac4* expression levels were analysed semi-quantitatively using ImageJ software and plotted as *Tac4* specific total dot area/number detected either in SGC or sensory neuron soma (Figure 12.). Sensory neurons and SGCs were identified morphologically (Figure 12.). In addition, histological co-localization of *Tac4* with neuronal [285] (NeuN, encoded by *Rbfox3*) and satellite glial marker [95] (SK3, encoded by *Kcnn3*, Figure 14.) was performed. *Tac4* positive transcripts were also detected on Schwann cells, identified only morphologically. RNAscope was validated by RNAscope 3-plex negative control probes designed to bacterial *dapB* gene giving no detectable fluorescent signal on any channel (Appendix Figure 1.).

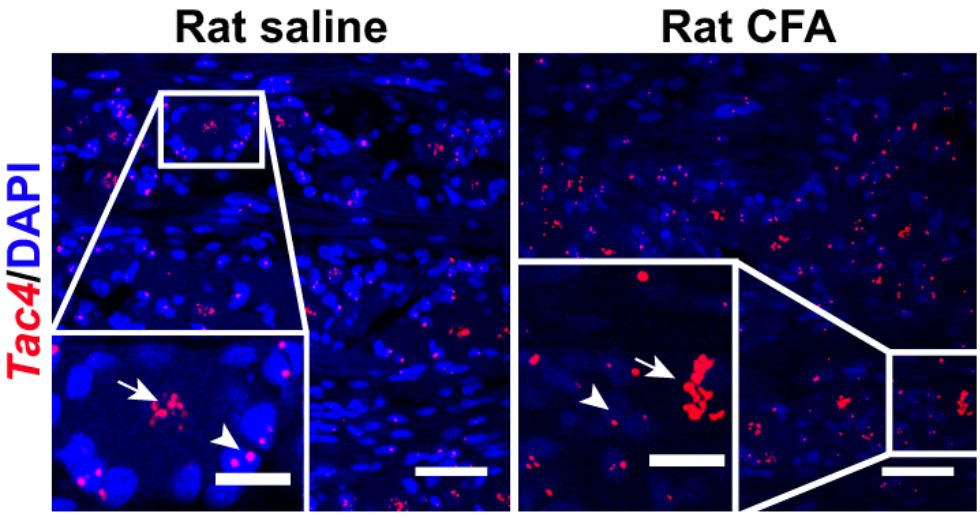

Figure 12. Representative images of *Tac4* mRNA (red) counterstained with DAPI are displayed on longitudinal slices of rat trigeminal ganglia after injection of saline or CFA. Arrows: sensory neurons; arrowhead: SGCs; scale bar: 50 µm; inset scale bar: 20 µm.

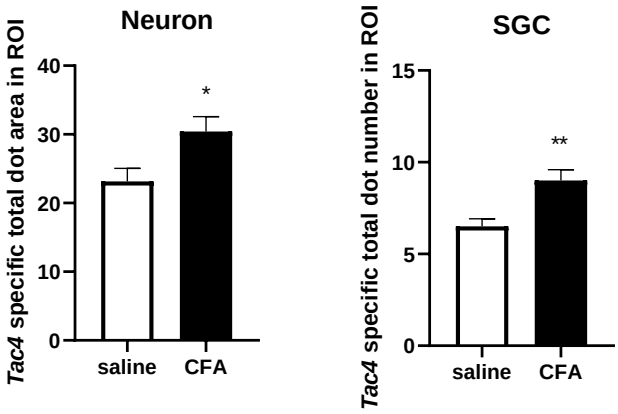

Figure 13. Quantification of *Tac4* mRNA. CFA induced upregulation of transcripts when compared to saline group in neurons (CFA: n=120, saline: n=68) and in SGCs (CFA: n=69, saline: n=52) of n=4-6 rats/group. Asterisks: significant differences in saline vs CFA samples (*p≤0.05, **p≤0.01); Student's *t*-test for unpaired samples; ROI: region of interest; unit of the area: µm2.

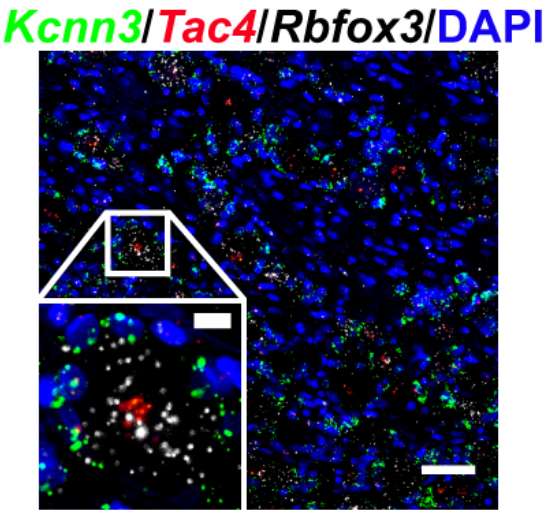

Figure 14. Representative image of rat longitudinal TG section. RNAscope probes specific to *Kcnn3* (green encoding SK3) to detect SGCs, and to *Rbfox3* (white encoding NeuN) to visualize sensory neurons were used to co-localize with *Tac4* mRNA (red). Scale bar: 50 µm; inset scale bar 10 µm.

Behavioural tests suggested anxiety-like behaviour in Tac4$^{-/-}$ gene-deficient mice

To examine the effect of the lack of *Tac4* gene on behaviour, we applied our orofacial inflammation model on *Tac4*$^{-/-}$ mice. CFA administration caused significantly decreased orofacial mechanonociceptive threshold one and three days after injection in both WT and *Tac4* $^{-/-}$ mice. However, saline injection caused similar, although non-significant changes. No significant changes were observed between the thresholds of WT and *Tac4*$^{-/-}$ mice. However, saline and CFA treated groups seem to be better separated in WT mice (Figure 15.). No

substantial change in spontaneous behaviour was seen due to CFA injection (saline vs CFA). However, *Tac4*$^{-/-}$ mice spent less time in the centre zone of the open field box, suggesting an anxiety-like behaviour compared to their littermates (Figure 16.).

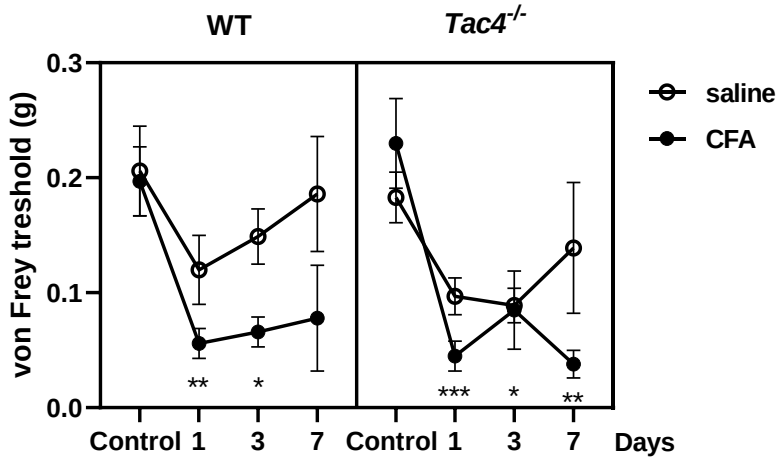

Figure 15. Changes in orofacial mechanical threshold in responses to mechanical stimuli during the von Frey test before (control) and one, three, seven days after CFA (10 µl s.c. complete Freund's adjuvant) inflammation or saline injection. The mean of the orofacial thresholds on both sides was calculated. Data: means ± S.E.M; n=7-18; asterisks: significant differences between control and saline/CFA-treated samples (*p≤0.05, **p≤0.01, ***p≤0.001); two-way ANOVA followed by Tukey's multiple comparison test.

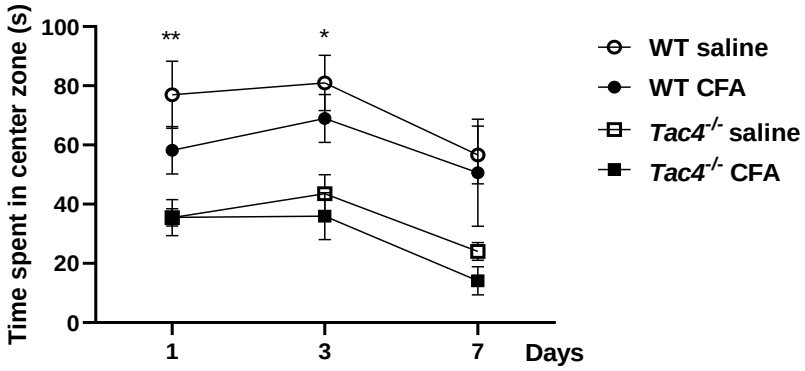

Figure 16. Changes in spontaneous behaviour measured in the open field test. Data: means ± SEM; n=3-15; asterisk: significant differences in WT saline vs *Tac4*$^{-/-}$ saline comparison (*p<0.05, **p≤0.01); two-way ANOVA followed by Tukey's multiple comparison tests.

CFA induced upregulation Tac4 mRNA in both primary sensory neurons and SGCs of the mice TG

Similar to *Tac4* expression found in rat TG, basal *Tac4* mRNA was detected both in sensory neurons and SGCs of mouse TG (Figure 17.). Moreover, CFA-induced upregulation in mouse *Tac4* mRNA (Figure 18.). Sensory neurons and SGCs were identified morphologically (Figure 17.).

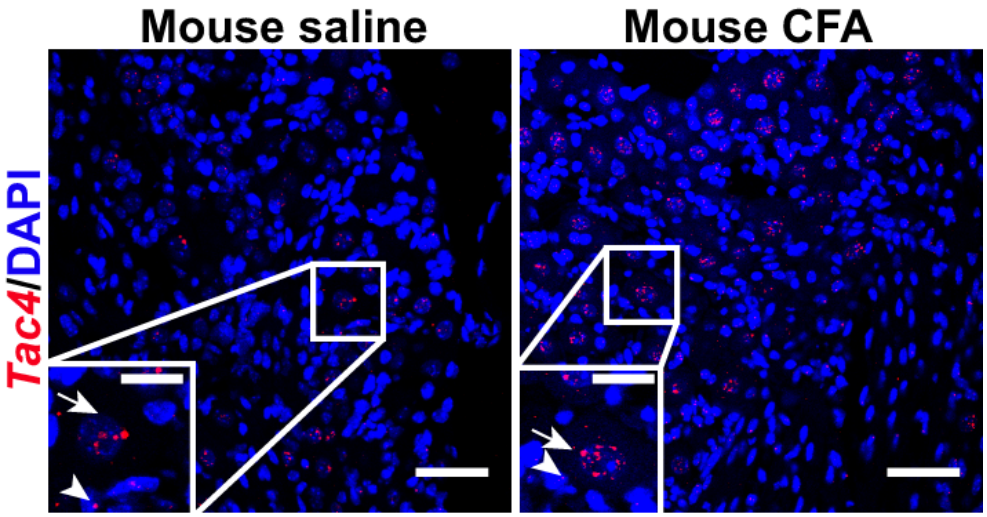

Figure 17. Representative images of *Tac4* mRNA (red) counterstained with DAPI is shown on longitudinal slices of mouse TG after saline or CFA administration. Arrows: sensory neurons; arrowheads: SGCs; scale bar: 50 µm; inset scale bar: 20 µm.

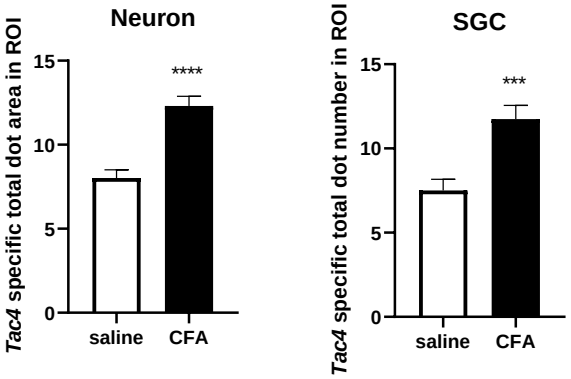

Figure 18. Quantification of *Tac4* mRNA. CFA induced upregulation of transcripts when compared to saline group in neurons (CFA: n=119, saline: n=71) and in SGCs (CFA: n=54, saline: n=38). n=4-5 mice/group; ROI: region of interest; unit of the area: µm2.

CFA-induced changes in neuronal and glial activation marker levels in the TG of Tac4 gene-deficient mice

Mouse TG samples showed a relatively low value of *Tac4* expression, and thus it could not be reliably quantified by RT-qPCR. With this method, we could not reliably detect *Tac4* in TNC and PBMC samples either, similarly to rat TNC and PBMC samples.

The gene pattern of neuronal and glial activation markers in the rat TG and TNC was presented in the previous chapter. We also investigated the same markers in the mouse samples after orofacial inflammation. Since this chapter focuses on peripheral trigeminal ganglia, in the following, only results of the TG are going to be described. In WT mice, neuronal *FosB* gene expression was significantly upregulated by day three compared to intact samples (data not shown). However, both CFA injection and the saline administration increased *FosB* expression level. The differences between saline- and CFA-treated samples were significant only on day one. A significant upregulation of the *FosB* was only detected in *Tac4*$^{-/-}$ animals at a later time point, on day seven. Upregulation of the neuronal marker on days three and seven was significantly lower in the TG of *Tac4*$^{-/-}$ mice when compared to its matching WT (Figure 19.).

In intact animals, the microglia/macrophage activation marker (*Aif1*) presented lower expression levels in *Tac4*$^{-/-}$ mice compared to WT (data not shown). *Aif1* expression was slightly higher in both saline- and CFA-treated *Tac4*$^{-/-}$ mice than their corresponding WT groups, significant on days one and three. Although, these changes were probably too small to be biologically meaningful (Figure 19.). After treatment, the SGC/astrocyte activation marker was upregulated in all groups on all days compared to intact samples (data not shown). CFA induced a significant elevation in WT compared to the respective saline-treated group on days one and three. Interestingly, inflammation did not cause alteration in *Gfap* levels in *Tac4*$^{-/-}$ mice. Moreover, most of the comparisons showed that *Gfap* mRNA expression levels were lower in all Tac4$^{-/-}$ groups than in the WT group (Figure 19.).

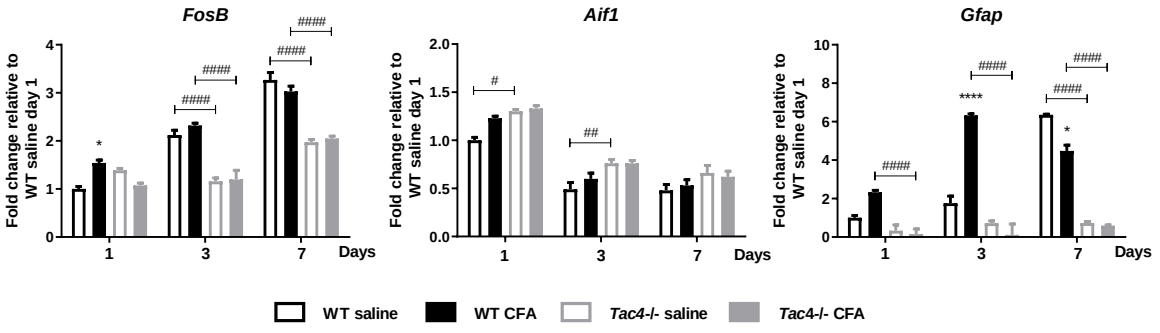

Figure 19. Time course of fold changes relative to WT saline day one group of *FosB, Aif1*, *Gfap* mRNA expression in the trigeminal ganglia of WT and *Tac4*$^{-/-}$ mice one, three and seven days after saline/CFA injection. Housekeeping gene: *Ppia*. Data: means ± SEM; asterisks: significant differences between saline and CFA treated samples (*p≤0.05, ***p≤0.001); n=3-10; hash marks: significant differences in WT and *Tac4*$^{-/-}$ samples (#p≤0.05, ##p≤0.01, ### p≤0.001, ####p≤0.0001); two-way ANOVA followed by Tukey's multiple comparison test.

Neuroinflammation-related genes were differently altered in TG of saline-or CFA-treated Tac4$^{-/-}$ *and WT mice*

Nanostring analysis was performed on TG samples collected on day three after CFA or saline injection in the whisker pad of WT and *Tac4*$^{-/-}$ mice. Results revealed various neuroinflammation-related differentially expressed genes and significant cell type-specific gene expressions correlations. In the saline-treated *Tac4*$^{-/-}$ group, 15 genes were differentially (9 upregulated, 6 downregulated) expressed (p-value threshold of 0.05) in comparison with saline-treated WT samples (Figure 20.). Significant alterations in microglia/macrophage and cytotoxic cell-specific genes were enlisted when saline-treated *Tac4*$^{-/-}$ mice were compared to saline-treated WTs (Figure 21.). In the TG of CFA-treated *Tac4*$^{-/-}$ mice, 22 genes were differentially expressed (p-value threshold of 0.05) compared to the CFA-treated WT group. 13 genes were upregulated, nine were downregulated in the *Tac4*$^{-/-}$ TG samples (Figure 22.). Alterations in genes specific to neutrophil granulocytes were significantly correlated in CFA-treated *Tac4*$^{-/-}$ vs CFA-treated WT comparison (Figure 23.). The treatment effect was reflected in the clustering of the samples in all cases.

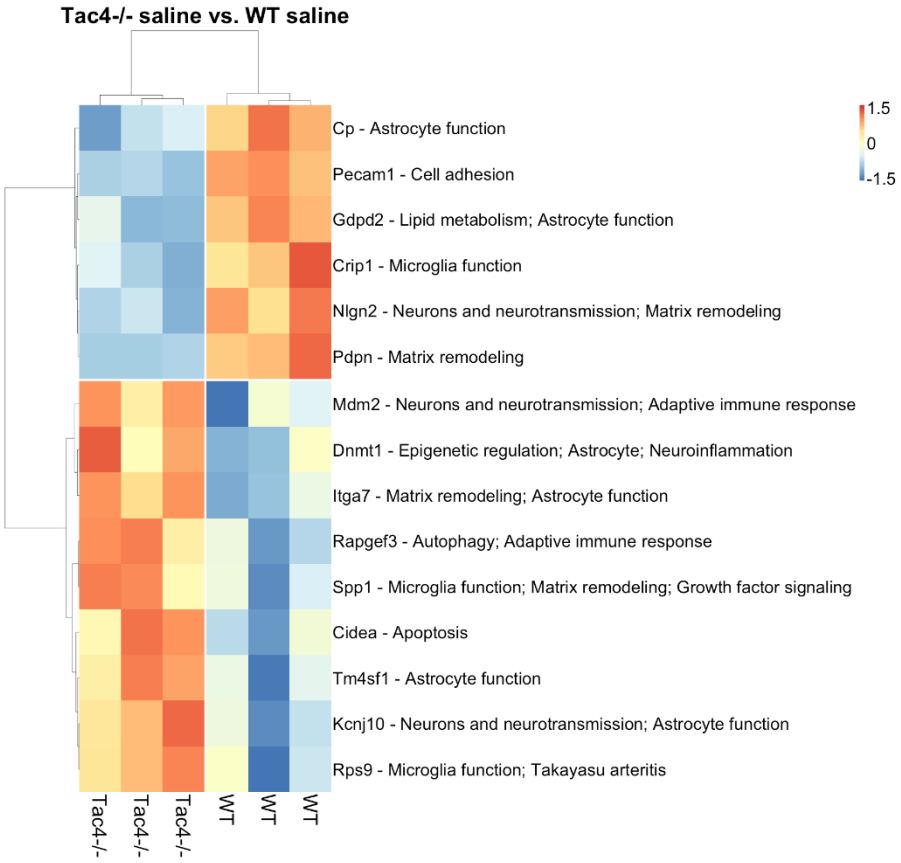

Figure 20. Heat map of the DE genes with annotations between TG saline groups of *Tac4*$^{-/-}$ and WT mice. Rows: genes; columns: samples; n=3-3. Normalized gene counts data are shown as row-wise z-scores (scale is shown on legend). Rows and columns were hierarchically clustered using Pearson correlation distance measure and average method. Distances are displayed as dendrograms. References for the functional annotations: *Cp* [286] *Pecam1* [287] *Gdpd2* [288] *Crip1* [289] *Nlgn2* [290] *Pdpn* [291] *Mdm2* [292] *Dnmt1* [293] *Itga7* [294] *Rapgef3* [295] *Spp1* [296] *Cidea* [297] *Tm4sf1* [298] *Kcnj10* [299] *Rps9* [299].

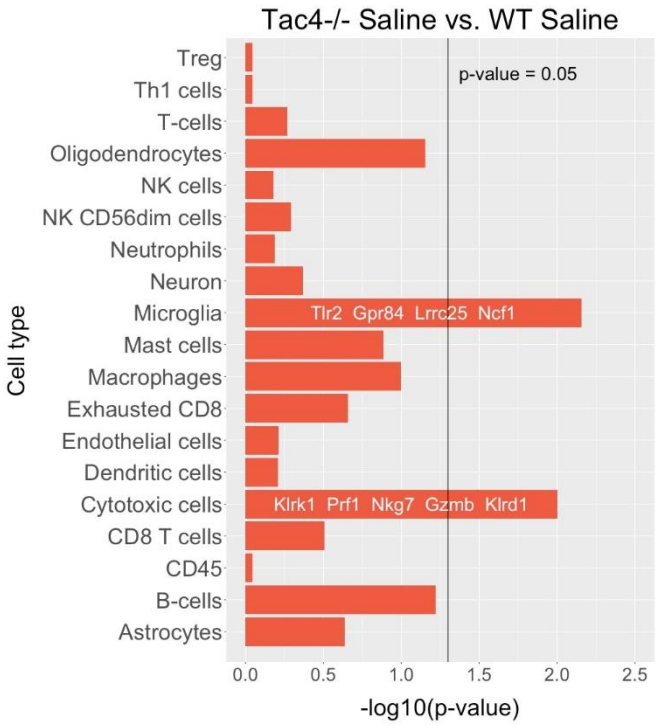

Figure 21. Barplots of p-values for correlation of cell-type-specific gene expressions in saline groups of *Tac4*$^{-/-}$ *vs* WT mice. p-values are -$\log_{10}$ transformed.

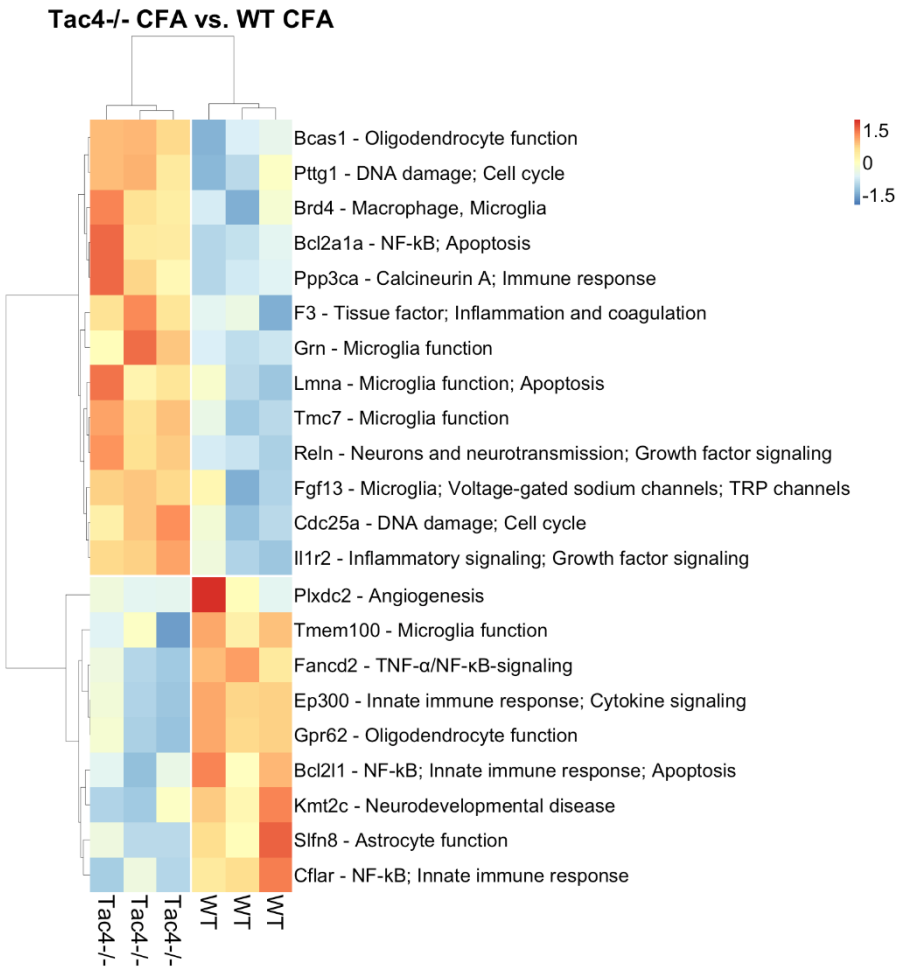

Figure 22. Heat map of the DE genes with annotations between CFA groups of *Tac4*$^{-/-}$ and WT mice. Rows: genes; columns: samples; n=3-3. Normalized gene counts data are shown as row-wise z-scores (scale is shown on legend). Rows and columns were hierarchically clustered using Pearson correlation distance measure and average method. Distances are displayed as dendrograms. References for the functional annotations: *Bcas1* [300] *Pttg1* [301] *Brd4* [302,303] *Bcl2a1a* [304] *Ppp3ca* [305] *F3* [306,307] *Grn* [308,309] *Lmna* [310] *Tmc7* [311,312] *Reln* [313] *Fgf13* [314–317] *Cdc25a* [318] *Il1r2* [319] *Plxdc2* [320] *Tmem100* [321,322] *Fancd2* [323] *Gpr62* [324,325] *Bcl2l1* [326] *Kmt2c* [327] *Slfn8* [328,329] *Cflar* [330].

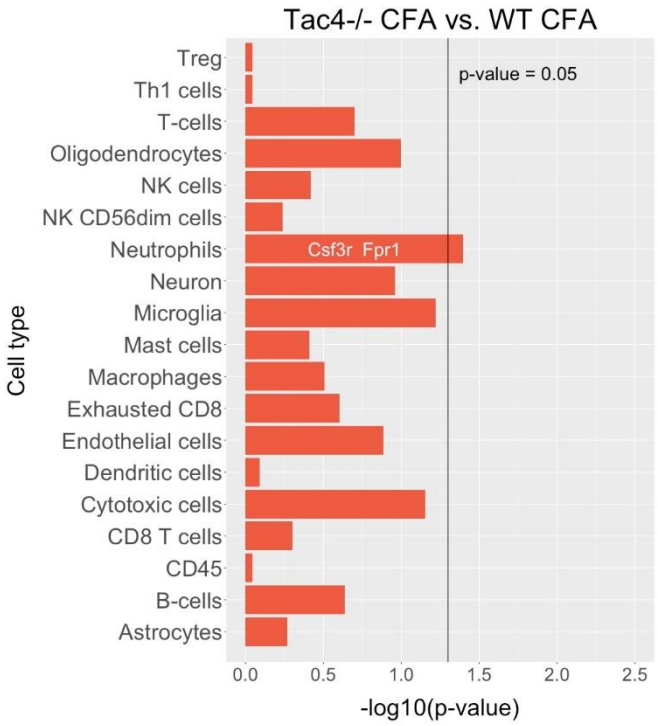

Figure 23. Barplots of p-values for correlation of cell-type-specific gene expressions in CFA groups *Tac4*$^{-/-}$ vs WT mice. p-values are -$\log_{10}$ transformed.

Discussion

In the current chapter, results confirmed the presence of *Tac4* mRNA in the trigeminal ganglion and its upregulation due to orofacial inflammation. However, it was already previously shown that HK-1 is distributed throughout the CNS and the TG [129,134]; and little data exists on describing *Tac4* alteration in human studies [331,332]; to our knowledge, ours is the first study to assess the changes of *Tac4* expression under a pathological condition in an animal trigeminal sensitisation model. Hemokinin-1 had only been shown in small and medium-size neurons using immunohistochemistry in the TG [134]. In turn, we detected Tac4 transcripts on neurons and all types of glial cells of the TG in the present study. In addition, significant inflammation-induced upregulation of *Tac4* was demonstrated in both neurons and satellite glial cells. Based on our orofacial mechanonociceptive threshold measurements in the rat and the qPCR results, we have shown that *Tac4* upregulation happened parallel to the development of allodynia which suggests a potential role in the sensitisation process. There is growing evidence for the crucial role of neuron-glia crosstalk in chronic pain conditions, including orofacial pain [82,221,333]. Therefore, simultaneous upregulation of *Tac4* in trigeminal sensory neurons and SGCs might be particularly important. Other neuropeptides such as CGRP have already been suggested to have a role in glial cell activation during sensitisation [334] and appears to be an essential mediator in the neuron-glia interactions in the TG [64,335,336]. Our results suggest a role of the neuropeptide in question in two-way communication between neuronal and glial cells. Furthermore, a possible physiological role of HK-1 in the trigeminal system can be suspected by detecting baseline differences in the expression of genes associated with glial cell activity.

Previous studies proved that HK-1 could contribute to hyperalgesia in acute and chronic pain models. HK-1 can elicit pain when injected intrathecally [129,136]. Recent articles of our workgroup described reduced nocifensive behaviour of *Tac4*$^{-/-}$ mice in chemically-induced pain models and suppressed hyperalgesia/allodynia in chronic inflammatory and neuropathic pain models [138,337]. In models of inflammatory pain and arthritis, a proinflammatory component is also likely to contribute since the expression of HK-1 have been described in the immune system as well [125,128,338], and *Tac4* deficiency also alleviated experimental lung inflammation [137]. After nerve injury, spinal microglia and astrocyte activation were damped in *Tac4*$^{-/-}$ mice, proving a potential role in central nociceptive sensitisation [138]. Few human data exist on *Tac4* gene expression alteration. *Tac4* mRNA was upregulated in the mucosa of ulcerative colitis patients [331]. Using a commercially available ELISA kit, a recent study

declared that serum protein levels of patients with chronic spontaneous urticaria were decreased compared to the control group [332]. In addition, its serum level increased in patients with fibromyalgia syndrome [339].

HK-1 is a potent NK-1 receptor agonist [129]. Though, more evidence propounds a different mechanism of action, suggesting the existence of a possible unknown target. This hypothesis is underlined by the difference between the phenotypes of *Tac4*- and SP- or NK-1 receptor-deficient mice in chronic pain models [135].

We aimed to investigate the role of HK-1/*Tac4* in trigeminal sensitisation by adapting the CFA-induced orofacial pain model to *Tac4*$^{-/-}$ and wild-type mice. Although a certain tendency was seen in the temporal change of the mechanical thresholds, we could not prove clearly that orofacial allodynia was attenuated in *Tac4* deficient mice. Unlike rats, mice do not adapt well to repeated handling [340], and stress might cause hyperalgesia in humans and animal models [341]. We limited the handling and the number of repeated measurements, but even light restraint seemed to be a significant stress factor. This could explain why the mechanical thresholds of saline and CFA mice decreased from the baseline. Alterations in spontaneous behaviour measured in the open field test are in line with previous results, suggesting a possible role of HK-1 in mediating anxiolytic effects [135].

In the previous chapter, temporal changes of mRNA levels of neuronal and glial activation markers in rat TG, TNC and PBMC were detected, which correlated with changes in the orofacial allodynia. Unfortunately, we could not reproduce these results clearly in mice. In addition, PBMC isolation from pooled mice blood failed to give the necessary quantity and quality mRNA; thus, we did not follow with further quantification. In the intact *Tac4*$^{-/-}$ mice, there was a lower baseline expression of microglia/macrophage marker *Aif1* and SGC/astrocyte marker *Gfap* in all the sampled tissues. The basal difference might be conceivable since macrophages express both HK-1 and the NK-1 receptor, and the *Tac4* mRNA was also present in cultured microglia. Resident CNS cell types like astrocytes and microglia also express the NK-1 receptor, through which glial NK-1 receptors might be necessary to regulate CNS neuroimmune responses [342].

All activation markers increased significantly in both saline and CFA groups, probably due to the restraint-induced stress. *Tac4*$^{-/-}$ mice presented a substantially lower *FosB* and *Gfap* upregulation than their respective WT counterparts due to all treatments. The mentioned difference in *Gfap* between wild-type and gene-deficient mice could also suggest that HK-1 might activate SGCs and astrocytes during stress.

NanoString neuroinflammation panel methodology revealed additional DE genes to explore our orofacial inflammation model better. To our knowledge, these are the first results using this technology in mouse TG samples to investigate neuroinflammation in a pain model. Compared to saline-treated wild-type and *Tac4*$^{-/-}$ animals, the cell type-specific profiling showed significantly altered microglia and cytotoxic cell-related genes. Thus, *Tac4* deficiency might be involved in macrophage/microglia-related gene expression changes, not surprising since the allocation of *Tac4* and the NK-1 receptor has been described on these cells. DE genes found in this comparison highlight that not only macrophage-like microglia functioning seem to be altered, but the functions of SGCs as well.

Interestingly, downregulation of the *Kcnj10* gene has been observed. *Kcnj10* encodes Kir4.1, a member of the inward rectifier-type potassium channel family. Takeda and his colleagues have already suggested that inflammation could dampen Kir4.1 in SGC of the TG, resulting in impaired glial potassium microenvironment and pain [299]; these findings are in line with our results. Comparing the cell type-specific profiling of differentially expressed genes between CFA-treated wild-type and *Tac4*$^{-/-}$ mice resulted in significantly concerned neutrophil granulocytes. Furthermore, the list of DE genes revealed alterations in transcripts regarding microglia, inflammatory and immune modulation. Nevertheless, future validation is required to strengthen the role of detected genes in the effects of HK-1 in the TG.

In conclusion, our present findings support the importance of HK-1 in the inflammatory processes and nociceptive sensitisation underlying orofacial pain. We have also revealed that HK-1 participates in neuron-glia interactions both under physiological conditions and after inflammation. Although we provide evidence for expression changes at the mRNA level only which is an explicit limitation of the study, the concomitant behavioural alterations suggest that the protein products of the examined mRNAs were also affected. A limitation of our study is the lack of clear behavioural, functional data for the *Tac4*$^{-/-}$ phenotype in this model; therefore, the link and the precise mechanism between HK-1 and glial activation should be further investigated in other models of trigeminal sensitisation.

Chapter 4. Hemokinin-1 expression and effect on a mixed glial cell culture

Results

Tac4 transcripts were co-localised with Aif1 (Iba1), Gfap, Olig2-expressing cells of mouse MGCs

To investigate the basal level of *Tac4* mRNA expression in mouse MGCs, we performed fluorescent RNAscope *in situ* hybridization that provides cellular resolution. *Tac4* transcripts localized uniformly throughout the cell culture (Figure 24.).

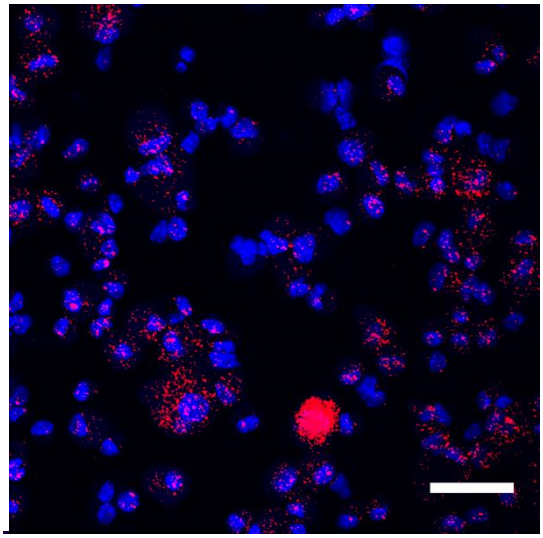

Figure 24. Representative confocal images of *Tac4* mRNA (red) counterstained with DAPI are presented on 3-week-old mixed glial cell culture derived from whole brains of 1-3-day-old mouse pups. Scale bar: 50 µm.

All glial cell types show *Tac4* transcripts, both in nucleus and cytoplasm, although it appears that co-expression is higher in oligodendrocytes and astrocytes than with microglia. Different glial cell types were identified based on *Aif1*, *Gfap*, *Olig2* (specific markers of microglia, astrocyte, oligodendrocyte, respectively) cell positivity (Figure 25.).

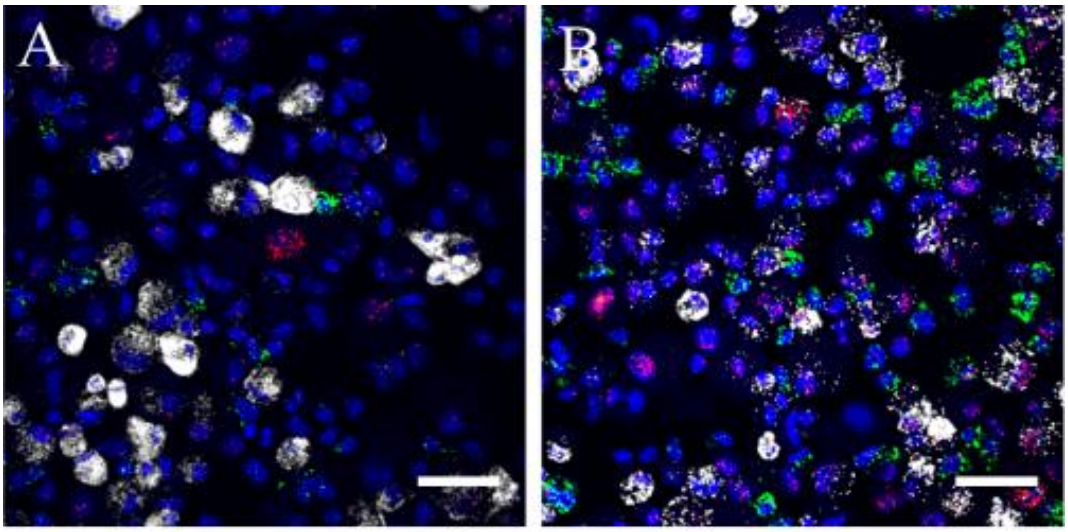

Figure 25. Representative confocal images of *Aif1/Tac4/Gfap (A)* and *Aif1/Tac4/Olig2 (B)* mRNA *(green, red, white, respectively)* counterstained with DAPI are presented on 3-week-old mixed glial cell culture from whole brains of 1-3-day-old mouse pups. Scale bar: 50 µm.

Hemokinin-1 treatment induced radioactive $^{45}Ca^{2+}$ uptake in mouse MGCs

Incubation of MGCs with HK-1 resulted in concentration-dependent radioactive $^{45}Ca^{2+}$ uptake. Whereas the 1 μM HK-1 could increase the $^{45}Ca^{2+}$ uptake in the cells compared to ECS, the 5 μM HK-1 treatment generated a significant influx (Figure 26.).

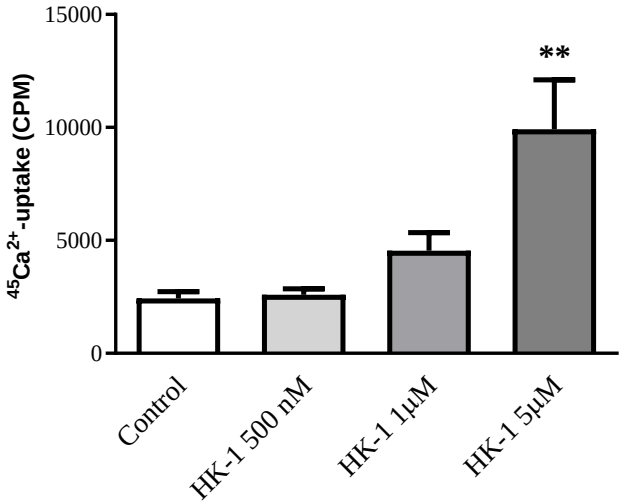

Figure 26. Effect of 500 nM, 1 and 5 μM hemokinin-1 (HK-1) on $^{45}Ca^{2+}$-uptake on mixed glial cell cultures. Data: means ± SEM; asterisks: significant differences between treated and ECS control groups (*p≤ 0.05, ** p≤0.01); one-way ANOVA followed by Tuckey's multiple comparison test. $^{45}Ca^{2+}$-isotope retention is given in Counts Per Minute (CPM).

Hemokinin-1 treatment increased the inflammatory cytokine production in mouse MGCs

Figure 27. shows changes of 5 inflammatory cytokines/chemokines concentrations: CCL5 (RANTES), CXCL1 (KC), interleukin 1 beta (IL-1β), interleukin 6 (IL-6), monocyte chemoattractant protein-1 (MCP-1/CCL2), tumor necrosis factor-alpha (TNFα) in interest, after 24-hour treatment of MGCs with mouse HK-1. IL-1β presented nondetectable levels (concentrations below 2.06 pg/mL) in supernatants of treated MGC samples. In the case of MCP-1 and TNFα, significant differences were seen in concentrations when MGSs were treated with 5 μM, but not lower HK-1 concentrations, compared with the control (ECS) treatment. Although different HK-1 treatments did not significantly affect RANTES, KC and IL-6 levels, the observed tendencies were similar to the previously mentioned cytokines.

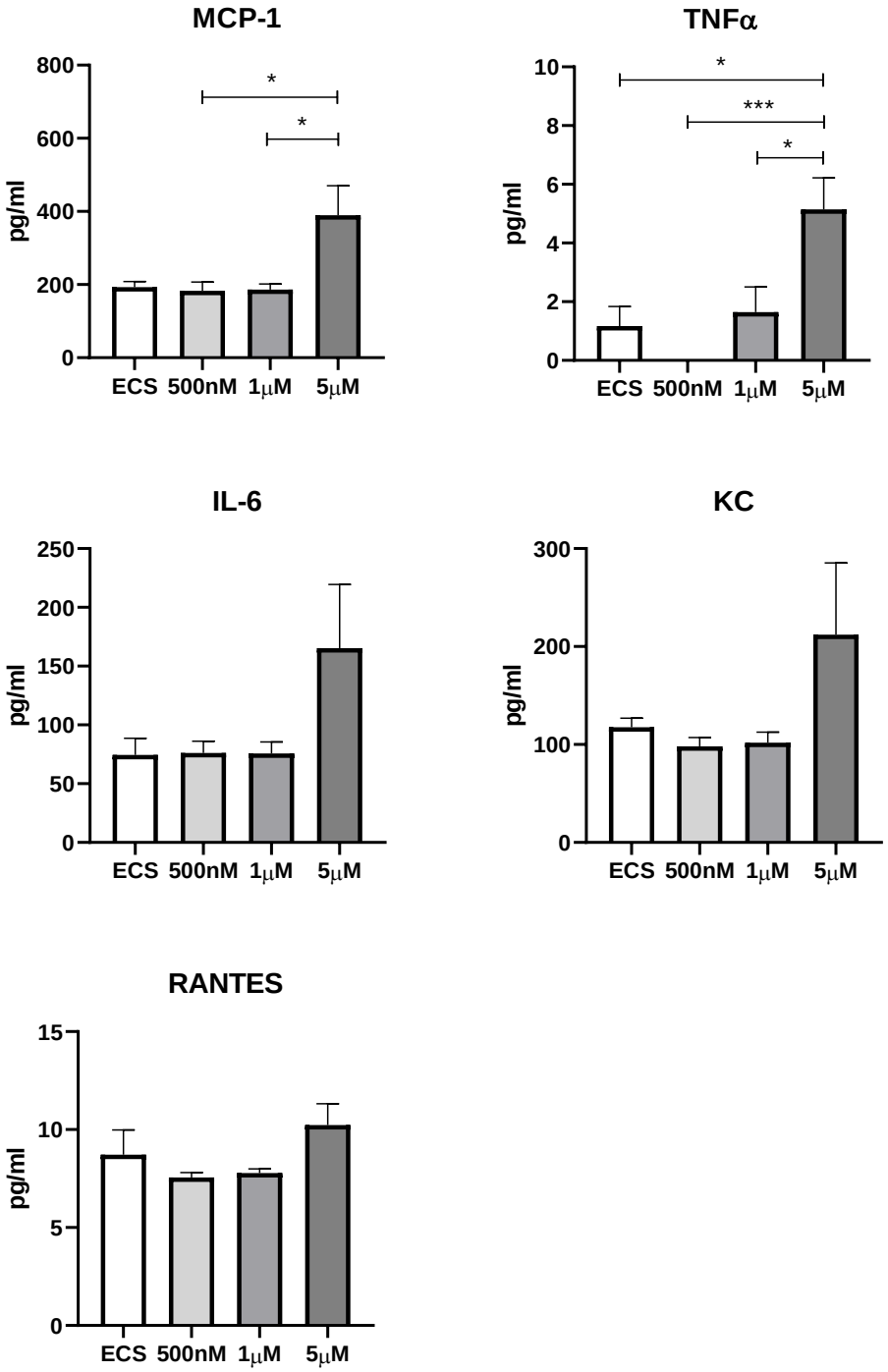

Figure 27. Effect of hemokinin-1 on cytokine expression of mixed glial cell cultures. Levels of CCL5 (RANTES), CXCL1 (KC), Interleukin 6 (IL-6), Monocyte chemoattractant protein-1 (MCP-1/CCL2), Tumor necrosis factor-alpha (TNFα) are shown in pg/ml. Data: means ± SEM; n=6 (from two separate MGC); asterisks: significant differences between treated and ECS control groups (*$p \leq 0.05$, ***$p \leq 0.001$); one-way ANOVA followed by Tukey's multiple comparison test.

Discussion

In the present chapter, we show the presence of *Tac4* mRNA in several glial cells derived from cerebral tissue. While it was previously proved that *Tac4 is* expressed in both peripheral and central nervous system tissues [129,134], ours is the first study to assess the expression of *Tac4* on mRNA level, including localization of the transcripts on a cellular level. Recently, an immunohistochemistry based study located HK-1 only in small and medium-size neurons in the TG [134]. We showed previously that *Tac4* mRNA was expressed by neurons and all types of glial cells of the TG. Besides, we demonstrated significant inflammation-related upregulation of *Tac4* occurs in both neurons and satellite glial cells. These data suggest a role of *Tac4* in glial cell function in the periphery, which is supplemented with its existence in glial cells derived from central nervous tissue. Our RT-qPCR methodology seemed to fail in the reliable detection of *Tac4* mRNA in TNC rodent tissues (very low values close to detection limit). Fortunately, the ISH technique can unmask signals on their transcript levels, adding localization as an essential value to the results.

HK-1 is a potent NK-1 receptor agonist [130]. Some of its effects, but not all, might be explained by NK-1-receptor activation. Even the first study describing cloning of the *Tac4* gene suggests a possible existence of a fourth tachykinin receptor [125]. Since then, several lines of evidence point to a different mechanism of action and even the possibility of a yet unknown target. According to our group's previous results, interestingly HK-1 (1 μM), but not SP, caused a slow and reproducible Ca^{2+} influx into the TG neurons obtained from both WT and $NK1^{-/-}$ mice [145], suggesting that HK-1 directly activates the primary sensory neurons via an NK1-independent, possibly an ion channel-coupled receptor mechanism. In our study, we showed a similar Ca^{2+} influx into the MGCs. However, a higher concentration HK-1 had to be used to achieve significant results, suggesting that neurons excluded from our setup might also have a role in this process, and HK-1 functions are more prominent in the periphery.

Various cytokines released from glial cells have been described in the literature [85,104,343,344]. We were interested in which are mainly involved in HK-1 induced responses. Although several studies focus on IL-1β expression, in our experiments, IL-1β presented at non-detectable levels. In the case of other inflammatory markers like MCP-1 and TNFα, a significant increase of RANTES, KC, IL-6 levels an increased tendency was seen when MGSs were treated with 5 μM HK-1. Therefore, we showed that these proinflammatory molecules are involved in HK-1 mediated signalling for the first time. Thus, our finding supports that glial cell activation is of great importance in the context of inflammatory progression. It should be

highlighted that results originate from cell cultures, where the lack of neuron and natural composition exists; thus, in vivo validation is necessary.

Chapter 3. is based on experiments performed by Angéla Kecskés, Anita Steib, Éva Szőke, Ágnes Kemény and Timea Aczél. Confocal images were taken by Balázs Gaszner (unpublished data).

Novelty and relevance of our findings

- We have described some up-and downregulated genes at the levels of the trigeminovascular system's primary and secondary sensory neurons that might play essential roles in peripheral and central sensitisation mechanisms.
- We are the first to present transcriptomic alterations in the PBMCs similar to the changes detected in the neuronal tissues. These results open new perspectives and initiate further investigations in the research of trigeminal pain disorders.
- These are the first data revealed from transcriptome analysis of PBMCs isolated from both ictal and interictal samples of migraineurs. Comparing these groups with healthy controls made possible the identification of both disease-specific and headache-specific alterations and revealed the importance of inflammatory pathways and the potential contribution of various cytokines to migraine susceptibility.
- Furthermore, our results suggest the possible implication of mitochondrial dysfunction, oxidative stress, cytokine and immune activity in migraine.
- We have confirmed the presence of *Tac4* mRNA in the trigeminal ganglion and established the upregulation of the gene after orofacial inflammation, this being the first study to assess the changes of *Tac4* expression under pathological conditions.
- We have shown *Tac4* mRNA expression and localization on the cellular level on sensory neurons and all types of glial cells of the trigeminal ganglion. Furthermore, significant inflammation-induced upregulation of *Tac4* was shown in both neurons and satellite glial cells. Our findings support the importance of HK-1 in the inflammatory processes and nociceptive sensitisation underlying orofacial pain.
- We have confirmed the presence of *Tac4* mRNA in several glial cells derived from cerebral tissue. Our work is the first to assess the expression of *Tac4* on mRNA level, including localization of the transcripts on the cellular level, in all glial cell types driven from central nervous tissue.
- We have shown that inflammatory molecules, mostly MCP-1 and TNFα and eventually RANTES, KC, IL-6, are involved in HK-1 mediated signalling.

Future perspectives

Migraine and orofacial pain disorders are specifically human and very complex diseases; therefore, it is impossible to model them precisely in animals. However, clinically relevant models of TVS activation are fundamental to reveal mechanisms related to the neuronal sensitisation pathways neuro-vascular-immune interactions and identify functional evidence for key mediators and targets in the brain.

In migraine research, reverse translation (from humans to animals) is necessary to prove the validity of the model and its clinical relevance. Forward translation (from animals to humans) is also crucial for the appropriate interpretation of the experimental findings on the disease. Such an approach has been planned to validate the functional importance of the several differentially expressed genes described in the thesis. The human migraine study is still in progress to increase the number of participants, to validate and expand results using an integrative transcriptomic and metabolomic approach.

Acknowledgements

First of all, I would like to thank my supervisor, Kata Bölcskei, for tutoring me through all these years. I am most grateful for the guidance, support, and knowledge that she shared with me and the friendship she showed towards me.

I want to express my deep gratitude to Prof. Erika Pintér, the leader of the Neuropharmacology doctoral program, for giving me the chance to be part of the Department of Pharmacology and Pharmacotherapy. I especially thank her for her ongoing support throughout the years.

I want to express my special thanks to Prof. Zsuzsanna Helyes for giving me the opportunity to work on her projects. Her enthusiasm, positive thinking and dedication to the research served as an example to follow.

I wish to express my gratitude to Prof. János Szolcsányi, the founder of this research group; I feel honoured to have known him.

I would like to also thank my roommates, ex-roommates, PhD fellows and all members of the Department of Pharmacology and Pharmacotherapy for creating a cheerful atmosphere, sharing their friendship, meanwhile constantly advising and helping me professionally through all these years.

Many thanks to our collaborators: colleagues from the Szentágothai Research Centre Bioinformatics Research Group who assured my work a professional statistical and analysis background and colleagues from the University of Szeged, who, with their expertise, made it possible to conduct the human migraine study successfully.

Finally, I cannot be grateful enough to my family for standing beside me and my husband for encouraging and supporting me all the time with his patience and love.

References

1. IASP Task Force on Taxonomy, edited by H. Merskey and N. Bogduk. Classification of Chronic Pain. Second Edition. Seattle: IASP Press; 1994.
2. Shephard MK, MacGregor EA, Zakrzewska JM. Orofacial Pain: A Guide for the Headache Physician. Headache J Head Face Pain. 2014;54: 22–39. doi:10.1111/head.12272
3. Lipton JA, Ship JA, Larach-Robinson D. Estimated prevalence and distribution of reported orofacial pain in the United States. J Am Dent Assoc 1939. 1993;124: 115–121. doi:10.14219/jada.archive.1993.0200
4. Macfarlane TV, Blinkhorn AS, Davies RM, Ryan P, Worthington HV, Macfarlane GJ. Orofacial pain: just another chronic pain? Results from a population-based survey. Pain. 2002;99: 453–458. doi:10.1016/s0304-3959(02)00181-1
5. Benoliel R, Birman N, Eliav E, Sharav Y. The International Classification of Headache Disorders: Accurate Diagnosis of Orofacial Pain? Cephalalgia. 2008;28: 752–762. doi:10.1111/j.1468-2982.2008.01586.x
6. Shueb SS, Nixdorf DR, John MT, Alonso BF, Durham J. What is the impact of acute and chronic orofacial pain on quality of life? J Dent. 2015;43: 1203–1210. doi:10.1016/j.jdent.2015.06.001
7. Hargreaves KM. Orofacial pain: Pain. 2011;152: S25–S32. doi:10.1016/j.pain.2010.12.024
8. Renton T, Durham J, Aggarwal VR. The classification and differential diagnosis of orofacial pain. Expert Rev Neurother. 2012;12: 569–576. doi:10.1586/ern.12.40
9. Shinoda M, Kubo A, Hayashi Y, Iwata K. Peripheral and Central Mechanisms of Persistent Orofacial Pain. Front Neurosci. 2019;13. doi:10.3389/fnins.2019.01227
10. Iwata K, Shinoda M. Role of neuron and non-neuronal cell communication in persistent orofacial pain. J Dent Anesth Pain Med. 2019;19: 77–82. doi:10.17245/jdapm.2019.19.2.77
11. Matsuka Y, Afroz S, Dalanon JC, Iwasa T, Waskitho A, Oshima M. The role of chemical transmitters in neuron-glia interaction and pain in sensory ganglion. Neurosci Biobehav Rev. 2020;108: 393–399. doi:10.1016/j.neubiorev.2019.11.019
12. Réus JC, Polmann H, Souza BDM, Flores-Mir C, Gonçalves DAG, de Queiroz LP, et al. Association between primary headaches and temporomandibular disorders: A systematic review and meta-analysis. J Am Dent Assoc 1939. 2021; S0002-8177(21)00479–7. doi:10.1016/j.adaj.2021.07.021
13. Romero-Reyes M, Uyanik JM. Orofacial pain management: current perspectives. J Pain Res. 2014;7: 99–115. doi:10.2147/JPR.S37593
14. Sharav Y, Katsarava Z, Charles A. Facial presentations of primary headache disorders. Cephalalgia. 2017;37: 714–719. doi:10.1177/0333102417705374
15. Bigal ME, Ashina S, Burstein R, Reed ML, Buse D, Serrano D, et al. Prevalence and characteristics of allodynia in headache sufferers: A population study. Neurology. 2008;70: 1525–1533. doi:10.1212/01.wnl.0000310645.31020.b1

16. Goadsby PJ, Holland PR, Martins-Oliveira M, Hoffmann J, Schankin C, Akerman S. Pathophysiology of Migraine: A Disorder of Sensory Processing. Physiol Rev. 2017;97: 553–622. doi:10.1152/physrev.00034.2015

17. Smitherman TA, Burch R, Sheikh H, Loder E. The prevalence, impact, and treatment of migraine and severe headaches in the United States: a review of statistics from national surveillance studies. Headache. 2013;53: 427–436. doi:10.1111/head.12074

18. Mulder E, Van Baal, C., Gaist, D., Kallela, M., Palotie, A. Genetic and Environmental Influences on Migraine: A Twin Study Across Six Countries. Twin Res. 2003;6(5), 422-431. doi:doi:10.1375/twin.6.5.422

19. Global Burden of Disease Study. Global, regional, and national incidence, prevalence, and years lived with disability for 328 diseases and injuries for 195 countries, 1990–2016: a systematic analysis for the Global Burden of Disease Study 2016. Lancet Lond Engl. 2017;390: 1211–1259. doi:10.1016/S0140-6736(17)32154-2

20. Katsarava Z, Mania M, Lampl C, Herberhold J, Steiner TJ. Poor medical care for people with migraine in Europe – evidence from the Eurolight study. J Headache Pain. 2018;19. doi:10.1186/s10194-018-0839-1

21. Steiner TJ, Stovner LJ, Vos T, Jensen R, Katsarava Z. Migraine is first cause of disability in under 50s: will health politicians now take notice? J Headache Pain. 2018;19. doi:10.1186/s10194-018-0846-2

22. Steiner TJ, Stovner LJ, Jensen R, Uluduz D, Katsarava Z, on behalf of Lifting The Burden: the Global Campaign against Headache. Migraine remains second among the world's causes of disability, and first among young women: findings from GBD2019. J Headache Pain. 2020;21: 137. doi:10.1186/s10194-020-01208-0

23. Buse DC, Loder EW, Gorman JA, Stewart WF, Reed ML, Fanning KM, et al. Sex Differences in the Prevalence, Symptoms, and Associated Features of Migraine, Probable Migraine and Other Severe Headache: Results of the American Migraine Prevalence and Prevention (AMPP) Study. Headache J Head Face Pain. 2013;53: 1278–1299. doi:10.1111/head.12150

24. Goadsby PJ. Pathophysiology of migraine. Ann Indian Acad Neurol. 2012;15: S15–S22. doi:10.4103/0972-2327.99993

25. Lipton RB, Bigal ME, Diamond M, Freitag F, Reed ML, Stewart WF, et al. Migraine prevalence, disease burden, and the need for preventive therapy. Neurology. 2007;68: 343–349. doi:10.1212/01.wnl.0000252808.97649.21

26. Olesen J, Burstein R, Ashina M, Tfelt-Hansen P. Origin of pain in migraine: evidence for peripheral sensitisation. Lancet Neurol. 2009;8: 679–690.

27. Weatherall MW. The diagnosis and treatment of chronic migraine. Ther Adv Chronic Dis. 2015;6: 115–123. doi:10.1177/2040622315579627

28. Evers S, Áfra J, Frese A, Goadsby PJ, Linde M, May A, et al. EFNS guideline on the drug treatment of migraine - revised report of an EFNS task force. Eur J Neurol. 2009;16: 968–981. doi:10.1111/j.1468-1331.2009.02748.x

29. Silberstein SD, Holland S, Freitag F, Dodick DW, Argoff C, Ashman E. Evidence-based guideline update: Pharmacologic treatment for episodic migraine prevention in adults: Report of the Quality Standards Subcommittee of the American Academy of Neurology and the American Headache Society. Neurology. 2012;78: 1337–1345. doi:10.1212/WNL.0b013e3182535d20

30. Tajti J, Majláth Z, Szok D, Csáti A, Vécsei L. Drug safety in acute migraine treatment. Expert Opin Drug Saf. 2015;14: 891–909. doi:10.1517/14740338.2015.1026325

31. Burch R. Antidepressants for Preventive Treatment of Migraine. Curr Treat Options Neurol. 2019;21: 18. doi:10.1007/s11940-019-0557-2

32. D'Amico D. Antiepileptic drugs in the prophylaxis of migraine, chronic headache forms and cluster headache: a review of their efficacy and tolerability. Neurol Sci. 2007;28: S188–S197. doi:10.1007/s10072-007-0775-3

33. Goadsby PJ, Lipton RB, Ferrari MD. Migraine — Current Understanding and Treatment. Wood AJJ, editor. N Engl J Med. 2002;346: 257–270. doi:10.1056/NEJMra010917

34. Moskowitz MA. Trigeminovascular System. Cephalalgia. 1992;12: 127–127. doi:10.1046/j.1468-2982.1992.1203127.x

35. Moskowitz MA. Neurogenic inflammation in the pathophysiology and treatment of migraine. Neurology. 1993;43: S16-20.

36. Tajti J, Párdutz á., Vámos E, Tuka B, Kuris A, Bohár Zs, et al. Migraine is a neuronal disease. J Neural Transm. 2011;118: 511–524. doi:10.1007/s00702-010-0515-3

37. L Kelman. The Triggers or Precipitants of the Acute Migraine Attack. Cephalalgia. 2007;27: 394–402. doi:10.1111/j.1468-2982.2007.01303.x

38. Martin VT, Behbehani MM. TOWARD A RATIONAL UNDERSTANDING OF MIGRAINE TRIGGER FACTORS. Med Clin North Am. 2001;85: 911–941. doi:10.1016/S0025-7125(05)70351-5

39. Sauro KM, Becker WJ. The stress and migraine interaction. Headache. 2009;49: 1378–1386. doi:10.1111/j.1526-4610.2009.01486.x

40. Buture A, Gooriah R, Nimeri R, Ahmed F. Current Understanding on Pain Mechanism in Migraine and Cluster Headache. Anesthesiol Pain Med. 2016;6: e35190. doi:10.5812/aapm.35190

41. Edvinsson L, Villalón CM, MaassenVanDenBrink A. Basic mechanisms of migraine and its acute treatment. Pharmacol Ther. 2012;136: 319–333. doi:10.1016/j.pharmthera.2012.08.011

42. Pietrobon D, Moskowitz MA. Pathophysiology of Migraine. Annu Rev Physiol. 2013;75: 365–391. doi:10.1146/annurev-physiol-030212-183717

43. Tepper SJ. History and Review of anti-Calcitonin Gene-Related Peptide (CGRP) Therapies: From Translational Research to Treatment. Headache. 2018;58 Suppl 3: 238–275. doi:10.1111/head.13379

44. Whyte CA, Tepper SJ. Adverse effects of medications commonly used in the treatment of migraine. Expert Rev Neurother. 2009;9: 1379–1391. doi:10.1586/ern.09.47

45. Barbanti P, Aurilia C, Egeo G, Fofi L. Future trends in drugs for migraine prophylaxis. Neurol Sci. 2012;33: 137–140. doi:10.1007/s10072-012-1058-1

46. de Vries T, Villalón CM, MaassenVanDenBrink A. Pharmacological treatment of migraine: CGRP and 5-HT beyond the triptans. Pharmacol Ther. 2020; 107528. doi:10.1016/j.pharmthera.2020.107528

47. Henson B, Hollingsworth H, Nevois E, Herndon C. Calcitonin Gene-Related Peptide (CGRP) Antagonists and Their Use in Migraines. J Pain Palliat Care Pharmacother. 2020;34: 22–31. doi:10.1080/15360288.2019.1690616

48. Ho TW, Ho AP, Ge Y (Joy), Assaid C, Gottwald R, MacGregor EA, et al. Randomized controlled trial of the CGRP receptor antagonist telcagepant for prevention of headache in women with perimenstrual migraine. Cephalalgia. 2016;36: 148–161. doi:10.1177/0333102415584308

49. Nelson DL, Phebus LA, Johnson KW, Wainscott DB, Cohen ML, Calligaro DO, et al. Preclinical pharmacological profile of the selective 5-HT $_{1F}$ receptor agonist lasmiditan. Cephalalgia. 2010;30: 1159–1169. doi:10.1177/0333102410370873

50. Reuter U, Israel H, Neeb L. The pharmacological profile and clinical prospects of the oral 5-HT1F receptor agonist lasmiditan in the acute treatment of migraine. Ther Adv Neurol Disord. 2015;8: 46–54. doi:10.1177/1756285614562419

51. Tso AR, Goadsby PJ. Anti-CGRP Monoclonal Antibodies: the Next Era of Migraine Prevention? Curr Treat Options Neurol. 2017;19: 27. doi:10.1007/s11940-017-0463-4

52. Ailani J, Lipton RB, Goadsby PJ, Guo H, Miceli R, Severt L, et al. Atogepant for the Preventive Treatment of Migraine. N Engl J Med. 2021;385: 695–706. doi:10.1056/NEJMoa2035908

53. Drugs@FDA: FDA-Approved Drugs. [cited 12 Feb 2022]. Available: https://www.accessdata.fda.gov/scripts/cder/daf/

54. EMA: Medicines. In: European Medicines Agency [Internet]. [cited 12 Feb 2022]. Available: https://www.ema.europa.eu/en/medicines

55. Fan W, Zhu X, He Y, Zhu M, Wu Z, Huang F, et al. The role of satellite glial cells in orofacial pain. J Neurosci Res. 2019;97: 393–401. doi:10.1002/jnr.24341

56. Goadsby PJ. The vascular theory of migraine—a great story wrecked by the facts. Brain. 2009;132: 6–7. doi:10.1093/brain/awn321

57. Dux M, Sántha P, Jancsó G. Capsaicin-sensitive neurogenic sensory vasodilatation in the dura mater of the rat. J Physiol. 2003;552: 859–867. doi:10.1113/jphysiol.2003.050633

58. Holland PR, Hoffmann J, Goadsby PJ. Neurobiological Basis of Migraine. In: Wood JN, editor. The Oxford Handbook of the Neurobiology of Pain. Oxford University Press; 2019. doi:10.1093/oxfordhb/9780190860509.013.27

59. Bolay H, Reuter U, Dunn AK, Huang Z, Boas DA, Moskowitz MA. Intrinsic brain activity triggers trigeminal meningeal afferents in a migraine model. Nat Med. 2002;8: 136. doi:10.1038/nm0202-136

60. Erdener SE, Dalkara T. Modelling headache and migraine and its pharmacological manipulation. Br J Pharmacol. 2014;171: 4575–4594. doi:10.1111/bph.12651

61. Bernstein C, Burstein R. Sensitization of the Trigeminovascular Pathway: Perspective and Implications to Migraine Pathophysiology. J Clin Neurol. 2012;8: 89. doi:10.3988/jcn.2012.8.2.89

62. Ahn AH, Basbaum AI. Where do triptans act in the treatment of migraine?: Pain. 2005;115: 1–4. doi:10.1016/j.pain.2005.03.008

63. Ahn AH, Basbaum AI. Tissue Injury Regulates Serotonin 1D Receptor Expression: Implications for the Control of Migraine and Inflammatory Pain. J Neurosci. 2006;26: 8332–8338. doi:10.1523/JNEUROSCI.1989-06.2006

64. Messlinger K, Balcziak LK, Russo AF. Cross-talk signaling in the trigeminal ganglion: role of neuropeptides and other mediators. J Neural Transm. 2020 [cited 2 Mar 2020]. doi:10.1007/s00702-020-02161-7

65. Lopes DM, Denk F, McMahon SB. The Molecular Fingerprint of Dorsal Root and Trigeminal Ganglion Neurons. Front Mol Neurosci. 2017;10. doi:10.3389/fnmol.2017.00304

66. Viana F. Chemosensory Properties of the Trigeminal System. ACS Chem Neurosci. 2010;2: 38–50. doi:10.1021/cn100102c

67. Durham PL, Garrett FG. Development of functional units within trigeminal ganglia correlates with increased expression of proteins involved in neuron–glia interactions. Neuron Glia Biol. 2010;6: 171–181. doi:10.1017/S1740925X10000232

68. Lee Y, Kawai Y, Shiosaka S, Takami K, Kiyama H, Hillyard CJ, et al. Coexistence of calcitonin gene-related peptide and substance P-like peptide in single cells of the trigeminal ganglion of the rat: immunohistochemical analysis. Brain Res. 1985;330: 194–196. doi:10.1016/0006-8993(85)90027-7

69. Ma Q-P, Hill R, Sirinathsinghji D. Colocalization of CGRP with 5-HT1B/1D receptors and substance P in trigeminal ganglion neurons in rats. Eur J Neurosci. 2001;13: 2099–2104. doi:10.1046/j.0953-816x.2001.01586.x

70. Schueler M, Neuhuber WL, De Col R, Messlinger K. Innervation of Rat and Human Dura Mater and Pericranial Tissues in the Parieto-Temporal Region by Meningeal Afferents. Headache J Head Face Pain. 2014;54: 996–1009. doi:10.1111/head.12371

71. Fernandes ES, Schmidhuber SM, Brain SD. Sensory-nerve-derived neuropeptides: possible therapeutic targets. Handb Exp Pharmacol. 2009; 393–416. doi:10.1007/978-3-540-79090-7_11

72. Seybold VS. The role of peptides in central sensitization. Handb Exp Pharmacol. 2009; 451–491. doi:10.1007/978-3-540-79090-7_13

73. Cady RJ, Glenn JR, Smith KM, Durham PL. Calcitonin gene-related peptide promotes cellular changes in trigeminal neurons and glia implicated in peripheral and central sensitization. Mol Pain. 2011;7: 94. doi:10.1186/1744-8069-7-94

74. Tajti J, Uddman R, Edvinsson L. Neuropeptide localization in the “migraine generator” region of the human brainstem. Cephalalgia Int J Headache. 2001;21: 96–101. doi:10.1046/j.1468-2982.2001.00140.x

75. Lee J, Saloman JL, Weiland G, Auh Q-S, Chung M-K, Ro JY. Functional interactions between NMDA receptors and TRPV1 in trigeminal sensory neurons mediate mechanical hyperalgesia in the rat masseter muscle: Pain. 2012;153: 1514–1524. doi:10.1016/j.pain.2012.04.015

76. Mickle AD, Shepherd AJ, Mohapatra DP. Sensory TRP Channels: The Key Transducers of Nociception and Pain. Prog Mol Biol Transl Sci. 2015;131: 73–118. doi:10.1016/bs.pmbts.2015.01.002

77. Dux M, Sántha P, Jancsó G. The role of chemosensitive afferent nerves and TRP ion channels in the pathomechanism of headaches. Pflüg Arch - Eur J Physiol. 2012;464: 239–248. doi:10.1007/s00424-012-1142-7

78. Dux M, Rosta J, Messlinger K. TRP Channels in the Focus of Trigeminal Nociceptor Sensitization Contributing to Primary Headaches. Int J Mol Sci. 2020;21: 342. doi:10.3390/ijms21010342

79. Iannone LF, De Logu F, Geppetti P, De Cesaris F. The role of TRP ion channels in migraine and headache. Neurosci Lett. 2022;768: 136380. doi:10.1016/j.neulet.2021.136380

80. Shinoda M, Ozaki N, Sugiura Y. Involvement of ATP and its receptors on nociception in rat model of masseter muscle pain: Pain. 2008;134: 148–157. doi:10.1016/j.pain.2007.04.006

81. Woolf CJ. Central sensitization: Implications for the diagnosis and treatment of pain: Pain. 2011;152: S2–S15. doi:10.1016/j.pain.2010.09.030

82. Hanani M. Satellite glial cells in sensory ganglia: from form to function. Brain Res Rev. 2005;48: 457–476. doi:10.1016/j.brainresrev.2004.09.001

83. Su M, Yu S. Chronic migraine: A process of dysmodulation and sensitization. Mol Pain. 2018;14: 174480691876769. doi:10.1177/1744806918767697

84. Li T, Chen X, Zhang C, Zhang Y, Yao W. An update on reactive astrocytes in chronic pain. J Neuroinflammation. 2019;16. doi:10.1186/s12974-019-1524-2

85. Ohara PT, Vit J-P, Bhargava A, Romero M, Sundberg C, Charles AC, et al. Gliopathic Pain: When Satellite Glial Cells Go Bad. Neurosci Rev J Bringing Neurobiol Neurol Psychiatry. 2009;15: 450–463. doi:10.1177/1073858409336094

86. Ren K, Dubner R. Interactions between the immune and nervous systems in pain. Nat Med. 2010;16: 1267–1276. doi:10.1038/nm.2234

87. Ren K, Dubner R. Activity-triggered tetrapartite neuron-glial interactions following peripheral injury. Curr Opin Pharmacol. 2016;26: 16–25. doi:10.1016/j.coph.2015.09.006

88. Robinson RR, Dietz AK, Maroof AM, Asmis R, Forsthuber TG. The role of glial–neuronal metabolic cooperation in modulating progression of multiple sclerosis and neuropathic pain. Immunotherapy. 2019;11: 129–147. doi:10.2217/imt-2018-0153

89. Aczél T, Körtési T, Kun J, Urbán P, Bauer W, Herczeg R, et al. Identification of disease- and headache-specific mediators and pathways in migraine using blood transcriptomic and metabolomic analysis. J Headache Pain. 2021;22: 117. doi:10.1186/s10194-021-01285-9

90. Damodaram S, Thalakoti S, Freeman SE, Garrett FG, Durham PL. Tonabersat Inhibits Trigeminal Ganglion Neuronal-Satellite Glial Cell Signaling. Headache J Head Face Pain. 2009;49: 5–20. doi:10.1111/j.1526-4610.2008.01262.x

91. Paramel Mohan S, Ramalingam M. Neuroscience of Peripheral Nerve Regeneration. J Pharm Bioallied Sci. 2021;13: S913–S916. doi:10.4103/jpbs.jpbs_182_21

92. Liu H, Zhao L, Gu W, Liu Q, Gao Z, Zhu X, et al. Activation of satellite glial cells in trigeminal ganglion following dental injury and inflammation. J Mol Histol. 2018;49: 257–263. doi:10.1007/s10735-018-9765-4

93. Villa G, Ceruti S, Zanardelli M, Magni G, Jasmin L, Ohara PT, et al. Temporomandibular joint inflammation activates glial and immune cells in both the trigeminal ganglia and in the spinal trigeminal nucleus. Mol Pain. 2010;6: 89. doi:10.1186/1744-8069-6-89

94. Takeda M, Tanimoto T, Kadoi J, Nasu M, Takahashi M, Kitagawa J, et al. Enhanced excitability of nociceptive trigeminal ganglion neurons by satellite glial cytokine following peripheral inflammation. Pain. 2007;129: 155–166. doi:10.1016/j.pain.2006.10.007

95. Donegan M, Kernisant M, Cua C, Jasmin L, Ohara PT. Satellite Glial Cell Proliferation in the Trigeminal Ganglia After Chronic Constriction Injury of the Infraorbital Nerve. Glia. 2013;61: 2000–2008. doi:10.1002/glia.22571

96. Liu Q, Liu C, Jiang L, Li M, Long T, He W, et al. α7 Nicotinic acetylcholine receptor-mediated anti-inflammatory effect in a chronic migraine rat model via the attenuation of glial cell activation. J Pain Res. 2018;11: 1129–1140. doi:10.2147/JPR.S159146

97. Ceruti S, Villa G, Fumagalli M, Colombo L, Magni G, Zanardelli M, et al. Calcitonin Gene-Related Peptide-Mediated Enhancement of Purinergic Neuron/Glia Communication by the Algogenic Factor Bradykinin in Mouse Trigeminal Ganglia from Wild-Type and R192Q Cav2.1 Knock-In Mice: Implications for Basic Mechanisms of Migraine Pain. J Neurosci. 2011;31: 3638–3649. doi:10.1523/JNEUROSCI.6440-10.2011

98. Zhang Y, Song N, Liu F, Lin J, Liu M, Huang C, et al. Activation of mitogen-activated protein kinases in satellite glial cells of the trigeminal ganglion contributes to substance P-mediated inflammatory pain. Int J Oral Sci. 2019;11. doi:10.1038/s41368-019-0055-0

99. Kushnir R, Cherkas PS, Hanani M. Peripheral inflammation upregulates P2X receptor expression in satellite glial cells of mouse trigeminal ganglia: A calcium imaging study. Neuropharmacology. 2011;61: 739–746. doi:10.1016/j.neuropharm.2011.05.019

100. Afroz S, Arakaki R, Iwasa T, Oshima M, Hosoki M, Inoue M, et al. CGRP Induces Differential Regulation of Cytokines from Satellite Glial Cells in Trigeminal Ganglia and Orofacial Nociception. Int J Mol Sci. 2019;20. doi:10.3390/ijms20030711

101. Messlinger K, Russo A. Current understanding of trigeminal ganglion structure and function in headache. Cephalalgia Int J Headache. 2018. doi:10.1177/0333102418786261

102. Lynch MA. The Multifaceted Profile of Activated Microglia. Mol Neurobiol. 2009;40: 139–156. doi:10.1007/s12035-009-8077-9

103. Carniglia L, Ramírez D, Durand D, Saba J, Turati J, Caruso C, et al. Neuropeptides and Microglial Activation in Inflammation, Pain, and Neurodegenerative Diseases. Mediators Inflamm. 2017;2017. doi:10.1155/2017/5048616

104. Berta T, Qadri YJ, Chen G, Ji RR. Microglial Signaling in Chronic Pain with a Special Focus on Caspase 6, p38 MAP Kinase, and Sex Dependence. J Dent Res. 2016;95: 1124–1131. doi:10.1177/0022034516653604

105. Franceschini A, Vilotti S, Ferrari MD, van den Maagdenberg AMJM, Nistri A, Fabbretti E. TNFα Levels and Macrophages Expression Reflect an Inflammatory Potential of Trigeminal Ganglia in a Mouse Model of Familial Hemiplegic Migraine. PLoS ONE. 2013;8. doi:10.1371/journal.pone.0052394

106. Franceschini A, Nair A, Bele T, Maagdenberg AM, Nistri A, Fabbretti E. Functional crosstalk in culture between macrophages and trigeminal sensory neurons of a mouse genetic model of migraine. BMC Neurosci. 2012;13: 143. doi:10.1186/1471-2202-13-143

107. Fischer M, Wille G, Klien S, Shanib H, Holle D, Gaul C, et al. Brain-derived neurotrophic factor in primary headaches. J Headache Pain. 2012;13: 469–475. doi:10.1007/s10194-012-0454-5

108. Burmeister AR, Johnson MB, Chauhan VS, Moerdyk-Schauwecker MJ, Young AD, Cooley ID, et al. Human microglia and astrocytes constitutively express the neurokinin-1 receptor and functionally respond to substance P. J Neuroinflammation. 2017;14. doi:10.1186/s12974-017-1012-5

109. Brain SD, Cox HM. Neuropeptides and their receptors: innovative science providing novel therapeutic targets. Br J Pharmacol. 2006;147 Suppl 1: S202-211. doi:10.1038/sj.bjp.0706461

110. Garcia-Recio S, Gascón P. Biological and Pharmacological Aspects of the NK1-Receptor. Rapoport BL, editor. BioMed Res Int. 2015;2015: 495704. doi:10.1155/2015/495704

111. Muñoz M, Coveñas R. Involvement of substance P and the NK-1 receptor in human pathology. Amino Acids. 2014;46: 1727–1750. doi:10.1007/s00726-014-1736-9

112. Rupniak N, Carlson E, Boyce S, Webb J, Hill R. Enantioselective inhibition of the formalin paw late phase by the NK1 receptor antagonist L-733,060 in gerbils. Pain. 1996;67: 189–195. doi:10.1016/0304-3959(96)03109-0

113. Jang JH, Nam TS, Paik KS, Leem JW. Involvement of peripherally released substance P and calcitonin gene-related peptide in mediating mechanical hyperalgesia in a traumatic neuropathy model of the rat. Neurosci Lett. 2004;360: 129–132. doi:10.1016/j.neulet.2004.02.043

114. Edvinsson JC, Reducha PV, Sheykhzade M, Warfvinge K, Haanes KA, Edvinsson L. Neurokinins and their receptors in the rat trigeminal system: Differential localization and release with implications for migraine pain. Mol Pain. 2021;17: 17448069211059400. doi:10.1177/17448069211059400

115. Teodoro FC, Tronco Júnior MF, Zampronio AR, Martini AC, Rae GA, Chichorro JG. Peripheral substance P and neurokinin-1 receptors have a role in inflammatory and neuropathic orofacial pain models. Neuropeptides. 2013;47: 199–206. doi:10.1016/j.npep.2012.10.005

116. King KA, Hu C, Rodriguez MM, Romaguera R, Jiang X, Piedimonte G. Exaggerated Neurogenic Inflammation and Substance P Receptor Upregulation in RSV-Infected Weanling Rats. Am J Respir Cell Mol Biol. 2001;24: 101–107. doi:10.1165/ajrcmb.24.2.4264

117. Rittner HL, Lux C, Labuz D, Mousa SA, Schäfer M, Stein C, et al. Neurokinin-1 Receptor Antagonists Inhibit the Recruitment of Opioid-containing Leukocytes and Impair Peripheral Antinociception. Anesthesiol J Am Soc Anesthesiol. 2007;107: 1009–1017. doi:10.1097/01.anes.0000291454.90754.de

118. Connor HE CH. Clinical evaluation of a novel, potent, CNS penetrating NK-1 receptor antagonist in the acute treatment of migraine. Cephalalgia. 1998;18: 392.

119. Diener H-C. Rpr100893, A Substance-P Antagonist, is Not Effective in the Treatment of Migraine Attacks. Cephalalgia. 2003;23: 183–185. doi:10.1046/j.1468-2982.2003.00496.x

120. Norman B. A placebo-controlled, in-clinic study to explore the preliminary safety and efficacy of intravenous L-758,298 (a prodrug of the NK-1 receptor antagonist L-754,030) in the acute treatment of migraine. Cephalalgia. 1998;18: 407.

121. Reinhardt R. Comparison of neurokinin-1 antagonist, L-745,030, to placebo, acetaminophen and ibuprofen in the dental pain model. Clin Pharmacol Ther. 1998;63: 168.

122. Goldstein D, Wang O, Gitter B, Iyengar S. Dose-Response Study of the Analgesic Effect of Lanepitant in Patients with Painful Diabetic Neuropathy. Clin Neuropharmacol. 2001;24: 16–22.

123. Borsook D, Upadhyay J, Klimas M, Schwarz AJ, Coimbra A, Baumgartner R, et al. Decision-making using fMRI in clinical drug development: revisiting NK-1 receptor antagonists for pain. Drug Discov Today. 2012;17: 964–973. doi:10.1016/j.drudis.2012.05.004

124. Herbert MK, Holzer P. Warum versagen Substanz P (NK1)-Rezeptorantagonisten in der Schmerztherapie? Anaesthesist. 2002;51: 308–319. doi:10.1007/s00101-002-0296-7

125. Zhang Y, Lu L, Furlonger C, Wu GE, Paige CJ. Hemokinin is a hematopoietic-specific tachykinin that regulates B lymphopoiesis. Nat Immunol. 2000;1: 392–397. doi:10.1038/80826

126. Dai L, Perera DS, King DW, Southwell BR, Burcher E, Liu L. Hemokinin-1 Stimulates Prostaglandin E $_2$ Production in Human Colon through Activation of Cyclooxygenase-2 and Inhibition of 15-Hydroxyprostaglandin Dehydrogenase. J Pharmacol Exp Ther. 2012;340: 27–36. doi:10.1124/jpet.111.186155

127. Metwali A, Blum AM, Elliott DE, Setiawan T, Weinstock JV. Cutting Edge: Hemokinin Has Substance P-Like Function and Expression in Inflammation. J Immunol. 2004;172: 6528–6532. doi:10.4049/jimmunol.172.11.6528

128. Nelson DA, Marriott I, Bost KL. Expression of hemokinin 1 mRNA by murine dendritic cells. J Neuroimmunol. 2004;155: 94–102. doi:10.1016/j.jneuroim.2004.06.005

129. Duffy RA, Hedrick JA, Randolph G, Morgan CA, Cohen-Williams ME, Vassileva G, et al. Centrally administered hemokinin-1 (HK-1), a neurokinin NK1 receptor agonist, produces substance P-like behavioral effects in mice and gerbils. Neuropharmacology. 2003;45: 242–250. doi:10.1016/S0028-3908(03)00150-3

130. Morteau, O., Lu, B., Gerard, C., Gerard, N.P. Hemokinin 1 is a full agonist at the substance P receptor. Nat Immunol. 2001;2: 1088.

131. Borbély É, Helyes Z. Role of hemokinin-1 in health and disease. Neuropeptides. 2017;64: 9–17. doi:10.1016/j.npep.2016.12.003

132. Page NM. Hemokinins and endokinins. Cell Mol Life Sci. 2004;61. doi:10.1007/s00018-004-4035-x

133. Jin L, Jin B, Song C, Zhang Y. Murine Monoclonal Antibodies Generated Against Mouse/Rat Hemokinin-1. Hybridoma. 2009;28: 259–267. doi:10.1089/hyb.2009.0009

134. Igawa K, Funahashi H, Miyahara Y, Naono-Nakayama R, Matsuo H, Yamashita Y, et al. Distribution of hemokinin-1 in the rat trigeminal ganglion and trigeminal sensory nuclear complex. Arch Oral Biol. 2017;79: 62–69. doi:10.1016/j.archoralbio.2017.03.004

135. Borbély É, Hajna Z, Nabi L, Scheich B, Tékus V, László K, et al. Hemokinin-1 mediates anxiolytic and anti-depressant-like actions in mice. Brain Behav Immun. 2017;59: 219–232. doi:10.1016/j.bbi.2016.09.004

136. Endo D, Ikeda T, Ishida Y, Yoshioka D, Nishimori T. Effect of intrathecal administration of hemokinin-1 on the withdrawal response to noxious thermal stimulation of the rat hind paw. Neurosci Lett. 2006;392: 114–117. doi:10.1016/j.neulet.2005.09.005

137. Hajna Z, Borbély É, Kemény Á, Botz B, Kereskai L, Szolcsányi J, et al. Hemokinin-1 is an important mediator of endotoxin-induced acute airway inflammation in the mouse. Peptides. 2015;64: 1–7. doi:10.1016/j.peptides.2014.12.002

138. Hunyady Á, Hajna Z, Gubányi T, Scheich B, Kemény Á, Gaszner B, et al. Hemokinin-1 is an important mediator of pain in mouse models of neuropathic and inflammatory mechanisms. Brain Res Bull. 2019;147: 165–173. doi:10.1016/j.brainresbull.2019.01.015

139. Watanabe C, Mizoguchi H, Bagetta G, Sakurada S. Involvement of spinal glutamate in nociceptive behavior induced by intrathecal administration of hemokinin-1 in mice. Neurosci Lett. 2016;617: 236–239. doi:10.1016/j.neulet.2016.02.027

140. Fu C-Y, Xia R-L, Zhang T-F, Lu Y, Zhang S-F, Yu Z-Q, et al. Hemokinin-1(4-11)-Induced Analgesia Selectively Up-Regulates δ-Opioid Receptor Expression in Mice. Price TJ, editor. PLoS ONE. 2014;9: e90446. doi:10.1371/journal.pone.0090446

141. Fu CY, Zhao YL, Dong L, Chen Q, Ni JM, Wang R. In vivo characterization of the effects of human hemokinin-1 and human hemokinin-1(4-11), mammalian tachykinin peptides, on the modulation of pain in mice. Brain Behav Immun. 2008;22: 850–860. doi:10.1016/j.bbi.2007.12.010

142. Xia R-L, Fu C-Y, Zhang S-F, Jin Y-T, Zhao F-K. Study on the distribution sites and the molecular mechanism of analgesia after intracerebroventricular injection of rat/mouse hemokinin-1 in mice. Peptides. 2013;43: 113–120. doi:10.1016/j.peptides.2013.02.020

143. Sakai A, Takasu K, Sawada M, Suzuki H. Hemokinin-1 Gene Expression Is Upregulated in Microglia Activated by Lipopolysaccharide through NF-κB and p38 MAPK Signaling Pathways. Rameshwar P, editor. PLoS ONE. 2012;7: e32268. doi:10.1371/journal.pone.0032268

144. Ando, Y. Expression of hemokinin-1 in rat spinal cord after peripheral inflammation. Kokubyo Gakkai Zasshi. 2009;76: 81-90.

145. Borbély É, Hunyady Á, Pohóczky K, Payrits M, Botz B, Mócsai A, et al. Hemokinin-1 as a Mediator of Arthritis-Related Pain via Direct Activation of Primary Sensory Neurons. Front Pharmacol. 2020;11: 594479. doi:10.3389/fphar.2020.594479

146. Gerring ZF, Powell JE, Montgomery GW, Nyholt DR. Genome-wide analysis of blood gene expression in migraine implicates immune-inflammatory pathways. Cephalalgia Int J Headache. 2017; 333102416686769. doi:10.1177/0333102416686769

147. Perry C, Blake P, Buettner C, Papavassiliou E, Schain A, Bhasin M, et al. Upregulation of inflammatory gene transcripts in periosteum of chronic migraineurs: implications to extracranial origin of headache. Ann Neurol. 2016;79: 1000–1013. doi:10.1002/ana.24665

148. Burstein R, Yarnitsky D, Goor-Aryeh I, Ransil BJ, Bajwa ZH. An association between migraine and cutaneous allodynia. Ann Neurol. 2000;47: 614–624.

149. Sandrini G, Cecchini AP, Milanov I, Tassorelli C, Buzzi MG, Nappi G. Electrophysiological evidence for trigeminal neuron sensitization in patients with migraine. Neurosci Lett. 2002;317: 135–138.

150. Burstein R, Yamamura H, Malick A, Strassman AM. Chemical Stimulation of the Intracranial Dura Induces Enhanced Responses to Facial Stimulation in Brain Stem Trigeminal Neurons. J Neurophysiol. 1998;79: 964–982.

151. Levy D, Jakubowski M, Burstein R. Disruption of communication between peripheral and central trigeminovascular neurons mediates the antimigraine action of 5HT1B/1D receptor agonists. Proc Natl Acad Sci. 2004;101: 4274–4279.

152. Kunkler PE, Ballard CJ, Oxford GS, Hurley JH. TRPA1 receptors mediate environmental irritant-induced meningeal vasodilatation: Pain. 2011;152: 38–44. doi:10.1016/j.pain.2010.08.021

153. Filipović B, Matak I, Bach-Rojecky L, Lacković Z. Central Action of Peripherally Applied Botulinum Toxin Type A on Pain and Dural Protein Extravasation in Rat Model of Trigeminal Neuropathy. Premkumar LS, editor. PLoS ONE. 2012;7: e29803. doi:10.1371/journal.pone.0029803

154. Burstein R. Deconstructing migraine headache into peripheral and central sensitization. Pain. 2001;89: 107–110.

155. Landy S, Rice K, Lobo B. Central sensitisation and cutaneous allodynia in migraine: implications for treatment. CNS Drugs. 2004;18: 337–342.

156. Bigal ME, Ashina S, Burstein R, Reed ML, Buse D, Serrano D, et al. Prevalence and characteristics of allodynia in headache sufferers: A population study. Neurology. 2008;70: 1525–1533. doi:10.1212/01.wnl.0000310645.31020.b1

157. Tajti J, Szok D, Majláth Z, Tuka B, Csáti A, Vécsei L. Migraine and neuropeptides. Neuropeptides. 2015;52: 19–30. doi:10.1016/j.npep.2015.03.006

158. Greco R, Demartini C, De Icco R, Martinelli D, Putortì A, Tassorelli C. Migraine neuroscience: from experimental models to target therapy. Neurol Sci. 2020;41: 351–361. doi:10.1007/s10072-020-04808-5

159. Harriott AM, Strother LC, Vila-Pueyo M, Holland PR. Animal models of migraine and experimental techniques used to examine trigeminal sensory processing. J Headache Pain. 2019;20: 91. doi:10.1186/s10194-019-1043-7

160. Romero-Reyes M, Akerman S. Update on Animal Models of Migraine. Curr Pain Headache Rep. 2014;18. doi:10.1007/s11916-014-0462-z

161. Ren K, Dubner R. Inflammatory Models of Pain and Hyperalgesia. ILAR J. 1999;40: 111–118.

162. Krzyzanowska A, Avendaño C. Behavioral testing in rodent models of orofacial neuropathic and inflammatory pain. Brain Behav. 2012;2: 678–697. doi:10.1002/brb3.85

163. Gregory NS, Harris AL, Robinson CR, Dougherty PM, Fuchs PN, Sluka KA. An overview of animal models of pain: disease models and outcome measures. J Pain. 2013;14: 1255–1269. doi:10.1016/j.jpain.2013.06.008

164. Martinez-Garcia M, Miguelanez-Medran B, Goicoechea C. Animal models in the study and treatment of orofacial pain. J Clin Exp Dent. 2019; 0–0. doi:10.4317/jced.55429

165. Perrino C, Barabási A-L, Condorelli G, Davidson SM, De Windt L, Dimmeler S, et al. Epigenomic and transcriptomic approaches in the post-genomic era: path to novel targets for diagnosis and therapy of the ischaemic heart? Position Paper of the European Society of Cardiology Working Group on Cellular Biology of the Heart. Cardiovasc Res. 2017;113: 725–736. doi:10.1093/cvr/cvx070

166. Okumura M, Iwata K, Yasuda K, Inoue K, Shinoda M, Honda K, et al. Alternation of Gene Expression in Trigeminal Ganglion Neurons Following Complete Freund's Adjuvant or Capsaicin Injection into the Rat Face. J Mol Neurosci. 2010;42: 200–209. doi:10.1007/s12031-010-9348-7

167. Chung M-K, Park J, Asgar J, Ro JY. Transcriptome analysis of trigeminal ganglia following masseter muscle inflammation in rats. Mol Pain. 2016;12: 1. doi:10.1177/1744806916668526

168. Rollins B, Martin MV, Morgan L, Vawter MP. Analysis of whole genome biomarker expression in blood and brain. Am J Med Genet B Neuropsychiatr Genet. 2010;153B: 919–936. doi:10.1002/ajmg.b.31062

169. Sullivan PF, Fan C, Perou CM. Evaluating the comparability of gene expression in blood and brain. Am J Med Genet B Neuropsychiatr Genet. 2006;141B: 261–268. doi:10.1002/ajmg.b.30272

170. Mosallaei M, Ehtesham N, Rahimirad S, Saghi M, Vatandoost N, Khosravi S. PBMCs: a new source of diagnostic and prognostic biomarkers. Arch Physiol Biochem. 2020;0: 1–7. doi:10.1080/13813455.2020.1752257

171. Berger A, Benveniste P, Corfe SA, Tran AH, Barbara M, Wakeham A, et al. Targeted deletion of the tachykinin 4 gene (TAC4−/−) influences the early stages of B lymphocyte development. Blood. 2010;116: 3792–3801. doi:10.1182/blood-2010-06-291062

172. Edgar R, Domrachev M, Lash AE. Gene Expression Omnibus: NCBI gene expression and hybridization array data repository. Nucleic Acids Res. 2002;30: 207–210.

173. Hofmann M, Kordás KS, Gravius A, Bölcskei K, Parsons CG, Dekundy A, et al. Assessment of the effects of NS11394 and L-838417, α2/3 subunit-selective GABAA receptor-positive allosteric modulators, in tests for pain, anxiety, memory and motor function. Behav Pharmacol. 2012;23: 790–801. doi:10.1097/FBP.0b013e32835a7c7e

174. Sághy É, Payrits M, Bíró-Sütő T, Skoda-Földes R, Szánti-Pintér E, Erostyák J, et al. Carboxamido steroids inhibit the opening properties of transient receptor potential ion channels by lipid raft modulation. J Lipid Res. 2018;59: 1851–1863. doi:10.1194/jlr.M084723

175. Headache Classification Committee of the International Headache Society (IHS) The International Classification of Headache Disorders, 3rd edition. Cephalalgia. 2018;38: 1–211. doi:10.1177/0333102417738202

176. Gentleman RC, Carey VJ, Bates DM, Bolstad B, Dettling M, Dudoit S, et al. Bioconductor: open software development for computational biology and bioinformatics. Genome Biol. 2004;5: R80. doi:10.1186/gb-2004-5-10-r80

177. R Development Core Team. R: A Language and Environment for Statistical Computing. Vienna, Austria: R Foundation for Statistical Computing; 2008. Available: http://www.R-project.org

178. Ritchie ME, Phipson B, Wu D, Hu Y, Law CW, Shi W, et al. limma powers differential expression analyses for RNA-sequencing and microarray studies. Nucleic Acids Res. 2015;43: e47. doi:10.1093/nar/gkv007

179. Ashburner M, Ball CA, Blake JA, Botstein D, Butler H, Cherry JM, et al. Gene ontology: tool for the unification of biology. The Gene Ontology Consortium. Nat Genet. 2000;25: 25–29. doi:10.1038/75556

180. Kanehisa M, Goto S. KEGG: kyoto encyclopedia of genes and genomes. Nucleic Acids Res. 2000;28: 27–30.

181. Fabregat A, Jupe S, Matthews L, Sidiropoulos K, Gillespie M, Garapati P, et al. The Reactome Pathway Knowledgebase. Nucleic Acids Res. 2018;46: D649–D655. doi:10.1093/nar/gkx1132

182. Alexa A, Rahnenführer J. topGO: Enrichment Analysis for Gene Ontology. R package version 2.30.0. 2016.

183. Luo W, Friedman MS, Shedden K, Hankenson KD, Woolf PJ. GAGE: generally applicable gene set enrichment for pathway analysis. BMC Bioinformatics. 2009;10: 161. doi:10.1186/1471-2105-10-161

184. Morpheus. https://software.broadinstitute.org/morpheus/ Broad Institute, Cambridge, MA, USA;

185. Coste J, Voisin DL, Luccarini P, Dallel R. A role for wind-up in trigeminal sensory processing: intensity coding of nociceptive stimuli in the rat. Cephalalgia Int J Headache. 2008;28: 631–639. doi:10.1111/j.1468-2982.2008.01568.x

186. Hucho T, Levine JD. Signaling pathways in sensitization: toward a nociceptor cell biology. Neuron. 2007;55: 365–376. doi:10.1016/j.neuron.2007.07.008

187. Matsumoto S, Yoshida S, Takahashi M, Saiki C, Takeda M. The Roles of ID, IA and IK in the Electrophysiological Functions of Small-Diameter Rat Trigeminal Ganglion Neurons. Curr Mol Pharmacol. 2010;3: 30–36.

188. Weyer AD, Zappia KJ, Garrison SR, O'Hara CL, Dodge AK, Stucky CL. Nociceptor Sensitization Depends on Age and Pain Chronicity(1,2,3). eNeuro. 2016;3. doi:10.1523/ENEURO.0115-15.2015

189. Flegel C, Schöbel N, Altmüller J, Becker C, Tannapfel A, Hatt H, et al. RNA-Seq Analysis of Human Trigeminal and Dorsal Root Ganglia with a Focus on Chemoreceptors. McKemy DD, editor. PLOS ONE. 2015;10: e0128951. doi:10.1371/journal.pone.0128951

190. Manteniotis S, Lehmann R, Flegel C, Vogel F, Hofreuter A, Schreiner BSP, et al. Comprehensive RNA-Seq Expression Analysis of Sensory Ganglia with a Focus on Ion Channels and GPCRs in Trigeminal Ganglia. Zhang Z, editor. PLoS ONE. 2013;8: e79523. doi:10.1371/journal.pone.0079523

191. Tremblay C, Frasnelli J. Olfactory and Trigeminal Systems Interact in the Periphery. Chem Senses. 2018;43: 611–616. doi:10.1093/chemse/bjy049

192. Demarquay G, Royet JP, Mick G, Ryvlin P. Olfactory hypersensitivity in migraineurs: a H(2)(15)O-PET study. Cephalalgia Int J Headache. 2008;28: 1069–1080. doi:10.1111/j.1468-2982.2008.01672.x

193. Schreiber AO, Calvert PC. Migrainous olfactory hallucinations. Headache. 1986;26: 513–514.

194. Kelman L. Osmophobia and Taste Abnormality in Migraineurs: A Tertiary Care Study. Headache. 2004;44: 1019–1023. doi:10.1111/j.1526-4610.2004.04197.x

195. Rubino E, Rainero I, Garino F, Vicentini C, Govone F, Vacca A, et al. Subclinical hypothyroidism is associated with migraine: A case-control study. Cephalalgia. 2019;39: 15–20. doi:10.1177/0333102418769917

196. Kamata Y, Kuhara A, Iwamoto T, Hayashi K, Koido S, Kimura T, et al. Identification of HLA Class I-binding Peptides Derived from Unique Cancer-associated Proteins by Mass Spectrometric Analysis. Anticancer Res. 2013;33: 1853–1859.

197. Bayam E, Sahin GS, Guzelsoy G, Guner G, Kabakcioglu A, Ince-Dunn G. Genome-wide target analysis of NEUROD2 provides new insights into regulation of cortical projection neuron migration and differentiation. BMC Genomics. 2015;16: 681. doi:10.1186/s12864-015-1882-9

198. Chen F, Moran JT, Zhang Y, Ates KM, Yu D, Schrader LA, et al. The transcription factor NeuroD2 coordinates synaptic innervation and cell intrinsic properties to control excitability of cortical pyramidal neurons. J Physiol. 2016;594: 3729–3744. doi:10.1113/JP271953

199. Bröhl D, Strehle M, Wende H, Hori K, Bormuth I, Nave K-A, et al. A transcriptional network coordinately determines transmitter and peptidergic fate in the dorsal spinal cord. Dev Biol. 2008;322: 381–393. doi:10.1016/j.ydbio.2008.08.002

200. Khan MZ, He L. Neuro-psychopharmacological perspective of Orphan receptors of Rhodopsin (class A) family of G protein-coupled receptors. Psychopharmacology (Berl). 2017;234: 1181–1207. doi:10.1007/s00213-017-4586-9

201. Laitakari A, Liu L, Frimurer TM, Holst B. The Zinc-Sensing Receptor GPR39 in Physiology and as a Pharmacological Target. Int J Mol Sci. 2021;22: 3872. doi:10.3390/ijms22083872

202. Muneoka S, Goto M, Kadoshima-Yamaoka K, Kamei R, Terakawa M, Tomimori Y. G protein-coupled receptor 39 plays an anti-inflammatory role by enhancing IL-10 production from macrophages under inflammatory conditions. Eur J Pharmacol. 2018;834: 240–245. doi:10.1016/j.ejphar.2018.07.045

203. de Roux N, Genin E, Carel J-C, Matsuda F, Chaussain J-L, Milgrom E. Hypogonadotropic hypogonadism due to loss of function of the KiSS1-derived peptide receptor GPR54. Proc Natl Acad Sci U S A. 2003;100: 10972–10976. doi:10.1073/pnas.1834399100

204. Seminara SB. Mechanisms of Disease: the first kiss—a crucial role for kisspeptin-1 and its receptor, G-protein-coupled receptor 54, in puberty and reproduction. Nat Rev Endocrinol. 2006;2: 328–334. doi:10.1038/ncpendmet0139

205. Kauffman AS, Clifton DK, Steiner RA. Emerging ideas about kisspeptin– GPR54 signaling in the neuroendocrine regulation of reproduction. Trends Neurosci. 2007;30: 504–511. doi:10.1016/j.tins.2007.08.001

206. Colledge WH. Kisspeptins and GnRH neuronal signalling. Trends Endocrinol Metab. 2009;20: 115–121. doi:10.1016/j.tem.2008.10.005

207. Mi W-L, Mao-Ying Q-L, Liu Q, Wang X-W, Li X, Wang Y-Q, et al. The distribution of kisspeptin and its receptor GPR54 in rat dorsal root ganglion and up-regulation of its expression after CFA injection. Brain Res Bull. 2009;78: 254–260. doi:10.1016/j.brainresbull.2008.12.003

208. Spampinato S, Trabucco A, Biasiotta A, Biagioni F, Cruccu G, Copani A, et al. Hyperalgesic activity of kisspeptin in mice. Mol Pain. 2011;7: 90. doi:10.1186/1744-8069-7-90

209. Elhabazi K, Humbert J-P, Bertin I, Schmitt M, Bihel F, Bourguignon J-J, et al. Endogenous mammalian RF-amide peptides, including PrRP, kisspeptin and 26RFa, modulate nociception and morphine analgesia via NPFF receptors. Neuropharmacology. 2013;75: 164–171. doi:10.1016/j.neuropharm.2013.07.012

210. Sobrino V, Avendaño MS, Perdices-López C, Jimenez-Puyer M, Tena-Sempere M. Kisspeptins and the neuroendocrine control of reproduction: Recent progress and new frontiers in kisspeptin research. Front Neuroendocrinol. 2022;65: 100977. doi:10.1016/j.yfrne.2021.100977

211. Morgan JR, Gebhart GF. Characterization of a Model of Chronic Orofacial Hyperalgesia in the Rat: Contribution of NAV 1.8. J Pain. 2008;9: 522–531. doi:10.1016/j.jpain.2008.01.326

212. Koltzenburg M, Wall PD, McMahon SB. Does the right side know what the left is doing? Trends Neurosci. 1999;22: 122–127.

213. Shenker N, Haigh R, Roberts E, Mapp P, Harris N, Blake D. A review of contralateral responses to a unilateral inflammatory lesion. Rheumatol Oxf Engl. 2003;42: 1279–1286. doi:10.1093/rheumatology/keg397

214. Benemei S, Nicoletti P, Capone JG, Geppetti P. CGRP receptors in the control of pain and inflammation. Curr Opin Pharmacol. 2009;9: 9–14. doi:10.1016/j.coph.2008.12.007

215. Bigal ME, Walter S, Rapoport AM. Calcitonin gene-related peptide (CGRP) and migraine current understanding and state of development. Headache. 2013;53: 1230–1244. doi:10.1111/head.12179

216. Doods H, Arndt K, Rudolf K, Just S. CGRP antagonists: unravelling the role of CGRP in migraine. Trends Pharmacol Sci. 2007;28: 580–587. doi:10.1016/j.tips.2007.10.005

217. Durham PL. Calcitonin Gene-Related Peptide (CGRP) and Migraine. Headache. 2006;46: S3–S8.

218. Russo AF. Calcitonin Gene-Related Peptide (CGRP). Annu Rev Pharmacol Toxicol. 2015;55: 533–552. doi:10.1146/annurev-pharmtox-010814-124701

219. Dong Y, Li P, Ni Y, Zhao J, Liu Z. Decreased MicroRNA-125a-3p Contributes to Upregulation of p38 MAPK in Rat Trigeminal Ganglions with Orofacial Inflammatory Pain. PLOS ONE. 2014;9: e111594. doi:10.1371/journal.pone.0111594

220. Kuzawińska O, Lis K, Cudna A, Ba\lkowiec-Iskra E. Gender differences in the neurochemical response of trigeminal ganglion neurons to peripheral inflammation in mice. Acta Neurobiol Exp. 2014;74: 227–232.

221. Shinoda M, Iwata K. Neural communication in the trigeminal ganglion contributes to ectopic orofacial pain. J Oral Biosci. 2013;55: 165–168. doi:10.1016/j.job.2013.06.003

222. Yasuda M, Shinoda M, Kiyomoto M, Honda K, Suzuki A, Tamagawa T, et al. P2X3 receptor mediates ectopic mechanical allodynia with inflamed lower lip in mice. Neurosci Lett. 2012;528: 67–72. doi:10.1016/j.neulet.2012.08.067

223. Körtési T, Tuka B, Nyári A, Vécsei L, Tajti J. The effect of orofacial complete Freund's adjuvant treatment on the expression of migraine-related molecules. J Headache Pain. 2019;20: 43. doi:10.1186/s10194-019-0999-7

224. Alibhai IN, Green TA, Potashkin JA, Nestler EJ. Regulation of fosB and ΔfosB mRNA Expression: In Vivo and In Vitro Studies. Brain Res. 2007;1143: 22–33. doi:10.1016/j.brainres.2007.01.069

225. Knight WD, Little JT, Carreno FR, Toney GM, Mifflin SW, Cunningham JT. Chronic intermittent hypoxia increases blood pressure and expression of FosB/ FosB in central autonomic regions. AJP Regul Integr Comp Physiol. 2011;301: R131–R139. doi:10.1152/ajpregu.00830.2010

226. Nestler EJ, Barrot M, Self DW. ΔFosB: A sustained molecular switch for addiction. Proc Natl Acad Sci. 2001;98: 11042–11046. doi:10.1073/pnas.191352698

227. Middeldorp J, Hol EM. GFAP in health and disease. Prog Neurobiol. 2011;93: 421–443. doi:10.1016/j.pneurobio.2011.01.005

228. Kelemen SE, Autieri MV. Expression of Allograft Inflammatory Factor-1 in T Lymphocytes. Am J Pathol. 2005;167: 619–626.

229. Pawlik A, Kotrych D, Paczkowska E, Roginska D, Dziedziejko V, Safranow K, et al. Expression of allograft inflammatory factor-1 in peripheral blood monocytes and synovial membranes in patients with rheumatoid arthritis. Hum Immunol. 2016;77: 131–136. doi:10.1016/j.humimm.2015.11.008

230. Niebrój-Dobosz I, Rafałowska J, Lukasiuk M, Pfeffer A, Mossakowski MJ. Immunochemical analysis of some proteins in cerebrospinal fluid and serum of patients with ischemic strokes. Folia Neuropathol. 1994;32: 129–137.

231. Missler U, Wiesmann M, Wittmann G, Magerkurth O, Hagenström H. Measurement of Glial Fibrillary Acidic Protein in Human Blood: Analytical Method and Preliminary Clinical Results. Clin Chem. 1999;45: 138–141.

232. Brunkhorst R, Pfeilschifter W, Foerch C. Astroglial Proteins as Diagnostic Markers of Acute Intracerebral Hemorrhage—Pathophysiological Background and Clinical Findings. Transl Stroke Res. 2010;1: 246–251. doi:10.1007/s12975-010-0040-6

233. Mayer CA, Brunkhorst R, Niessner M, Pfeilschifter W, Steinmetz H, Foerch C. Blood levels of glial fibrillary acidic protein (GFAP) in patients with neurological diseases. PloS One. 2013;8: e62101. doi:10.1371/journal.pone.0062101

234. Foerch C, Luger S, Group BFS. Glial fibrillary acidic protein (GFAP) plasma levels distinguish intracerebral hemorrhage from cerebral ischemia in the early phase of acute stroke. J Neurol Sci. 2015;357: e430. doi:10.1016/j.jns.2015.09.042

235. Bembea MM, Savage W, Strouse JJ, Schwartz JM, Graham E, Thompson CB, et al. Glial fibrillary acidic protein as a brain injury biomarker in children undergoing extracorporeal membrane oxygenation. Pediatr Crit Care Med J Soc Crit Care Med World Fed Pediatr Intensive Crit Care Soc. 2011;12: 572–579. doi:10.1097/PCC.0b013e3181fe3ec7

236. Lei J, Gao G, Feng J, Jin Y, Wang C, Mao Q, et al. Glial fibrillary acidic protein as a biomarker in severe traumatic brain injury patients: a prospective cohort study. Crit Care Lond Engl. 2015;19: 362. doi:10.1186/s13054-015-1081-8

237. Zhang Y, Song N, Liu F, Lin J, Liu M, Huang C, et al. Activation of mitogen-activated protein kinases in satellite glial cells of the trigeminal ganglion contributes to substance P-mediated inflammatory pain. Int J Oral Sci. 2019;11: 24. doi:10.1038/s41368-019-0055-0

238. Kiyomoto M, Shinoda M, Okada-Ogawa A, Noma N, Shibuta K, Tsuboi Y, et al. Fractalkine signaling in microglia contributes to ectopic orofacial pain following trapezius muscle inflammation. J Neurosci Off J Soc Neurosci. 2013;33: 7667–7680. doi:10.1523/JNEUROSCI.4968-12.2013

239. Cano-Martínez D, Monserrat J, Hernández-Breijo B, Sanmartín Salinas P, Álvarez-Mon M, Val Toledo-Lobo M, et al. Extracellular allograft inflammatory factor-1 (AIF-1) potentiates Th1 cell differentiation and inhibits Treg response in human peripheral blood mononuclear cells from normal subjects. Hum Immunol. 2020;81: 91–100. doi:10.1016/j.humimm.2020.01.011

240. McDaniel DO, Zhou X, Moore CK, Aru G. Cardiac Allograft Rejection Correlates with Increased Expressions of Toll-Like Receptors 2 and 4 and Allograft Inflammatory Factor 1. Transplant Proc. 2010;42: 4235–4237. doi:10.1016/j.transproceed.2010.09.091

241. Pilka R, Neubert D, Stejskal D, Krejčí G, Švesták M, Marek R, et al. Serum concentrations of TFF3, S100-A11 and AIF-1 in association with systemic inflammatory response, disease stage and nodal involvement in endometrial cancer. Pteridines. 2018;29: 6–12. doi:10.1515/pteridines-2018-0003

242. Anders QS, Klauss J, Rodrigues LC de M, Nakamura-Palacios EM. FosB mRNA Expression in Peripheral Blood Lymphocytes in Drug Addicted Patients. Front Pharmacol. 2018;9: 1205. doi:10.3389/fphar.2018.01205

243. Eising E, de Vries B, Ferrari MD, Terwindt GM, van den Maagdenberg AM. Pearls and pitfalls in genetic studies of migraine. Cephalalgia. 2013;33: 614–625. doi:10.1177/0333102413484988

244. Tolner EA, Houben T, Terwindt GM, de Vries B, Ferrari MD, van den Maagdenberg AMJM. From migraine genes to mechanisms. Pain. 2015;156: S64–S74. doi:10.1097/01.j.pain.0000460346.00213.16

245. Hershey AD, Tang Y, Powers SW, Kabbouche MA, Gilbert DL, Glauser TA, et al. Genomic Abnormalities in Patients With Migraine and Chronic Migraine: Preliminary Blood Gene Expression Suggests Platelet Abnormalities. Headache. 2004;44: 994–1004. doi:10.1111/j.1526-4610.2004.04193.x

246. Conti P, D'Ovidio C, Conti C, Gallenga CE, Lauritano D, Caraffa A, et al. Progression in migraine: Role of mast cells and pro-inflammatory and anti-inflammatory cytokines. Eur J Pharmacol. 2019;844: 87–94. doi:10.1016/j.ejphar.2018.12.004

247. Kursun O, Yemisci M, van den Maagdenberg AMJM, Karatas H. Migraine and neuroinflammation: the inflammasome perspective. J Headache Pain. 2021;22: 55. doi:10.1186/s10194-021-01271-1

248. Levy D, Burstein R, Kainz V, Jakubowski M, Strassman AM. Mast cell degranulation activates a pain pathway underlying migraine headache: Pain. 2007;130: 166–176. doi:10.1016/j.pain.2007.03.012

249. Uzar E, Evliyaoglu O, Yucel Y, Ugur Cevik M, Acar A, Guzel I, et al. Serum cytokine and pro-brain natriuretic peptide (BNP) levels in patients with migraine. Eur Rev Med Pharmacol Sci. 2011;15: 1111–1116.

250. Covelli V, Massari F, Fallacara C, Munno I, Pellegrino NM, Jirillo E, et al. Increased spontaneous release of tumor necrosis factor-alpha/cachectin in headache patients. A possible correlation with plasma endotoxin and hypothalamic-pituitary-adrenal axis. Int J Neurosci. 1991;61: 53–60. doi:10.3109/00207459108986270

251. Duarte H, Teixeira AL, Rocha NP, Domingues RB. Increased interictal serum levels of CXCL8/IL-8 and CCL3/MIP-1α in migraine. Neurol Sci Off J Ital Neurol Soc Ital Soc Clin Neurophysiol. 2015;36: 203–208. doi:10.1007/s10072-014-1931-1

252. Domingues RB, Duarte H, Senne C, Bruniera G, Brunale F, Rocha NP, et al. Serum levels of adiponectin, CCL3/MIP-1α, and CCL5/RANTES discriminate migraine from tension-type headache patients. Arq Neuropsiquiatr. 2016;74: 626–631. doi:10.1590/0004-282X20160096

253. Vanmolkot FH, de Hoon JN. Increased C-reactive protein in young adult patients with migraine. Cephalalgia Int J Headache. 2007;27: 843–846. doi:10.1111/j.1468-2982.2007.01324.x

254. Güzel I, Taşdemir N, Celik Y. Evaluation of serum transforming growth factor β1 and C-reactive protein levels in migraine patients. Neurol Neurochir Pol. 2013;47: 357–362. doi:10.5114/ninp.2013.36760

255. Perini F, D'Andrea G, Galloni E, Pignatelli F, Billo G, Alba S, et al. Plasma cytokine levels in migraineurs and controls. Headache J Head Face Pain. 2005;45: 926–931.

256. Sarchielli P, Alberti A, Baldi A, Coppola F, Rossi C, Pierguidi L, et al. Proinflammatory cytokines, adhesion molecules, and lymphocyte integrin expression in the internal jugular blood of migraine patients without aura assessed ictally. Headache. 2006;46: 200–207. doi:10.1111/j.1526-4610.2006.00337.x

257. Woolf CJ, Allchorne A, Safieh-Garabedian B, Poole S. Cytokines, nerve growth factor and inflammatory hyperalgesia: the contribution of tumour necrosis factor α. Br J Pharmacol. 1997;121: 417–424. doi:10.1038/sj.bjp.0701148

258. Watkins LR, Maier SF. Beyond Neurons: Evidence That Immune and Glial Cells Contribute to Pathological Pain States. Physiol Rev. 2002;82: 981–1011. doi:10.1152/physrev.00011.2002

259. Sommer C, Kress M. Recent findings on how proinflammatory cytokines cause pain: peripheral mechanisms in inflammatory and neuropathic hyperalgesia. Neurosci Lett. 2004;361: 184–187. doi:10.1016/j.neulet.2003.12.007

260. Kawasaki Y, Zhang L, Cheng J-K, Ji R-R. Cytokine Mechanisms of Central Sensitization: Distinct and Overlapping Role of Interleukin-1β, Interleukin-6, and Tumor Necrosis Factor-α in Regulating Synaptic and Neuronal Activity in the Superficial Spinal Cord. J Neurosci. 2008;28: 5189–5194. doi:10.1523/JNEUROSCI.3338-07.2008

261. Zhang X-C, Kainz V, Burstein R, Levy D. Tumor necrosis factor-α induces sensitization of meningeal nociceptors mediated via local COX and p38 MAP kinase actions. Pain. 2011;152: 140–149. doi:10.1016/j.pain.2010.10.002

262. Zhang X, Burstein R, Levy D. Local action of the proinflammatory cytokines IL-1 and IL-6 on intracranial meningeal nociceptors. Cephalalgia. 2012;32: 66–72. doi:10.1177/0333102411430848

263. Silva RL, Lopes AH, Guimarães RM, Cunha TM. CXCL1/CXCR2 signaling in pathological pain: Role in peripheral and central sensitization. Neurobiol Dis. 2017;105: 109–116. doi:10.1016/j.nbd.2017.06.001

264. Piotrowska A, Rojewska E, Pawlik K, Kreiner G, Ciechanowska A, Makuch W, et al. Pharmacological Blockade of Spinal CXCL3/CXCR2 Signaling by NVP CXCR2 20, a Selective CXCR2 Antagonist, Reduces Neuropathic Pain Following Peripheral Nerve Injury. Front Immunol. 2019;10: 2198. doi:10.3389/fimmu.2019.02198

265. Manjavachi MN, Passos GF, Trevisan G, Araújo SB, Pontes JP, Fernandes ES, et al. Spinal blockage of CXCL1 and its receptor CXCR2 inhibits paclitaxel-induced peripheral neuropathy in mice. Neuropharmacology. 2019;151: 136–143. doi:10.1016/j.neuropharm.2019.04.014

266. Moraes TR, Elisei LS, Malta IH, Galdino G. Participation of CXCL1 in the glial cells during neuropathic pain. Eur J Pharmacol. 2020;875: 173039. doi:10.1016/j.ejphar.2020.173039

267. Liang D-Y, Shi X, Liu P, Sun Y, Sahbaie P, Li W-W, et al. The Chemokine Receptor CXCR2 Supports Nociceptive Sensitization after Traumatic Brain Injury. Mol Pain. 2017;13: 1744806917730212. doi:10.1177/1744806917730212

268. Sahbaie P, Irvine K-A, Liang D-Y, Shi X, Clark JD. Mild Traumatic Brain Injury Causes Nociceptive Sensitization through Spinal Chemokine Upregulation. Sci Rep. 2019;9: 19500. doi:10.1038/s41598-019-55739-x

269. Nees TA, Rosshirt N, Zhang JA, Reiner T, Sorbi R, Tripel E, et al. Synovial Cytokines Significantly Correlate with Osteoarthritis-Related Knee Pain and Disability: Inflammatory Mediators of Potential Clinical Relevance. J Clin Med. 2019;8: 1343. doi:10.3390/jcm8091343

270. Riese DJ, Cullum RL. Epiregulin: Roles in normal physiology and cancer. Semin Cell Dev Biol. 2014;28: 49–56. doi:10.1016/j.semcdb.2014.03.005

271. Singh B, Carpenter G, Coffey RJ. EGF receptor ligands: recent advances. F1000Research. 2016;5: 2270. doi:10.12688/f1000research.9025.1

272. Martin LJ, Smith SB, Khoutorsky A, Magnussen CA, Samoshkin A, Sorge RE, et al. Epiregulin and EGFR interactions are involved in pain processing. J Clin Invest. 2017;127: 3353–3366. doi:10.1172/JCI87406

273. Yamane S, Ishida S, Hanamoto Y, Kumagai K, Masuda R, Tanaka K, et al. Proinflammatory role of amphiregulin, an epidermal growth factor family member whose expression is augmented in rheumatoid arthritis patients. J Inflamm. 2008;5: 5. doi:10.1186/1476-9255-5-5

274. Grosche L, Knippertz I, König C, Royzman D, Wild AB, Zinser E, et al. The CD83 Molecule – An Important Immune Checkpoint. Front Immunol. 2020;11: 721. doi:10.3389/fimmu.2020.00721

275. Gross EC, Lisicki M, Fischer D, Sándor PS, Schoenen J. The metabolic face of migraine — from pathophysiology to treatment. Nat Rev Neurol. 2019;15: 627–643. doi:10.1038/s41582-019-0255-4

276. Cevoli S, Favoni V, Cortelli P. Energy Metabolism Impairment in Migraine. Curr Med Chem. 2019;26: 6253–6260. doi:10.2174/0929867325666180622154411

277. Neri M, Frustaci A, Milic M, Valdiglesias V, Fini M, Bonassi S, et al. A meta-analysis of biomarkers related to oxidative stress and nitric oxide pathway in migraine. Cephalalgia Int J Headache. 2015;35: 931–937. doi:10.1177/0333102414564888

278. Welch KM, Levine SR, D'Andrea G, Schultz LR, Helpern JA. Preliminary observations on brain energy metabolism in migraine studied by in vivo phosphorus 31 NMR spectroscopy. Neurology. 1989;39: 538–541. doi:10.1212/wnl.39.4.538

279. Barbiroli B, Montagna P, Cortelli P, Funicello R, Iotti S, Monari L, et al. Abnormal brain and muscle energy metabolism shown by 31P magnetic resonance spectroscopy in

patients affected by migraine with aura. Neurology. 1992;42: 1209–1214. doi:10.1212/wnl.42.6.1209

280. Lodi R, Kemp GJ, Montagna P, Pierangeli G, Cortelli P, Iotti S, et al. Quantitative analysis of skeletal muscle bioenergetics and proton efflux in migraine and cluster headache. J Neurol Sci. 1997;146: 73–80. doi:10.1016/s0022-510x(96)00287-0

281. Kim JH, Kim S, Suh S-I, Koh S-B, Park K-W, Oh K. Interictal metabolic changes in episodic migraine: a voxel-based FDG-PET study. Cephalalgia Int J Headache. 2010;30: 53–61. doi:10.1111/j.1468-2982.2009.01890.x

282. Borkum JM. Migraine Triggers and Oxidative Stress: A Narrative Review and Synthesis: Headache. Headache J Head Face Pain. 2016;56: 12–35. doi:10.1111/head.12725

283. Borkum JM. The Migraine Attack as a Homeostatic, Neuroprotective Response to Brain Oxidative Stress: Preliminary Evidence for a Theory. Headache. 2018;58: 118–135. doi:10.1111/head.13214

284. Gerring ZF, Powell JE, Montgomery GW, Nyholt DR. Genome-wide analysis of blood gene expression in migraine implicates immune-inflammatory pathways. Cephalalgia. 2018;38: 292–303. doi:10.1177/0333102416686769

285. Wolf HK, Buslei R, Schmidt-Kastner R, Schmidt-Kastner PK, Pietsch T, Wiestler OD, et al. NeuN: a useful neuronal marker for diagnostic histopathology. J Histochem Cytochem Off J Histochem Soc. 1996;44: 1167–1171. doi:10.1177/44.10.8813082

286. Wang B, Wang X-P. Does Ceruloplasmin Defend Against Neurodegenerative Diseases? Curr Neuropharmacol. 2019;17: 539–549. doi:10.2174/1570159X16666180508113025

287. Cheng G-Y, Jiang Q, Deng A-P, Wang Y, Liu J, Zhou Q, et al. CD31 induces inflammatory response by promoting hepatic inflammatory response and cell apoptosis. Eur Rev Med Pharmacol Sci. 2018;22: 7543–7550. doi:10.26355/eurrev_201811_16296

288. Dobrowolski M, Cave C, Levy-Myers R, Lee C, Park S, Choi B-R, et al. GDE3 regulates oligodendrocyte precursor proliferation via release of soluble CNTFRα. Dev Camb Engl. 2020;147. doi:10.1242/dev.180695

289. Hallquist NA, Khoo C, Cousins RJ. Lipopolysaccharide regulates cysteine-rich intestinal protein, a zinc-finger protein, in immune cells and plasma. J Leukoc Biol. 1996;59: 172–177. doi:10.1002/jlb.59.2.172

290. Kim J-YV, Megat S, Moy JK, Asiedu MN, Mejia GL, Vagner J, et al. Neuroligin 2 regulates spinal GABAergic plasticity in hyperalgesic priming, a model of the transition from acute to chronic pain. Pain. 2016;157: 1314–1324. doi:10.1097/j.pain.0000000000000513

291. Quintanilla M, Montero-Montero L, Renart J, Martín-Villar E. Podoplanin in Inflammation and Cancer. Int J Mol Sci. 2019;20. doi:10.3390/ijms20030707

292. Heyne K, Winter C, Gerten F, Schmidt C, Roemer K. A novel mechanism of crosstalk between the p53 and NFκB pathways: MDM2 binds and inhibits p65RelA. Cell Cycle Georget Tex. 2013;12: 2479–2492. doi:10.4161/cc.25495

293. Tang R-Z, Zhu J-J, Yang F-F, Zhang Y-P, Xie S-A, Liu Y-F, et al. DNA methyltransferase 1 and Krüppel-like factor 4 axis regulates macrophage inflammation and atherosclerosis. J Mol Cell Cardiol. 2019;128: 11–24. doi:10.1016/j.yjmcc.2019.01.009

294. Flanagan LA, Rebaza LM, Derzic S, Schwartz PH, Monuki ES. Regulation of human neural precursor cells by laminin and integrins. J Neurosci Res. 2006;83: 845–856. doi:10.1002/jnr.20778

295. Robichaux WG, Cheng X. Intracellular cAMP Sensor EPAC: Physiology, Pathophysiology, and Therapeutics Development. Physiol Rev. 2018;98: 919–1053. doi:10.1152/physrev.00025.2017

296. Icer MA, Gezmen-Karadag M. The multiple functions and mechanisms of osteopontin. Clin Biochem. 2018;59: 17–24. doi:10.1016/j.clinbiochem.2018.07.003

297. Sans A, Bonnafous S, Rousseau D, Patouraux S, Canivet CM, Leclere PS, et al. The Differential Expression of Cide Family Members is Associated with Nafld Progression from Steatosis to Steatohepatitis. Sci Rep. 2019;9: 7501. doi:10.1038/s41598-019-43928-7

298. Zamanian JL, Xu L, Foo LC, Nouri N, Zhou L, Giffard RG, et al. Genomic Analysis of Reactive Astrogliosis. J Neurosci. 2012;32: 6391–6410. doi:10.1523/JNEUROSCI.6221-11.2012

299. Takeda M, Takahashi M, Nasu M, Matsumoto S. Peripheral inflammation suppresses inward rectifying potassium currents of satellite glial cells in the trigeminal ganglia. Pain. 2011;152: 2147–2156. doi:10.1016/j.pain.2011.05.023

300. Ishimoto T, Ninomiya K, Inoue R, Koike M, Uchiyama Y, Mori H. Mice lacking BCAS1, a novel myelin-associated protein, display hypomyelination, schizophrenia-like abnormal behaviors, and upregulation of inflammatory genes in the brain. Glia. 2017;65: 727–739. doi:10.1002/glia.23129

301. Vihervuori H, Autere TA, Repo H, Kurki S, Kallio L, Lintunen MM, et al. Tumor-infiltrating lymphocytes and CD8+ T cells predict survival of triple-negative breast cancer. J Cancer Res Clin Oncol. 2019;145: 3105–3114. doi:10.1007/s00432-019-03036-5

302. Dey A, Yang W, Gegonne A, Nishiyama A, Pan R, Yagi R, et al. BRD4 directs hematopoietic stem cell development and modulates macrophage inflammatory responses. EMBO J. 2019;38. doi:10.15252/embj.2018100293

303. Hajmirza A, Emadali A, Gauthier A, Casasnovas O, Gressin R, Callanan MB. BET Family Protein BRD4: An Emerging Actor in NFκB Signaling in Inflammation and Cancer. Biomedicines. 2018;6. doi:10.3390/biomedicines6010016

304. Berberich I, Hildeman DA. The Bcl2a1 gene cluster finally knocked out: first clues to understanding the enigmatic role of the Bcl-2 protein A1. Cell Death Differ. 2017;24: 572–574. doi:10.1038/cdd.2017.25

305. Gaud G, Lesourne R, Love PE. Regulatory mechanisms in T cell receptor signalling. Nat Rev Immunol. 2018;18: 485–497. doi:10.1038/s41577-018-0020-8

306. Witkowski M, Landmesser U, Rauch U. Tissue factor as a link between inflammation and coagulation. Trends Cardiovasc Med. 2016;26: 297–303. doi:10.1016/j.tcm.2015.12.001

307. Zelaya H, Rothmeier AS, Ruf W. Tissue factor at the crossroad of coagulation and cell signaling. J Thromb Haemost JTH. 2018;16: 1941–1952. doi:10.1111/jth.14246

308. Horinokita I, Hayashi H, Oteki R, Mizumura R, Yamaguchi T, Usui A, et al. Involvement of Progranulin and Granulin Expression in Inflammatory Responses after Cerebral Ischemia. Int J Mol Sci. 2019;20. doi:10.3390/ijms20205210

309. Bateman A, Cheung ST, Bennett HPJ. A Brief Overview of Progranulin in Health and Disease. Methods Mol Biol Clifton NJ. 2018;1806: 3–15. doi:10.1007/978-1-4939-8559-3_1

310. Tran JR, Chen H, Zheng X, Zheng Y. Lamin in inflammation and aging. Curr Opin Cell Biol. 2016;40: 124–130. doi:10.1016/j.ceb.2016.03.004

311. Corey DP, Holt JR. Are TMCs the Mechanotransduction Channels of Vertebrate Hair Cells? J Neurosci. 2016;36: 10921–10926. doi:10.1523/JNEUROSCI.1148-16.2016

312. Yue X, Sheng Y, Kang L, Xiao R. Distinct functions of TMC channels: a comparative overview. Cell Mol Life Sci. 2019;76: 4221–4232. doi:10.1007/s00018-019-03214-1

313. Micera A, Balzamino BO, Biamonte F, Esposito G, Marino R, Fanelli F, et al. Current progress of Reelin in development, inflammation and tissue remodeling: from nervous to visual systems. Curr Mol Med. 2016.

314. Barbosa C, Xiao Y, Johnson AJ, Xie W, Strong JA, Zhang J-M, et al. FHF2 isoforms differentially regulate Nav1.6-mediated resurgent sodium currents in dorsal root ganglion neurons. Pflugers Arch. 2017;469: 195–212. doi:10.1007/s00424-016-1911-9

315. Yang L, Dong F, Yang Q, Yang P-F, Wu R, Wu Q-F, et al. FGF13 Selectively Regulates Heat Nociception by Interacting with Nav1.7. Neuron. 2017;93: 806-821.e9. doi:10.1016/j.neuron.2017.01.009

316. Effraim PR, Huang J, Lampert A, Stamboulian S, Zhao P, Black JA, et al. Fibroblast growth factor homologous factor 2 (FGF-13) associates with Nav1.7 in DRG neurons and alters its current properties in an isoform-dependent manner. Neurobiol Pain Camb Mass. 2019;6: 100029. doi:10.1016/j.ynpai.2019.100029

317. Carpio Horta K, Weiss SG, Miranda K, Sebastiani AM, Costa DJ da, Matsumoto MAN, et al. Polymorphisms in FGF3, FGF10, and FGF13 May Contribute to the Presence of Temporomandibular Disorders in Patients Who Required Orthognathic Surgery. J Craniofac Surg. 2019;30: 2082–2084. doi:10.1097/SCS.0000000000006029

318. Boutros R, Lobjois V, Ducommun B. CDC25 phosphatases in cancer cells: key players? Good targets? Nat Rev Cancer. 2007;7: 495–507. doi:10.1038/nrc2169

319. Boraschi D, Italiani P, Weil S, Martin MU. The family of the interleukin-1 receptors. Immunol Rev. 2018;281: 197–232. doi:10.1111/imr.12606

320. Cheng G, Zhong M, Kawaguchi R, Kassai M, Al-Ubaidi M, Deng J, et al. Identification of PLXDC1 and PLXDC2 as the transmembrane receptors for the multifunctional factor PEDF. eLife. 2014;3: e05401. doi:10.7554/eLife.05401

321. Weng H-J, Patel KN, Jeske NA, Bierbower SM, Zou W, Tiwari V, et al. Tmem100 is a regulator of TRPA1-TRPV1 complex and contributes to persistent pain. Neuron. 2015;85: 833–846. doi:10.1016/j.neuron.2014.12.065

322. Yu H, Shin SM, Wang F, Xu H, Xiang H, Cai Y, et al. Transmembrane protein 100 is expressed in neurons and glia of dorsal root ganglia and is reduced after painful nerve injury. Pain Rep. 2019;4: e703. doi:10.1097/PR9.0000000000000703

323. Ma D, Li S-J, Wang L-S, Dai J, Zhao S, Zeng R. Temporal and spatial profiling of nuclei-associated proteins upon TNF-alpha/NF-kappaB signaling. Cell Res. 2009;19: 651–664. doi:10.1038/cr.2009.46

324. Cahoy JD, Emery B, Kaushal A, Foo LC, Zamanian JL, Christopherson KS, et al. A Transcriptome Database for Astrocytes, Neurons, and Oligodendrocytes: A New Resource for Understanding Brain Development and Function. J Neurosci. 2008;28: 264–278. doi:10.1523/JNEUROSCI.4178-07.2008

325. Hay CM. Investigating the role of Gpr62 in oligodendrocyte development and central nervous system myelination. PhD Thesis Univ Melb Httphdlhandlenet1134358589. 2015 [cited 29 Feb 2020]. doi:http://hdl.handle.net/11343/58589

326. Kollek M, Müller A, Egle A, Erlacher M. Bcl-2 proteins in development, health, and disease of the hematopoietic system. FEBS J. 2016;283: 2779–2810. doi:10.1111/febs.13683

327. Shen E, Shulha H, Weng Z, Akbarian S. Regulation of histone H3K4 methylation in brain development and disease. Philos Trans R Soc Lond B Biol Sci. 2014;369. doi:10.1098/rstb.2013.0514

328. Geserick P, Kaiser F, Klemm U, Kaufmann SHE, Zerrahn J. Modulation of T cell development and activation by novel members of the Schlafen (slfn) gene family harbouring an RNA helicase-like motif. Int Immunol. 2004;16: 1535–1548. doi:10.1093/intimm/dxh155

329. Nakagawa K, Matsuki T, Zhao L, Kuniyoshi K, Tanaka H, Ebina I, et al. Schlafen-8 is essential for lymphatic endothelial cell activation in experimental autoimmune encephalomyelitis. Int Immunol. 2018;30: 69–78. doi:10.1093/intimm/dxx079

330. Silke J, Strasser A. The FLIP Side of Life. Sci Signal. 2013;6: pe2. doi:10.1126/scisignal.2003845

331. Liu L, Markus I, Saghire HE, Perera D s, King DW, Burcher E. Distinct differences in tachykinin gene expression in ulcerative colitis, Crohn's disease and diverticular disease: a role for hemokinin-1? Neurogastroenterol Motil. 2011;23: 475-e180. doi:10.1111/j.1365-2982.2011.01685.x

332. Nishimori N, Toyoshima S, Sasaki-Sakamoto T, Hayama K, Terui T, Okayama Y. Serum level of hemokinin-1 is significantly lower in patients with chronic spontaneous urticaria than in healthy subjects. Allergol Int. 2021;70: 480–488. doi:10.1016/j.alit.2021.05.002

333. Goto T, Oh SB, Takeda M, Shinoda M, Sato T, Gunjikake KK, et al. Recent advances in basic research on the trigeminal ganglion. J Physiol Sci. 2016;66: 381–386. doi:10.1007/s12576-016-0448-1

334. Edvinsson L, Haanes KA, Warfvinge K, Krause DN. CGRP as the target of new migraine therapies — successful translation from bench to clinic. Nat Rev Neurol. 2018;14: 338–350. doi:10.1038/s41582-018-0003-1

335. Messlinger K, Fischer MJ, Lennerz JK. Neuropeptide effects in the trigeminal system: pathophysiology and clinical relevance in migraine. Keio J Med. 2011;60: 82–89.

336. Tajti J, Szok D, Majláth Z, Tuka B, Csáti A, Vécsei L. Migraine and neuropeptides. Neuropeptides. 2015;52: 19–30. doi:10.1016/j.npep.2015.03.006

337. Borbély E, Hajna Z, Sándor K, Kereskai L, Tóth I, Pintér E, et al. Role of tachykinin 1 and 4 gene-derived neuropeptides and the neurokinin 1 receptor in adjuvant-induced

chronic arthritis of the mouse. PloS One. 2013;8: e61684. doi:10.1371/journal.pone.0061684

338. Klassert TE, Pinto F, Hernández M, Candenas ML, Hernández MC, Abreu J, et al. Differential expression of neurokinin B and hemokinin-1 in human immune cells. J Neuroimmunol. 2008;196: 27–34. doi:10.1016/j.jneuroim.2008.02.010

339. Tsilioni I, Russell IJ, Stewart JM, Gleason RM, Theoharides TC. Neuropeptides CRH, SP, HK-1, and Inflammatory Cytokines IL-6 and TNF Are Increased in Serum of Patients with Fibromyalgia Syndrome, Implicating Mast Cells. J Pharmacol Exp Ther. 2016;356: 664–672. doi:10.1124/jpet.115.230060

340. Wilson SG, Mogil JS. Measuring pain in the (knockout) mouse: big challenges in a small mammal. Behav Brain Res. 2001;125: 65–73.

341. Jennings EM, Okine BN, Roche M, Finn DP. Stress-induced hyperalgesia. Prog Neurobiol. 2014;121: 1–18. doi:10.1016/j.pneurobio.2014.06.003

342. Marriott I. The role of tachykinins in central nervous system inflammatory responses. Front Biosci J Virtual Libr. 2004;9: 2153–2165. doi:10.2741/1377

343. Cunin P, Caillon A, Corvaisier M, Garo E, Scotet M, Blanchard S, et al. The tachykinins substance P and hemokinin-1 favor the generation of human memory Th17 cells by inducing IL-1β, IL-23, and TNF-like 1A expression by monocytes. J Immunol Baltim Md 1950. 2011;186: 4175–4182. doi:10.4049/jimmunol.1002535

344. Lau LT, Yu AC. Astrocytes produce and release interleukin-1, interleukin-6, tumor necrosis factor alpha and interferon-gamma following traumatic and metabolic injury. J Neurotrauma. 2001;18: 351–359. doi:10.1089/08977150151071035

345. Benoliel R, Svensson P, Evers S, Wang S-J, Barke A, Korwisi B, et al. The IASP classification of chronic pain for ICD-11: chronic secondary headache or orofacial pain. Pain. 2019;160: 60–68. doi:10.1097/j.pain.0000000000001435

346. Orofacial Pain - American Academy of Orofacial Pain. [cited 23 Feb 2020]. Available: https://aaop.clubexpress.com/content.aspx?page_id=22&club_id=508439&module_id=107325

Appendix

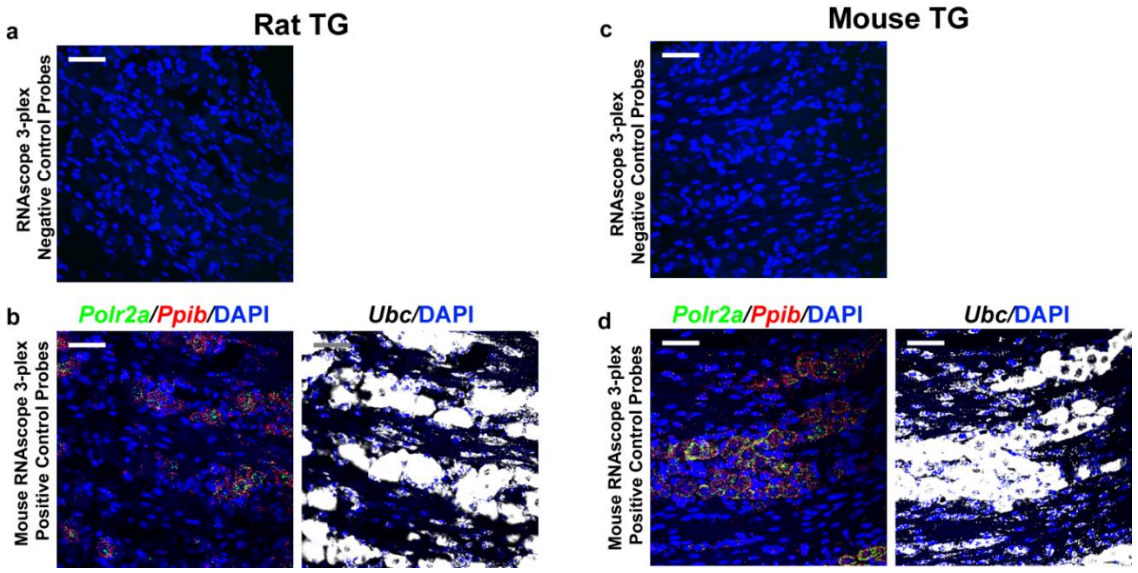

Appendix Figure 1. RNAscope control conditions were performed on saline-injected rat and mouse longitudinal TG sections counterstained with DAPI. **(a)** Representative confocal image of 3-plex negative control probes specific to the bacterial *dabP* gene giving no specific signal on rat TG; **(b)** Representative confocal images of 3-plex positive control probes specific to mouse *Polr2a* (in green), *Ppib* (in red) and *Ubc* (in white) mRNA targets on rat TG; **(c)** Representative confocal image of 3-plex negative control probes specific to the bacterial *dabP* gene giving no specific signal on mouse TG; **(d)** Representative confocal images of 3-plex positive control probes specific to mouse *Polr2a* (in green), *Ppib* (in red) and *Ubc* (in white) mRNA targets on mouse TG. Scale bar: 50 µm. Note that the sensitivity of mouse 3-plex positive control probes applied on rat tissue samples reflects the highly conserved mouse and rat genome.

Appendix Table 1. Classifications of primary and secondary headache and orofacial pain disorders.

The International Association for the Study of Pain [345]	International Headache Society - ICHD-3 [175]	The American Academy of Orofacial Pain [346]
Chronic primary headache or orofacial pain		
Chronic migraine without or with aura **Chronic tension-type headache** **Chronic trigeminal autonomic cephalalgias (TACs):** Chronic cluster headache Chronic paroxysmal hemicranias Short-lasting unilateral neuralgiform headache with conjunctival injection and tearing Hemicrania continua **Chronic primary temporomandibular disorder pains** Myalgia Myofascial pain with referral Arthralgia **Chronic burning mouth** Glossodynia **Chronic primary orofacial pain** Orofacial pain as a presentation of primary headaches Persistent idiopathic dentoalveolar pain Atypical facial pain (persistent idiopathic facial pain)	Migraine Tension-type headache (TTH) Trigeminal autonomic cephalalgias (TACs): Cluster headache and other trigeminal autonomic cephalalgias Other primary headache disorders	Temporomandibular Joint disorders Masticatory musculoskeletal pain Cervical musculoskeletal pain Neurovascular pain Neuropathic pain Sleep disorders related to orofacial pain Orofacial Dystonias Headaches Intraoral, intracranial, extracranial, and systemic disorders that cause orofacial pain
Chronic secondary headache or orofacial pain		
Chronic headache/orofacial pain attributed to trauma or injury to the head and/or neck **Chronic headache/orofacial pain attributed to a cranial or cervical vascular disorder** **Chronic headache/orofacial pain attributed to nonvascular intracranial disorder** **Chronic headache attributed to a substance or its withdrawal** **Chronic headache/orofacial pain attributed to infection** **Chronic headache/orofacial pain attributed to disorders of homeostasis or their nonpharmacological treatment** **Chronic headache/orofacial pain attributed to disorder of the cranium, neck, eyes, ears, sinuses, salivary glands, and oral mucosa** **Chronic dental pain** Diseases of pulp and periapical tissues Other diseases of hard tissues of teeth **Chronic neuropathic orofacial pain** Pain attributed to a lesion or disease of the trigeminal nerve, including trigeminal neuralgia (primary parent: chronic peripheral neuropathic pain) Other cranial and regional neuralgias and neuropathies **Chronic secondary temporomandibular disorder pain** Chronic secondary orofacial muscle pain Systemic disorders or trauma Chronic secondary temporomandibular joint pain Systemic disorders, trauma, or infection	Headache attributed to trauma or injury to the head and/or neck Headache attributed to a cranial or cervical vascular disorder Headache attributed to nonvascular intracranial disorder Headache attributed to a substance or its withdrawal Headache attributed to infection Headache attributed to disorder of homeostasis Headache or facial pain attributed to disorder of cranium, neck, eyes, ears, nose, sinuses, teeth, mouth, or other facial or cranial structures Headache attributed to psychiatric disorder Painful lesions of the cranial nerves and other facial pain Other headache disorders	

Appendix Table 2. Sequences of primers for real-time PCR.

Gene symbol	Species	Accession number	Forward primer sequence (F, 5' - 3') Reverse primer sequence (R, 5' - 3')
Aif1 (Iba1)	mouse	NM_001361501.1	F: CAA CAA GCA ATT CCT CGA TGA TCC R: CTC CAG CAT TCG CTT CAA GG
B2m	mouse	NM_009735.3	F: TTC TGG TGC TTG TCT CAC TGA R: CAG TAT GTT CGG CTT CCC ATT C
FosB	mouse	NM_001347586.1 NM_008036.2	F: CGA GAA GAG ACA CTT ACC CCA R: GTT TCC GCC TGA AGT CGA TCT
Gapdh	mouse	AY618199.1	F: GTG GAG TCA TAC TGG AAC ATG TAG R: AAT GGT GAA GGT CGG TGT G
Gfap	mouse	NM_010277.3	F: CGG AGA CGC ATC ACC TCT G R: TGG AGG AGT CAT TCG AGA CAA
Hprt1	mouse	NM_013556.2	F: CCC CAA AAT GGT TAA GGT TGC R: AAC AAA GTC TGG CCT GTA TCC
Ppia	mouse	NM_008907.2	F: GAG CTG TTT GCA GAC AAA GTT R: CCC TGG CAC ATG AAT CTT GG
Tac4	mouse	NM_053093.2	F: CCG TGA ACC TGA AGG GAA T R: CCC ATC AGA CCA TAG AAC TGG
Aif1 (Iba1)	rat	NM_017196; XM_006256062; XM_006256065; XM_006256061; XM_006256063	F: TCC GAG GAG ACG TTC AGT TA R: GTT GGC TTC TGG TGT TCT TTG
B2m	rat	NM_012512	F: CCC ACC CTC ATG GCT ACT TC R: CCA CTT CAC TTC ACT CTG GCA
Calca (Cgrp)	rat	NM_017338; NM_001033955; NM_001033956; XM_008759676	F: TTG TCA GCA TCT TGC TCC TGT AC R: GCC TGG GCT GCT TTC CA
FosB	rat	NM_001256509	F: CAC TTC CAA CAT GTC TCC TCT C R: CCA CCC AGT CAC ACT TAC TTA C
Gapdh	rat	NM_017008	F: GTA ACC AGG CGT CCG ATA C R: TCC TCT GCT CCT CCC TGT TC
Gfap	rat	NM_017009	F: GAT CCG AGA AAC CAG CCT GGA C R: TGG GCA CAC CTC ACA TCA CAT
Gpr39	rat	NM_001114392; NM_001100943	F: GTC TTC CAG TCC AGC ATC TTT R: GCT TGC TCT TCA TTA GCA CTT TC
Hprt1	rat	NM_012583	F: GCT TTT CCA ACT TTC GCT GAT G R: GGT GAA AAG GAC CTC TCG AAG
Kiss1	rat	NM_181692; XM_008769443; XM_017598697	F: ATG ATC TCG CTG GCT TCT TGG R: GGT TCA CCA CAG GTG CCA TTT T
Kiss1r	rat	NM_001301151; NM_023992	F: TTC TAC ATC GCT AAC CTG GC R: AAA GTG GCA CAT GTG GCT TG

Lkaaear1	rat	NM_001106551; XM_006235763; XM_008762502; XM_006235764; XM_008762501	F: CTC TCC TGA TCC AGA AGC AAA G R: GTC CAA AGG ATC AGG GAT CTT C
Neurod2	rat	NM_019326	F: GGC TCT CTC GGA GAT CTT GC R: TGC TCC GTG AGG AAG TTA CG
Ppia	rat	NM_017101	F: CCA TTA TGG CGT GTG AAG TC R: GCA GAC AAA GTT CCA AAG ACA G
Tac4	rat	NM_172328.2	F: CTG TCC CCA GCA TCG AAC TT R: CCA GCT GAT ACC CCG TTC TC

Appendix Table 3. Probes applied dilutions of fluorophores.

Target	Catalog number	Fluorophores	Dilutions
Mm-Aif1 (Iba1)	319141	TSA Plus Fluorescein	1:750
Mm-Gfap	313211-C3	TSA Plus Cyanine 3	1:3000
Mm-Olig2	447091-C3	TSA Plus Cyanine 5	1:3000
Mm-Tac4	449651-C2	TSA Plus Cyanine 3	1:750
Mm-Kcnn3	427961	TSA Plus Fluorescein	1:750
Mm-Rbfox3	313311-C3	TSA Plus Cyanine 5	1:750
Mm-3-plex positive ctrl probes	320881	TSA Plus Fluorescein, Cyanine 3, 5	1:750
3-plex negative ctrl probes	320871		1:750

Appendix Table 4. The top 25 up-and downregulated genes. ID: microarray feature identifier; FC: expression ratio (fold-change) between CFA-treated and contralateral sample groups.

ID	FC	P-value	SystematicName	GeneSymbol	Description	EnsemblID
948	**5.20**	0.0381	MRAK049104	**NA**	**lncRNA (chromosome 1)**	NA
11131	**4.55**	0.0353	TC598318	**NA**	**NA**	NA
9725	**4.35**	0.0214	NM_199489.3	**Ccr7**	**C-C motif chemokine receptor 7**	ENSRNOG00000010665
5534	**4.34**	0.0076	NM_001011951.1	**Sf3b4**	**splicing factor 3b, subunit 4**	ENSRNOG00000021181
12278	**4.29**	0.0010	NM_001037518.1	**Defb23**	**defensin beta 23**	ENSRNOG00000023477
519	**4.28**	0.0218	NM_001000099.1	**Olr1640**	**olfactory receptor 1640**	ENSRNOG00000048857
13893	**4.13**	0.0236	NM_001106821.1	**Atm**	**ATM serine/threonine kinase**	ENSRNOG00000029773
40839	**4.08**	0.0135	NM_134399.2	**Mk1**	**Mk1 protein**	ENSRNOG00000019657
6132	**4.01**	0.0172	NM_001106551.1	**Lkaaear1**	**LKAAEAR motif containing 1**	ENSRNOG00000024815
10158	**3.83**	0.0477	NM_001013956.1	**RGD1309049**	**similar to RIKEN cDNA 4933415F23**	ENSRNOG00000014123
10494	**3.80**	0.0138	NM_001013147.1	**Axl**	**Axl receptor tyrosine kinase**	ENSRNOG00000020716
2571	**3.78**	0.0404	NM_019128.4	**Ina**	**internexin neuronal intermediate filament protein, alpha**	ENSRNOG00000020248
12538	**3.73**	0.0232	NM_198133.2	**Uts2b**	**urotensin 2B**	ENSRNOG00000038512
3346	**3.72**	0.0156	NM_001047878.1	**F5**	**coagulation factor V**	ENSRNOG00000057855
6931	**3.71**	0.0198	uc.339+	**NA**	**lncRNA (chromosome 7)**	NA
5544	**3.70**	0.0316	NM_001001034.1	**Olr199**	**olfactory receptor 199**	ENSRNOG00000029755

9136	**3.69**	0.0250	NM_012735.1	**Hk2**	**hexokinase 2**	ENSRNOG00000006116
4102	**3.67**	0.0212	NM_001001010.1	**Olr283**	**olfactory receptor 283**	ENSRNOG00000030782
3492	**3.67**	0.0159	uc.470+	**NA**	**lncRNA (chromosome X)**	NA
1789	**3.66**	0.0240	XR_005913	**NA**	**lncRNA (chromosome 16)**	NA
4451	**3.64**	0.0064	NM_173305.1	**Hsd17b6**	**hydroxysteroid (17-beta) dehydrogenase 6**	ENSRNOG00000002597
11677	**3.63**	0.0013	NM_001000387.1	**Olr416**	**olfactory receptor 416**	ENSRNOG00000029069
6676	**3.62**	0.0322	NM_001107582.2	**Pdcd1lg2**	**programmed cell death 1 ligand 2**	ENSRNOG00000016136
9724	**3.61**	0.0247	NM_153466.1	**Gzmf**	**granzyme F**	ENSRNOG00000028810
5556	**3.60**	0.0103	NM_001099514.1	**Vom2r48**	**vomeronasal 2 receptor, 48**	ENSRNOG00000028538
39867	**-3.50**	0.0007	NM_001047931.1	**LOC498460**	**LRRGT00055**	ENSRNOG00000028821
41314	**-3.62**	0.0313	NM_001080939.1	**Tas2r109**	**taste receptor, type 2, member 109**	ENSRNOG00000032724
38176	**-3.63**	0.0005	NM_001164826.1	**RT1-Db2**	**RT1 class II, locus Db2**	ENSRNOG00000030431
44381	**-3.64**	0.0049	NM_001130497.1	**Pnpla5**	**patatin-like phospholipase domain containing 5**	ENSRNOG00000022296
35607	**-3.67**	0.0016	MRAK078136	**NA**	**lncRNA (chromosome 1)**	NA
16902	**-3.73**	0.0186	uc.163+	**NA**	**NA**	NA
41319	**-3.76**	0.0102	NM_001012084.1	**Adh6**	**alcohol dehidrogenase 6**	NA
37492	**-3.78**	0.0025	NM_001003979.1	**Tmprss11c**	**transmembrane protease, serine 11C**	ENSRNOG00000033910
36560	**-3.87**	0.0023	NM_001000338.1	**Olr619**	**olfactory receptor 619**	ENSRNOG00000021473

43356	**-4.15**	0.0009	NM_022673.2	**Mecp2**	**methyl CpG binding protein 2**	ENSRNOG00000056659
42598	**-4.17**	0.0001	NM_001017480.1	**Hoxb7**	**homeo box B7**	ENSRNOG00000007611
38934	**-4.62**	0.0036	NM_052808.1	**Bpifa2**	**BPI fold containing family A, member 2**	ENSRNOG00000013540
38765	**-4.64**	0.0056	NM_001000575.1	**Olr741**	**olfactory receptor 741**	ENSRNOG00000053815
37233	**-4.69**	0.0053	NM_012689.1	**Esr1**	**estrogen receptor 1**	ENSRNOG00000019358
43878	**-4.71**	0.0017	NM_001000307.1	**Olr485**	**olfactory receptor 485**	ENSRNOG00000009747
38741	**-4.80**	0.0043	NM_001001355.1	**Olr905**	**olfactory receptor 905**	ENSRNOG00000057325
44809	**-4.86**	0.0006	NM_001109459.1	**LOC685171**	**similar to protein disulfide isomerase-associated 6**	ENSRNOG00000058543
40038	**-4.88**	0.0012	uc.400-	**NA**	**lncRNA (chromosome 19)**	NA
43786	**-5.14**	0.0023	NM_001109285.1	**C2cd4c**	**C2 calcium-dependent domain containing 4C**	ENSRNOG00000008026
43442	**-5.40**	0.0004	uc.225+	**NA**	**lncRNA (chromosome 4)**	NA
40720	**-5.65**	0.0041	NM_001000692.1	**Olr25**	**olfactory receptor 25**	ENSRNOG00000046609
41996	**-6.14**	0.0014	uc.47-	**NA**	**lncRNA (chromosome 6)**	NA
43609	**-6.60**	0.0018	NM_001000394.1	**Olr428**	**olfactory receptor 428**	ENSRNOG00000030460
36293	**-8.03**	0.0021	XR_008902	**NA**	**lncRNA (chromosome 19)**	NA
44472	**-9.20**	0.0012	NM_019326.1	**Neurod2**	**neuronal differentiation 2**	ENSRNOG00000028417

Appendix Table 5. Results of gene set enrichment analysis of a subset of genes DE between the control (contralateral) and seven-day CFA (ipsilateral) samples from TG as detected by microarray. Enrichment analysis for the differentially expressed filtered gene lists tests whether the genes within a certain KEGG or Reactome pathway or GO term are statistically over-represented in a given comparison.

	Term	Annotated	Significant	Expected	P-value
GO.ID	**Biological process**				
GO:0008202	steroid metabolic process	223	3	0.3	0.0031
GO:0005975	carbohydrate metabolic process	400	3	0.54	0.0155
GO:0007600	sensory perception	1453	5	1.97	0.0380
GO:0050911	detection of chemical stimulus involved in sensory perception of smell	1059	4	1.43	0.0487
	Cellular component				
GO:0005576	extracellular region	3051	6	3.95	0.181
GO:0005615	extracellular space	2639	5	3.41	0.243
GO:0071944	cell periphery	4053	7	5.24	0.246
GO:0044421	extracellular region part	2763	5	3.57	0.276
GO:0016021	integral component of membrane	4420	7	5.72	0.334
GO:0031224	intrinsic component of membrane	4505	7	5.83	0.356
GO:0044425	membrane part	5350	8	6.92	0.381
GO:0005886	plasma membrane	3959	6	5.12	0.407
GO:0044464	cell part	11048	15	14.29	0.476
GO:0005623	Cell	11071	15	14.32	0.486

	Molecular function				
GO:0004984	olfactory receptor activity	1059	4	1.21	0.0269
GO:0099600	transmembrane receptor activity	1749	5	2	0.0374
KEGG.ID	**KEGG Pathway Term**				
604	Glycosphingolipid biosynthesis - ganglio series	12	1	0.012067578	0.012014279
603	Glycosphingolipid biosynthesis - globo series	13	1	0.01307321	0.013010232
533	Glycosaminoglycan biosynthesis - keratan sulfate	14	1	0.014078842	0.014005382
512	Mucin type O-Glycan biosynthesis	20	1	0.020112631	0.019959439
500	Starch and sucrose metabolism	28	1	0.028157683	0.027853402
4740	Olfactory transduction	842	3	0.846741754	0.036986751
Reactome.ID	**Downregulated Reactome Term**	**GeneRatio**	**BgRatio**	**P-value**	
R-RNO-8957275	Post-translational protein phosphorylation	2/5	74/5483	0.001750444	
R-RNO-381426	Regulation of Insulin-like Growth Factor (IGF) transport and uptake by Insulin-like Growth Factor Binding Proteins (IGFBPs)	2/5	82/5483	0.002145931	

Appendix Table 6. Top 10 differentially expressed genes in interictal vs healthy comparison. Avg rank: average rank of p-value and fold change (FC) ranks; ID: Ensembl gene identifier.

Interictal vs Healthy						
Avg rank	**ID**	**FC**	**P-Value**	**adj. P-value**	**Description**	**geneName**
1	ENSG00000125538	13.6	1.27E-04	0.98947	interleukin 1 beta	IL1B
2	ENSG00000073756	7.8	4.85E-04	1	prostaglandin-endoperoxide synthase 2 (cyclooxygenase 2)	PTGS2 (COX2)
3	ENSG00000169429	7.0	9.72E-04	1	C-X-C motif chemokine ligand 8	IL8
4	ENSG00000232810	7.0	1.19E-03	1	tumor necrosis factor	TNF
5	ENSG00000163739	8.7	2.80E-03	1	C-X-C motif chemokine ligand 1	CXCL1
6	ENSG00000165685	5.3	3.84E-04	1	transmembrane protein 52B	TMEM52B
7	ENSG00000205021	8.5	2.91E-03	1	C-C Motif Chemokine Ligand 3 Like 1	CCL3L1
8	ENSG00000205595	7.0	2.55E-03	1	amphiregulin B	AREGB
9	ENSG00000120738	6.1	1.56E-03	1	early growth response 1	EGR1
10	ENSG00000124882	8.4	3.62E-03	1	epiregulin	EREG

Appendix Table 7. Top 10 differentially expressed genes in ictal vs interictal comparison. Avg rank: average rank of p-value and fold change (FC) ranks; ID: Ensembl gene identifier.

Ictal vs Interictal						
Avg rank	**ID**	**FC**	**P-value**	**adj. P-value**	**Description**	**geneName**
1	ENSG00000179172	-3.2	1.09E-07	0.0018	heterogeneous nuclear ribonucleoprotein C like 1	HNRNPCL1
2	ENSG00000267908	-2.8	5.96E-04	1	zinc finger and SCAN domain containing 5D pseudogene	ZSCAN5D
3	ENSG00000268154	-3.0	3.48E-03	1	Metazoan signal recognition particle RNA	AL591806.1
4	ENSG00000248874	3.4	4.86E-03	1	chromosome 5 open reading frame 17 (putative)	C5orf17
5	ENSG00000229937	2.6	1.60E-03	1	phosphoribosyl pyrophosphate synthetase 1 like 1	PRPS1L1
6	ENSG00000180389	-2.5	2.05E-04	1	ATP synthase F1 subunit epsilon pseudogene 2	ATP5EP2
7	ENSG00000255582	3.1	4.90E-03	1	olfactory receptor family 10 subfamily G member 2	OR10G2
8	ENSG00000133136	-2.5	1.47E-03	1	G protein subunit gamma 5 pseudogene 2	GNG5P2
9	ENSG00000120156	2.7	4.55E-03	1	TEK receptor tyrosine kinase	TEK
10	ENSG00000125207	-2.6	4.47E-03	1	piwi like RNA-mediated gene silencing 1	PIWIL1

Appendix Table 8. Top 10 differentially expressed genes in ictal vs healthy comparison. Avg rank: average rank of p-value and fold change (FC) ranks; ID: Ensembl gene identifier.

Ictal vs Healthy						
Avg Rank	**ID**	**FC**	**P-Value**	**adj. P-value**	**Description**	**geneName**
1	ENSG00000125538	21.7	1.14E-04	1	interleukin 1 beta	IL1B
2	ENSG00000073756	10.8	3.27E-04	1	prostaglandin-endoperoxide synthase 2 (cyclooxygenase 2)	PTGS2 (COX2)
3	ENSG00000205021	13.9	9.44E-04	1	C-C Motif Chemokine Ligand 3 Like 1	CCL3L1
4	ENSG00000232810	10.8	5.02E-04	1	tumor necrosis factor	TNF
5	ENSG00000124882	11.8	1.33E-03	1	epiregulin	EREG
6	ENSG00000256515	14.5	1.72E-03	1	C-C Motif Chemokine Ligand 3 Like 3	CCL3L3
7	ENSG00000197262	8.4	1.18E-03	1	C-C Motif Chemokine Ligand 4 Like 2	CCL4L2
8	ENSG00000006075	12.6	1.83E-03	1	C-C Motif Chemokine Ligand 3	CCL3
9	ENSG00000169429	9.2	1.43E-03	1	C-X-C motif chemokine ligand 8	IL8
10	ENSG00000205020	8.2	1.35E-03	1	C-C Motif Chemokine Ligand 4 Like 1	CCL4L1

Appendix Table 9. Functional enrichment results of migraine study data in all group comparisons. DE list enrichment: overrepresentation of functional terms in the differentially expressed gene list. Ranked list enrichment: enrichment of genes associated with a specific pathway towards the top of the ranked whole data. GO: gene ontology, BP: biological process, CC: cellular component, MF molecular function. KEGG: Kyoto Encyclopedia of Genes and Genomes. R: Reactome database. Significant: number of statistically associated genes with the given term.

Interictal vs healthy			**Ictal vs interictal**			**Ictal vs healthy**		
ID	DE list enrichment	p-value	ID	DE list enrichment	p-value	ID	DE list enrichment	p-value
GO:0006954 BP	inflammatory response	2.60E-14	GO:1902305 BP	regulation of sodium ion transmembrane transport	2.60E-14	GO:1901700 BP	response to oxygen-containing compound	2.60E-14
GO:0005126 MF	cytokine receptor binding	6.10E-09	GO:0070382 CC	exocytic vesicle	0.0019	GO:0070851 MF	growth factor receptor binding	0.000019
GO:0042379 MF	chemokine receptor binding	8.90E-07	GO:0005179	hormone activity	0.00924			
R-HSA-6783783	Interleukin-10 signaling	2.60E-14	KEGG 4742	Taste transduction	0.019843	R-HSA-6783783	Interleukin-10 signaling	2.60E-14
	Ranked list enrichment	p-value		Ranked list enrichment	p-value	R-HSA-6785807	Interleukin-4 and Interleukin-13 signaling	1.71E-09
GO:0022900 BP	electron transport chain	2.60E-14	GO:0005746 CC	mitochondrial respiratory chain	2.60E-14	R-HSA-179812	GRB2 events in EGFR signaling	0.00013
GO:0005746 CC	mitochondrial respiratory chain	2.17E-05	GO:0005125 MF	cytokine activity	0.000001		Ranked list enrichment	p-value
GO:0016684 MF	oxidoreductase activity	0.000016	GO:0005179 MF	hormone activity	6.95E-05	GO:0070098 BP	chemokine-mediated signaling pathway	2.60E-14
KEGG 190	Oxidative phosphorylation	8.82E-06	GO:0030594 MF	neurotransmitter receptor activity	0.000107	KEGG 4080	Neuroactive ligand-receptor interaction	1.86E-14
KEGG 4080	Neuroactive ligand-receptor interaction	2.28E-05	GO:0004984 MF	olfactory receptor activity	0.000433	KEGG 4740	Olfactory transduction	0.000817
			KEGG 4080	Neuroactive ligand-receptor interaction	9.04E-05			
			KEGG 190	Oxidative phosphorylation	0.000845			
			KEGG 140	Steroid hormone biosynthesis	0.00112			

List of Publications

Articles related to the thesis

Aczél, T. *, Kun, J. *, Szőke, É., Rauch, T., Junttila, S., Gyenesei, A., Bölcskei, K., & Helyes, Z. (2018). Transcriptional Alterations in the Trigeminal Ganglia, Nucleus and Peripheral Blood Mononuclear Cells in a Rat Orofacial Pain Model. Frontiers in molecular neuroscience, 11, 219. https://doi.org/10.3389/fnmol.2018.00219 (IF: 3.720)

Aczél, T., Kecskés, A., Kun, J., Szenthe, K., Bánáti, F., Szathmary, S., Herczeg, R., Urbán, P., Gyenesei, A., Gaszner, B., Helyes, Z., & Bölcskei, K. (2020). Hemokinin-1 Gene Expression Is Upregulated in Trigeminal Ganglia in an Inflammatory Orofacial Pain Model: Potential Role in Peripheral Sensitization. International journal of molecular sciences, 21(8), 2938. https://doi.org/10.3390/ijms21082938 (IF: 5.923)

Aczél, T. *, Körtési, T. *, Kun, J. *, Urbán, P., Bauer, W., Herczeg, R., Farkas, R., Kovács, K., Vásárhelyi, B., Karvaly, G. B., Gyenesei, A., Tuka, B., Tajti, J., Vécsei, L., Bölcskei, K., & Helyes, Z. (2021). Identification of disease- and headache-specific mediators and pathways in migraine using blood transcriptomic and metabolomic analysis. The journal of headache and pain, 22(1), 117. https://doi.org/10.1186/s10194-021-01285-9 (IF: 7.277)

Cumulative impact factor (without citable abstracts): **16.92**

Articles not related to the thesis

Takács-Lovász, K., Kun, J., **Aczél, T.**, Urbán, P., Gyenesei, A., Bölcskei, K., Szőke, É., & Helyes, Z. (2022). PACAP-38 Induces Transcriptomic Changes in Rat Trigeminal Ganglion Cells Related to Neuroinflammation and Altered Mitochondrial Function Presumably via PAC1/VPAC2 Receptor-Independent Mechanism. International journal of molecular sciences, 23(4), 2120. https://doi.org/10.3390/ijms23042120 (IF: 5.923)

Nemes, B., Bölcskei, K., Kecskés, A., Kormos, V., Gaszner, B., **Aczél, T.**, Hegedüs, D., Pintér, E., Helyes, Z., & Sándor, Z. (2021). Human Somatostatin SST4 Receptor Transgenic Mice: Construction and Brain Expression Pattern Characterization. International journal of molecular sciences, 22(7), 3758. https://doi.org/10.3390/ijms22073758 (IF: 5.923)

Kovács-Ábrahám, Z., **Aczél, T.**, Jancsó, G., Horváth-Szalai, Z., Nagy, L., Tóth, I., Nagy, B., Molnár, T., & Szabó, P. (2021). Cerebral and Systemic Stress Parameters in Correlation with Jugulo-Arterial CO2 Gap as a Marker of Cerebral Perfusion during Carotid Endarterectomy. Journal of clinical medicine, 10(23), 5479. https://doi.org/10.3390/jcm10235479 (IF: 4.241)

Pohóczky, K., Kun, J., Szentes, N., **Aczél, T.**, Urbán, P., Gyenesei, A., Bölcskei, K., Szőke, É., Sensi, S., Dénes, Á., Goebel, A., Tékus, V., Helyes, Z. Discovery of novel targets in a Complex Regional Pain Syndrome mouse model by transcriptomics: TNF and JAK-STAT pathways. *Under revision in Pharmacological research. (IF:7.68)*

Cumulative impact factor of all publications (without citable abstracts): **33.007**

Citations MTMT: 18

Citations Google Scholar: 28

Oral presentations related to the thesis

2019- European Pain School (EPS), Siena, Italy
Investigation of gene expression changes in animal models of trigeminal sensitization
Timea Aczél, Angéla Kecskés, Éva Szőke, József Kun, Balázs Gaszner, Zsuzsanna Helyes, Kata Bölcskei

2018 – III. Neuroscience Center PhD and TDK Conference, Pécs, Hungary
Génexpresszió-változások vizsgálata trigeminális szenzitizációban (3rd prize)
Timea Aczél, József Kun, Eva Szőke, Tibor Rauch, Sini Junttila, Attila Gyenesei, Kata Bölcskei, Zsuzsanna Helyes

2018 – Pain Mechanisms and Therapeutics Conference, Taormina, Sicily
Temporal changes of gene expression in trigeminal ganglia, trigeminal nucleus caudalis and peripheral blood mononuclear cells in a rodent orofacial pain model.
Timea Aczél, József Kun, Eva Szőke, Tibor Rauch, Sini Junttila, Attila Gyenesei, Kata Bölcskei, Zsuzsanna Helyes

Oral presentations not related to the thesis

2016 – V. Interdisciplinary Doctoral Conference, Pécs, Hungary
Cortical spreading depression-induced blood flow changes measured by Laser Speckle Contrast imaging in Transient Receptor Potential Ankyrin 1 (TRPA1) and Vanilloid 1 (TRPV1) deficient mice
Timea Aczél, Kata Bölcskei, Zsuzsanna Helyes, Erika Pintér

2014 – VI. EFIS-EJI South Eastern European Immunology School (SEEIS2014), Timisoara, Romania
Cardiomyocyte inflammation model in Sirt3$^{-/-}$ mouse
Timea Aczél, Manuel Vázquez-Carrera, Xavier Palomer, Előd Nagy

2014 – The 21st Students' Scientific Conference, Târgu Mures, Romania
Sirt3$^{-/-}$ egér szívizomsejt hipertrófia-gyulladás modellje (1st prize)
Timea Aczél, Manuel Vázquez-Carrera, Xavier Palomer, Előd Nagy
abstract: Bulletin of Medical Sciences – Orvostudományi Értesítő 87 (2014)

Poster presentations related to the thesis

2019 – Hungarian Pain Society's Conference, Szeged, Hungary
Tac4 szerepének vizsgálata orofaciális és dura gyulladással kiváltott trigeminális szenzitizáció állatmodelljeiben
Timea Aczél, Angéla Kecskés, Éva Szőke, József Kun, Balázs Gaszner, Zsuzsanna Helyes, Kata Bölcskei

2019 – The 7th Mediterranean Neuroscience Conference, Marrakesh, Morocco
Hemokinin-1 is involved in trigeminal sensitization
Timea Aczél, Angéla Kecskés, Éva Szőke, József Kun, Balázs Gaszner, Zsuzsanna Helyes, Kata Bölcskei

2019 – III. Gyógyszer Innovációs Kongresszus, Gárdony, Hungary
Orofaciális gyulladással kiváltott génexpressziós változások Tac4 génhiányos egerekben
Timea Aczél, Éva Szőke, József Kun, Anikó Perkecz, Zsuzsanna Helyes, Kata Bölcskei

2017 – Hungarian Physiological Society's Conference, Debrecen, Hungary
Trigeminális neuronok és perifériás leukociták génexpresszió-változásai patkány orofaciális fájdalommodellben (Society's Main Prize)
Timea Aczél, József Kun, Éva Szőke, Tibor Rauch, Kata Bölcskei, Zsuzsanna Helyes

2017 – 7th BBBB International Conference on Pharmaceutical Sciences, Balatonfüred, Hungary
Time course of gene expression changes in trigeminal neurones and peripheral blood mononuclear cells in a rat orofacial pain model
Timea Aczél, József Kun, Éva Szőke, Tibor Rauch, Kata Bölcskei, Zsuzsanna Helyes
abstract: Acta Pharmaceutica Hungarica 87, (043) 85–244. (2017) (IF:0.12)

2017 – Federation of European Neuroscience Societies FENS Regional Meeting, Pécs, Hungary
Gene expression analysis of trigeminal ganglia and peripheral blood mononuclear cells in a rat orofacial pain model
Timea Aczél, József Kun, Éva Szőke, Tibor Rauch, Kata Bölcskei, Zsuzsanna Helyes

Poster presentations not related to the thesis

2018 – Association of Medical Schools in Europe Conference, Pécs, Hungary
Role of sirtuin 1 activation in trigeminal sensitization
Timea Aczél, Maja Payrits, Éva Szőke, József Kun, Zsuzsanna Helyes, Kata Bölcskei

2018 – Hungarian Physiological Society's Conference, Szeged, Hungary
A sirtuin 1 aktiváció szerepe trigeminalis neuronok szenzitizációjában
Timea Aczél, Maja Payrits, Éva Szőke, József Kun, Zsuzsanna Helyes, Kata Bölcskei

2016 – Hungarian Physiological Society's Conference, Pécs, Hungary
Agykérgi kúszó depolarizáció által kiváltott perfúzióváltozások és a Tranziens Receptor Potenciál Ankyrin 1 (TRPA1) és Vanilloid 1 (TRPV1) ioncsatornák szerepének vizsgálata egérmodellben
Timea Aczél, Kata Bölcskei, Zsuzsanna Helyes, Erika Pintér

Other contribution to oral presentations

2018 - 22nd International Symposium on Regulatory Peptides, Acapulco, Mexico
Neuropeptide-mediated sensitization mechanisms in models of trigeminovascular activation: focus on PACAP and hemokinin-1
Zsuzsanna Helyes, Éva Szőke, József Kun, Timea Aczél, Maja Mayrits, Tibor Rauch, Sini Junttilla, Attila Gyenesei, Adrienn Markovics, Viktória Kormos, Balázs Gaszner, Sándor Farkas, Dóra Reglődi, Kata Bölcskei

2017 - Hungarian Pain Society's Conference, Szeged, Hungary
Génexpresszió-változások patkány orofaciális fájdalommodellben
Bölcskei Kata, Aczél Timea, Kun József, Szőke Éva, Rauch Tibor, Helyes Zsuzsanna

2017 - 13th International Symposium on VIP, PACAP and Related Peptides, Hong Kong
Hemokinin-1 activates cultured trigeminal neurones its mRNA Tac4 is upregulated in a rat orofacial pain model
József Kun, Timea Aczél, Éva Szőke, Maja Payrits, Kata Bölcskei, Zsuzsanna Helyes

2017 – Magyar Élettani Társaság, a Magyar Kísérletes és Klinikai Farmakológiai Társaság és a Magyar Mikocirkulációs és Vaszkuláris Biológiai Tárasaság közös Vándorgyűlése, Debrecen, Hungary
A hemokinin-1 szerepének vizsgálata akut és krónikus artritisz egérmodelljeiben
Szőke Éva, Borbély Éva, Payrits Maja, Sághy Éva, Bölcskei Kata, Kun József, Aczél Timea, Békefi Katinka, Alexandra Berger, Christopher J. Paige, Mócsai Attila, Csepregi Janka, Jason J. McDougall, Pintér Erika, Zsuzsanna Helyes

2014 - University Days, Târgu Mures, Romania
Characterization of cytokine response in a monoiodoacetate-induced rat osteoarthritis model
Nagy Előd, Vajda Enikő, Aczél Timea, Farr Ana-Maria, Muntean Daniela-Lucia

Other contribution to poster presentations

2021 - Medical Conference for PhD Students and Experts of Clinical Sciences
Transcriptomic changes in trigeminal ganglion cells induced by pituitary adenylate cyclase activating polypeptide (PACAP)-38 or PACAP-38 treatment
Krisztina Takács-Lovász, Timea Aczél, József Kun, Péter Urbán, Attila Gyenesei, Kata Bölcskei, Dóra Reglődi, Éva Szőke, Zsuzsanna Helyes

2020 – Federation of European Neuroscience Societies FENS Virtual Forum
Transcriptome analysis of peripheral blood mononuclear cells isolated from migraine patients during and between headaches: a pilot study
Kata Bölcskei, Timea Aczél, József Kun, Tamás Körtési, Péter Urbán, Attila Gyenesei, Bernadett Tuka, János Tajti, László Vécsei, Zsuzsanna Helyes

2019 – 11th congress of the European Pain Federation EFIC, Valencia Spain
Involvement of Hemokinin-1 in trigeminal sensitization after orofacial inflammation
Kata Bölcskei, Timea Aczél, József Kun, Éva Szőke, Zsuzsanna Helyes

2019 – Summer School on Stress, St. Petersburg, Russia
Novel humanized model for pharmacological research: generating human somatostatin receptor 4 (hSSTR4) expressing transgenic mice
Balázs Nemes, Kata Bölcskei, Timea Aczél, Adnan Ahmad Alkurdi, Y. Abuawwad, András Dinnyés, Julianna Kobolák, Zoltán Sándor, Erika Pintér, Zsuzsanna

2019 – Hungarian Physiological Society's Conference, Budapest, Hungary
Humanizált szomatostatin receptor 4 expresszáló transzgenikus egerek: egy új modell a transzlációs medicinában
Balázs Nemes, Kata Bölcskei, Timea Aczél, Adnan Ahmad Alkurdi, Y. Abuawwad, András Dinnyés, Julianna Kobolák, Zoltán Sándor, Erika Pintér, Zsuzsanna Helyes

2019 - 16th Annual Conference of the Hungarian Neuroscience Society Hungarian Academy of Sciences, Debrecen, Hungary
Transgenetic mice expressing the human somatostatin receptor 4: a novel humanized model for translational research
Balázs Nemes, Kata Bölcskei, Timea Aczél, Adnan Ahmad Alkurdi, Erika Pintér, Zsuzsanna Helyes, Zoltán Sándor

2017 – Federation of European Neuroscience Societies FENS Regional Meeting, Pécs, Hungary
Expression and inflammation-induced up-regulation of hemokinin-1 in the trigeminal system, and its effect on cultured trigeminal ganglion neurons
József Kun, Timea Aczél, Éva Szőke, Maja Payrits, Kata Bölcskei, Zsuzsanna Helyes

frontiers in Molecular Neuroscience

ORIGINAL RESEARCH
published: 26 June 2018
doi: 10.3389/fnmol.2018.00219

Transcriptional Alterations in the Trigeminal Ganglia, Nucleus and Peripheral Blood Mononuclear Cells in a Rat Orofacial Pain Model

Timea Aczél[1,2†], *József Kun*[1,2,3†], *Éva Szőke*[1,2,3], *Tibor Rauch*[4], *Sini Junttila*[5], *Attila Gyenesei*[2,5], *Kata Bölcskei*[1,2†] *and Zsuzsanna Helyes*[1,2,3*†]

[1] *Department of Pharmacology and Pharmacotherapy, Medical School, University of Pécs, Pécs, Hungary,* [2] *Szentágothai Research Centre and Centre for Neuroscience, University of Pécs, Pécs, Hungary,* [3] *MTA-PTE Chronic Pain Research Group, Pécs, Hungary,* [4] *Section of Molecular Medicine, Rush University Medical Center, Chicago, IL, United States,* [5] *Bioinformatics and Scientific Computing, Vienna Biocenter Core Facilities, Vienna, Austria*

OPEN ACCESS

Edited by:
Hermona Soreq,
Hebrew University of Jerusalem, Israel

Reviewed by:
Parisa Gazerani,
Aalborg University, Denmark
Hans-Georg Schaible,
Friedrich-Schiller-Universität-Jena, Germany

***Correspondence:**
Zsuzsanna Helyes
zsuzsanna.helyes@aok.pte.hu

[†] *These authors have contributed equally to this work.*

Received: *04 April 2018*
Accepted: *06 June 2018*
Published: *26 June 2018*

Citation:
Aczél T, Kun J, Szőke É, Rauch T, Junttila S, Gyenesei A, Bölcskei K and Helyes Z (2018) Transcriptional Alterations in the Trigeminal Ganglia, Nucleus and Peripheral Blood Mononuclear Cells in a Rat Orofacial Pain Model. Front. Mol. Neurosci. 11:219. doi: 10.3389/fnmol.2018.00219

Orofacial pain and headache disorders are among the most debilitating pain conditions. While the pathophysiological basis of these disorders may be diverse, it is generally accepted that a common mechanism behind the arising pain is the sensitization of extra- and intracranial trigeminal primary afferents. In the present study we investigated gene expression changes in the trigeminal ganglia (TRG), trigeminal nucleus caudalis (TNC) and peripheral blood mononuclear cells (PBMC) evoked by Complete Freund's Adjuvant (CFA)-induced orofacial inflammation in rats, as a model of trigeminal sensitization. Microarray analysis revealed 512 differentially expressed genes between the ipsi- and contralateral TRG samples 7 days after CFA injection. Time-dependent expression changes of G-protein coupled receptor 39 (*Gpr39*), kisspeptin-1 receptor (*Kiss1r*), kisspeptin (*Kiss1*), as well as synaptic plasticity-associated Lkaaear1 (*Lkr*) and Neurod2 mRNA were described on the basis of qPCR results. The greatest alterations were observed on day 3 ipsilaterally, when orofacial mechanical allodynia reached its maximum. This corresponded well with patterns of neuronal (*Fosb*), microglia (*Iba1*), and astrocyte (*Gfap*) activation markers in both TRG and TNC, and interestingly also in PBMCs. This is the first description of up- and downregulated genes both in primary and secondary sensory neurones of the trigeminovascular system that might play important roles in neuroinflammatory activation mechanisms. We are the first to show transcriptomic alterations in the PBMCs that are similar to the neuronal changes. These results open new perspectives and initiate further investigations in the research of trigeminal pain disorders.

Keywords: orofacial pain, trigeminovascular system, Kisspeptin-1 receptor, *Gpr39, Neurod2*, differential gene expression data analysis

INTRODUCTION

Orofacial pain and headache disorders are among the most debilitating pain conditions. While the pathophysiological basis of these disorders may be diverse, it is generally accepted that a common mechanism behind the arising pain is the sensitization of extra- and intracranial trigeminal primary afferents. The trigeminal nerve provides most of the sensory innervation to the face and oral cavity as well as the meninges where the nociceptive primary afferents are closely associated with the vasculature. The cell bodies of these neurons are located in the trigeminal ganglion (TRG) and their central projections terminate in the trigeminal nucleus caudalis (TNC). It has been described that there is convergence of extra- and intracranial primary afferents in the TNC (Burstein et al., 1998). Sensitization of these secondary nociceptive neurons might be responsible for the phenomenon of the facial allodynia developing in primary headaches (Burstein et al., 2000). A similar mechanism could induce the headache associated with disorders of extracranial structures. Inflammation of the temporal artery, temporomandibular joint, sinuses or orbit can induce headache which could have the same characteristics as the primary disorders. Co-morbidity of migraine and temporomandibular disorders has also been reported (Romero-Reyes and Uyanik, 2014).

Inflammatory pain models adapted to the orofacial area induce trigeminal sensitization and can constitute a possible way to understand the mechanisms of pain associated with orofacial disorders and headaches (Krzyzanowska et al., 2011; Krzyzanowska and Avendaño, 2012; Romero-Reyes et al., 2013). A commonly used model of peripheral inflammation in animals is injection of Complete Freund's Adjuvant (CFA) (Ren and Dubner, 1999; Takeda et al., 2007; Krzyzanowska and Avendaño, 2012; Gregory et al., 2013). Orofacial inflammation induces mechanical hyperalgesia/allodynia on the face by activation/sensitization of trigeminal primary and secondary sensory neurons (Iwata et al., 2017).

Since the mechanisms of trigeminal sensitization are not known, global transcriptomic analysis allows an unbiased approach to reveal key pathways responsible for the pathophysiological changes (Perrino et al., 2017). Gene expression changes in the trigeminal ganglion (TRG) had been assessed by microarray analysis after CFA injection in whisker pad (Okumura et al., 2010) or masseter muscle (Chung et al., 2016). However, no study has evaluated TRG gene expression changes in parallel with the central gene expression variances in the trigeminal nucleus caudalis (TNC) and correlate it with the time course and extent of facial allodynia. This comprehensive approach might facilitate the identification of differentially regulated genes with a relevant role in the cascade of events resulting in the sensitization of primary and secondary trigeminal neurons. Moreover, there is growing evidence that transcriptome changes in the central nervous system could be reflected in peripheral blood cells. Investigation of gene expression changes in migraine patients identified differential expression of major genes from the peripheral blood (Gardiner et al., 1998; Hershey et al., 2004, 2012; Du et al., 2006; Plummer et al., 2011; Gerring et al., 2017). Gene transcription changes of PBMCs have not been analysed in animal models of trigeminal sensitization, although it could provide a good opportunity to compare with human data.

The aim of the present study was to follow the temporal changes of facial mechanonociceptive thresholds and gene expression in TRG, TNC neurones and PBMCs after CFA inflammation using microarray and qPCR analyses in order to get a better insight into the mechanisms of trigeminal pain disorders.

Abbreviations: TRG, trigeminal ganglion; TNC, trigeminal nucleus caudalis; PBMC, peripheral blood mononuclear cells; CFA, Complete Freund's Adjuvant; Iba1, Ionized calcium binding adaptor molecule 1; Gfap, Glial fibrillary acidic protein.

MATERIALS AND METHODS

Animals

Twenty male Wistar rats (Toxicoop Zrt., Hungary) weighing between 200–300 g were used. Animals were kept under standard light-dark cycle (12-h light/dark cycle) and temperature (24–25°C) conditions, food and water were provided *ad libitum*, in the local animal house of the Pécs University Department of Pharmacology and Pharmacotherapy. In order to minimise stress, all rats were habituated to handling and the light restraint used for the facial von Frey test for 3 days prior to the start of the experiments.

The study was carried out in accordance with the Ethical Codex of Animal Experiments of the University of Pécs and the 1998/XXVIII Act of the Hungarian Parliament on Animal Protection and Consideration Decree of Scientific Procedures of Animal Experiments (243/1988). The protocol was approved by the local Ethics Committee on Animal Research of University of Pécs (license No.: BA02/2000-9/2011).

CFA Injection

Orofacial inflammation was induced by unilateral s.c. injection of 50 μl complete Freund's adjuvant (CFA; Sigma-Aldrich, Saint Louis, USA; killed mycobacteria suspended in paraffin oil; 1 mg/ml) into the whisker pad of male rats, while under ketamine (72 mg/kg) and xylazine (8 mg/kg) anaesthesia. In the second series of experiments, a control group received the same volume of saline injection.

Microarray

Orofacial inflammation-associated gene expression was analysed using Agilent microarray platforms. Rat TRG tissue samples were collected from animals 7 days after receiving s.c. CFA injection ($n = 8$). Animals were anaesthetized with thiopental (100 mg/kg i.p.) and sacrificed by exsanguination. TRGs were excised and snap-frozen in liquid nitrogen. Contralateral sides of CFA-injected rats served as controls. Total RNA were isolated from snap-frozen samples using RNeasy Mini Kit (Qiagen, Carlsbad, CA) and high-quality samples (RIN > 8.0) were used for subsequent expression analyses. Sample labelling, array hybridization and primary data analysis was performed by ArrayStar Inc. (Rockville, MD, USA). Briefly, total RNA samples

were amplified and labelled with Cy3-dCTP. Labeled amplicons were purified, fragmented and hybridized to rat LncRNA Array v1.0 (4 × 44 K, Arraystar Inc.) slides. One-color microarray-based gene expression analysis was used. After hybridization slides were washed, fixed and scanned. Gene expression data files were deposited to NCBI's Gene Expression Omnibus (Edgar et al., 2002) and are accessible through GEO Series accession number GSE111160.

Orofacial Pain Sensitivity Tested With Von Frey Filaments

In a second experiment, mechanical pain thresholds of the orofacial region were determined with a series of von Frey filaments. Tests were performed on days 0 (control day) before and 1, 3, 7 after CFA ($n = 9$)/saline ($n = 3$) injection. Animals were lightly restrained using a soft cotton glove in order to allow an easier habituation, then a set of calibrated nylon monofilaments (Stoelting, Wood Dale, Illinois, U.S.A) was used with increasing strengths (0.8–12 g) to measure facial mechanosensitivity. Filaments were applied in ascending order, starting from the 5.2 g filament during control measurements and the 0.8 g filament after CFA treatment. The mechanonociceptive threshold was defined as the lowest force evoking at least two withdrawal responses (face stroking with the forepaw or head shaking) out of five stimulations.

Experimental Setup of the Second Experiment

At each time point (1, 3, and 7 days) animals ($n = 3$) were anaesthetized with thiopental and blood was collected by cardiac puncture. Tissue samples (TRG, TNC) were quickly frozen in liquid nitrogen and stored at −80°C until RNA extraction and real-time PCR processing.

Isolation of Peripheral Blood Mononuclear Cells

Mononuclear cells were purified from fresh peripheral blood according to Ficoll-PaquePREMIUM (Cat. No. 17-5446-02, GE Healthcare, Budapest, Hungary) manufacturer's instructions. Fresh anticoagulant-treated blood and an equal volume of balanced salt solution (final volume of 8 ml) were transferred to 15 ml sterile centrifuge tubes. The mixture was carefully overlaid on 5 ml Ficoll-PaquePREMIUM and centrifuged 40 min at 2,100 RPM, 20°C. The mononuclear layer was transferred into a new 15 ml centrifuge tube, suspended with approximately 6 ml of salt solution and centrifuged 15 min at 2300 RPM, 20°C. The supernatant was removed and the pellet was resuspended in another 6 ml of salt solution, followed by another centrifugation (10 min, 2300 RPM, 20°C). After the removal of the supernatant the cells were resuspended with 1 ml of TRI Reagent (Molecular Research Center, Inc., Cincinnati, OH, USA) and transferred to Eppendorf and stored at −80°C until use.

Quantitative Real-Time RT-PCR (qRT-PCR)

Purification of total RNA was carried out according to the TRI Reagent manufacturer's (Molecular Research Center, Inc., Cincinnati, OH, USA) protocol up to the step of acquiring the aqueous phase. Briefly, tissue samples were homogenized in 1 ml of TRI Reagent, and then, 200 µl of bromo-chloro-propane (Sigma-Aldrich, Saint Louis, USA) was added. RNA was purified from the aqueous phase using the Direct-zol RNA MiniPrep kit (Cat. No. R2052; Zymo Research, Irvine, CA, USA) according to the manufacturer's protocol. Briefly, 400 µl of the aqueous phase was mixed with 400 µl absolute ethanol, the mixture was loaded onto the column, washed, and the RNA was eluted in 50 µl of RNase-free water. The quantity and purity of the extracted RNA were assessed on Nanodrop ND-1000 Spectrophotometer V3.5 (Nano-Drop Technologies, Inc., Wilmington, DE, USA). 200 ng of PBMCs/TRG and 250 ng of TNC total RNA was reverse transcribed using Maxima First Strand cDNA Synthesis Kit (Cat. No. K1642, ThermoScientific, Santa Clara, CA, USA) according to the manufacturer's instructions. qRT-PCR was performed on a Stratagene Mx3000P qPCR System (Agilent Technologies, Santa Clara, USA). PCR amplification was performed using SensiFast SYBR Lo-ROX Kit (Cat. No. BIO-94020). Transcripts of the reference genes glyceraldehyde 3-phosphate dehydrogenase (*Gapdh*), hypoxanthine phosphoribosyltransferase 1 (*Hprt1*), beta-2-microglobulin (*β2m*) and Peptidyl-prolyl cis-trans isomerase (*Ppia*) were detected in all samples. *Ppia* and *Hprt1* for PBMCs and *β2m, Hprt1* for TRG and TNC samples were eventually chosen as internal controls, the geometric mean of their Cq values was calculated. Primers of similar efficiencies were used and $2^{-\Delta\Delta Cq}$ fold change values were calculated. Sequences of primers used for qRT-PCR are given in Supplementary Table 1.

Statistical Analysis

The raw microarray data were analysed using R and Bioconductor (Gentleman et al., 2004; R Development Core Team, 2008) The data were quantile normalised to reduce technical noise with Limma package (Ritchie et al., 2015). The statistical testing for differential expression was also performed using Limma, which applies linear modeling with a modified *t*-test to calculate the *p*-values and fold change values. One-way analysis of variance (ANOVA) followed by Tukeys' multiple comparison tests on RT-PCR data and in case of mechanical pain threshold detection two-way ANOVA with repeated measures followed by Bonferroni's post-test for time-matching samples were performed using GraphPad Prism software (GraphPad Software, Inc., La Jolla, CA, USA). Probability values $p \leq 0.05$ were accepted as significant. Results are presented as the mean ± standard error of the mean (SEM). Log2 mRNA fold change data measured by qPCR were further analysed by hierarchical cluster analysis (1-Pearson correlation and average linkage method) and then visualised by heat map using the free web tool Morpheus (Morpheus)[1].

Functional Classification of Differentially Regulated Genes

The functional enrichment analyses against Gene Ontology (GO) (Ashburner et al., 2000; The Gene Ontology Consortium, 2017),

[1]https://software.broadinstitute.org/morpheus/ Broad Institute, Cambridge, MA, USA.

TABLE 1 | The top 25 up- and downregulated genes.

ID	FC	*P*.Value	SystematicName	GeneSymbol	Description	EnsemblID	EntrezGene
948	**5.20**	0.0381	MRAK049104	**NA**	**lncRNA (chromosome 1)**	NA	NA
11131	**4.55**	0.0353	TC598318	**NA**	**NA**	NA	NA
9725	**4.35**	0.0214	NM_199489.3	**Ccr7**	**C-C motif chemokine receptor 7**	ENSRNOG00000010665	287673
5534	**4.34**	0.0076	NM_001011951.1	**Sf3b4**	**splicing factor 3b, subunit 4**	ENSRNOG00000021181	295270
12278	**4.29**	0.0010	NM_001037518.1	**Defb23**	**defensin beta 23**	ENSRNOG00000023477	641621
519	**4.28**	0.0218	NM_001000099.1	**Olr1640**	**olfactory receptor 1640**	ENSRNOG00000048857	290049
13893	**4.13**	0.0236	NM_001106821.1	**Atm**	**ATM serine/threonine kinase**	ENSRNOG00000029773	300711
40839	**4.08**	0.0135	NM_134399.2	**Mk1**	**Mk1 protein**	ENSRNOG00000019657	171436
6132	**4.01**	0.0172	NM_001106551.1	**Lkaaear1**	**LKAAEAR motif containing 1**	ENSRNOG00000024815	296483
10158	**3.83**	0.0477	NM_001013956.1	**RGD1309049**	**similar to RIKEN cDNA 4933415F23**	ENSRNOG00000014123	301306
10494	**3.80**	0.0138	NM_001013147.1	**Axl**	**Axl receptor tyrosine kinase**	ENSRNOG00000020716	308444
2571	**3.78**	0.0404	NM_019128.4	**Ina**	**internexin neuronal intermediate filament protein, alpha**	ENSRNOG00000020248	24503
12538	**3.73**	0.0232	NM_198133.2	**Uts2b**	**urotensin 2B**	ENSRNOG00000038512	378939
3346	**3.72**	0.0156	NM_001047878.1	**F5**	**coagulation factor V**	ENSRNOG00000057855	NA
6931	**3.71**	0.0198	uc.339+	**NA**	**lncRNA (chromosome 7)**	NA	NA
5544	**3.70**	0.0316	NM_001001034.1	**Olr199**	**olfactory receptor 199**	ENSRNOG00000029755	405920
9136	**3.69**	0.0250	NM_012735.1	**Hk2**	**hexokinase 2**	ENSRNOG00000006116	25059
4102	**3.67**	0.0212	NM_001001010.1	**Olr283**	**olfactory receptor 283**	ENSRNOG00000030782	405384
3492	**3.67**	0.0159	uc.470+	**NA**	**lncRNA (chromosome X)**	NA	NA
1789	**3.66**	0.0240	XR_005913	**NA**	**lncRNA (chromosome 16)**	NA	NA
4451	**3.64**	0.0064	NM_173305.1	**Hsd17b6**	**hydroxysteroid (17-beta) dehydrogenase 6**	ENSRNOG00000002597	286964
11677	**3.63**	0.0013	NM_001000387.1	**Olr416**	**olfactory receptor 416**	ENSRNOG00000029069	296678
6676	**3.62**	0.0322	NM_001107582.2	**Pdcd1lg2**	**programmed cell death 1 ligand 2**	ENSRNOG00000016136	309304
9724	**3.61**	0.0247	NM_153466.1	**Gzmf**	**granzyme F**	ENSRNOG00000028810	266704
5556	**3.60**	0.0103	NM_001099514.1	**Vom2r48**	**vomeronasal 2 receptor, 48**	ENSRNOG00000028538	686145
39867	**−3.50**	0.0007	NM_001047931.1	**LOC498460**	**LRRGT00055**	ENSRNOG00000028821	498460
41314	**−3.62**	0.0313	NM_001080939.1	**Tas2r109**	**taste receptor, type 2, member 109**	ENSRNOG00000032724	690572
38176	**−3.63**	0.0005	NM_001164826.1	**RT1-Db2**	**RT1 class II, locus Db2**	ENSRNOG00000030431	24981
44381	**−3.64**	0.0049	NM_001130497.1	**Pnpla5**	**patatin-like phospholipase domain containing 5**	ENSRNOG00000022296	300108
35607	**−3.67**	0.0016	MRAK078136	**NA**	**lncRNA (chromosome 1)**	NA	NA
16902	**−3.73**	0.0186	uc.163+	**NA**	**NA**	NA	NA
41319	**−3.76**	0.0102	NM_001012084.1	**Adh6**	**alcohol dehidrogenase 6**	NA	NA
37492	**−3.78**	0.0025	NM_001003979.1	**Tmprss11c**	**transmembrane protease, serine 11C**	ENSRNOG00000033910	408213
36560	**−3.87**	0.0023	NM_001000338.1	**Olr619**	**olfactory receptor 619**	ENSRNOG00000021473	295843
43356	**−4.15**	0.0009	NM_022673.2	**Mecp2**	**methyl CpG binding protein 2**	ENSRNOG00000056659	29386
42598	**−4.17**	0.0001	NM_001017480.1	**Hoxb7**	**homeo box B7**	ENSRNOG00000007611	497985
38934	**−4.62**	0.0036	NM_052808.1	**Bpifa2**	**BPI fold containing family A, member 2**	ENSRNOG00000013540	50585
38765	**−4.64**	0.0056	NM_001000575.1	**Olr741**	**olfactory receptor 741**	ENSRNOG00000053815	366120
37233	**−4.69**	0.0053	NM_012689.1	**Esr1**	**estrogen receptor 1**	ENSRNOG00000019358	24890
43878	**−4.71**	0.0017	NM_001000307.1	**Olr485**	**olfactory receptor 485**	ENSRNOG00000009747	295751
38741	**−4.80**	0.0043	NM_001001355.1	**Olr905**	**olfactory receptor 905**	ENSRNOG00000057325	288875
44809	**−4.86**	0.0006	NM_001109459.1	**LOC685171**	**similar to protein disulfide isomerase-associated 6**	ENSRNOG00000058543	685171
40038	**−4.88**	0.0012	uc.400−	**NA**	**lncRNA (chromosome 19)**	NA	NA
43786	**−5.14**	0.0023	NM_001109285.1	**C2cd4c**	**C2 calcium-dependent domain containing 4C**	ENSRNOG00000008026	500798
43442	**−5.40**	0.0004	uc.225+	**NA**	**lncRNA (chromosome 4)**	NA	NA
40720	**−5.65**	0.0041	NM_001000692.1	**Olr25**	**olfactory receptor 25**	ENSRNOG00000046609	404897
41996	**−6.14**	0.0014	uc.47−	**NA**	**lncRNA (chromosome 6)**	NA	NA
43609	**−6.60**	0.0018	NM_001000394.1	**Olr428**	**olfactory receptor 428**	ENSRNOG00000030460	296689
36293	**−8.03**	0.0021	XR_008902	**NA**	**lncRNA (chromosome 19)**	NA	NA
44472	**−9.20**	0.0012	NM_019326.1	**Neurod2**	**neuronal differentiation 2**	ENSRNOG00000028417	NA

ID, microarray feature identifier; FC, expression ratio (fold-change) between CFA-treated and contralateral sample groups.

KEGG (Kanehisa and Goto, 2000) and Reactome (Fabregat et al., 2018) databases were performed using the topGO (Alexa and Rahnenführer, 2016) and gage (Luo et al., 2009) packages in R.

RESULT

Microarray Analysis

The microarray data analysis identified 512 differentially expressed (319 up- and 191 downregulated) transcripts between the control (contralateral) and 7-day CFA (ipsilateral) samples from TRG at a statistically significant level ($p \leq 0.05$) and with fold change $|FC| > 2$ (Supplementary Table 2; Supplementary Figures 1, 2). All but 15 of these have absolute fold change values below 4. Original data files have been uploaded to the NCBI GEO Database. The top 25 up- and downregulated genes are included in **Table 1**. The most upregulated (5.20 fold) transcript was found to be a lncRNA (MRAK049104) with unknown function. The most downregulated transcript (−9.20 fold), Neurod2, is involved in neuronal differentiation. **Figure 1** shows the 44 differentially expressed genes at a significance level $p \leq 0.001$ and $|FC| > 2$, including a number of olfactory, taste and pheromone receptors, as well as the chemokine receptor (*Ccr7*) and the estrogen receptor 1 (Esr1) genes as well as long non-coding RNAs.

Gene Ontology

Gene set enrichment analysis was performed on the microarray data to find common features of genes. The most differentially expressed genes ($|FC| > 2$, $p \leq 0.001$) between the control (contralateral) and 7-day CFA (ipsilateral) samples from TRG were functionally annotated based on gene ontology (GO), KEGG Pathway and Reactome terms to gain an overview of the affected biological processes and pathways (**Table 2**). The identified enriched GO terms include steroid and carbohydrate metabolism, sensory perception and olfactory transduction.

Mechanonociceptive Threshold

The facial mechanonociceptive threshold of CFA-injected rats was significantly decreased compared to the contralateral side starting from day 1 after injection. The allodynia reached its maximum on day 3 ($p \leq 0.001$), as the threshold change was lower on day 7 (**Figure 2**). No significant changes in the contralateral threshold were observed in the whisker pad area.

RT-PCR Analysis

Validation of Differentially Expressed mRNAs in TRG by Real-Time RT-PCR

To validate the microarray results, the transcription levels of five differentially expressed, microarray-identified genes were further determined using quantitative real-time RT-PCR. The following genes were chosen for validation: *Lkaaear1, Neurod2* (**Table 1**), as well as G-protein coupled receptor 39 (*Gpr39*), kisspeptin (*Kiss1*) and kisspeptin-1 receptor (*Kiss1r*) (microarray data not shown). The relative fold changes (up-regulated) of *Gpr39* and *Lkaaear1* for CFA TRG samples were 3.04 and 4.01

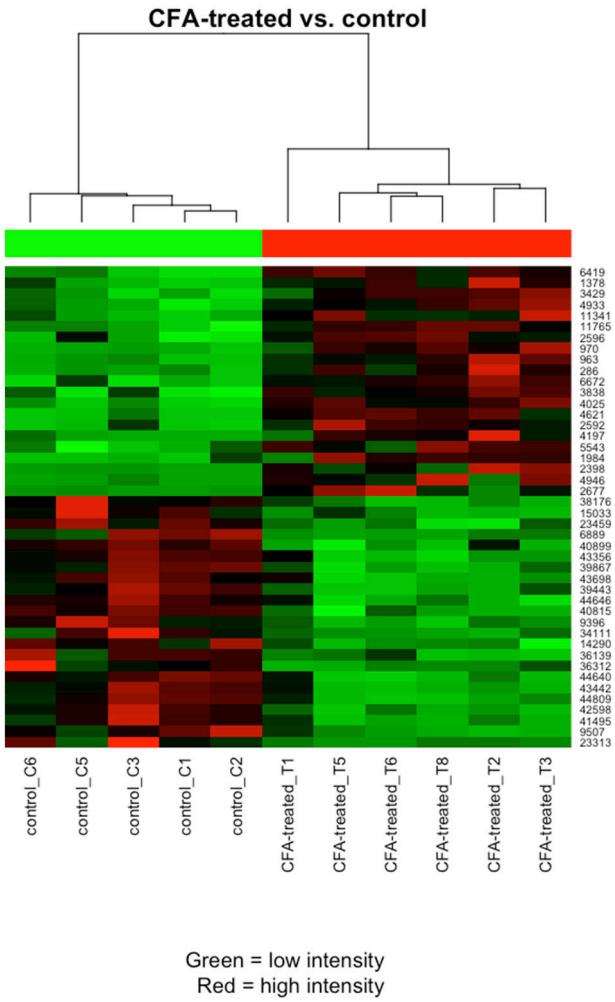

FIGURE 1 | Heat map clustering of the most differentially expressed transcripts for the comparison between CFA-treated and contralateral side TRG samples. Pearson's metrics has been used in hierarchical clustering of the samples and filtered features. The clustering is based on the general expression measurement similarity. Red colour means high expression and green low expression. Each row represents one differentially expressed (DE) feature (microarray feature identifiers) and each column represents one sample.

respectively, while the relative fold changes (down-regulated) of *Kiss1, Kiss1r* and *Neurod2* were −1.74, −2.63, and −9.2 (**Table 1**, Supplementary Table 2). On day 7, *Gpr39* and *Kiss1r* alterations were similar to the microarray data (**Figure 3**). PCR results could not confirm microarray data on *Lkaaear1, Neurod2* and *Kiss1*. *Lkaaear1* presented decreased mRNA levels on day 7 compared to contralateral CT side. In addition, we were unable to detect *Neurod2* expression changes in TRG with our PCR protocol. We also chose to investigate the time course of neuronal and activation marker expressions. Although *Fosb*, Ionized calcium binding adaptor molecule 1 (*Iba1*), Glial fibrillary acidic protein (*Gfap*) and Calcitonin gene-related peptide (*Cgrp*) were not listed in microarray data, meaning no significant changes between the two groups of interest, we analysed the variation of these mRNA levels as well. No significant differences were detected on day

TABLE 2 | Results of gene set enrichment analysis of a subset of genes differentially expressed between the control (contralateral) and 7-day CFA (ipsilateral) samples from TRG as detected by microarray.

	Term	Annotated	Significant	Expected	*P*-Value
GO.ID	**Biological process**				
GO:0008202	Steroid metabolic process	223	3	0.3	0.0031
GO:0005975	Carbohydrate metabolic process	400	3	0.54	0.0155
GO:0007600	Sensory perception	1,453	5	1.97	0.0380
GO:0050911	Detection of chemical stimulus involved in sensory perception of smell	1,059	4	1.43	0.0487
CELLULAR COMPONENT					
GO:0005576	Extracellular region	3,051	6	3.95	0.181
GO:0005615	Extracellular space	2,639	5	3.41	0.243
GO:0071944	Cell periphery	4,053	7	5.24	0.246
GO:0044421	Extracellular region part	2,763	5	3.57	0.276
GO:0016021	Integral component of membrane	4,420	7	5.72	0.334
GO:0031224	Intrinsic component of membrane	4,505	7	5.83	0.356
GO:0044425	Membrane part	5,350	8	6.92	0.381
GO:0005886	Plasma membrane	3,959	6	5.12	0.407
GO:0044464	Cell part	11,048	15	14.29	0.476
GO:0005623	Cell	11,071	15	14.32	0.486
MOLECULAR FUNCTION					
GO:0004984	Olfactory receptor activity	1,059	4	1.21	0.0269
GO:0099600	Transmembrane receptor activity	1,749	5	2	0.0374
KEGG.ID	**KEGG pathway term**				
604	Glycosphingolipid biosynthesis - ganglio series	12	1	0.012067578	0.012014279
603	Glycosphingolipid biosynthesis - globo series	13	1	0.01307321	0.013010232
533	Glycosaminoglycan biosynthesis - keratan sulfate	14	1	0.014078842	0.014005382
512	Mucin type O-Glycan biosynthesis	20	1	0.020112631	0.019959439
500	Starch and sucrose metabolism	28	1	0.028157683	0.027853402
4740	Olfactory transduction	842	3	0.846741754	0.036986751
Reactome.ID	**Downregulated reactome term**	**GeneRatio**	**BgRatio**	***P*-Value**	
R-RNO-8957275	Post-translational protein phosphorylation	2/5	74/5483	0.001750444	
R-RNO-381426	Regulation of Insulin-like Growth Factor (IGF) transport and uptake by Insulin-like Growth Factor Binding Proteins (IGFBPs)	2/5	82/5483	0.002145931	

Enrichment analysis for the differentially expressed filtered gene lists test whether the genes within a certain KEGG or Reactome pathway or GO term are statistically over-represented in a given comparison.

7 related to the mentioned genes which further confirmed the consistency and reliability of the microarray data.

Gene Expression Analysis in TRG Tissues

We measured mRNA levels of eight genes in TRG tissues on three different time points after CFA injection. On day 1, CFA-induced significant up-regulation of Kiss1r, as well as of neuronal (*Fosb*), glial (*Iba1*), and astrocyte (*Gfap*) activation markers compared to saline-treated control group. By day 3, seven genes reached their maximum at a level of 9.18- (Gpr39), 2.97- (*Lkaaear1*), 9.51- (*Kiss1)*, 14.31- (*Kiss1r*), 117.82- (*Cgrp*), 7.40- (*Fosb*), and 27.80-fold (Gfap). Iba1 reached a 3.6-fold peak at day 1 before declining. mRNA levels of *Lkaaear1*, *Kiss1r*, *Iba1* gradually decreased at last time point until reaching a non-significant level compared to saline-treated control side (**Figure 3**).

Gene Expression Analysis in TNC Tissues

Briefly, main changes in the relative gene expression were observed directly 1, 3 and 7 days post-CFA treatment. All measured mRNA levels, except *Kiss1r*, showed significantly altered temporal change in TNC of CFA-injected samples when compared to both CFA CT and Saline CT, presenting a maximum at day 3 ($p \leq 0.001$ or $p \leq 0.0001$). There was no significant difference in mRNA abundance of *Kiss1r* on different time points (**Figure 4**).

Gene Expression Analysis in PBMCs

Finally, low but significant expressional changes of *Lkaaear1* and *Kiss1r* gene mRNA in peripheral blood from CFA-treated rats have been observed. *Lkaaear1* displayed a gene expression

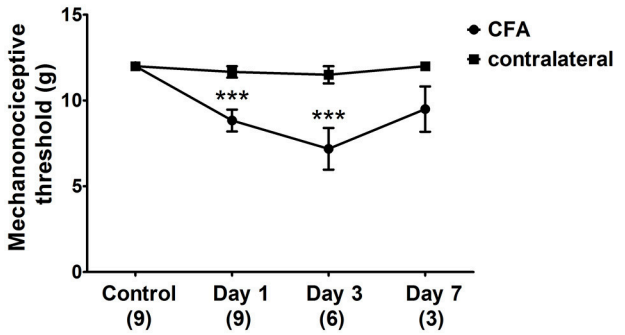

FIGURE 2 | Changes in mechanical threshold in response to von Frey filaments before and 1, 3, 7 days after CFA (50 μl s.c. complete Freund's adjuvant) inflammation. Orofacial thresholds in both ipsilateral and contralateral sides were measured. Data are means ± S.E.M. ($n = 9$ at control and day 1; $n = 6$ at day 3; $n = 3$ at day 7). Asterisks denote statistically significant differences between contralateral (CT) and ipsilateral (CFA) sides (***$p \leq 0.001$) as analysed by two-way ANOVA followed by Bonferroni's post-test.

pattern similar to *Kiss1r*, where Lkaaear1 presented a maximum of 2.33 and *Kiss1r* a 3.86 fold change at day one. We noted no significant changes in *Gpr39* mRNA levels of PBMCs after CFA exposure. Interestingly, *Fosb* and *Iba1* seem to be up-regulated ($p \leq 0.01$ or $p \leq 0.001$) at each time point due to CFA treatment, while Gfap only on day 7 (**Figure 5**).

Heat Map Plotting

Fold change data were plotted on a heat map to summarize changes in mRNA levels measured by qPCR (**Figure 6**). Genes with a similar level of expression were grouped into three major clusters in TRG samples: *1. Kiss1r, Gpr39*; *2. Kiss, Fosb, Lkr, Cgrp*; *3. Gfap, Iba1*. In the TNC, all but one gene fall into a large cluster with highly similar temporal patterns, except for Kiss1r that changed the opposite way, however, its alterations were not found to be significant. Group 3 genes distinctly upregulated in CFA-treated TRG samples on days 1 and 3 but not on respective contralateral sides while they were substantially upregulated in TNC samples from both sides on these days, as well as on day 7. Genes upregulated in TRG and TNC were also elevated in PBMCs, although starting at an earlier time point (day 1) for most genes.

DISCUSSION

To our knowledge, this is the first comprehensive study which compared gene expression changes in the TRG, TNC and peripheral blood leukocytes in an inflammatory orofacial pain model. Simultaneous measurement of the transcriptional changes of PBMCs had been suggested to reflect alterations in the CNS (Arosio et al., 2014; Gerring et al., 2016; Srinivasan et al., 2017). We described up- and downregulation of distinct genes that are likely to be involved in the activation and sensitization of primary and secondary trigeminal neurons.

The mechanisms of nociceptor sensitization after inflammation have been extensively studied in rodents by electrophysiological, histological and molecular biological approaches (Hucho and Levine, 2007; Coste et al., 2008; Matsumoto et al., 2010; Cady et al., 2011; Bernstein and Burstein, 2012; Weyer et al., 2016). Nevertheless, we cannot extrapolate all the findings to the trigeminovascular system, since it is considerably different from other regions of the somatosensory system. As mentioned before, the central terminals of extra- and intracranial trigeminal primary afferents converge considerably in the TNC. As a consequence, inflammatory sensitization of primary meningeal afferents and secondary trigeminal neurons resulted in an enhanced response to cutaneous stimulation of the face (Burstein et al., 1998; Levy et al., 2004). On the other hand, experimental data also confirm that noxious stimulation (e.g., intranasal capsaicin), inflammation or nerve lesion on the face can induce meningeal vasodilation or neurogenic inflammation (Kunkler et al., 2011; Filipović et al., 2012). Intriguingly, it was revealed that there are trigeminal afferents which project to both the meninges and extracranial tissues (Schueler et al., 2013). Both human and rodent data point out that gene expression of TRGs is distinct from DRGs (Manteniotis et al., 2013; Flegel et al., 2015; Kogelman et al., 2017; LaPaglia et al., 2017). Yet, there have only been few rodent studies investigating gene expression changes in the TRGs after chronic orofacial inflammation (Okumura et al., 2010; Chung et al., 2016).

Our microarray study revealed a high number of differentially expressed olfactory, taste and pheromone receptor genes between the ipsi- and contralateral sides 7 days after CFA treatment. A large number of transcripts of chemoreceptors had been detected in murine and human TRGs using next-generation sequencing (Manteniotis et al., 2013), however their involvement in trigeminal sensitisation is not known. It is appealing to draw parallels between the perturbation of TRG chemoreceptors in our model and the known phenomena of an odour or perfume-triggered migraine, as well as odour hypersensitivity, osmophobia, odour hallucination and taste abnormalities associated with migraine (Schreiber and Calvert, 1986; Kelman, 2004; Goadsby et al., 2017). The microarray analysis implicated thyroid hormone receptor beta which had been previously associated with migraine (Gormley et al., 2015), and chemokine signalling (*Ccr7*), among many others as well as long non-coding RNAs (lncRNA) putatively involved in gene regulation.

On the basis of these microarray results, we further investigated the time-dependent changes of one of the most upregulated genes (*Lkaaear1*) and the most downregulated (*Neurod2*) gene with qPCR. Transcripts of genes with possible roles in nociception, which also have the potential to be future drug targets, were also chosen to be studied, such as two G-protein-coupled receptors (*Gpr39* and *Kiss1r*) and the neuropeptide kisspeptin (*Kiss1*). *Lkaaear1* encodes an LKAAEAR motive containing protein with unclear function. It is highly expressed in the brain and testis and during organ development (NCBI Gene database)[2] *Neurod2* is involved in

[2]https://www.ncbi.nlm.nih.gov/gene/198437

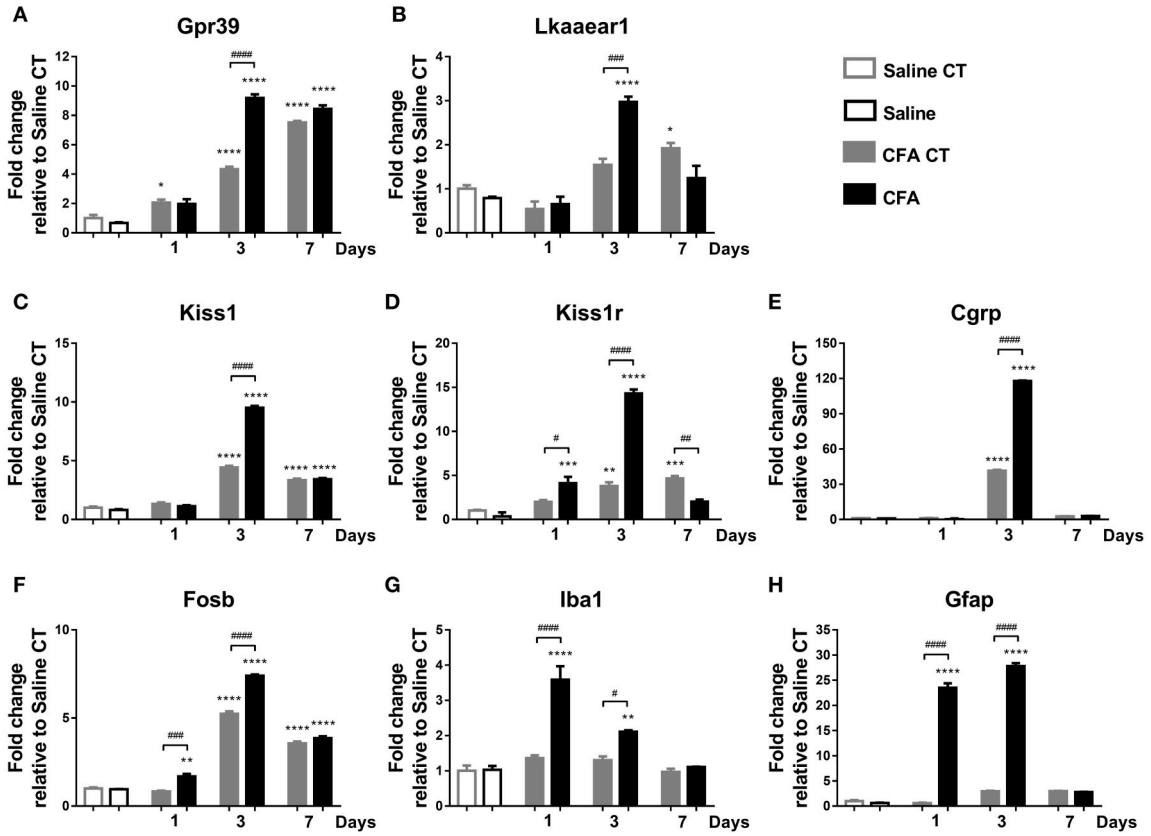

FIGURE 3 | Time course of normalized fold changes in the trigeminal ganglia of Gpr39 **(A)**, Lkaaear1 **(B)**, Kiss1 **(C)**, Kiss1r **(D)**, Cgrp **(E)**, Fosb **(F)**, Iba1 **(G)**, and Gfap **(H)** mRNA expression one, 3 and 7 days after CFA injection. The mRNA levels were normalised to β2m and Hprt1, as detailed in materials and methods. Data are means ± S.E.M. ($n = 3$ at each time point). Asterisks denote statistically significant differences between CT Saline and CT/CFA groups (*$p \leq 0.05$, **$p \leq 0.01$, ***$p \leq 0.001$, ****$p \leq 0.0001$), while hash marks label statistically significant differences between respective CT and CFA groups ($\#p \leq 0.05$, $\#\#p \leq 0.01$, $\#\#\#p \leq 0.001$, $\#\#\#\#p \leq 0.0001$) as analysed by one-way ANOVA followed by Tukeys' multiple comparison tests.

neuronal differentiation and has been implicated in synaptic plasticity (Bayam et al., 2015; Chen et al., 2016). Gpr39 is a Zn^{2+}-sensing $G_{\alpha q}$-coupled receptor which is expressed in a wide range of tissues including some areas of the brain. Activation of Gpr39 induces the release of Ca^{2+} via the IP_3 pathway. The receptor may play a role in depression, and as a specific and direct sensor of Zn^{2+}, in many physiological functions where the cation is involved such as synaptic transmission (Popovics and Stewart, 2011; Sato et al., 2016). Kisspeptin, encoded by the Kiss1 gene, is considered to have an emerging role in the neuroendocrine regulation of reproduction and puberty (de Roux et al., 2003; Seminara, 2006; Kauffman et al., 2007; Colledge, 2009). Kisspeptin-expressing neurons and Kiss1r are found in areas other than the hypothalamus: amygdala, hippocampus, periaqueductal grey (Oakley et al., 2009; Herbison et al., 2010). In addition, DRG and dorsal horns neurons of the spinal cord have been shown to express kisspeptin and Kiss1r, whose expression might be upregulated due to intra-articular injection of CFA (Mi et al., 2009). There are studies showing hyperalgesic effect of peripheral and intrathecal kisspeptin (Spampinato et al., 2011). Likewise, i.c.v. administration of kisspeptin-10 induces both hyperalgesia and opioid antagonistic activity (Elhabazi et al., 2013), suggesting its possible involvement in the regulation of pain sensitivity.

We successfully reproduced the changes detected with the microarray by qPCR in cases of *Gpr39* and *Kiss1r*. *Neurod2* transcripts were not detected in the TRG and Lkaaear1 expression was higher on day 3 but not on day 7 compared to the contralateral side. It is important to highlight that there was a delayed but considerable increase of mRNA levels on the contralateral side of CFA-treated animals when compared to saline-treated animals. This is consistent with earlier reports found after inflammation or nerve injury of the hind limbs in which structural and biochemical changes appeared both centrally and in the periphery on the contralateral side (Koltzenburg et al., 1999; Shenker et al., 2003) However, we did not only use the contralateral side of CFA injected animals as controls, but we also included a saline-injected group as well. We aimed at keeping the animal number at a minimum level and meanwhile taking into account the possible trauma caused by only the injection itself. In addition, there was no detectable allodynia on the contralateral side in our model, therefore the comparison to the contralateral side is still valid from a functional

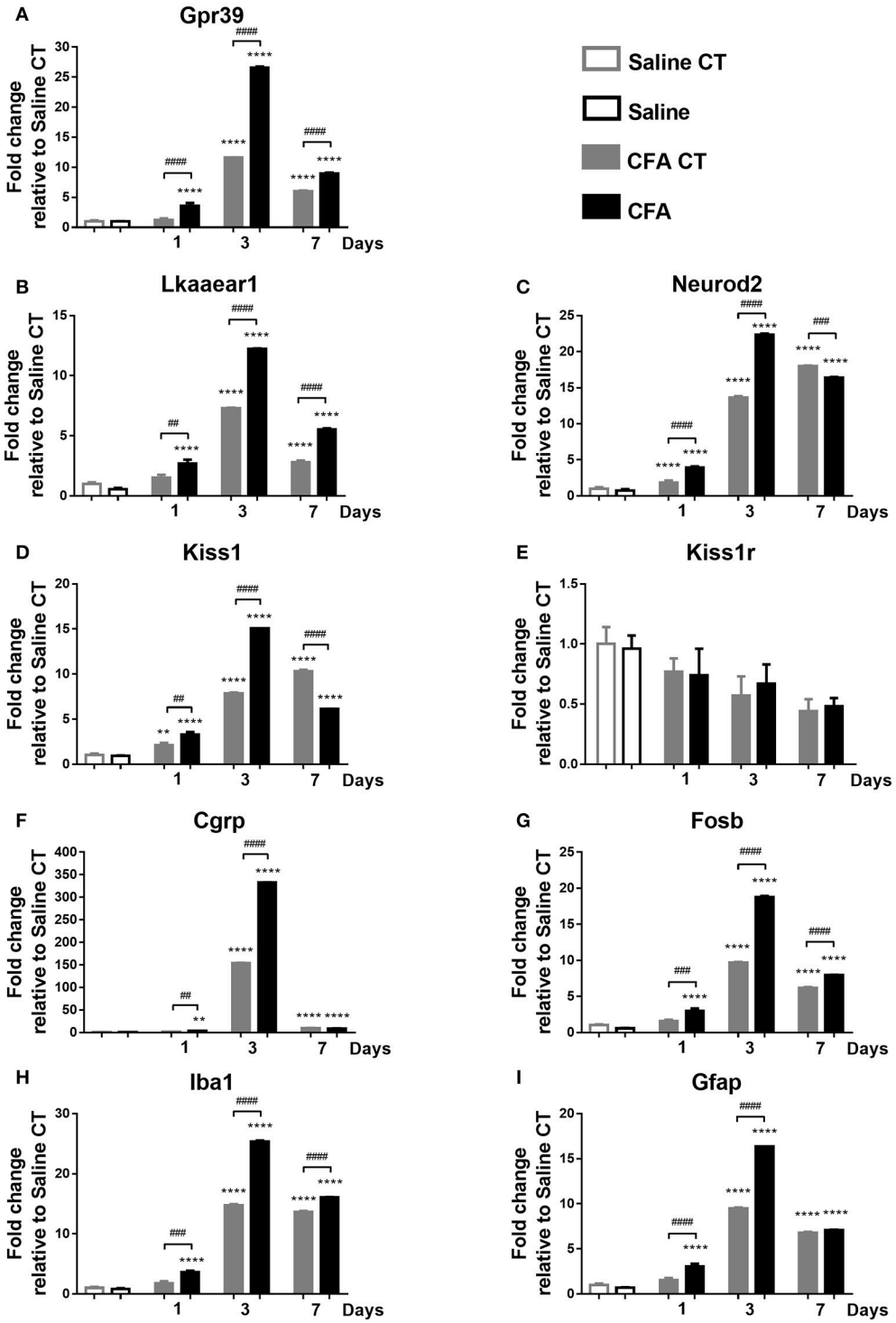

FIGURE 4 | Time course of normalized fold changes in the trigeminal nucleus caudalis of Gpr39 **(A)**, Lkaaear1 **(B)**, Neurod2 **(C)**, Kiss1 **(D)**, Kiss1r **(E)**, Cgrp **(F)**, Fosb **(G)**, Iba1 **(H),** and Gfap **(I)** mRNA expression one, 3 and 7 days after CFA injection. The mRNA levels were normalised to β2m and Hprt1, as detailed in materials and methods. Data are means ± S.E.M. ($n = 3$ at each time point). Asterisks denote statistically significant differences between CT Saline and CT/CFA groups (**$p \leq 0.01$, ****$p \leq 0.0001$), while hash marks label statistically significant differences between respective CT and CFA groups (##$p \leq 0.01$, ###$p \leq 0.001$, ####$p \leq 0.0001$) as analysed by one-way ANOVA followed by Tukeys' multiple comparison tests.

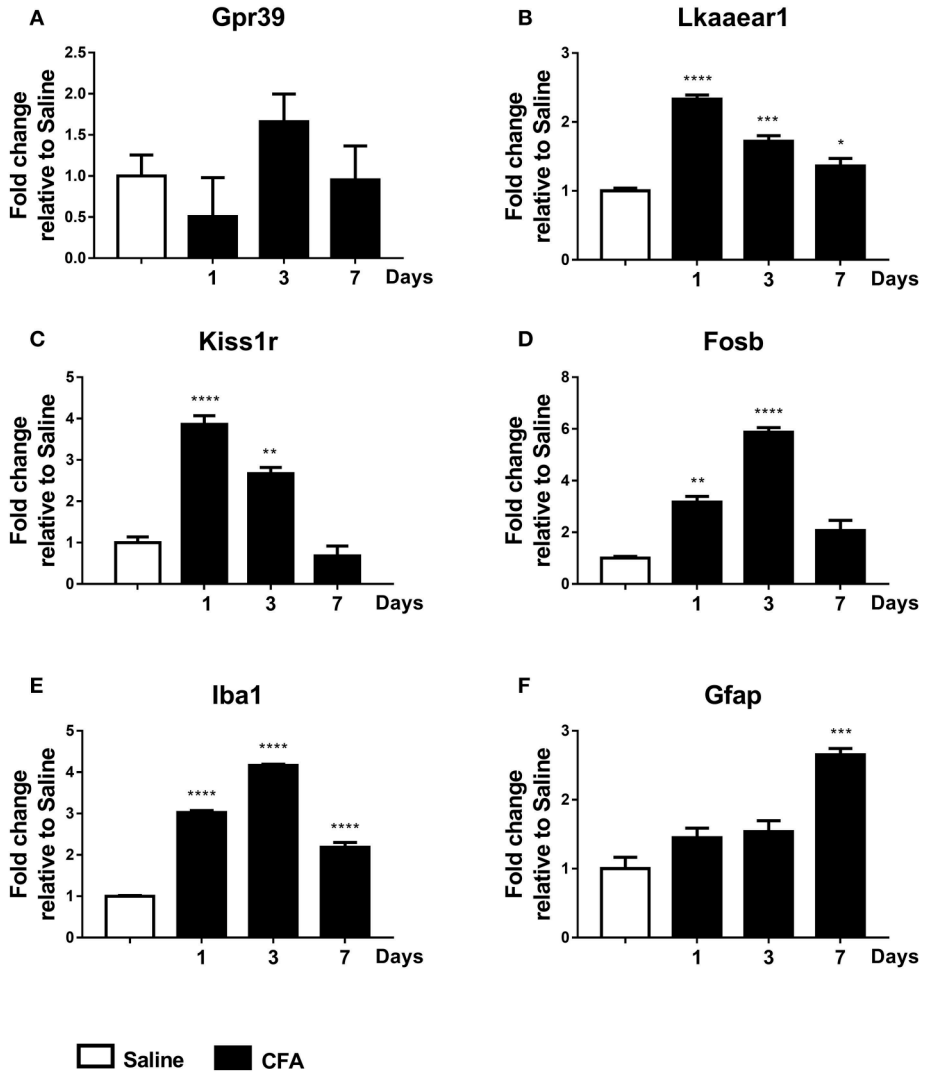

FIGURE 5 | Time course of normalized fold changes in PBMC of Gpr39 **(A)**, Lkaaear1 **(B)**, Kiss1r **(C)**, Fosb **(D)**, Iba1 **(E)**, and Gfap **(F)** mRNA expression one, 3 and 7 days after CFA injection. The mRNA levels were normalised to Ppia and Hprt1, as detailed in materials and methods. Data are means ± S.E.M. ($n = 3$ at each time point). Asterisks denote statistically significant differences between respective Saline and CT/CFA groups (*$p \leq 0.05$, **$p \leq 0.01$, ***$p \leq 0.001$, ****$p \leq 0.0001$) as analysed by one-way ANOVA followed by Tukeys' multiple comparison tests.

aspect and provides additional information based on this double comparison.

We added Cgrp to the list of investigated markers to validate the model, since it is a well-known mediator and even a novel pharmacological target of migraine (Durham, 2006; Doods et al., 2007; Benemei et al., 2009; Edvinsson et al., 2012; Bigal et al., 2013; Russo, 2015). Moreover, its expression was shown to be elevated in TRGs in rodent models of orofacial inflammation (Yasuda et al., 2012; Shinoda and Iwata, 2013; Kuzawinska et al., 2014). Our results are consistent with these previous findings, Cgrp transcripts were significantly increased in the TRG at day 3 after CFA treatment corresponding to the peak of the facial allodynia.

In addition to the TRG, we also examined the transcriptional changes in the TNC, reflecting mechanisms involved in central sensitization, as well as PBMCs in the peripheral blood. In the TNC, significant changes were observed for the examined genes with the exception of *Kiss1r*. Intriguingly, the Kiss1 expression in the TNC was mirroring the changes of the receptor expression in the TRG which suggests a presynaptic effect on primary afferents. Lkaaear1 and *Kiss1r* expression were also significantly increased in PBMCs with a similar time course.

Besides allodynia, as the main functional parameter, neuronal and glial activation markers were also assessed by comparing their gene expression profiles. Therefore, we determined the widely-used neuronal activation marker *Fosb, Gfap* for astrocytes and *Iba1* for microglia (Nestler et al., 2001; Alibhai et al., 2007; Knight et al., 2011). *Gfap* has been shown to play a role in astrocyte migration, the function of the blood-brain barrier, signal transduction pathways and neuron-glia

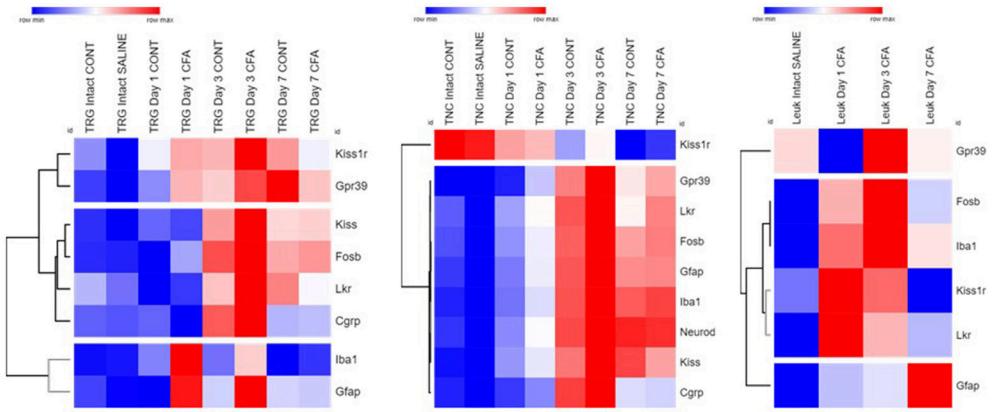

FIGURE 6 | Summary of all qPCR results in TRG, TNC and PBMCs one, 3 and 7 days after CFA injection and in saline-treated controls. Fold change values were log2 transformed and plotted on a heat map. Rows: genes; columns: sample groups; scale: blue (low) to red (high). Hierarchical cluster analysis (1-Pearson correlation and average linkage method) was performed. Dendrograms on the left side of each figure demonstrate similarities between expression patterns of genes.

interactions (Middeldorp and Hol, 2011). *Iba1*, also known as *AIF1* (Allograft Inflammatory Factor 1) expressed in various cells such as monocyte/macrophages and activated T lymphocytes, is mostly used as a microglia marker (Kelemen and Autieri, 2005; Pawlik et al., 2016). All the three activation markers were significantly increased already at day 1 of the inflammation in both TRGs and TNCs, peaked by day 3 and decreased by day 7 when allodynia was declining. Remarkably and most interestingly, a smaller but significant increase of expression was also detectable in PBMCs which highlights the relevance of blood transcriptomics data in CNS diseases. To our knowledge, this is the first study to determine these transcripts in the peripheral blood of experimental animals, however, there are relevant human data for *Gfap* as a blood biomarker. It was first presented in acute stroke diagnosis in adults (Niebrój-Dobosz et al., 1994) and head trauma (Missler et al., 1999). Recently, it has been suggested that Gfap might be a potential biomarker of intracerebral haemorrhage (IHC) with symptoms of acute stroke (Brunkhorst et al., 2010; Mayer et al., 2013; Foerch et al., 2015). It is also an early marker of traumatic brain injury (Bembea et al., 2011; Lei et al., 2015), during different phases of cardiopulmonary bypass (Vedovelli et al., 2017), with predictiveness of neurological outcome (Lei et al., 2015). It is clear that the measurement of *Gfap* changes at the periphery is not a specific diagnostic tool and it is too early to draw a final conclusion on its utility at this stage. However, it would be interesting to see in future studies whether it could have a prognostic value to predict the conversion of orofacial pain or headache conditions from episodic to chronic. In our model, Gfap expression remained high even at the end of the experiment which could reflect a persistent neuroinflammation.

In conclusion, the main novelty of the present findings is the description of some up- and downregulated genes at the levels of both primary and secondary sensory neurones of the trigeminovascular system that might play important roles in neuroinflammatory activation mechanisms. Furthermore, we are the first to show transcriptomic alterations in the PBMCs that are similar to the changes detected in the neuronal tissues. These results open new perspectives and initiate further investigations in the research of trigeminal pain disorders.

AUTHOR CONTRIBUTIONS

ZH, KB, and ÉS: Study concept and design; KB, TA, and ÉS: Animal model, behavioural studies and sample collection conducted by; JK, SJ, AG, TR, TA: Microarray/qPCR analysis and interpretation of genetic data; ZH and TR: Funding. All authors contributed to the analysis of the results, drafting of manuscript and approved the final version.

FUNDING

The present study was supported by Hungarian Grants: National Brain Research Program 2(2017-1.2.1-NKP-2017-00002), EFOP-3.6.1.-16-2016-0004, GINOP 2.3.2-15-2016-00050 PEPSYS and University of Pécs, Medical School Grant: KA-2015-20. JK was supported by a scholarship from the European Union and the State of Hungary, co-financed by the European Social Fund in the framework of TAMOP-4.2.4.A/2-11/1-2012-0001 National Excellence Program Apáczai Scholarship.

ACKNOWLEDGMENTS

The authors wish to thank Mrs. Dóra Ömböli for expert technical assistance.

SUPPLEMENTARY MATERIAL

The Supplementary Material for this article can be found online at: https://www.frontiersin.org/articles/10.3389/fnmol.2018.00219/full#supplementary-material

REFERENCES

Alexa, A., and Rahnenführer, J. (2016). *topGO: Enrichment Analysis for Gene Ontology*. R package version 2.30.30. doi: 10.18129/B9.bioc.topGO

Alibhai, I. N., Green, T. A., Potashkin, J. A., and Nestler, E. J. (2007). Regulation of fosB and ΔfosB mRNA expression: *in vivo* and *in vitro* studies. *Brain Res.* 1143, 22–33. doi: 10.1016/j.brainres.2007.01.069

Arosio, B., D'Addario, C., Gussago, C., Casati, M., Tedone, E., Ferri, E., et al. (2014). Peripheral blood mononuclear cells as a laboratory to study dementia in the elderly. *BioMed Res. Int.* 2014:169203. doi: 10.1155/2014/169203

Ashburner, M., Ball, C. A., Blake, J. A., Botstein, D., Butler, H., Cherry, J. M., et al. (2000). Gene ontology: tool for the unification of biology. *Gene Ontol. Consortium. Nat. Genet.* 25, 25–29. doi: 10.1038/75556

Bayam, E., Sahin, G. S., Guzelsoy, G., Guner, G., Kabakcioglu, A., and Ince-Dunn, G. (2015). Genome-wide target analysis of NEUROD2 provides new insights into regulation of cortical projection neuron migration and differentiation. *BMC Genomics* 16:681. doi: 10.1186/s12864-015-1882-9

Bembea, M. M., Savage, W., Strouse, J. J., Schwartz, J. M., Graham, E., Thompson, C. B., et al. (2011). Glial fibrillary acidic protein as a brain injury biomarker in children undergoing extracorporeal membrane oxygenation. *Pediatr. Crit. Care Med. J. Soc. Crit. Care Med. World Fed. Pediatr. Intensive Crit. Care Soc.* 12, 572–579. doi: 10.1097/PCC.0b013e3181fe3ec7

Benemei, S., Nicoletti, P., Capone, J. G., and Geppetti, P. (2009). CGRP receptors in the control of pain and inflammation. *Curr. Opin. Pharmacol.* 9, 9–14. doi: 10.1016/j.coph.2008.12.007

Bernstein, C., and Burstein, R. (2012). Sensitization of the trigeminovascular pathway: perspective and implications to migraine pathophysiology. *J. Clin. Neurol. Seoul Korea* 8, 89–99. doi: 10.3988/jcn.2012.8.2.89

Bigal, M. E., Walter, S., and Rapoport, A. M. (2013). Calcitonin gene-related peptide (CGRP) and migraine current understanding and state of development. *Headache* 53, 1230–1244. doi: 10.1111/head.12179

Brunkhorst, R., Pfeilschifter, W., and Foerch, C. (2010). Astroglial proteins as diagnostic markers of acute intracerebral hemorrhage—pathophysiological background and clinical findings. *Transl. Stroke Res.* 1, 246–251. doi: 10.1007/s12975-010-0040-6

Burstein, R., Cutrer, M. F., and Yarnitsky, D. (2000). The development of cutaneous allodynia during a migraine attack Clinical evidence for the sequential recruitment of spinal and supraspinal nociceptive neurons in migraine. *Brain* 123, 1703–1709. doi: 10.1093/brain/123.8.1703

Burstein, R., Yamamura, H., Malick, A., and Strassman, A. M. (1998). Chemical stimulation of the intracranial dura induces enhanced responses to facial stimulation in brain stem trigeminal neurons. *J. Neurophysiol.* 79, 964–982. doi: 10.1152/jn.1998.79.2.964

Cady, R. J., Glenn, J. R., Smith, K. M., and Durham, P. L. (2011). Calcitonin gene-related peptide promotes cellular changes in trigeminal neurons and glia implicated in peripheral and central sensitization. *Mol. Pain* 7:94. doi: 10.1186/1744-8069-7-94

Chen, F., Moran, J. T., Zhang, Y., Ates, K. M., Yu, D., Schrader, L. A., et al. (2016). The transcription factor NeuroD2 coordinates synaptic innervation and cell intrinsic properties to control excitability of cortical pyramidal neurons. *J. Physiol.* 594, 3729–3744. doi: 10.1113/JP271953

Chung, M.-K., Park, J., Asgar, J., and Ro, J. Y. (2016). Transcriptome analysis of trigeminal ganglia following masseter muscle inflammation in rats. *Mol. Pain* 12:1. doi: 10.1177/1744806916668526

Colledge, W. H. (2009). Kisspeptins and GnRH neuronal signalling. *Trends Endocrinol. Metab.* 20, 115–121. doi: 10.1016/j.tem.2008.10.005

Coste, J., Voisin, D. L., Luccarini, P., and Dallel, R. (2008). A role for wind-up in trigeminal sensory processing: intensity coding of nociceptive stimuli in the rat. *Cephalalgia Int. J. Headache* 28, 631–639. doi: 10.1111/j.1468-2982.2008.01568.x

de Roux, N., Genin, E., Carel, J.-C., Matsuda, F., Chaussain, J.-L., and Milgrom, E. (2003). Hypogonadotropic hypogonadism due to loss of function of the KiSS1-derived peptide receptor GPR54. *Proc. Natl. Acad. Sci. U.S.A.* 100, 10972–10976. doi: 10.1073/pnas.1834399100

Doods, H., Arndt, K., Rudolf, K., and Just, S. (2007). CGRP antagonists: unravelling the role of CGRP in migraine. *Trends Pharmacol. Sci.* 28, 580–587. doi: 10.1016/j.tips.2007.10.005

Du, X., Tang, Y., Xu, H., Lit, L., Walker, W., Ashwood, P., et al. (2006). Genomic profiles for human peripheral blood T cells, B cells, natural killer cells, monocytes, and polymorphonuclear cells: comparisons to ischemic stroke, migraine, and Tourette syndrome. *Genomics* 87, 693–703. doi: 10.1016/j.ygeno.2006.02.003

Durham, P. L. (2006). Calcitonin Gene-Related Peptide (CGRP) and migraine. *Headache* 46, S3–S8. doi: 10.1111/j.1526-4610.2006.00483.x

Edgar, R., Domrachev, M., and Lash, A. E. (2002). Gene expression omnibus: NCBI gene expression and hybridization array data repository. *Nucleic Acids Res.* 30, 207–210. doi: 10.1093/nar/30.1.207

Edvinsson, L., Villalón, C. M., and MaassenVanDenBrink, A. (2012). Basic mechanisms of migraine and its acute treatment. *Pharmacol. Ther.* 136, 319–333. doi: 10.1016/j.pharmthera.2012.08.011

Elhabazi, K., Humbert, J.-P., Bertin, I., Schmitt, M., Bihel, F., Bourguignon, J.-J., et al. (2013). Endogenous mammalian RF-amide peptides, including PrRP, kisspeptin and 26RFa, modulate nociception and morphine analgesia via NPFF receptors. *Neuropharmacology* 75, 164–171. doi: 10.1016/j.neuropharm.2013.07.012

Fabregat, A., Jupe, S., Matthews, L., Sidiropoulos, K., Gillespie, M., Garapati, P., et al. (2018). The Reactome Pathway Knowledgebase. *Nucleic Acids Res.* 46, D649–D655. doi: 10.1093/nar/gkx1132

Filipović, B., Matak, I., Bach-Rojecky, L., and Lacković, Z. (2012). Central action of peripherally applied botulinum toxin Type A on pain and dural protein extravasation in rat model of trigeminal neuropathy. *PLoS ONE* 7:e29803. doi: 10.1371/journal.pone.0029803

Flegel, C., Schöbel, N., Altmüller, J., Becker, C., Tannapfel, A., Hatt, H., et al. (2015). RNA-Seq analysis of human trigeminal and dorsal root ganglia with a focus on chemoreceptors. *PLoS ONE* 10:e0128951. doi: 10.1371/journal.pone.0128951

Foerch, C., Luger, S., and Group, B. F. S. (2015). Glial fibrillary acidic protein (GFAP) plasma levels distinguish intracerebral hemorrhage from cerebral ischemia in the early phase of acute stroke. *J. Neurol. Sci.* 357:e430. doi: 10.1016/j.jns.2015.09.042

Gardiner, I., Ahmed, F., Steiner, T., McBain, A., Kennard, C., and de Belleroche, J. (1998). A study of adaptive responses in cell signaling in migraine and cluster headache: correlations between headache type and changes in gene expression. *Cephalalgia* 18, 192–196. doi: 10.1046/j.1468-2982.1998.1804192.x

Gentleman, R. C., Carey, V. J., Bates, D. M., Bolstad, B., Dettling, M., Dudoit, S., et al. (2004). Bioconductor: open software development for computational biology and bioinformatics. *Genome Biol.* 5:R80. doi: 10.1186/gb-2004-5-10-r80

Gerring, Z. F., Powell, J. E., Montgomery, G. W., and Nyholt, D. R. (2017). Genome-wide analysis of blood gene expression in migraine implicates immune-inflammatory pathways. *Cephalalgia* 38, 292–303. doi: 10.1177/0333102416686769

Gerring, Z., Rodriguez-Acevedo, A. J., Powell, J. E., Griffiths, L. R., Montgomery, G. W., and Nyholt, D. R. (2016). Blood gene expression studies in migraine: potential and caveats. *Cephalalgia* 36, 669–678. doi: 10.1177/0333102416628463

Goadsby, P. J., Holland, P. R., Martins-Oliveira, M., Hoffmann, J., Schankin, C., and Akerman, S. (2017). Pathophysiology of migraine: a disorder of sensory processing. *Physiol. Rev.* 97, 553–622. doi: 10.1152/physrev.00034.2015

Gormley, P., Anttila, V., Winsvold, B. S., Palta, P., Esko, T., Pers, T. H., et al. (2015). Meta-analysis of 375,000 individuals identifies 38 susceptibility loci for migraine. *bioRxiv* 030288. doi: 10.1101/030288

Gregory, N. S., Harris, A. L., Robinson, C. R., Dougherty, P. M., Fuchs, P. N., and Sluka, K. A. (2013). An overview of animal models of pain: disease models and outcome measures. *J. Pain* 14, 1255–1269. doi: 10.1016/j.jpain.2013.06.008

Herbison, A. E., d'Anglemont de Tassigny, X., Doran, J., and Colledge, W. H. (2010). Distribution and postnatal development of Gpr54 gene expression in mouse brain and gonadotropin-releasing hormone neurons. *Endocrinology* 151, 312–321. doi: 10.1210/en.2009-0552

Hershey, A. D., Tang, Y., Powers, S. W., Kabbouche, M. A., Gilbert, D. L., Glauser, T. A., et al. (2004). Genomic abnormalities in patients with migraine and chronic migraine: preliminary blood gene expression suggests platelet abnormalities. *Headache* 44, 994–1004. doi: 10.1111/j.1526-4610.2004.04193.x

Hershey, A., Horn, P., Kabbouche, M., O'Brien, H., and Powers, S. (2012). Genomic expression patterns in menstrually-related migraine in adolescents. *Headache* 52, 68–79. doi: 10.1111/j.1526-4610.2011.02049.x

Hucho, T., and Levine, J. D. (2007). Signaling pathways in sensitization: toward a nociceptor cell biology. *Neuron* 55, 365–376. doi: 10.1016/j.neuron.2007.07.008

Iwata, K., Takeda, M., Bae Oh, S., and Shinoda, M. (2017). "Neurophysiology of orofacial pain," in *Contemporary Oral Medicine*, eds C. Farah, R. Balasubramaniam, and M. McCullough (Cham: Springer), 1–23.

Kanehisa, M., and Goto, S. (2000). KEGG: kyoto encyclopedia of genes and genomes. *Nucleic Acids Res.* 28, 27–30. doi: 10.1093/nar/28.1.27

Kauffman, A. S., Clifton, D. K., and Steiner, R. A. (2007). Emerging ideas about kisspeptin– GPR54 signaling in the neuroendocrine regulation of reproduction. *Trends Neurosci.* 30, 504–511. doi: 10.1016/j.tins.2007.08.001

Kelemen, S. E., and Autieri, M. V. (2005). Expression of Allograft Inflammatory Factor-1 in T Lymphocytes. *Am. J. Pathol.* 167, 619–626. doi: 10.1016/S0002-9440(10)63003-9

Kelman, L. (2004). Osmophobia and taste abnormality in migraineurs: a tertiary care study. *Headache* 44, 1019–1023. doi: 10.1111/j.1526-4610.2004.04197.x

Knight, W. D., Little, J. T., Carreno, F. R., Toney, G. M., Mifflin, S. W., and Cunningham, J. T. (2011). Chronic intermittent hypoxia increases blood pressure and expression of FosB/ FosB in central autonomic regions. *Am. J. Physiol. Regul. Integr. Comp. Physiol.* 301, R131–R139. doi: 10.1152/ajpregu.00830.2010

Kogelman, L. J. A., Christensen, R. E., Pedersen, S. H., Bertalan, M., Hansen, T. F., Jansen-Olesen, I., et al. (2017). Whole transcriptome expression of trigeminal ganglia compared to dorsal root ganglia in Rattus Norvegicus. *Neuroscience* 350, 169–179. doi: 10.1016/j.neuroscience.2017.03.027

Koltzenburg, M., Wall, P. D., and McMahon, S. B. (1999). Does the right side know what the left is doing? *Trends Neurosci.* 22, 122–127. doi: 10.1016/S0166-2236(98)01302-2

Krzyzanowska, A., and Avendaño, C. (2012). Behavioral testing in rodent models of orofacial neuropathic and inflammatory pain. *Brain Behav.* 2, 678–697. doi: 10.1002/brb3.85

Krzyzanowska, A., Pittolo, S., Cabrerizo, M., Sánchez-López, J., Krishnasamy, S., Venero, C., et al. (2011). Assessing nociceptive sensitivity in mouse models of inflammatory and neuropathic trigeminal pain. *J. Neurosci. Methods* 201, 46–54. doi: 10.1016/j.jneumeth.2011.07.006

Kunkler, P. E., Ballard, C. J., Oxford, G. S., and Hurley, J. H. (2011). TRPA1 receptors mediate environmental irritant-induced meningeal vasodilatation. *Pain* 152, 38–44. doi: 10.1016/j.pain.2010.08.021

Kuzawinska, O., Lis, K., Cudna, A., and Balkowiec-Iskra, E. (2014). Gender differences in the neurochemical response of trigeminal ganglion neurons to peripheral inflammation in mice. *Acta Neurobiol Exp* 74, 227–232.

LaPaglia, D. M., Sapio, M. R., Burbelo, P. D., Thierry-Mieg, J., Thierry-Mieg, D., Raithel, S. J., et al. (2017). RNA-Seq investigations of human post-mortem trigeminal ganglia. *Cephalalgia* 38, 912–932. doi: 10.1177/0333102417720216

Lei, J., Gao, G., Feng, J., Jin, Y., Wang, C., Mao, Q., et al. (2015). Glial fibrillary acidic protein as a biomarker in severe traumatic brain injury patients: a prospective cohort study. *Crit. Care Lond. Engl.* 19:362. doi: 10.1186/s13054-015-1081-8

Levy, D., Jakubowski, M., and Burstein, R. (2004). Disruption of communication between peripheral and central trigeminovascular neurons mediates the antimigraine action of 5HT1B/1D receptor agonists. *Proc. Natl. Acad. Sci. U.S.A.* 101, 4274–4279. doi: 10.1073/pnas.0306147101

Luo, W., Friedman, M. S., Shedden, K., Hankenson, K. D., and Woolf, P. J. (2009). GAGE: generally applicable gene set enrichment for pathway analysis. *BMC Bioinformatics* 10:161. doi: 10.1186/1471-2105-10-161

Manteniotis, S., Lehmann, R., Flegel, C., Vogel, F., Hofreuter, A., Schreiner, B. S. P., et al. (2013). Comprehensive RNA-Seq expression analysis of sensory ganglia with a focus on ion channels and GPCRs in trigeminal ganglia. *PLoS ONE* 8:e79523. doi: 10.1371/journal.pone.0079523

Matsumoto, S., Yoshida, S., Takahashi, M., Saiki, C., and Takeda, M. (2010). The roles of ID, IA and IK in the electrophysiological functions of small-diameter rat trigeminal ganglion neurons. *Curr. Mol. Pharmacol.* 3, 30–36. doi: 10.2174/1874467211003010030

Mayer, C. A., Brunkhorst, R., Niessner, M., Pfeilschifter, W., Steinmetz, H., and Foerch, C. (2013). Blood levels of glial fibrillary acidic protein (GFAP) in patients with neurological diseases. *PLoS ONE* 8:e62101. doi: 10.1371/journal.pone.0062101

Mi, W.-L., Mao-Ying, Q.-L., Liu, Q., Wang, X.-W., Li, X., Wang, Y.-Q., et al. (2009). The distribution of kisspeptin and its receptor GPR54 in rat dorsal root ganglion and up-regulation of its expression after CFA injection. *Brain Res. Bull.* 78, 254–260. doi: 10.1016/j.brainresbull.2008.12.003

Middeldorp, J., and Hol, E. M. (2011). GFAP in health and disease. *Prog Neurobiol.* 93, 421–443. doi: 10.1016/j.pneurobio.2011.01.005

Missler, U., Wiesmann, M., Wittmann, G., Magerkurth, O., and Hagenström, H. (1999). Measurement of glial fibrillary acidic protein in human blood: analytical method and preliminary clinical results. *Clin. Chem.* 45, 138–141.

Nestler, E. J., Barrot, M., and Self, D. W. (2001). ΔFosB: a sustained molecular switch for addiction. *Proc. Natl. Acad. Sci. U.S.A.* 98, 11042–11046. doi: 10.1073/pnas.191352698

Niebrój-Dobosz, I., Rafałowska, J., Lukasiuk, M., Pfeffer, A., and Mossakowski, M. J. (1994). Immunochemical analysis of some proteins in cerebrospinal fluid and serum of patients with ischemic strokes. *Folia Neuropathol.* 32, 129–137.

Oakley, A. E., Clifton, D. K., and Steiner, R. A. (2009). Kisspeptin Signaling in the Brain. *Endocr. Rev.* 30, 713–743. doi: 10.1210/er.2009-0005

Okumura, M., Iwata, K., Yasuda, K., Inoue, K., Shinoda, M., Honda, K., et al. (2010). Alternation of Gene Expression in Trigeminal Ganglion Neurons Following Complete Freund's Adjuvant or Capsaicin Injection into the Rat Face. *J. Mol. Neurosci.* 42, 200–209. doi: 10.1007/s12031-010-9348-7

Pawlik, A., Kotrych, D., Paczkowska, E., Roginska, D., Dziedziejko, V., Safranow, K., et al. (2016). Expression of allograft inflammatory factor-1 in peripheral blood monocytes and synovial membranes in patients with rheumatoid arthritis. *Hum. Immunol.* 77, 131–136. doi: 10.1016/j.humimm.2015.11.008

Perrino, C., Barabási, A.-L., Condorelli, G., Davidson, S. M., De Windt, L., Dimmeler, S., et al. (2017). Epigenomic and transcriptomic approaches in the post-genomic era: path to novel targets for diagnosis and therapy of the ischaemic heart? Position Paper of the European Society of Cardiology Working Group on Cellular Biology of the Heart.*Cardiovasc. Res.* 113, 725–736. doi: 10.1093/cvr/cvx070

Plummer, P. N., Colson, N. J., Lewohl, J. M., MacKay, R. K., Fernandez, F., Haupt, L. M., et al. (2011). Significant differences in gene expression of GABA receptors in peripheral blood leukocytes of migraineurs. *Gene* 490, 32–36. doi: 10.1016/j.gene.2011.08.031

Popovics, P., and Stewart, A. J. (2011). GPR39: a Zn^{2+}-activated G protein-coupled receptor that regulates pancreatic, gastrointestinal and neuronal functions. *Cell. Mol. Life Sci.* 68, 85–95. doi: 10.1007/s00018-010-0517-1

R Development Core Team (2008). *R: A Language and Environment for Statistical Computing*. Vienna: R Foundation for Statistical Computing.

Ren, K., and Dubner, R. (1999). Inflammatory models of pain and hyperalgesia. *ILAR J.* 40, 111–118. doi: 10.1093/ilar.40.3.111

Ritchie, M. E., Phipson, B., Wu, D., Hu, Y., Law, C. W., Shi, W., et al. (2015). limma powers differential expression analyses for RNA-sequencing and microarray studies. *Nucleic Acids Res.* 43:e47. doi: 10.1093/nar/gkv007

Romero-Reyes, M., Akerman, S., Nguyen, E., Vijjeswarapu, A., Hom, B., Dong, H.-W., et al. (2013). Spontaneous behavioral responses in the orofacial region: a model of trigeminal pain in mouse. *Headache* 53, 137–151. doi: 10.1111/j.1526-4610.2012.02226.x

Romero-Reyes, M., and Uyanik, J. M. (2014). Orofacial pain management: current perspectives. *J. Pain Res.* 7, 99–115. doi: 10.2147/JPR.S37593

Russo, A. F. (2015). Calcitonin Gene-Related Peptide (CGRP). *Annu. Rev. Pharmacol. Toxicol.* 55, 533–552. doi: 10.1146/annurev-pharmtox-010814-124701

Sato, S., Huang, X.-P., Kroeze, W. K., and Roth, B. L. (2016). Discovery and characterization of novel GPR39 agonists allosterically modulated by Zinc. *Mol. Pharmacol.* 90, 726–737. doi: 10.1124/mol.116.106112

Schreiber, A. O., and Calvert, P. C. (1986). Migrainous olfactory hallucinations. *Headache* 26, 513–514. doi: 10.1111/j.1526-4610.1986.hed2610513.x

Schueler, M., Messlinger, K., Dux, M., Neuhuber, W. L., and De, R. (2013). Extracranial projections of meningeal afferents and their impact on meningeal nociception and headache. *Pain* 154, 1622–1631. doi: 10.1016/j.pain.2013.04.040

Seminara, S. B. (2006). Mechanisms of Disease: the first kiss—a crucial role for kisspeptin-1 and its receptor, G-protein-coupled receptor 54, in puberty and reproduction. *Nat. Rev. Endocrinol.* 2, 328–334. doi: 10.1038/ncpendmet0139

Shenker, N., Haigh, R., Roberts, E., Mapp, P., Harris, N., and Blake, D. (2003). A review of contralateral responses to a unilateral inflammatory lesion. *Rheumatol. Oxf. Engl.* 42, 1279–1286. doi: 10.1093/rheumatology/keg397

Shinoda, M., and Iwata, K. (2013). Neural communication in the trigeminal ganglion contributes to ectopic orofacial pain. *J. Oral Biosci.* 55, 165–168. doi: 10.1016/j.job.2013.06.003

Spampinato, S., Trabucco, A., Biasiotta, A., Biagioni, F., Cruccu, G., Copani, A., et al. (2011). Hyperalgesic activity of kisspeptin in mice. *Mol. Pain* 7:90. doi: 10.1186/1744-8069-7-90

Srinivasan, S., Di Dario, M., Russo, A., Menon, R., Brini, E., Romeo, M., et al. (2017). Dysregulation of MS risk genes and pathways at distinct stages of disease. *Neurol. - Neuroimmunol. Neuroinflammation* 4:e337. doi: 10.1212/NXI.0000000000000337

Takeda, M., Tanimoto, T., Kadoi, J., Nasu, M., Takahashi, M., Kitagawa, J., et al. (2007). Enhanced excitability of nociceptive trigeminal ganglion neurons by satellite glial cytokine following peripheral inflammation. *Pain* 129, 155–166. doi: 10.1016/j.pain.2006.10.007

The Gene Ontology Consortium (2017). Expansion of the Gene Ontology knowledgebase and resources. *Nucleic Acids Res.* 45, D331–D338. doi: 10.1093/nar/gkw1108

Vedovelli, L., Padalino, M., D'Aronco, S., Stellin, G., Ori, C., Carnielli, V. P., et al. (2017). Glial fibrillary acidic protein plasma levels are correlated with degree of hypothermia during cardiopulmonary bypass in congenital heart disease surgery. *Interact. Cardiovasc. Thorac. Surg.* 24, 436–442. doi: 10.1093/icvts/ivw395

Weyer, A. D., Zappia, K. J., Garrison, S. R., O'Hara, C. L., Dodge, A. K., and Stucky, C. L. (2016). Nociceptor Sensitization Depends on Age and Pain Chronicity(1,2,3). *eNeuro* 3: ENEURO.0115-15.2015. doi: 10.1523/ENEURO.0115-15.2015

Yasuda, M., Shinoda, M., Kiyomoto, M., Honda, K., Suzuki, A., Tamagawa, T., et al. (2012). P2X3 receptor mediates ectopic mechanical allodynia with inflamed lower lip in mice. *Neurosci. Lett.* 528, 67–72. doi: 10.1016/j.neulet.2012.08.067

Conflict of Interest Statement: The authors declare that the research was conducted in the absence of any commercial or financial relationships that could be construed as a potential conflict of interest.

Aczél et al. The Journal of Headache and Pain (2021) 22:117
https://doi.org/10.1186/s10194-021-01285-9

The Journal of Headache and Pain

RESEARCH ARTICLE Open Access

Identification of disease- and headache-specific mediators and pathways in migraine using blood transcriptomic and metabolomic analysis

Timea Aczél[1†], Tamás Körtési[2,3,4†], József Kun[1,5†], Péter Urbán[5], Witold Bauer[5], Róbert Herczeg[5], Róbert Farkas[6], Krisztián Kovács[6], Barna Vásárhelyi[6], Gellért B. Karvaly[6], Attila Gyenesei[5], Bernadett Tuka[2,3], János Tajti[2], László Vécsei[2,3], Kata Bölcskei[1†] and Zsuzsanna Helyes[1*†]

Abstract

Background: Recent data suggest that gene expression profiles of peripheral white blood cells can reflect changes in the brain. We aimed to analyze the transcriptome of peripheral blood mononuclear cells (PBMC) and changes of plasma metabolite levels of migraineurs in a self-controlled manner during and between attacks.

Methods: Twenty-four patients with migraine were recruited and blood samples were collected in a headache-free (interictal) period and during headache (ictal) to investigate disease- and headache-specific alterations. Control samples were collected from 13 age- and sex-matched healthy volunteers. RNA was isolated from PBMCs and single-end 75 bp RNA sequencing was performed using Illumina NextSeq 550 instrument followed by gene-level differential expression analysis. Functional analysis was carried out on information related to the role of genes, such as signaling pathways and biological processes. Plasma metabolomic measurement was performed with the Biocrates MxP Quant 500 Kit.

Results: We identified 144 differentially-expressed genes in PBMCs between headache and headache-free samples and 163 between symptom-free patients and controls. Network analysis revealed that enriched pathways included inflammation, cytokine activity and mitochondrial dysfunction in both headache and headache-free samples compared to controls. Plasma lactate, succinate and methionine sulfoxide levels were higher in migraineurs while spermine, spermidine and aconitate were decreased during attacks.

Conclusions: It is concluded that enhanced inflammatory and immune cell activity, and oxidative stress can play a role in migraine susceptibility and headache generation.

Keywords: Migraine, Transcriptomic analysis, Peripheral blood mononuclear cells, Cytokines, Mitochondrial dysfunction

* Correspondence: zsuzsanna.helyes@aok.pte.hu
†Timea Aczél, Tamás Körtési, József Kun, Kata Bölcskei and Zsuzsanna Helyes contributed equally to this work.
[1]Department of Pharmacology and Pharmacotherapy, Molecular Pharmacology Research Group and Centre for Neuroscience, University of Pécs Szentágothai Research Centre, University of Pécs Medical School, Szigeti út 12, Pécs H-7624, Hungary
Full list of author information is available at the end of the article

Background

Migraine is a primary headache condition characterized by moderate-to-severe unilateral pain of pulsating or throbbing quality and accompanying symptoms, such as nausea/vomiting or photo−/phonophobia. The headache can be triggered by a variety of factors such as alcohol, stress or hormonal changes [1]. There has been an ongoing debate about the precise pathophysiological mechanism of the disease, but the most accepted theory is that migraine is a disorder affecting the sensory processing of the brain [1]. However, the headache is most likely to be generated by the activation of the trigeminovascular system resulting in neurogenic vasodilation and inflammation of the meninges [2]. It is now evident that major contributors to headache development are the neuropeptides calcitonin gene-related peptide (CGRP) [3–5] and pituitary adenylate cyclase activating polypeptide (PACAP) [6–8]. Yet, the exact sequence of events during the phases of headache episode and the relative importance of central and peripheral mechanisms are still unclear. Except for the recently approved anti-CGRP monoclonal antibodies, most of the preventive treatment is based on empirical observations rather than the understanding of the pathophysiology. Elucidating the pathophysiological mechanisms is crucial to identify the key mediators and determine novel therapeutic targets.

It is also accepted that migraine susceptibility has a genetic background [9, 10]. However, most of the research using linkage, candidate gene- and genome-wide association studies (GWAS) provided limited results. GWAS have revealed susceptibility genes or loci implicating vascular and smooth muscle tissues, synaptic function, astrocyte-, microglia- and oligodendrocyte roles [11–13]. The few genomic next-generation sequencing studies mainly focused on certain candidate genes associated with glutamatergic neurotransmission and synaptic function/development, pain-sensing mechanisms, metalloproteinases and vascular metabolism [9]. Quite recently, the interaction between single nucleotide polymorphisms of three genes involved in synaptic transmission was also linked to migraine susceptibility [14]. None of the candidate genes could be conclusive as genetic biomarkers of the disease, each having small impact individually and limited predictive value [15]. The reason for this could be that genetic-environmental interactions play an important role in disease mechanisms in specific clinical conditions. Gene expression patterns associated with migraine reflect genetic and non-genetic effects and may inform of migraine susceptibility and outcome [16].

Recent results have pointed out that interactions between external stimuli and brain pathological processes may be reflected in peripheral tissues, such as the blood, which facilitates clinical research of several central nervous system diseases without invasive tissue sampling [16–18]. Differentially expressed genes have been described in peripheral whole blood of migraineurs by microarray or bead array [19, 20]. More recently, whole blood next-generation RNA sequencing studies were also performed to compare healthy individuals and migraineurs. While the study by Gerring and coworkers revealed significant changes in immune function and cytokine signaling [21], another study by Kogelman and coworkers reported largely negative results [22].

To unveil pathways responsible for headache generation, a self-controlled study design to compare samples of headache (ictal) and headache-free (interictal) periods is also necessary. Since previous data show that the transcriptome of mononuclear blood cells is more closely correlated with the transcriptome of brain samples [18], RNA sequencing was performed from separated peripheral blood mononuclear cells (PBMCs) instead of the whole blood. We have also complemented the transcriptome analysis of peripheral blood mononuclear cells with a plasma metabolome analysis from simultaneously taken samples.

Methods

Study design

The study was approved by the National Public Health Center, Ministry of Human Capacities of Hungary (28324–5/2019/EÜIG). All study participants gave their written informed consent in accordance with the Declaration of Helsinki.

Episodic migraine patients (with or without aura) between the age of 20–65 years were included in the study. Migraineurs were selected in accordance with the criteria of the third edition of International Classification of Headache Disorders [23]: recurrent unilateral, pulsating headache, which manifests in moderate or severe intensity attacks lasting 4–72 h. Headache was aggravated by routine physical activity and associated with nausea and/or vomiting, as well as photophobia and phonophobia. Exclusion criteria for enrolment included chronic inflammatory diseases and depression.

Blood samples were drawn from migraine sufferers in an attack-free period and during an attack. The attack-free (interictal) sample was collected if the patient had no headache for at least 24 h. For ictal samples, affected patients were asked not to start their usual attack treatment until the blood had been taken. There were no restrictions as regards food and drink intake. A detailed questionnaire was used to compile a homogeneous group of migraineurs concerning the features of their disease. Questions included the prophylactic or attack medication before sampling, number of attacks in the previous month, the time of the last attack, the

beginning of the current attack, other known diseases, applied drugs and contraceptives, relation of migraine attacks to the menstrual cycle, the presence of allodynia, attack frequency, duration of migraine, severity of pain during attacks as measured on a visual analog scale, comorbidities with other chronic diseases, familial manifestation of migraine, regular sport activity and the time of the last meal were recorded.

Enrolment took place between September 2018 and December 2019. Thirty six female and 1 male subjects were recruited: 24 episodic migraine patients with or without aura and 13 healthy controls. Sample size was determined based on literature data [24, 25]. Healthy volunteers serving as controls were screened for non-reported/non-treated headaches.

Sample collection

Human blood (13 mL/person) was collected from cubital veins of migraineurs and healthy volunteers into ice-cold glass tubes containing ethylenediaminetetraacetic acid (EDTA) or citrate. For the transcriptomic measurements, the PBMCs were isolated by Ficoll-Paque PREMIUM (GE Healthcare, Budapest, Hungary) according to the manufacturer's instructions. Four mL of anticoagulant-treated blood and 4 mL phosphate-buffered saline (PBS) - EDTA solution were mixed in sterile centrifuge tubes. Next, the diluted blood samples were layered on 5 mL Ficoll-Paque PREMIUM and centrifuged 40 min at 400×g, 20 °C. After the removal of the liquid phase, the PBMC layer was transferred into a new centrifuge tube, suspended with 6 mL PBS-EDTA solution and centrifuged 10 min at 500×g, 20 °C. The supernatant was removed also and the pellet was suspended in 6 mL PBS-EDTA solution, followed by centrifugation (10 min, 500×g, 20 °C). Liquid phase was removed and the cells were resuspended with 1 mL of TRI Reagent (Molecular Research Center, Cincinnati, OH, USA), transposed to Eppendorf tubes and stored at − 80 °C until the gene expression investigations.

For the metabolomic measurements, the total human blood samples were centrifuged at 300×g for 15 min, twice at 2500×g for 15 min and 18,000×g for 90 min at 4 °C. Plasma samples were stored at − 80 °C until analysis. Samples showing signs of hemolysis were excluded.

RNA extraction and quality control

Isolation and purification of total RNA were carried out as previously described [26] using the phenol-chloroform based TRI Reagent procedure (Molecular Research Center, Cincinnati, OH, USA), up to the step of acquiring the RNA-containing aqueous layer. The aqueous phase was mixed with an equal volume of absolute ethanol and was loaded into Zymo-Spin™ IICR Column. Direct-zol RNA MiniPrep kit (Zymo Research, Irvine, CA, USA) was used according to the manufacturer's protocol including the optional on-column DNase digestion.

RNA concentrations were measured using Qubit 3.0 (Invitrogen, Carlsbad, CA, USA). The RNA quality was verified on TapeStation 4200 using RNA ScreenTape (Agilent Technologies, Santa Clara, CA, USA). We proceeded with high quality (RIN > 8) RNA samples to library preparation.

Illumina library preparation and sequencing

The library for Illumina sequencing was prepared using NEBNext Ultra II Directional RNA Library Prep Kit for Illumina (NEB, Ipswitch, MA, USA). Briefly, mRNA was isolated from 500 ng total RNA using NEBNext Poly(A) mRNA MAgnetic Isolation Module (NEB, Ipswitch, MA, USA). Thereafter, the mRNA was fragmented, end prepped and adapter-ligated. Finally, the library was amplified according to the manufacturer's instructions. The quality of the libraries was checked on 4200 TapeSation System using D1000 Screen Tape, the quantity was measured on Qubit 3.0. Illumina sequencing was performed on the NextSeq550 instrument (Illumina, San Diego, CA, USA) with 1 × 76 run configuration.

Bioinformatics

The sequencing reads were aligned against the *Homo sapiens* reference genome (GRCh37 Ensembl release) with STAR v2.5.3a [27]. After alignment, the reads were associated with known protein-coding genes and the number of reads aligned within each gene was counted using Rsubread package v2.0.0 [28]. Gene count data were normalized using the trimmed mean of M values (TMM) normalization method of the edgeR R/Bioconductor package (v3.28, R v3.6.0, Bioconductor v3.9) [29]. For statistical testing the data were further log transformed using the voom approach [30] in the limma package [31]. Normalized counts were represented as transcripts per million (TPM) values. Fold change (FC) values between the compared groups resulting from linear modeling process and modified t-test *p*-values were produced by the limma package. The Benjamini–Hochberg method was used to control the False Discovery Rate (FDR) and adjusted *p*-values were calculated by limma. In case of paired ictal and interictal samples the correlation between samples originating from the same patient was taken into account using the duplicateCorrelation function of limma. Functional analysis was performed to take into account the annotations of genes using the Gene Ontology (GO), Kyoto Encyclopedia of Genes and Genomes (KEGG), and Reactome databases. Detection of functional enrichment was performed in the differentially expressed gene list (DE list enrichment: Fisher's exact test for GO, hypergeometric test for

KEGG and Reactome) and towards the top of the list when all genes have been ranked according to the evidence for being differentially expressed (ranked list enrichment: non-parametric Kolmogorov-Smirnov test for GO and KEGG, hypergeometric test for Reactome) applying the topGO v2.37.0, ReactomePA v1.30.0, gage v2.36.0 packages. The pathview package v1.26.0 [32] was used to visualize mapping data to KEGG pathways.

Targeted metabolomic measurements

Acetonitrile, formic acid, methanol and water, all LC-MS grade, as well as ammonium acetate for HPLC and ethanol 96% Ph. Eur. 9.0, were obtained from Molar Chemicals Kft. (Halásztelek, Hungary). The MxP Quant 500 Kit was purchased from Biocrates Life Sciences AG (Innsbruck, Austria). Phenyl isothiocyanate (PITC), phosphate buffered saline and pyridine were from Sigma Aldrich Kft (Budapest, Hungary). Phosphate buffered saline solution was prepared as per the recommendations of the manufacturer. 5 mmol/L ammonium acetate was prepared by adding 19 mg ammonium acetate to 50 mL methanol.

Plasma samples were processed for analysis as recommended by the kit manufacturer. Briefly, after being allowed to thaw and equilibrate to room temperature, samples were homogenized. 10-μL plasma aliquots, calibrators and controls were pipetted into the respective slots of a 96-well deep well reaction plate. The plate was dried for 30 min under nitrogen 5.0 (Messer Hungarogáz Kft., Budapest, Hungary). Derivatization was performed by adding 50 μL 5% PITC prepared in a mixture of ethanol, pyridine and water (1:1:1, v/v) to each slot, covering and incubating the plate for 60 min at ambient temperature and, after removing the plastic lid, by drying for 60 min under nitrogen. 300 μL 5 mmol/L ammonium acetate was subsequently added and the plate was shaken on an Allsheng MD-200 plate shaker at 450 rpm, ambient temperature, for 30 min. Elution of the analytes into a 96-well deep-well collection plate was performed by applying positive pressure on a Phenomenex Presston manifold (Gen-Lab Kft., Budapest, Hungary). For runs including chromatographic separation, 150 μL extract was pipetted to an LC collection plate and was diluted with 150 μL water. For flow injection analysis, 10 μl extract was transferred to a FIA collection plate and was diluted with 490 μL mobile phase employed for the FIA runs.

Analysis was conducted on a Shimadzu Nexera XR high performance liquid chromatograph (Simkon Kft, Budapest, Hungary) coupled to a low-resolution Sciex Qtrap 5500 mass spectrometer equipped with an electrospray ionization unit and operated in the multiple reaction monitoring mode (Per-form Hungária Kft, Budapest, Hungary). Sciex Analyst v.1.6.3 software was used for instrument control and data acquisition. Peak review and analyte quantitation was done using the Biocrates MetIDQ^{TM} (Nitrogen version) software as instructed by the kit manufacturer.

Samples were run using 4 different instrumental setups, with the liquid chromatographic separation of 106 metabolites, and the flow injection analysis of 524 metabolites. Both positive and negative ionization polarity was employed. Liquid chromatographic separation was performed using the stationary phase provided by the kit manufacturer and equipped with a precolumn Mixer (Biocrates A.G., Innsbruck, Austria). The mobile phases were water (A) and acetonitrile (B), both of which contained 0.2% formic acid. Analysis with positive ionization was carried out with an initial flow rate was 0.5 mL/min, then 0.6 mL/min at 5.5 min, then 8.0 mL/min at 7.0 min, and, finally, 0.5 mL/min at 7.5 min. The following linear gradient program was applied (% mobile phase B): initial, 0% for 0.25 min, 12% at 1 min, 17.5% at 3,0 min, 50% at 4.5 min, and 100% at 5.5 min. Analysis in the negative ionization mode was carried out with an initial flow rate of 0.5 mL/min, 0.7 mL/min at 4.5 min, 0.8 mL/min at 6.5 min, and, finally, 0.5 mL/min at 7.6 min. The following linear gradient program was applied: initial, 0% for 0.25 min, 25% at 0.5 min, 50% at 3.0 min, 75% at 4.0 min, and 100% at 4.5 min. The injection volume was 5 μL. The stationary phase was thermostatted at 50 °C. The general mass spectrometry settings in the positive and negative modes, respectively, were curtain gas, 45 L/min and 20 L/min, collision gas, 9 L/min and 8 L/min, ion spray voltage, 5500 V and − 4500 V, ion source temperature, 500 °C and 650 °C, ion source gas 1, 60 L/min and 40 L/min, and ion source gas 2, 70 L/min and 40 L/min. In the flow injection analysis mode, the mobile phase was prepared by adding 1 ampule FIA Mobile Phase Additive, supplied with the MxP Quant 500 kit, to 290 μL methanol. The flow rate was 0.2 mL/min, the sample injection volume was 20 μL. Ionization was performed in the positive mode. In the 2 runs, respectively, curtain gas was 20 L/min and 10 L/min, collision gas was 9 L/min, ion spray voltage was 5500 V, ion source temperature was 200 °C and 350 °C, ion source gas 1 was set at 40 L/min and 30 L/min, and ion source gas 2 was at 50 L/min and 90 L/min. Analyte-specific mass spectrometry settings were provided by the kit manufacturer.

Evaluation and statistical analysis of targeted metabolomic measurements

The calculation of the concentrations of the metabolites evaluated in the targeted metabolomic measurements, as well as quality control assessment, was performed automatically by the Biocrates MetIDQ^{TM} software. 42 metabolites, all determined in the liquid chromatography-

mass spectrometry (LC-MS/MS) assay, were quantitated using 6-point calibration curves. Linear regression was applied using 1/concentration weights, except for dopamine (quadratic regression, 1/concentration weights). The determination coefficients of the fitted lines ranged between 0.9894–0.9999 (median: 0.9972). 64 metabolites, assayed using LC-MS/MS, were evaluated by comparing their peak areas to those of their respective internal standards dried onto each slot of the sample preparation plate in known concentrations. The quantitation of the 524 metabolites measured using flow injection analysis-tandem mass spectrometry (FIA-MS/MS) was performed automatically by the MetIDQ™ software employing algorithms not disclosed to the users of the Biocrates MxP® Quant 500 kit. No data filtering or correction was applied in this phase of evaluation.

Raw metabolomic data treatment included cleaning of the background noise and unrelated ions through Molecular Feature Extraction (MFE) tool in Mass Hunter Qualitative Analysis Software (B.06.00, Agilent). Mass Profiler Professional (B.12.61, Agilent Technologies) software was used to perform quality assurance (QA) procedure and data filtration. QA procedure covered selection of metabolic features with good repeatability. To achieve this, only features detected in > 80% of the samples after QC, and samples having RSD < 30% were kept.

The differences between metabolomic profiles of the healthy controls and migraineurs (interictal and ictal) patients were studied. Homogeneity of variance and normality assumptions were studied using Levene's and Shapiro-Wilk tests respectively. Mean plasma concentrations of metabolites in 3 study groups were compared using one-way analysis of variance (ANOVA) test or Kruskal–Wallis test. For one-by-one comparisons, the t-test or Wilcoxon test were used. The statistical significance level was set at 0.05 for all two-sided tests and multivariate comparisons. All calculations were prepared in R (R version 3.6.2).

Results

Clinical characteristics of the patient population

The baseline demographic and clinical characteristic of the studied population is presented in Table 1. The studied groups were well matched, without any between-group differences in age, and anthropometric measurements such as body mass index (BMI). Interictal blood samples were collected from all 24 migraine patients,

Table 1 Demographic and clinical characteristics of study participants. Mean ± SD values are represented in the table

Group	Migraineurs with ($n = 3$) and without aura ($n = 21$)	Healthy control subjects ($n = 13$)
Gender	female $n = 23$ male $n = 1$	female $n = 13$
Age (years)	35 ± 12.25	35 ± 4.96
Body mass index (BMI)	22.21 ± 4.57	24 ± 3.47
Last meal (hours ago)	6.59 ± 6.29	3.69 ± 5.32
Co-morbidities and drugs of migraine patients		
Known other diseases	yes $n = 10$ no $n = 14$	
Regular medication (except for attack therapy)	yes $n = 7$ no $n = 17$	
Hormonal contraceptives	yes $n = 8$ no $n = 16$	
Antimigraine prophylactic therapy	no $n = 24$	
Clinical features of the headache		
Disease duration (years)	15 ± 12	
Attack frequency (attack/year)	32 ± 37.37	
Visual analogue scale (VAS)	7 ± 1.44	
Allodynia	yes $n = 9$ no $n = 15$	
Chronic pain	yes $n = 3$ no $n = 21$	
Menstruation-headache relationship	sensitive $n = 10$ independent $n = 13$	
Migraineurs in the family	yes $n = 15$ no $n = 9$	
Regular sport activity	yes $n = 13$ no $n = 11$	
Features of attacks before samplings		
Number of attacks in the previous month	3 ± 3.31	
Last attack before interictal blood sampling (days ago)	16.58 ± 28.35	
Beginning of attack before ictal blood sampling (hours)	17.91 ± 29.47	

while ictal samples were obtained from 8 of them for self-controlled comparison.

Transcriptome profile of PBMC samples

Twenty out of 24 interictal blood samples were used for PBMC RNA sequencing.

In interictal PBMC samples compared to healthy ones, 163 genes were found to be differentially expressed with a fold change threshold of 1.5 and a *p*-value threshold of 0.05, 135 genes were upregulated and 28 were downregulated. Based on the average of fold change and *p*-value ranks (average rank), the interleukin (IL)-1β gene (IL1B) was implicated at the top of the differentially expressed (DE) gene list (Table S1). Other highly implicated genes include prostaglandin-endoperoxide synthase 2 (PTGS2) also known as cyclooxygenase 2 (COX2), tumor necrosis factor (TNF), and numerous chemokines, such as IL-8 (IL8).

In ictal PBMC samples, when compared to the interictal ones, 144 genes were differentially expressed (fold change: 1.3, *p*-value: 0.05), 64 were upregulated, 80 downregulated. Heterogeneous nuclear ribonucleoprotein C like 1 (HNRNPCL1) was implicated most, along with olfactory receptor family 10 subfamily G member 2 (OR10G2) and interleukin 20 receptor subunit alpha (IL20RA), among others (Table S2). After FDR correction, two genes had adjusted *p*-values below 0.25, heterogeneous nuclear ribonucleoprotein C like 1 (HNRN PCL1) and cornichon family AMPA receptor auxiliary protein 3 (CNIH3).

In ictal PBMC samples compared to healthy samples, 131 genes were differentially expressed (fold change: 1.5, *p*-value: 0.05), 118 were upregulated, 13 downregulated. Similarly to the interictal and healthy sample comparison, IL1B gene was implicated at the top of the differentially expressed gene list (Table S3). Other highly implicated genes include PTGS2, TNF, and numerous chemokines such as IL8.

When DE genes were visualized on heat maps (Figs. 1, 2, 3), samples were clustered according to the original sample groups. Remarkably, the interictal group splits into two major and one minor subgroups based on gene expression patterns when compared to the healthy (Fig. 1) and ictal (Fig. 2) group.

Functional enrichment analysis of DE genes (DE list enrichment) and ranked list enrichment of all genes were carried out, which yielded statistically significant GO, KEGG and Reactome terms involved in PBMC cells of migraineurs (Tables 2, 3, 4).

In the interictal PBMC samples compared to healthy ones, cytokine and chemokine receptor binding, interleukin-10 (IL-10) signaling, as well as oxidative phosphorylation in the mitochondria were significantly affected.

In the ictal vs. interictal comparison, hormone and cytokine activity, oxidative phosphorylation, chemosensory receptors were implicated, among others.

In the ictal versus healthy comparison, IL-4, IL-10 and IL-13, as well as chemokine, growth factor and neuroactive ligand-receptor interactions were implicated.

Ranked list enrichment analysis of all genes statistically significantly implicated the metabolic pathway of oxidative phosphorylation (Tables 2, 3, 4) in the interictal PBMC samples when compared to the healthy control group (Fig. 4, upper panel) with a *p*-value of 8.82E-06, as well as in the ictal samples in comparison with the interictal group (Fig. 4, lower panel) with a *p*-value of 0.000845. Expression of most oxidative phosphorylation related genes on Fig. 4 were elevated in the interictal samples versus the healthy ones, while decreased in ictal samples during migraine attack when compared to the interictal groups. Expression of genes coding succinate dehydrogenase/fumarate reductase enzymes (SDHA, SDHB, SDHC, SDHD), for example, increased in the interictal samples versus the healthy ones, while decreased in ictal samples during migraine attack when compared to the interictal groups, albeit statistically non-significantly at the individual gene level.

Metabolic alterations in the plasma of migraine patients

Metabolomic measurements were performed on 14 interictal, 6 ictal and 6 healthy control plasma samples. During the migraine attack (ictal) spermine and spermidine levels were significantly reduced (Fig. 5A,B, *p*-values: 0.021 and < 0.001), in comparison to metabolite concentrations found in the samples from the attack-free period. Interestingly, the spermine/spermidine ratio was suppressed in migraineurs, but during headache the concentration ratio was restored to a healthy-like level (Fig. 5C, *p*-value: 0.014). Methionine sulfoxide levels significantly increased (Fig. 5D, *p*-values: 0.026) during the ictal phase, compared to the healthy group. Lactate and succinate levels were significantly elevated (Fig. 5E,F, *p*-values: 0.031 and 0.005) during the interictal phase when compared to healthy volunteers. Succinate concentration was also significantly higher (*p*-value: 0.0022) during the ictal phase compared to the healthy group, while aconitate was lower in the same comparison (Fig. 5G, *p*-value: 0.041).

Discussion

This is the first transcriptome analysis of PBMCs isolated from interictal and ictal samples of migraine patients in comparison with healthy controls suggesting the importance of inflammatory pathways and the potential contribution of various cytokines to migraine susceptibility. In addition to the inflammatory pathways, our results suggest potential implication of mitochondrial dysfunction in migraine. Moreover, significant

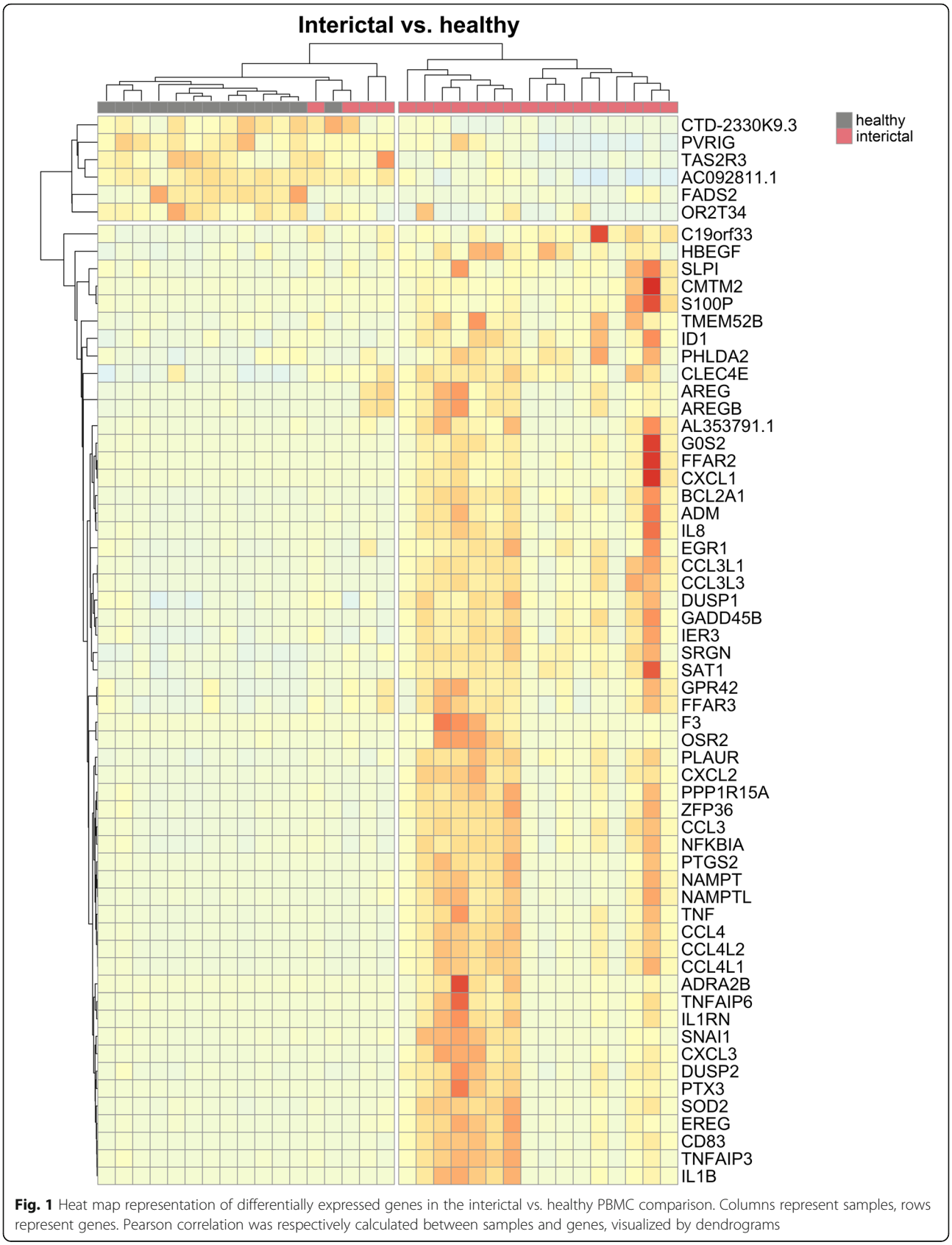

Fig. 1 Heat map representation of differentially expressed genes in the interictal vs. healthy PBMC comparison. Columns represent samples, rows represent genes. Pearson correlation was respectively calculated between samples and genes, visualized by dendrograms

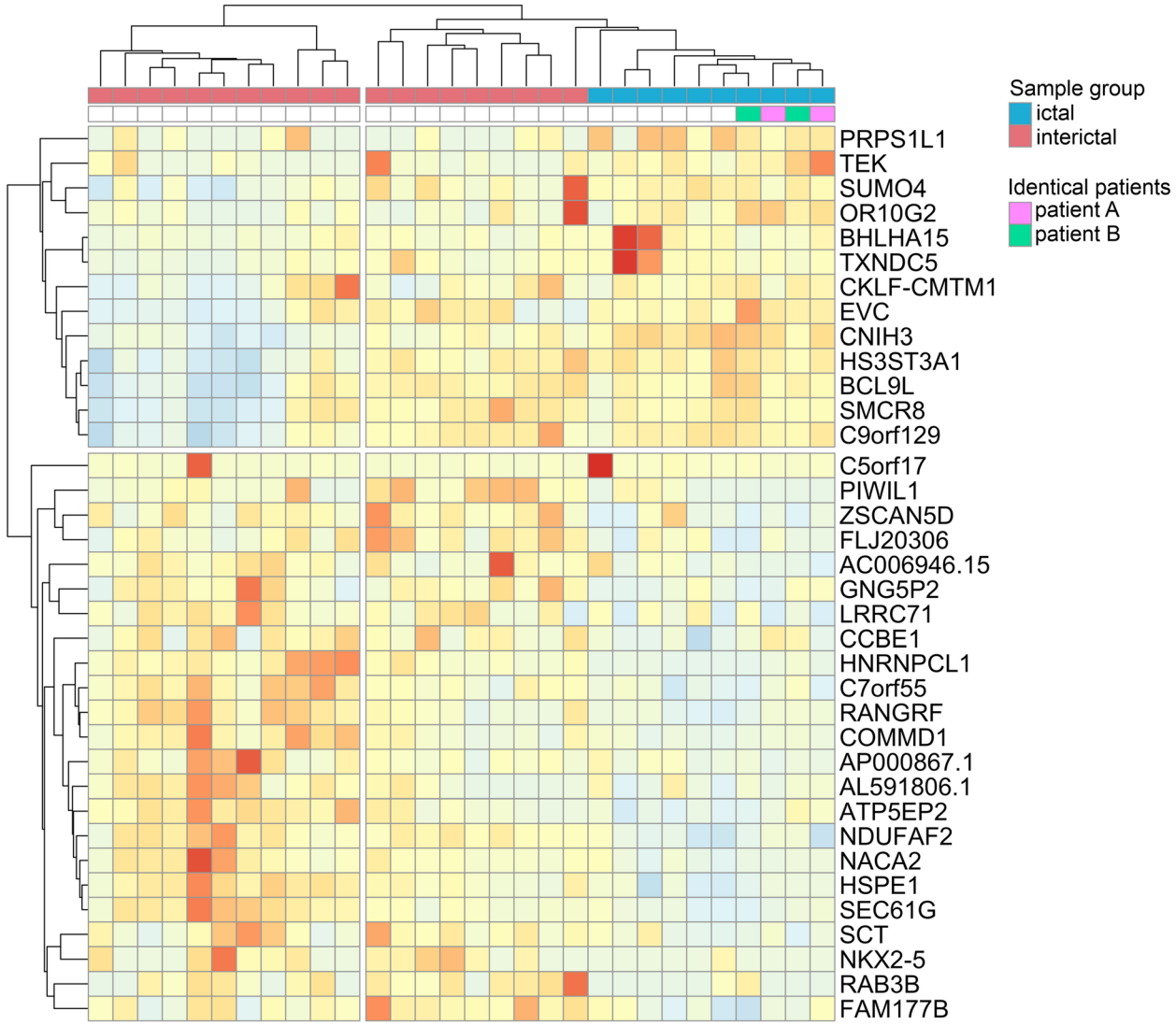

Fig. 2 Heat map representation of differentially expressed genes in the ictal vs. interictal comparison. Columns represent samples, rows represent genes. Pearson correlation was respectively calculated between samples and genes, visualized by dendrograms. Ictal samples from identical patients ("**A**", "**B**") are marked with respective colors in the legend

changes in some metabolites in the plasma also point to an alteration of mitochondrial electron transport chain or the citric acid cycle. There are two novel aspects of our analysis. On one hand, comparisons were made between healthy control samples to both the interictal and ictal samples of patients with the aim to identify both disease-specific and headache-specific alterations. On the other hand, instead of whole blood, we studied isolated mononuclear cells, the transcriptome of which had been reported to correlate better with the alterations in the brain [18]. Interestingly, significant gene expression and metabolite changes could be detected independently of headache episodes compared to healthy control samples which could be markers of migraine susceptibility, but not necessarily attack-specific.

A limitation of the study is that the RNA-based results are not confirmed by measuring the concentrations of the affected cytokines, but the results of the transcriptome analysis are in line with previous literature data which showed altered cytokine levels in migraine patients [33–36]. Our results showing immune pathway alterations are also in agreement with the findings of Gerring and coworkers' next-generation RNA sequencing study of the whole blood of migraine patients [21]. A further limitation is that only the ictal vs. interictal comparison yielded gene results after controlling for the

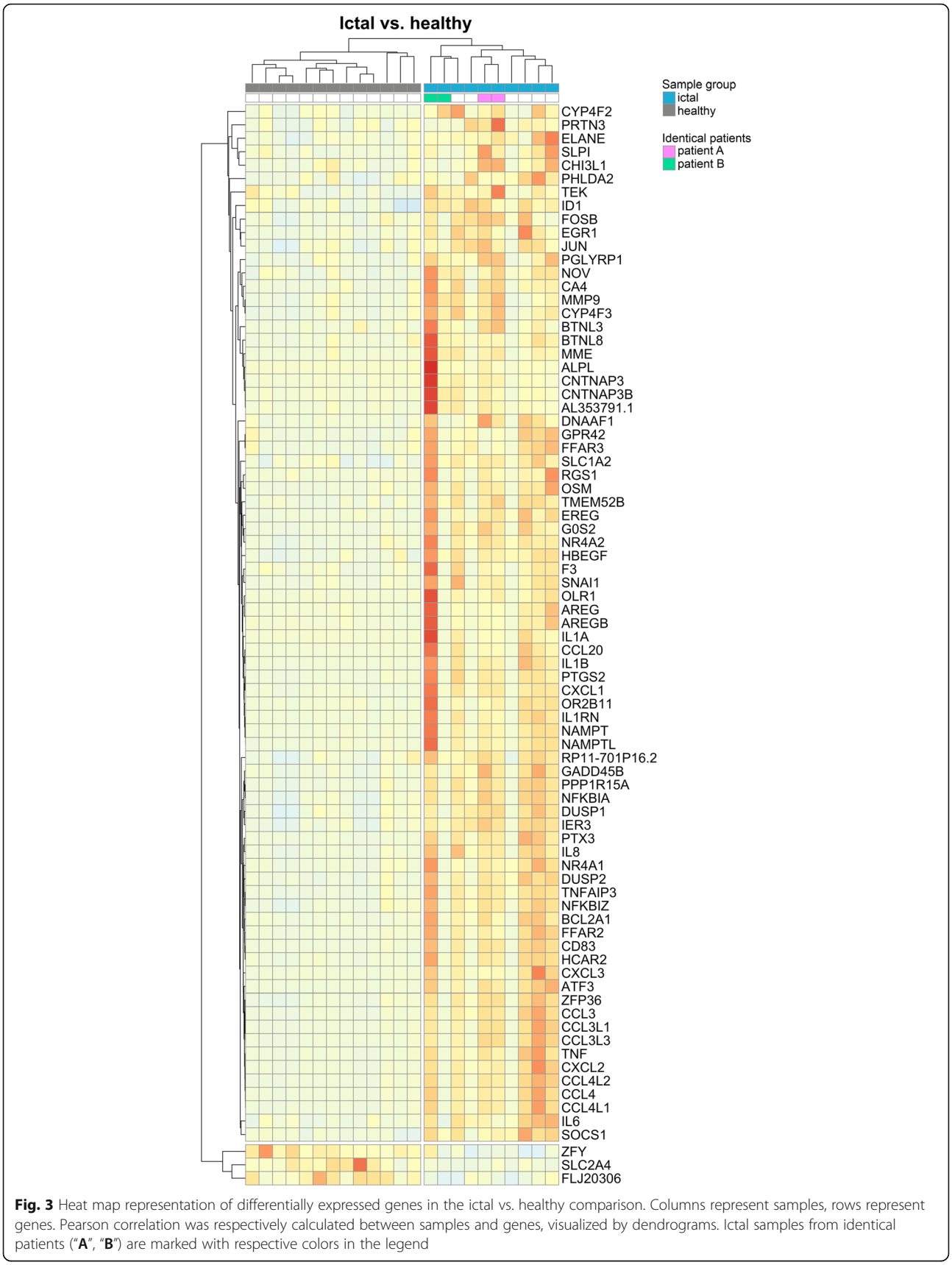

Fig. 3 Heat map representation of differentially expressed genes in the ictal vs. healthy comparison. Columns represent samples, rows represent genes. Pearson correlation was respectively calculated between samples and genes, visualized by dendrograms. Ictal samples from identical patients ("**A**", "**B**") are marked with respective colors in the legend

Table 2 Functional enrichment results of PBMC RNA-seq data of the interictal vs. healthy comparison. DE list enrichment: overrepresentation of functional terms in the differentially expressed gene list. Ranked list enrichment: enrichment of genes associated with a certain pathway towards the top of the ranked whole data. GO: gene ontology, BP: biological process, CC: cellular component, MF molecular function. KEGG: Kyoto Encyclopedia of Genes and Genomes. Annotated: number of genes associated with the given term. R: Reactome database. Significant: number of statistically significant associated with the given term. Expected: expected number of genes associated with the given term in the DE gene list. Gene ratio: ratio of number of genes in the DE list that overlap with genes associated with the given term, and the number of genes in the DE list which overlap with genes associated with all terms in the Reactome database. Bg ratio: ratio of the number of genes associated with the given term, and the total number of genes associated with Reactome terms

Interictal vs. healthy					
ID	**DE list enrichment**	**Annotated**	**Significant**	**Expected**	***p*-value**
GO:0006954 BP	inflammatory response	625	31	6.03	2.60E-14
GO:0005126 MF	cytokine receptor binding	210	14	1.89	6.10E-09
GO:0042379 MF	chemokine receptor binding	37	6	0.33	8.90E-07
		GeneRatio	BgRatio		p-value
R-HSA-6783783	Interleukin-10 signaling	11/96	40/8821		2.60E-14
	Ranked list enrichment	Annotated			p-value
GO:0022900 BP	electron transport chain	173			2.60E-14
GO:0005746 CC	mitochondrial respiratory chain	82			2.17E-05
GO:0016684 MF	oxidoreductase activity, acting on peroxide as acceptor	50			0.000016
KEGG 190	Oxidative phosphorylation	121			8.82E-06
KEGG 4080	Neuroactive ligand-receptor interaction	157			2.28E-05

Table 3 Functional enrichment results of PBMC RNA-seq data of the ictal vs. interictal comparison. DE list enrichment: overrepresentation of functional terms in the differentially expressed gene list. Ranked list enrichment: enrichment of genes associated with a certain pathway towards the top of the ranked whole data. GO: gene ontology, BP: biological process, CC: cellular component, MF molecular function. KEGG: Kyoto Encyclopedia of Genes and Genomes. Annotated: number of genes associated with the given term. R: Reactome database. Significant: number of statistically significant associated with the given term. Expected: expected number of genes associated with the given term in the DE gene list. Gene ratio: ratio of number of genes in the DE list that overlap with genes associated with the given term, and the number of genes in the DE list which overlap with genes associated with all terms in the Reactome database. Bg ratio: ratio of the number of genes associated with the given term, and the total number of genes associated with Reactome terms

Ictal vs. interictal					
ID	**DE list enrichment**	**Annotated**	**Significant**	**Expected**	***p*-value**
GO:1902305 BP	regulation of sodium ion transmembrane transport	55	4	0.39	2.60E-14
GO:0070382 CC	exocytic vesicle	175	6	1.3	0.0019
GO:0005179	hormone activity	61	3	0.43	0.00924
KEGG 4742	Taste transduction	35	2	0.219161	0.019843
	Ranked list enrichment	Annotated			p-value
GO:0005746 CC	mitochondrial respiratory chain	82			2.60E-14
GO:0005125 MF	cytokine activity	149			0.000001
GO:0005179 MF	hormone activity	61			6.95E-05
GO:0030594 MF	neurotransmitter receptor activity	57			0.000107
GO:0004984 MF	olfactory receptor activity	44			0.000433
KEGG 4080	Neuroactive ligand-receptor interaction	157			9.04E-05
KEGG 190	Oxidative phosphorylation	121			0.000845
KEGG 140	Steroid hormone biosynthesis	36			0.00112

Table 4 Functional enrichment results of PBMC RNA-seq data of the ictal vs. healthy comparison. DE list enrichment: overrepresentation of functional terms in the differentially expressed gene list. Ranked list enrichment: enrichment of genes associated with a certain pathway towards the top of the ranked whole data. GO: gene ontology, BP: biological process, CC: cellular component, MF molecular function. KEGG: Kyoto Encyclopedia of Genes and Genomes. Annotated: number of genes associated with the given term. R: Reactome database. Significant: number of statistically significant associated with the given term. Expected: expected number of genes associated with the given term in the DE gene list. Gene ratio: ratio of number of genes in the DE list that overlap with genes associated with the given term, and the number of genes in the DE list which overlap with genes associated with all terms in the Reactome database. Bg ratio: ratio of the number of genes associated with the given term, and the total number of genes associated with Reactome terms

Ictal vs. healthy					
ID	**DE list enrichment**	**Annotated**	**Significant**	**Expected**	***p*-value**
GO:1901700 BP	response to oxygen-containing compound	1347	45	10.86	2.60E-14
GO:0070851 MF	growth factor receptor binding	105	7	0.83	0.000019
		Gene ratio	Bg ratio		p-value
R-HSA-6783783	Interleukin-10 signaling	10/84	40/8821		2.60E-14
R-HSA-6785807	Interleukin-4 and Interleukin-13 signaling	11/84	98/8821		1.71E-09
R-HSA-179812	GRB2 events in EGFR signaling	3/84	11/8821		0.00013
	Ranked list enrichment	Annotated			p-value
GO:0070098 BP	chemokine-mediated signaling pathway	67			2.60E-14
KEGG 4080	Neuroactive ligand-receptor interaction	157			1.86E-14
KEGG 4740	Olfactory transduction	63			0.000817

false discovery rate. Migraine can have a prevalence of 20% of the population thus it can include a heterogeneous patient pool. In this regard our examination can be considered rather exploratory in nature with key results to be confirmed in a later study with a larger number of participants. Some similar migraine studies, however, have included patients in similar order of magnitude [22]. Controlling for FDR indeed reduces the number of false positive results but in turn increases false negatives. The cost of the latter is missing out on important discoveries [37]. Not having sufficient results after correction for multiple comparison also hinders finding associated biological functions. In a similar setting, examined the whole blood of migraineurs, Kogelman and colleagues performed correction for multiple testing and found two genes to be significantly differentially expressed [22]. They ran, however, functional enrichment analysis on the full non-corrected DE gene list, as well as co-expression network analysis on 5000 genes which is a multiple of the number of DE genes in their study. We carried out functional analysis by two approaches. One was DE list enrichment where potential false positive results at the gene level are expected to be randomly distributed among associated biological functions. Thus, significant biological terms supported by several DE genes are less likely to be false positive hits themselves. Our other method was ranked list enrichment that is not limited to the DE genes, hence it can circumvent the challenges of multiple comparison. The analysis considers the ranked list of all genes whose transcripts were detected.

While the vascular and neuronal origin of migraine has been debated for a long time, it is clear that there is an inflammatory component in the generation of the headache. NSAIDs are partially effective to relieve the headache pointing to the contribution of prostaglandins to nociceptor sensitization. Activation of resident mast cells in the meninges and release of proinflammatory cytokines such as IL-1β, IL-6, TNF-α and several chemokines have been proposed to play major roles in the progression of migraine headache (Fig. 6) [38, 39]. Moreover, cytokine release by glial cells is also likely to contribute to migraine pathomechanism, as it was shown that cortical spreading depression can result in inflammosome activation in the brain parenchyma, as well [40]. In our study upregulation of several cytokines, as well as COX-2 were detected in PBMCs of migraine patients in both interictal and ictal samples compared to healthy controls pointing to a systemic change of immune functions. These data are in line with previous reports of elevated plasma levels of various proinflammatory cytokines like IL-1, IL-6 [33], TNFα [34], IL-8, CCL3 and CCL5 [41, 42] and C-reactive proteins (CRP) [43, 44]. Moreover, during attacks, the concentration of IL-1β, IL-6, IL-8, IL-10 and TNF-α were further increased [35, 36]. Cytokines are fundamental regulators of inflammatory and immune reactions, and several of them have been directly implicated in pain sensitization by acting both on peripheral nociceptive nerve terminals and sensory ganglia, as well as participating in central sensitization. The pro-nociceptive role

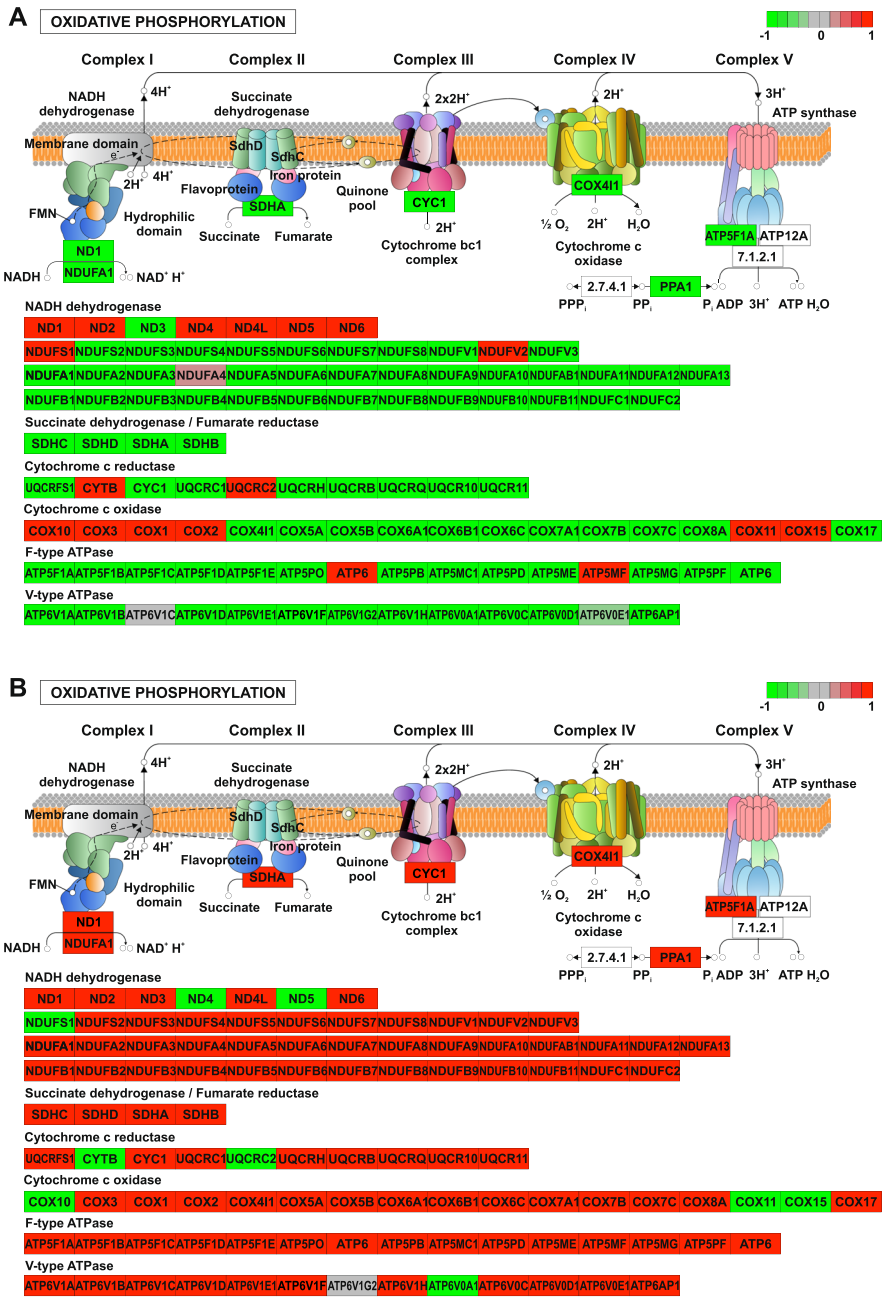

Fig. 4 Oxidative phosphorylation was implicated as a significantly altered metabolic pathway based on the ranked list enrichment analysis of all genes whose transcripts were detected from PBMC samples. Results of the analysis between ictal vs. interictal (upper panel) and interictal vs. healthy (lower panel) samples are shown. All detected genes are mapped to the pathway map. Original figure was rendered by Pathview

of IL-1β or TNFα in both peripheral and central pain mechanisms is well characterized [45–48]. Their potential contribution to headaches was supported by data that application of IL-1β or TNFα on rat dura resulted in activation and sensitization of meningeal nociceptors [49, 50]. Other cytokines from our top DE gene list, such as CXCL1, 2 or 3 (all ligands of the CXCR2 receptor), have also been shown to be pro-nociceptive [51]. Intrathecal administration of CXCL1, 2 or 3 produced hyperalgesia in mice [52]. These chemokines have also been implicated in neuropathic pain [52–54] and nociceptive sensitization after traumatic brain injury [55, 56]. CXCL1 in the synovial fluid of osteoarthritis patients correlated with the severity of pain [57]. Furthermore, significantly upregulated genes in our study include amphiregulin and epiregulin, which are epidermal

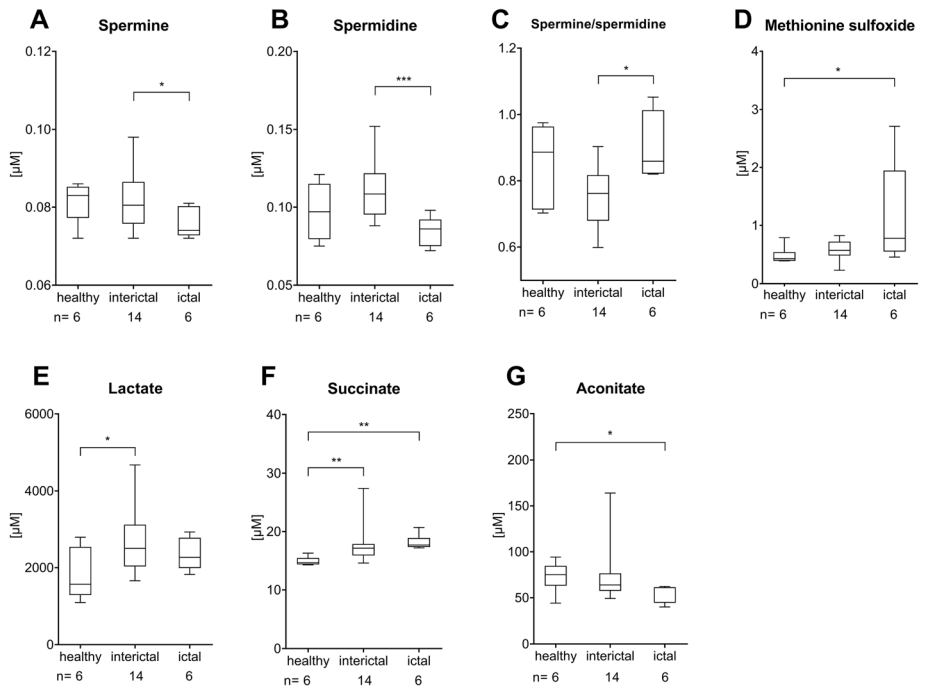

Fig. 5 Differences in plasma metabolomic profiles of healthy controls and migraineurs (interictal and ictal) for different classes of compounds: (**A**, **B**, **C**) biogenic amines; (**D**) amino acid-related; and (**E**, **F**, **G**) carboxylic acids. Plasma concentrations of different metabolites are compared between groups and are considered significantly different when $p \leq 0.05$. Asterisks denote significant differences (*$p \leq 0.05$, **$p \leq 0.01$, ***$p \leq 0.001$), as analyzed by one-way analysis of variance (ANOVA) for A, B, C, E and Kruskal–Wallis test for **D**, **F**, **G** samples

growth factor receptor (EGFR) ligands. These proteins have been implicated in tumor growth; however, a role in inflammation has also been described [58, 59]. Epiregulin, but not amphiregulin has been shown to be pronociceptive in mice, and EGFR inhibitors were analgesic in a variety of animal models of chronic pain [60]. Human data indicate that both amphiregulin and epiregulin expressions were higher in bone marrow-derived mononuclear cells of rheumatoid arthritis patients and increased expression of amphiregulin was also detected in PBMCs and synovial tissues [61].

Recently, the metabolic alterations in migraine have also been highlighted [62, 63] and a meta-analysis pointed to the importance of oxidative and nitrosative stress [64]. A possible link between mitochondrial dysfunction and neuroinflammation is the demonstration of NLRP3 inflammosome activation by mitochondrial reactive oxygen species which was postulated to participate in several CNS disorders including migraine [40]. Several lines of evidence demonstrate that in migraineurs there is an imbalance between energy requirement and supply of the brain [62, 63] and it has been hypothesized that the attack can be a consequence of an adaptive response to restore energy homeostasis. Impaired mitochondrial energy production has been detected in the brain and skeletal muscle of migraine patients during attacks, but also even interictally [65–68]. Moreover, it has also been raised that migraine triggers act as promoters of oxidative stress [69, 70] and various studies have consistently reported elevated levels of oxidative stress markers or a deficit of antioxidant mechanisms [62, 64]. Activities of various mitochondrial enzymes have been found to be altered in the platelets of migraine patients [71, 72].

In connection with the pathways identified with the PBMC transcriptome analysis, we have detected significant differences in several metabolites reflecting changes in mitochondrial function. These results provide a complementary viewpoint to a DE centric interpretation of our RNA-seq results. Lactate levels were increased in interictal, but not the ictal samples compared to the healthy plasma, while succinate levels were increased in both sets of migraine samples. Another intermediate metabolite of the citric acid cycle, aconitate was slightly decreased in parallel. Previous studies have already detected similar increases in plasma lactate and pyruvate levels [73], and it has also been reported that in migraine patients lactate levels rose higher upon exercise [74]. There are also data on increased lactate levels in some brain areas, although these were only detected in migraineurs with aura [62]. Abnormal “astrocyte-to-neuron lactate shuttle” has been considered to be behind the altered lactate metabolism, where astrocytes, through the end product of anaerobic glycolysis (lactate), provide

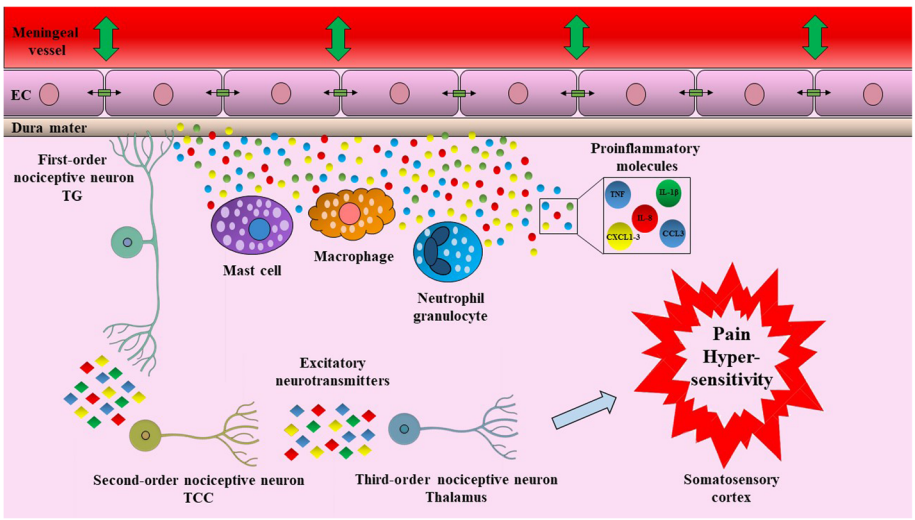

Fig. 6 Hypothetical contribution of inflammatory cytokines in migraine headache. Activation of immune cells alters the trigeminovascular microenvironment via the release of inflammatory molecules, such as cytokines and chemokines. These molecules cause vasodilation of dural vasculature and influence tight junction between endothelial cells. Activated trigeminal neurons transmit signals for the higher brain regions, which result in pain and hypersensitivity. CCL3: C-C motif ligand 3, CXCL1: C-X-C motif chemokine ligand 1, CXCL2: C-X-C motif chemokine ligand 2, CXCL3: C-X-C motif chemokine ligand 3, EC: endothelial cell, IL-1β: interleukin-1β, IL-8: interleukin-8, TCC: trigeminocervical complex, TNF: tumor necrosis factor, TG: trigeminal ganglion

energy to the activated neurons [75]. Regarding succinate, elevated levels were linked to a worse metabolic state in obese patients [76] and increased succinate concentrations have also been detected in the plasma of severely injured patients [77]. Also, succinate has been suggested to be a metabolic indicator of sepsis and mitochondrial dysfunction [78], with altered tissue concentrations under ischemia and inflammation [79–81]. However, novel data also indicate that succinate released for activated macrophages can act as a pro-inflammatory local mediator [80, 82], which could be another link between metabolic alterations in the plasma and inflammatory reactions. Other significantly changed metabolites include the polyamines spermine and spermidine and the oxidized metabolite of methionine, MetSO. Spermine and spermidine are involved in multiple cellular processes including the regulation of transcription and translation, alteration of ion channel and receptor function, and regulation of nitric oxide synthase. They act as scavengers of reactive oxygen radicals, thus represent important elements of normal mitochondrial functions. Polyamines also take part in protection from oxidative damage by stimulating the synthesis of superoxide dismutase, heat shock proteins and cell cycle regulators [83–89]. However, it has been described that overproduction or over-intake of these polyamines might contribute to cellular damage by oxidative mechanisms. In the brain, they might play a role in gap junction permeability and neuronal hyperexcitability under pathological conditions. Interestingly, spermine also can regulate the activity of glutamate-receptors, TRPV1 channels, and glial Kir4.1 channels [90–94]. Methionine, due to exposure to reactive oxygen species (ROS), oxidizes to MetSO. This procedure can be reversed by the methionine sulfoxide reductase (Msr) [95]. Currently, a correlation has been suggested between the increment in MetSO plasma levels and Alzheimer's disease progression [96]. Besides, altered Msr system function and MetSO accumulation have been proposed to be biomarkers of aging [97–99]. However, to our knowledge, this is the first study to link increased plasma levels of MetSO to migraine-related processes.

Conclusions

In summary, our results suggest that enhanced immune cell activity and oxidative stress generation play important roles in migraine susceptibility and headache-generation. Detection of altered gene expressions and metabolite levels in the peripheral blood point to the systemic nature of the disease. Our study also indicates that drugs targeting cytokines or reducing oxidative stress might be valuable for migraine treatment or prophylaxis.

Abbreviations

PBMC: Peripheral blood mononuclear cells; CGRP: Calcitonin gene-related peptide; PACAP: Pituitary adenylate cyclase activating polypeptide; GWAS: Genome-wide association studies; EDTA: Ethylenediaminetetraacetic acid; PBS: Phosphate-buffered saline; FC: Fold change; FDR: False discovery rate; GO: Gene ontology; KEGG: Kyoto encyclopedia of genes and genomes; DE: Differentially expressed; PITC: Phenyl isothiocyanate; LC-MS/MS: Liquid chromatography-mass spectrometry; FIA-MS/MS: Flow injection analysis-

tandem mass spectrometry; QA: Quality assurance; QC: Quality control; ANOVA: Analysis of variance; BMI: Body mass index; IL: Interleukin; PTGS2: Prostaglandin-endoperoxide synthase 2; COX2: Cyclooxygenase 2; TNF: Tumor necrosis factor; CRP: C-reactive protein; EGFR: Epidermal growth factor receptor; ROS: Reactive oxygen species

Supplementary Information

The online version contains supplementary material available at https://doi.org/10.1186/s10194-021-01285-9.

Additional file 1: Table S1. Top 20 differentially expressed genes in PBMCs comparing interictal and healthy control samples. *Avg rank*: average rank of *p*-value and fold change ranks; *ID*: Ensembl gene identifier. **Table S2.** Top 20 differentially expressed genes in PBMCs comparing interictal and ictal samples. *Avg rank*: average rank of *p*-value and fold change ranks; *ID*: Ensembl gene identifier. **Table S3.** Top 20 differentially expressed genes in PBMCs comparing ictal and healthy control samples. *Avg rank*: average rank of *p*-value and fold change ranks; *ID*: Ensembl gene identifier.

Acknowledgments

Not applicable.

Authors' contributions

Conceptualization: Z.H., K.B., J.K., A.G, L.V., J.T. Formal Analysis: J.K., R.H., W.B., A.G, G.B.K. Investigation: A.T., T.K., J.K., B.T., U.P., K.K., R.F., G.B.K. Resources: T.K., B.T., L.V, J.T., A.G., B.V., Z.H. Writing – Original Draft Preparation: A.T., T.K., J.K., U.P., W.B., G.B.K., K.B., Z.H. Writing – Review and Editing: A.T., T.K., J.K., P.U., W.B., R.H., R.F., K.K., B.V., G.B.K, A.G., B.T., J.T., L.V., K.B., Z.H. Visualization: A.T., T.K., J.K., W.B. Supervision: Z.H., K.B., A.G, L.V., J.T., V.B. Funding Acquisition: Z.H., K.B., A.G., L.V., J.T. The author(s) read and approved the final manuscript.

Funding

This research was supported by National Brain Research Program 2017–1.2.1-NKP-2017-00002 (NAP-2; Chronic Pain Research Group), Gazdaságfejlesztési és Innovációs Operatív Program (Economy Development and Innovation Operative Programme) (GINOP)-2.3.2-15-2016-00050 (Peptidergic Signaling in Health and Disease; PEPSYS), GINOP 2.3.2-15-2016-0034, Emberi Erőforrás Operatív Program (Human Resource Operative Programme) (EFOP) 3.6.2-16-2017-00008 (2017–2019), EFOP-3.6.1-16-2016-00004, TUDFO/47138–1/2019-ITM and National Research Development and Innovation Office grant OTKA FK132587. A.G. and J.K. were supported by the grants GINOP-2.3.4-15-2020-00010, GINOP-2.3.1-20-2020-00001 and Educating Experts of the Future: Developing Bioinformatics and Biostatistics competencies of European Biomedical Students (BECOMING, 2019–1-HU01-KA203–061251). Bioinformatics infrastructure was supported by ELIXIR Hungary (http://elixir-hungary.org/). The funders had no role in study design, data collection and analysis, decision to publish, or preparation of the manuscript.

Availability of data and materials

The RNA-Seq dataset supporting the conclusions of this article is available in the European Nucleotide Archive (https://www.ebi.ac.uk/ena), under accession number PRJEB40032.

Declarations

Ethics approval and consent to participate

The study was approved by the National Public Health Center, Ministry of Human Capacities of Hungary (28324–5/2019/EÜIG). All study participants gave their written informed consent in accordance with the Declaration of Helsinki.

Consent for publication

Not applicable.

Competing interests

The authors disclose no conflicts of interest.

Author details

[1]Department of Pharmacology and Pharmacotherapy, Molecular Pharmacology Research Group and Centre for Neuroscience, University of Pécs Szentágothai Research Centre, University of Pécs Medical School, Szigeti út 12, Pécs H-7624, Hungary. [2]Department of Neurology, Interdisciplinary Excellence Centre, Faculty of Medicine, Albert Szent-Györgyi Clinical Center, University of Szeged, Semmelweis u. 6, Szeged H-6725, Hungary. [3]MTA-SZTE Neuroscience Research Group, University of Szeged, Semmelweis u. 6, Szeged H-6725, Hungary. [4]Faculty of Health Sciences and Social Studies, University of Szeged, Temesvári krt. 31, Szeged H-6726, Hungary. [5]Szentágothai Research Centre, Bioinformatics Research Group, Genomics and Bioinformatics Core Facility, University of Pécs, Ifjúság útja 20, Pécs H-7624, Hungary. [6]Department of Laboratory Medicine, Semmelweis University, Nagyvárad tér 4, Budapest H-1089, Hungary.

Received: 14 May 2021 Accepted: 1 July 2021
Published online: 06 October 2021

References

1. Goadsby PJ, Holland PR, Martins-Oliveira M, Hoffmann J, Schankin C, Akerman S (2017) Pathophysiology of migraine: A disorder of sensory processing. Physiol Rev 97(2):553–622. https://doi.org/10.1152/physrev.00034.2015
2. Olesen J, Burstein R, Ashina M, Tfelt-Hansen P (2009) Origin of pain in migraine: evidence for peripheral sensitisation. Lancet Neurol 8(7):679–690. https://doi.org/10.1016/S1474-4422(09)70090-0
3. Tepper SJ (2018) History and review of anti-calcitonin gene-related peptide (CGRP) therapies: from translational research to treatment. Headache. 58(Suppl 3):238–275. https://doi.org/10.1111/head.13379
4. Charles A, Pozo-Rosich P (2019) Targeting calcitonin gene-related peptide: a new era in migraine therapy. Lancet 394(10210):1765–1774. https://doi.org/10.1016/S0140-6736(19)32504-8
5. Hargreaves R, Olesen J (2019) Calcitonin gene-related peptide modulators - the history and renaissance of a new migraine drug class. Headache. 59(6):951–970. https://doi.org/10.1111/head.13510
6. Amin FM, Asghar MS, Guo S, Hougaard A, Hansen AE, Schytz HW, van der Geest RJ, de Koning PJH, Larsson HBW, Olesen J, Ashina M (2012) Headache and prolonged dilatation of the middle meningeal artery by PACAP38 in healthy volunteers. Cephalalgia. 32(2):140–149. https://doi.org/10.1177/0333102411431333
7. Schytz HW, Birk S, Wienecke T, Kruuse C, Olesen J, Ashina M (2009) PACA P38 induces migraine-like attacks in patients with migraine without aura. Brain. 132(1):16–25. https://doi.org/10.1093/brain/awn307
8. Tuka B, Helyes Z, Markovics A, Bagoly T, Szolcsányi J, Szabó N, Tóth E, Kincses ZT, Vécsei L, Tajti J (2013) Alterations in PACAP-38-like immunoreactivity in the plasma during ictal and interictal periods of migraine patients. Cephalalgia. 33(13):1085–1095. https://doi.org/10.1177/0333102413483931
9. Tolner EA, Houben T, Terwindt GM, de Vries B, Ferrari MD, van den Maagdenberg AM (2015) From migraine genes to mechanisms. Pain 156(Suppl 1):S64–74. https://doi.org/10.1097/01.j.pain.0000460346.00213.16
10. Sutherland HG, Albury CL, Griffiths LR (2019) Advances in genetics of migraine. J Headache Pain 20(1):72. https://doi.org/10.1186/s10194-019-1017-9
11. Freilinger T, Anttila V, de Vries B, Malik R, Kallela M, Terwindt GM et al (2012) Genome-wide association analysis identifies susceptibility loci for migraine without aura. Nat Genet 44(7):777–782. https://doi.org/10.1038/ng.2307
12. Gormley P, Anttila V, Winsvold BS, Palta P, Esko T, Pers TH et al (2016) Meta-analysis of 375,000 individuals identifies 38 susceptibility loci for migraine. Nat Genet 48(8):856–866. https://doi.org/10.1038/ng.3598
13. Eising E, de Leeuw C, Min JL, Anttila V, Verheijen MH, Terwindt GM et al (2016) Involvement of astrocyte and oligodendrocyte gene sets in migraine. Cephalalgia. 36(7):640–647. https://doi.org/10.1177/0333102415618614
14. Alves-Ferreira M, Quintas M, Sequeiros J, Sousa A, Pereira-Monteiro J, Alonso I, Neto JL, Lemos C (2021) A genetic interaction of NRXN2 with GABRE, SYT1 and CASK in migraine patients: a case-control study. J Headache Pain. 22(1):57. https://doi.org/10.1186/s10194-021-01266-y
15. Di Lorenzo C, Santorelli FM, van den Maagdenberg AMJM (2015) Genetics of headache. In: Ashina M, Geppetti P (eds) Pathophysiology of headaches: from molecule to man. Springer International Publishing, Cham, pp 83–99. https://doi.org/10.1007/978-3-319-15621-7_4

16. Gerring Z, Rodriguez-Acevedo AJ, Powell JE, Griffiths LR, Montgomery GW, Nyholt DR (2016) Blood gene expression studies in migraine: potential and caveats. Cephalalgia. 36(7):669–678. https://doi.org/10.1177/0333102416628463
17. Sullivan PF, Fan C, Perou CM (2006) Evaluating the comparability of gene expression in blood and brain. Am J Med Genet B Neuropsychiatr Genet 141B(3):261–268. https://doi.org/10.1002/ajmg.b.30272
18. Rollins B, Martin MV, Morgan L, Vawter MP (2010) Analysis of whole genome biomarker expression in blood and brain. Am J Med Genet B Neuropsychiatr Genet 153B:919–936
19. Hershey AD, Tang Y, Powers SW, Kabbouche MA, Gilbert DL, Glauser TA, Sharp FR (2004) Genomic abnormalities in patients with migraine and chronic migraine: preliminary blood gene expression suggests platelet abnormalities. Headache. 44(10):994–1004. https://doi.org/10.1111/j.1526-4610.2004.04193.x
20. Hershey A, Horn P, Kabbouche M, O'Brien H, Powers S (2012) Genomic expression patterns in Menstrually-related migraine in adolescents. Headache. 52(1):68–79. https://doi.org/10.1111/j.1526-4610.2011.02049.x
21. Gerring ZF, Powell JE, Montgomery GW, Nyholt DR (2018) Genome-wide analysis of blood gene expression in migraine implicates immune-inflammatory pathways. Cephalalgia. 38(2):292–303. https://doi.org/10.1177/0333102416686769
22. Kogelman LJ, Falkenberg K, Halldorsson GH, Poulsen LU, Worm J, Ingason A et al (2019) Comparing migraine with and without aura to healthy controls using RNA sequencing. Cephalalgia. 39(11):1435–1444. https://doi.org/10.1177/0333102419851812
23. Headache Classification Committee of the International HeadacheSociety (IHS) (2018) The International Classification of Headache Disorders, vol 38, 3rd edn. Cephalalgia, pp 1–211. https://doi.org/10.1177/0333102417738202
24. Gardiner IM, Ahmed F, Steiner TJ, McBain A, Kennard C, de Belleroche J (1998) A study of adaptive responses in cell signaling in migraine and clusterheadache: correlations between headache type and changes in gene expression. Cephalalgia 18:192–196. https://doi.org/10.1046/j.1468-2982.1998.1804192.x
25. Plummer PN, Colson NJ, Lewohl JM, MacKay RK, Fernandez F, Haupt LM, Griffiths LR (2011) Significant differences in gene expression of GABA receptors inperipheral blood leukocytes of migraineurs. Gene 490:32–36. https://doi.org/10.1016/j.gene.2011.08.031
26. Aczél T, Kun J, Szőke É, Rauch T, Junttila S, Gyenesei A et al (2018) Transcriptional Alterations in the Trigeminal Ganglia, nucleus and peripheral blood mononuclear cells in a rat orofacial pain model. Front Mol Neurosci. 11:219. https://doi.org/10.3389/fnmol.2018.00219
27. Dobin A, Davis CA, Schlesinger F, Drenkow J, Zaleski C, Jha S, Batut P, Chaisson M, Gingeras TR (2013) STAR: ultrafast universal RNA-seq aligner. Bioinformatics 29(1):15–21. https://doi.org/10.1093/bioinformatics/bts635
28. Liao Y, Smyth GK, Shi W (2019) The R package Rsubread is easier, faster, cheaper and better for alignment and quantification of RNA sequencing reads. Nucleic Acids Res 47(8):e47–e47. https://doi.org/10.1093/nar/gkz114
29. Robinson MD, McCarthy DJ, Smyth GK (2010) edgeR: a Bioconductor package for differential expression analysis of digital gene expression data. Bioinformatics 26:139–140
30. Law CW, Chen Y, Shi W, Smyth GK (2014) Voom: precision weights unlock linear model analysis tools for RNA-seq read counts. Genome Biol 15:R29
31. Ritchie ME, Phipson B, Wu D, Hu Y, Law CW, Shi W et al (2015) Limma powers differential expression analyses for RNA-sequencing and microarray studies. Nucleic Acids Res 43:e47
32. Luo W, Brouwer C (2013) Pathview: an R/Bioconductor package for pathway-based data integration and visualization. Bioinformatics 29:1830–1831
33. Uzar E, Evliyaoglu O, Yucel Y, Ugur Cevik M, Acar A, Guzel I, Islamoglu Y, Colpan L, Tasdemir N (2011) Serum cytokine and pro-brain natriuretic peptide (BNP) levels in patients with migraine. Eur Rev Med Pharmacol Sci 15(10):1111–1116
34. Covelli V, Massari F, Fallacara C, Munno I, Pellegrino NM, Jirillo E, Savastano S, Ghiggi MR, Tommaselli AP, Lombardi G (1991) Increased spontaneous release of tumor necrosis factor-alpha/cachectin in headache patients. A possible correlation with plasma endotoxin and hypothalamic-pituitary-adrenal axis. Int J Neurosci 61(1-2):53–60. https://doi.org/10.3109/00207459108986270
35. Perini F, D'Andrea G, Galloni E, Pignatelli F, Billo G, Alba S et al (2005) Plasma cytokine levels in migraineurs and controls. Headache J Head Face Pain 45(7):926–931. https://doi.org/10.1111/j.1526-4610.2005.05135.x
36. Sarchielli P, Alberti A, Baldi A, Coppola F, Rossi C, Pierguidi L, Floridi A, Calabresi P (2006) Proinflammatory cytokines, adhesion molecules, and lymphocyte integrin expression in the internal jugular blood of migraine patients without aura assessed ictally. Headache. 46(2):200–207. https://doi.org/10.1111/j.1526-4610.2006.00337.x
37. McDonald JH (2014) Handbook of biological statistics, 3rd edn. Sparky House Publishing, Baltimore, Maryland, USA
38. Levy D, Burstein R, Kainz V, Jakubowski M, Strassman AM (2007) Mast cell degranulation activates a pain pathway underlying migraine headache. Pain 130(1-2):166–176. https://doi.org/10.1016/j.pain.2007.03.012
39. Conti P, D'Ovidio C, Conti C, Gallenga CE, Lauritano D, Caraffa A, Kritas SK, Ronconi G (2019) Progression in migraine: role of mast cells and pro-inflammatory and anti-inflammatory cytokines. Eur J Pharmacol 844:87–94. https://doi.org/10.1016/j.ejphar.2018.12.004
40. Kursun O, Yemisci M, van den Maagdenberg AMJM, Karatas H (2021) Migraine and neuroinflammation: the inflammasome perspective. J Headache Pain 22(1):55. https://doi.org/10.1186/s10194-021-01271-1
41. Duarte H, Teixeira AL, Rocha NP, Domingues RB (2015) Increased interictal serum levels of CXCL8/IL-8 and CCL3/MIP-1α in migraine. Neurol Sci 36(2):203–208. https://doi.org/10.1007/s10072-014-1931-1
42. Domingues RB, Duarte H, Senne C, Bruniera G, Brunale F, Rocha NP, Teixeira AL (2016) Serum levels of adiponectin, CCL3/MIP-1α, and CCL5/RANTES discriminate migraine from tension-type headache patients. Arq Neuropsiquiatr 74(8):626–631. https://doi.org/10.1590/0004-282X20160096
43. Vanmolkot FH, de Hoon JN (2007) Increased C-reactive protein in young adult patients with migraine. Cephalalgia. 27(7):843–846. https://doi.org/10.1111/j.1468-2982.2007.01324.x
44. Güzel I, Taşdemir N, Celik Y (2013) Evaluation of serum transforming growth factor β1 and C-reactive protein levels in migraine patients. Neurol Neurochir Pol 47(4):357–362. https://doi.org/10.5114/ninp.2013.36760
45. Woolf CJ, Allchorne A, Safieh-Garabedian B, Poole S (1997) Cytokines, nerve growth factor and inflammatory hyperalgesia: the contribution of tumour necrosis factor α. Br J Pharmacol 121(3):417–424. https://doi.org/10.1038/sj.bjp.0701148
46. Watkins LR, Maier SF (2002) Beyond neurons: evidence that immune and glial cells contribute to pathological pain states. Physiol Rev 82:981–1011
47. Sommer C, Kress M (2004) Recent findings on how proinflammatory cytokines cause pain: peripheral mechanisms in inflammatory and neuropathic hyperalgesia. Neurosci Lett 361(1-3):184–187. https://doi.org/10.1016/j.neulet.2003.12.007
48. Kawasaki Y, Zhang L, Cheng J-K, Ji R-R (2008) Cytokine mechanisms of central sensitization: distinct and overlapping role of interleukin-1β, Interleukin-6, and tumor necrosis factor-α in regulating synaptic and neuronal activity in the superficial spinal cord. J Neurosci 28(20):5189–5194. https://doi.org/10.1523/JNEUROSCI.3338-07.2008
49. Zhang X-C, Kainz V, Burstein R, Levy D (2011) Tumor necrosis factor-α induces sensitization of meningeal nociceptors mediated via local COX and p38 MAP kinase actions. Pain 152:140–149. https://doi.org/10.1016/j.pain.2010.10.002
50. Zhang X, Burstein R, Levy D (2012) Local action of the proinflammatory cytokines IL-1 and IL-6 on intracranial meningeal nociceptors. Cephalalgia. 32(1):66–72. https://doi.org/10.1177/0333102411430848
51. Silva RL, Lopes AH, Guimarães RM, Cunha TM (2017) CXCL1/CXCR2 signaling in pathological pain: role in peripheral and central sensitization. Neurobiol Dis 105:109–116. https://doi.org/10.1016/j.nbd.2017.06.001
52. Piotrowska A, Rojewska E, Pawlik K, Kreiner G, Ciechanowska A, Makuch W et al (2019) Pharmacological blockade of spinal CXCL3/CXCR2 signaling by NVP CXCR2 20, a selective CXCR2 antagonist, reduces neuropathic pain following peripheral nerve injury. Front Immunol 10:2198. https://doi.org/10.3389/fimmu.2019.02198
53. Manjavachi MN, Passos GF, Trevisan G, Araújo SB, Pontes JP, Fernandes ES, Costa R, Calixto JB (2019) Spinal blockage of CXCL1 and its receptor CXCR2 inhibits paclitaxel-induced peripheral neuropathy in mice. Neuropharmacology. 151:136–143. https://doi.org/10.1016/j.neuropharm.2019.04.014
54. Moraes TR, Elisei LS, Malta IH, Galdino G (2020) Participation of CXCL1 in the glial cells during neuropathic pain. Eur J Pharmacol 875:173039. https://doi.org/10.1016/j.ejphar.2020.173039
55. Liang D-Y, Shi X, Liu P, Sun Y, Sahbaie P, Li W-W et al (2017) The chemokine receptor CXCR2 supports nociceptive sensitization after traumatic brain injury. Mol Pain 13:1744806917730212

56. Sahbaie P, Irvine K-A, Liang D-Y, Shi X, Clark JD (2019) Mild traumatic brain injury causes nociceptive sensitization through spinal chemokine upregulation. Sci Rep 9(1):19500. https://doi.org/10.1038/s41598-019-55739-x
57. Nees TA, Rosshirt N, Zhang JA, Reiner T, Sorbi R, Tripel E, Walker T, Schiltenwolf M, Hagmann S, Moradi B (2019) Synovial cytokines significantly correlate with osteoarthritis-related knee pain and disability: inflammatory mediators of potential clinical relevance. J Clin Med 8(9):1343. https://doi.org/10.3390/jcm8091343
58. Riese DJ, Cullum RL (2014) Epiregulin: Roles in normal physiology and cancer. Semin Cell Dev Biol 28:49–56. https://doi.org/10.1016/j.semcdb.2014.03.005
59. Singh B, Carpenter G, Coffey RJ (2016) EGF receptor ligands: recent advances. F1000Res 5:2270. https://doi.org/10.12688/f1000research.9025.1
60. Martin LJ, Smith SB, Khoutorsky A, Magnussen CA, Samoshkin A, Sorge RE, Cho C, Yosefpour N, Sivaselvachandran S, Tohyama S, Cole T, Khuong TM, Mir E, Gibson DG, Wieskopf JS, Sotocinal SG, Austin JS, Meloto CB, Gitt JH, Gkogkas C, Sonenberg N, Greenspan JD, Fillingim RB, Ohrbach R, Slade GD, Knott C, Dubner R, Nackley AG, Ribeiro-da-Silva A, Neely GG, Maixner W, Zaykin DV, Mogil JS, Diatchenko L (2017) Epiregulin and EGFR interactions are involved in pain processing. J Clin Investig 127(9):3353–3366. https://doi.org/10.1172/JCI87406
61. Yamane S, Ishida S, Hanamoto Y, Kumagai K, Masuda R, Tanaka K, Shiobara N, Yamane N, Mori T, Juji T, Fukui N, Itoh T, Ochi T, Suzuki R (2008) Proinflammatory role of amphiregulin, an epidermal growth factor family member whose expression is augmented in rheumatoid arthritis patients. J Inflamm 5(1):5. https://doi.org/10.1186/1476-9255-5-5
62. Gross EC, Lisicki M, Fischer D, Sándor PS, Schoenen J (2019) The metabolic face of migraine — from pathophysiology to treatment. Nat Rev Neurol 15(11):627–643. https://doi.org/10.1038/s41582-019-0255-4
63. Cevoli S, Favoni V, Cortelli P (2019) Energy metabolism impairment in migraine. Curr Med Chem 26(34):6253–6260. https://doi.org/10.2174/0929867325666180622154411
64. Neri M, Frustaci A, Milic M, Valdiglesias V, Fini M, Bonassi S, Barbanti P (2015) A meta-analysis of biomarkers related to oxidative stress and nitric oxide pathway in migraine. Cephalalgia. 35(10):931–937. https://doi.org/10.1177/0333102414564888
65. Welch KM, Levine SR, D'Andrea G, Schultz LR, Helpern JA (1989) Preliminary observations on brain energy metabolism in migraine studied by in vivo phosphorus 31 NMR spectroscopy. Neurology. 39(4):538–541. https://doi.org/10.1212/WNL.39.4.538
66. Barbiroli B, Montagna P, Cortelli P, Funicello R, Iotti S, Monari L, Pierangeli G, Zaniol P, Lugaresi E (1992) Abnormal brain and muscle energy metabolism shown by 31P magnetic resonance spectroscopy in patients affected by migraine with aura. Neurology. 42(6):1209–1214. https://doi.org/10.1212/WNL.42.6.1209
67. Lodi R, Kemp GJ, Montagna P, Pierangeli G, Cortelli P, Iotti S, Radda GK, Barbiroli B (1997) Quantitative analysis of skeletal muscle bioenergetics and proton efflux in migraine and cluster headache. J Neurol Sci 146(1):73–80. https://doi.org/10.1016/S0022-510X(96)00287-0
68. Kim JH, Kim S, Suh S-I, Koh S-B, Park K-W, Oh K (2010) Interictal metabolic changes in episodic migraine: a voxel-based FDG-PET study. Cephalalgia. 30(1):53–61. https://doi.org/10.1111/j.1468-2982.2009.01890.x
69. Borkum JM (2016) Migraine triggers and oxidative stress: A narrative review and synthesis: headache. Headache: The Journal of Head and Face Pain. 56(1):12–35. https://doi.org/10.1111/head.12725
70. Borkum JM (2018) The migraine attack as a homeostatic, neuroprotective response to brain oxidative stress: preliminary evidence for a theory. Headache. 58(1):118–135. https://doi.org/10.1111/head.13214
71. Littlewood J, Glover V, Sandler M, Peatfield R, Petty R, Clifford RF (1984) Low platelet monoamine oxidase activity in headache: no correlation with phenolsulphotransferase, succinate dehydrogenase, platelet preparation method or smoking. J Neurol Neurosurg Psychiatry 47(4):338–343. https://doi.org/10.1136/jnnp.47.4.338
72. Sangiorgi S, Mochi M, Riva R, Cortelli P, Monari L, Pierangeli G, Montagna P (1994) Abnormal platelet mitochondrial function in patients affected by migraine with and without aura. Cephalalgia. 14(1):21–23. https://doi.org/10.1046/j.1468-2982.1994.1401021.x
73. Okada H, Araga S, Takeshima T, Nakashima K (1998) Plasma lactic acid and pyruvic acid levels in migraine and tension-type headache. Headache. 38(1):39–42. https://doi.org/10.1046/j.1526-4610.1998.3801039.x
74. Montagna P, Sacquegna T, Martinelli P, Cortelli P, Bresolin N, Moggio M, Baldrati A, Riva R, Lugaresi E (1988) Mitochondrial abnormalities in migraine. Preliminary findings. Headache 28(7):477–480. https://doi.org/10.1111/j.1526-4610.1988.hed2807477.x
75. Magistretti PJ, Pellerin L (1999) Cellular mechanisms of brain energy metabolism and their relevance to functional brain imaging. Philos Trans R Soc Lond Ser B Biol Sci 354(1387):1155–1163. https://doi.org/10.1098/rstb.1999.0471
76. Serena C, Ceperuelo-Mallafré V, Keiran N, Queipo-Ortuño MI, Bernal R, Gomez-Huelgas R et al (2018) Elevated circulating levels of succinate in human obesity are linked to specific gut microbiota. ISME J 12:1642–1657
77. D'Alessandro A, Moore HB, Moore EE, Reisz JA, Wither MJ, Ghasasbyan A, et al. (2017) Plasma succinate is a predictor of mortality in critically injured patients. J Trauma Acute Care Surg 83:491–495
78. Beloborodova N, Pautova A, Sergeev A, Fedotcheva N (2019) Serum Levels of Mitochondrial and Microbial Metabolites Reflect Mitochondrial Dysfunction in Different Stages of Sepsis. Metabolites 9:196. https://doi.org/10.3390/metabo9100196
79. Chouchani ET, Pell VR, Gaude E, Aksentijević D, Sundier SY, Robb EL et al (2014) Ischaemic accumulation of succinate controls reperfusion injury through mitochondrial ROS. Nature 515:431–435
80. Tannahill GM, Curtis AM, Adamik J, Palsson-McDermott EM, McGettrick AF, Goel G et al (2013) Succinate is an inflammatory signal that induces IL-1β through HIF-1α. Nature 496:238–242
81. Chinopoulos C (2019) Succinate in ischemia: where does it come from? Int J Biochem Cell Biol 115:105580. https://doi.org/10.1016/j.biocel.2019.105580
82. Mills E, O'Neill LAJ (2014) Succinate: a metabolic signal in inflammation. Trends Cell Biol 24(5):313–320. https://doi.org/10.1016/j.tcb.2013.11.008
83. Narayanan SP, Shosha E, Palani CD (2019) Spermine oxidase: A promising therapeutic target for neurodegeneration in diabetic retinopathy. Pharmacol Res 147:104299
84. Mandal S, Mandal A, Park MH (2015) Depletion of the polyamines spermidine and Spermine by overexpression of spermidine/spermine N1-Acetyltransferase1 (SAT1) leads to mitochondria-mediated apoptosis in mammalian cells. Biochem J 468(3):435–447. https://doi.org/10.1042/BJ20150168
85. Salvi M, Toninello A (2004) Effects of polyamines on mitochondrial Ca2+ transport. Biochim Biophys Acta Biomembr 1661(2):113–124. https://doi.org/10.1016/j.bbamem.2003.12.005
86. Ha HC, Sirisoma NS, Kuppusamy P, Zweier JL, Woster PM, Casero RA (1998) The natural polyamine spermine functions directly as a free radical scavenger. Proc Natl Acad Sci U S A 95(19):11140–11145. https://doi.org/10.1073/pnas.95.19.11140
87. Pegg AE (2014) The function of spermine. IUBMB Life 66(1):8–18. https://doi.org/10.1002/iub.1237
88. Hu J, Lu X, Zhang X, Shao X, Wang Y, Chen J, et al. Exogenous spermine attenuates myocardial fibrosis in diabetic cardiomyopathy by inhibiting endoplasmic reticulum stress and the canonical Wnt signaling pathway. Cell Biol Int 44:1660–1670. https://doi.org/10.1002/cbin.11360
89. Soda K (2020) Spermine and gene methylation: a mechanism of lifespan extension induced by polyamine-rich diet. Amino Acids 52(2):213–224. https://doi.org/10.1007/s00726-019-02733-2
90. Krauss M, Langnaese K, Richter K, Brunk I, Wieske M, Ahnert-Hilger G, Veh RW, Laube G (2006) Spermidine synthase is prominently expressed in the striatal patch compartment and in putative interneurones of the matrix compartment. J Neurochem 97(1):174–189. https://doi.org/10.1111/j.1471-4159.2006.03721.x
91. Skatchkov S, Woodbury M, Eaton M (2014) The role of glia in stress: polyamines and brain disorders. Psychiatr Clin North Am 37(4):653–678. https://doi.org/10.1016/j.psc.2014.08.008
92. Skatchkov SN, Bukauskas FF, Benedikt J, Inyushin M, Kucheryavykh YV (2015) Intracellular spermine prevents acid-induced uncoupling of Cx43 gap junction channels. NeuroReport. 26(9):528–532. https://doi.org/10.1097/WNR.0000000000000385
93. Benedikt J, Inyushin M, Kucheryavykh YV, Rivera Y, Kucheryavykh LY, Nichols CG, Eaton MJ, Skatchkov SN (2012) Intracellular polyamines enhance astrocytic coupling. Neuroreport. 23(17):1021–1025. https://doi.org/10.1097/WNR.0b013e32835aa04b
94. Skatchkov SN, Eaton MJ, Krusek J, Veh RW, Biedermann B, Bringmann A et al (2000) Spatial distribution of spermine/spermidine content and K(+)-current rectification in frog retinal glial (Müller) cells. Glia. 31(1):84–90. https://doi.org/10.1002/(SICI)1098-1136(200007)31:1<84::AID-GLIA80>3.0.CO;2-7
95. Lourenço dos Santos S, Petropoulos I, Friguet B (2018) The oxidized protein repair enzymes methionine sulfoxide reductases and their roles in

protecting against oxidative stress, in ageing and in regulating protein function. Antioxidants 7:191. https://doi.org/10.3390/antiox7120191
96. Deng Y, Marsh BM, Moskovitz J (2019) Increased levels of protein-methionine sulfoxide in plasma correlate with a shift from a mild cognitive impairment to an Alzheimer's disease stage. Innov Clin Neurosci 16(7-08): 29–31
97. Vanhooren V, Navarrete Santos A, Voutetakis K, Petropoulos I, Libert C, Simm A, Gonos ES, Friguet B (2015) Protein modification and maintenance systems as biomarkers of ageing. Mech Ageing Dev 151:71–84. https://doi.org/10.1016/j.mad.2015.03.009
98. Oien DB, Moskovitz J (2019) Genetic regulation of longevity and age-associated diseases through the methionine sulfoxide reductase system. Biochim Biophys Acta Mol Basis Dis 1865:1756–1762. https://doi.org/10.1016/j.bbadis.2018.11.016
99. Onorato JM, Thorpe SR, Baynes JW (1998) Immunohistochemical and ELISA assays for biomarkers of oxidative stress in aging and disease. Ann N Y Acad Sci 854:277–290. https://doi.org/10.1111/j.1749-6632.1998.tb09909.x

Publisher's Note

International Journal of
Molecular Sciences

MDPI

Article

Hemokinin-1 Gene Expression Is Upregulated in Trigeminal Ganglia in an Inflammatory Orofacial Pain Model: Potential Role in Peripheral Sensitization

Timea Aczél [1], Angéla Kecskés [1], József Kun [1,2], Kálmán Szenthe [3], Ferenc Bánáti [4], Susan Szathmary [5], Róbert Herczeg [2], Péter Urbán [2], Attila Gyenesei [2], Balázs Gaszner [6], Zsuzsanna Helyes [1,7] and Kata Bölcskei [1,*]

1 Department of Pharmacology and Pharmacotherapy, Medical School & Szentágothai Research Centre, Molecular Pharmacology Research Group, Centre for Neuroscience, University of Pécs, H-7624 Pécs, Hungary; aczel.timea@pte.hu (T.A.); angela.kecskes@aok.pte.hu (A.K.); kun.jozsef@pte.hu (J.K.); zsuzsanna.helyes@aok.pte.hu (Z.H.)
2 Szentágothai Research Centre, Bioinformatics Research Group, Genomics and Bioinformatics Core Facility, University of Pécs, H-7624 Pécs, Hungary; herczeg.robert@pte.hu (R.H.); urban.peter@pte.hu (P.U.); gyenesei.attila@pte.hu (A.G.)
3 Carlsbad Research Organization Ltd, H-9244 Újrónafő, Hungary; kszenthe@carlsbad.hu
4 RT-Europe Ltd, H-9200 Mosonmagyaróvár, Hungary; fbanati@rt-europe.org
5 Galenbio Ltd, H-9200 Mosonmagyaróvár, Hungary; sszathmary@galenbio.com
6 Department of Anatomy, University of Pécs Medical School, H-7624 Pécs, Hungary; balazs.b.gaszner@aok.pte.hu
7 PharmInVivo Ltd., H-7629 Pécs, Hungary
* Correspondence: kata.bolcskei@aok.pte.hu

Received: 27 March 2020; Accepted: 19 April 2020; Published: 22 April 2020

Abstract: A large percentage of primary sensory neurons in the trigeminal ganglia (TG) contain neuropeptides such as tachykinins or calcitonin gene-related peptide. Neuropeptides released from the central terminals of primary afferents sensitize the secondary nociceptive neurons in the trigeminal nucleus caudalis (TNC), but also activate glial cells contributing to neuroinflammation and consequent sensitization in chronic orofacial pain and migraine. In the present study, we investigated the newest member of the tachykinin family, hemokinin-1 (HK-1) encoded by the *Tac4* gene in the trigeminal system. HK-1 had been shown to participate in inflammation and hyperalgesia in various models, but its role has not been investigated in orofacial pain or headache. In the complete Freund's adjuvant (CFA)-induced inflammatory orofacial pain model, we showed that *Tac4* expression increased in the TG in response to inflammation. Duration-dependent *Tac4* upregulation was associated with the extent of the facial allodynia. *Tac4* was detected in both TG neurons and satellite glial cells (SGC) by the ultrasensitive RNAscope in situ hybridization. We also compared gene expression changes of selected neuronal and glial sensitization and neuroinflammation markers between wild-type and *Tac4*-deficient (*Tac4*$^{-/-}$) mice. Expression of the SGC/astrocyte marker in the TG and TNC was significantly lower in intact and saline/CFA-treated *Tac4*$^{-/-}$ mice. The procedural stress-related increase of the SGC/astrocyte marker was also strongly attenuated in *Tac4*$^{-/-}$ mice. Analysis of TG samples with a mouse neuroinflammation panel of 770 genes revealed that regulation of microglia and cytotoxic cell-related genes were significantly different in saline-treated *Tac4*$^{-/-}$ mice compared to their wild-types. It is concluded that HK-1 may participate in neuron-glia interactions both under physiological and inflammatory conditions and mediate pain in the trigeminal system.

Keywords: orofacial pain; hemokinin-1; trigeminal ganglia; complete Freund's adjuvant; macrophages; satellite glial cells; neuroinflammation

1. Introduction

Sensitization of trigeminal nociceptors by inflammatory mediators is a major factor of orofacial pain and headache disorders by causing hyperalgesia and allodynia. The orofacial area is mainly innervated by ophthalmic, maxillary and mandibular branches of the trigeminal nerve. The cell bodies of the primary sensory neurons are located in the trigeminal ganglia (TG) and their central terminals relay the protopathic information to the spinal trigeminal nucleus caudalis (TNC) and the upper cervical dorsal horn. When trigeminal nerve injury or orofacial inflammation occurs, TG neurons become sensitized and in turn release several mediators, which lead to enhanced responsiveness of the secondary afferent neurons. Satellite glial cells (SGC) and resident macrophages in the TG, as well as astrocytes and microglia in the central nervous system, are also activated in the process and contribute to the sensitization. There is growing evidence that the cross-talk between neurons and glial cells has a prominent modulatory role on nociceptive transmission under physiological and pathophysiological conditions [1–6].

A major percentage of nociceptive sensory neurons both in the trigeminal and dorsal root ganglia are peptidergic and release several neuropeptides, such as tachykinins (substance P (SP) and neurokinins) and calcitonin gene-related peptide (CGRP) in response to activation [7,8]. Tachykinins can be released both from the peripheral and central endings of primary sensory neurons contributing to inflammatory processes and pain transmission [9,10]. The biological actions of tachykinins are mediated by the G-protein coupled neurokinin NK-1, NK-2 and NK-3 receptors [11,12]. NK-1 receptor antagonists were shown to effectively reduce neuropathic mechanical hyperalgesia and inflammatory pain in animal models [13–15]. Since SP is expressed by trigeminal sensory neurons, it also became the focus of migraine studies. SP released from the peripheral terminals of trigeminal neurons induces plasma protein extravasation and vasodilatation in the dura mater [16], while centrally in the TNC it contributes to pain transmission [17,18]. It has been shown that the SP/NK-1 system participates in orofacial heat hyperalgesia in inflammatory and nerve injury-related animal models [19]. Preclinical data were promising regarding the use of NK-1 receptor antagonists in several pain conditions and inflammatory disease models [19–21]. Nevertheless, human studies could not prove the analgesic effect of these compounds, either in migraine [22–25] or in other conditions like post-operative dental pain [26] or neuropathic pain [27]. The explanation for the failure of NK-1 receptor antagonists as analgesics and anti-migraine drugs remains unclear, but it might be due to differences of the human NK-1 receptor structure and function as compared to the rodent receptor, or the ineffectiveness of competitively blocking the SP binding site [28,29].

The discovery of the newest member of the tachykinin family, the hemokinin-1 (HK-1) encoded by the *Tac4* gene [30], has given a new impetus to tachykinin research. HK-1 might be a novel key molecule in behavior, pain and inflammatory processes [31]. There is a growing amount of data regarding the mRNA expression of the *Tac4* gene both in the central and peripheral nervous systems. In contrast to other tachykinin members, relatively high expression of the *Tac4* gene can be found in the periphery (e.g., lung, spleen, adrenal gland). B and T lymphocytes, macrophages and dendritic cells also express *Tac4* [30,32–34]. While other tachykinins are conserved across mammals, HK-1 is highly homologous in mouse and rat, but not in humans. Both rodent peptides and the human HK-1 can bind to the NK-1 tachykinin receptor [35], but they also have distinct, NK-1-independent actions [36,37]. Since the structures of HK-1 and SP are very similar, it is difficult to proceed with peptide detection, localization and measurement. Although a few studies reported antibody development (e.g., [38]) or a recent immunohistochemical study on the TG with an in-house developed antibody [39], there are still no commercially available antibodies against HK-1. Despite the structural similarities and common receptors of HK-1 and SP, some of their functions appear to be different, even opposing each other [36,40–43]. This could be explained by different binding sites and different signalling pathways by HK-1 compared to SP even at the NK-1 receptor, but a specific target is suggested to mediate several actions of HK-1 [36]. Therefore, since the receptorial mechanisms of HK-1 are not precisely known, pharmacological interventions (e.g., antagonists) cannot be used to validate the target.

Studies investigating the pain modulatory function of HK-1 showed opposing effects, pointing to a complex role of the peptide. HK-1 had a pronociceptive effect after intrathecal or intracerebroventricular administration, causing pain and scratching behavior without influencing the withdrawal latency to a noxious heat stimulus [34,43]. However, in other studies, an analgesic effect was shown upon intracerebroventricular injection [44–46]. Its potential contribution to pain sensitization was shown by the upregulation of *Tac4* mRNA expression in lipopolysaccharide-stimulated cultured microglia [47], and in the rat spinal dorsal horn after complete Freund's adjuvant (CFA)-induced paw inflammation [48].

The role of HK-1 in orofacial pain and trigeminal sensitization have been poorly investigated. Therefore, we aimed to explore the potential role of HK-1 in the trigeminovascular system by (i) detecting expression changes of *Tac4* in the TG and TNC in a rat inflammatory orofacial pain model [49] (ii) investigating behavioral alterations and gene expression changes of selected markers of neuronal sensitization and neuroinflammation by comparing *Tac4*-deficient (*Tac4*$^{-/-}$) and wild-type mice.

2. Results

2.1. Tac4 mRNA Levels Are Upregulated in Response to CFA-Induced Inflammation in the Rat TG in Association with Facial Allodynia

The facial mechanonociceptive threshold of CFA-injected rats was significantly decreased compared to saline injection, starting from day one until day seven after injection. The allodynia reached its maximum on day three in the whisker pad area (Figure 1a), in accordance with our previous results [49]. *Tac4* mRNA expression was also measured in peripheral blood mononuclear cells (PBMCs), TG and TNC tissues. The fold changes of *Tac4* mRNA in TG (Figure 1b) followed the course of von Frey threshold changes, reaching its maximum on day three. In TNC and PBMC samples the *Tac4* expression could not be detected with sufficient reliability with this method, as C_q values were very close to the detection limit.

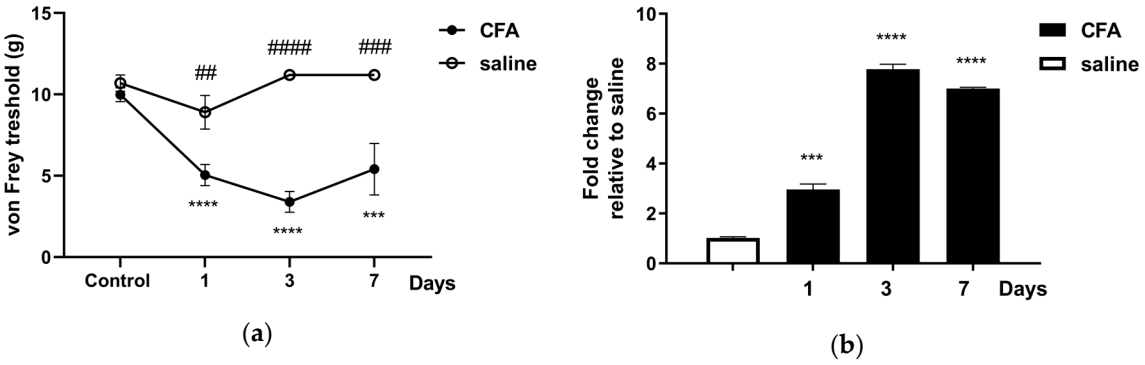

Figure 1. (**a**) Changes in mechanical threshold measured with von Frey filaments on day 1, 3, 7 after unilateral injection of complete Freund's adjuvant (CFA) or saline (50 µL s.c.). Data are means ± S.E.M. (CFA: n = 5–16, saline: n = 6). A sterisks denote statistically significant differences between the control day and the days after CFA treatment (*** $p \leq 0.001$, **** $p \leq 0.0001$), while hash marks label statistically significant differences between saline and CFA groups (## $p \leq 0.01$, ### $p \leq 0.001$, #### $p \leq 0.0001$) as analyzed by two-way ANOVA followed by Tukey's multiple comparison tests; (**b**) time course of normalized fold changes in *Tac4* mRNA expression of rat trigeminal ganglia (TG) on day 1, 3 and 7 after CFA or saline injection. The mRNA levels were normalized to *β2m* and *Hprt1*. Data are means ± S.E.M. (n = 3 at each time point). Asterisks denote statistically significant differences between saline and CFA groups (*** $p \leq 0.001$, **** $p \leq 0.0001$), as analyzed by one-way ANOVA followed by Tukey's multiple comparison tests.

2.2. CFA-Induced Orofacial Inflammation Upregulates Tac4 mRNA in Both Primary Sensory Neurons and SGCs of the Rat TG

To investigate the basal expression and inflammation-induced alterations of the *Tac4* mRNA in the rat TG, fluorescent RNAscope in situ hybridization (ISH) was performed, that provides cellular resolution and tissue context. *Tac4* transcripts were localized primarily on sensory neurons and SGCs in saline-treated samples (Figure 2a, left panel) and significantly upregulated in both cell types upon CFA treatment (Figure 2a, right panel). Basal and elevated *Tac4* mRNA levels were analyzed semi-quantitatively using ImageJ software and plotted as *Tac4*-specific total dot area/number detected in sensory neuron soma or SGC (Figure 2b). Sensory neurons and SGCs were identified morphologically (see arrows and arrowheads, respectively, Figure 2a) and histologically by colocalizing *Tac4* with neuronal (NeuN, encoded by *Rbfox3*) and satellite glial marker (SK3, encoded by *Kcnn3*, see Supplementary Figure S2). RNAscope performed on rat TG was validated by RNAscope 3-plex negative control probes designed to bacterial *dapB* gene giving no detectable fluorescent signal on any channel (Supplementary Figure S3a,b). RNAscope 3-plex mouse positive control probes were used to visualize the housekeeping genes: RNA polymerase II subunit A (*Polr2a*), peptidyl-prolyl cis-trans isomerase B (*Ppib*) and polyubiquitin-C (*Ubc*) mRNA on rat TG from saline-treated animals (Supplementary Figure S3c,d).

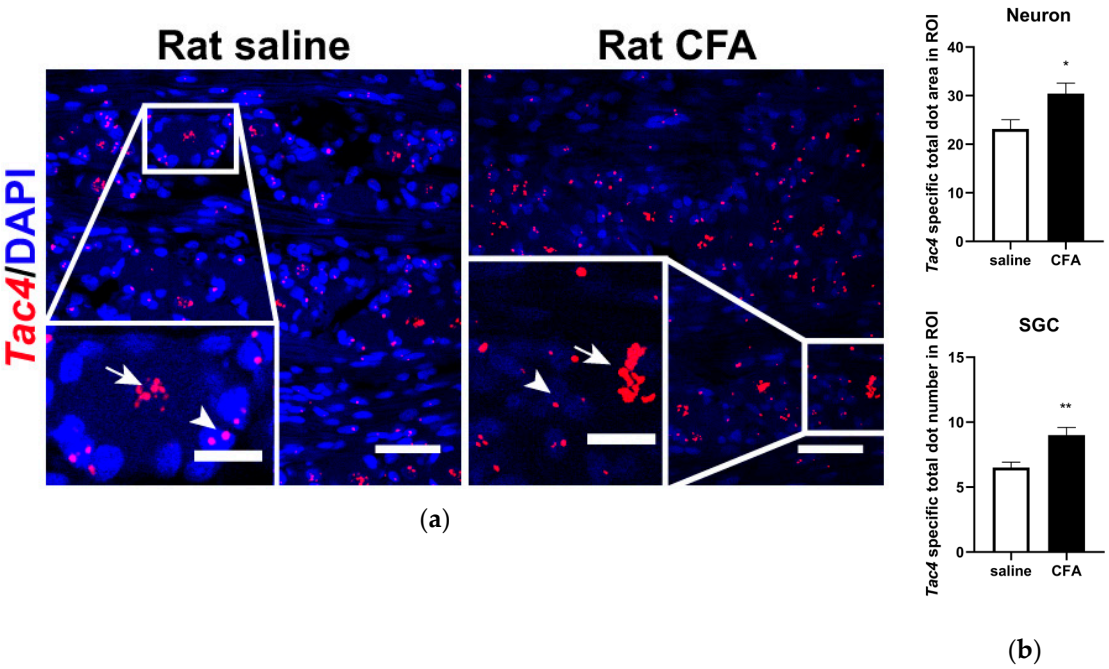

Figure 2. (**a**) Representative confocal images of *Tac4* mRNA (red) counterstained with DAPI are shown on longitudinal slices of rat TG after injection of saline or CFA. Arrows indicate sensory neurons, arrowheads refer to SGCs. Scale bar: 50 µm, inset scale bar: 20 µm; (**b**) quantification of *Tac4* mRNA showing upregulation after CFA compared to saline injection in *Tac4*-positive neurons and SGCs of $n = 4$ (saline)-6 (CFA) rats/group. Asterisks denote statistically significant differences between saline and CFA groups (* $p \leq 0.05$, ** $p \leq 0.01$), as analyzed by Student's *t*-test for unpaired samples. ROI: region of interest; unit of the area: μm^2.

2.3. CFA-Induced Orofacial Inflammation Upregulates Tac4 mRNA in Both Primary Sensory Neurons and SGCs of the Mouse TG

Similarly to *Tac4* expression found in rat TG, basal *Tac4* mRNA was detected both in sensory neurons and SGCs of the mouse TG (Figure 3a, left panel). Also, mouse *Tac4* mRNA was shown to be upregulated in response to CFA-induced inflammation (Figure 3a, right panel). Sensory neurons and SGCs were identified morphologically (see arrows and arrowheads, respectively, Figure 3a).

Technical control conditions using 3-plex negative (Supplementary Figure S3c) and mouse 3-plex positive (Supplementary Figure S3d) control probes were applied on longitudinal mouse TG from saline-injected animals.

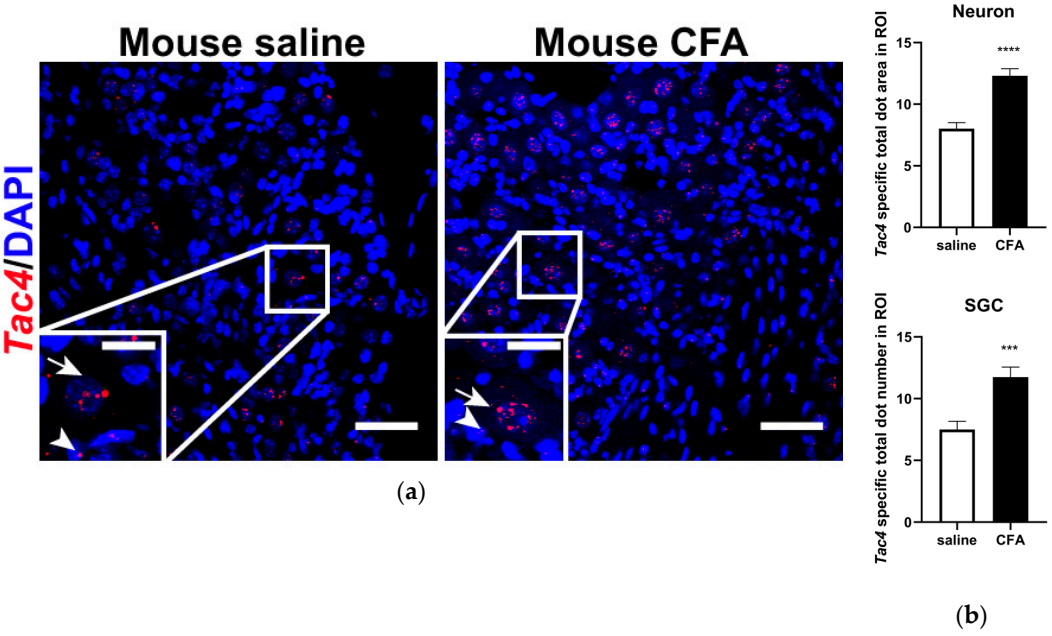

Figure 3. (**a**) Representative confocal images of *Tac4* mRNA (red) counterstained with DAPI is shown on longitudinal sections of mouse TG after saline or CFA treatment. Arrows indicate sensory neurons, arrowheads refer to SGCs. Scale bar: 50 μm, inset scale bar: 20 μm; (**b**) statistics showing *Tac4* mRNA upregulation after CFA compared to saline injection in *Tac4*-positive neurons and SGCs of $n = 4$ (saline) -5 (CFA) mice/group. Asterisks denote statistically significant differences between saline and CFA groups (*** $p \leq 0.001$, **** $p \leq 0.0001$), as analyzed by Student's *t*-test for unpaired samples. ROI: region of interest; unit of the area: μm^2.

2.4. CFA-Induced Alterations of Neuronal and Glial Activation Markers in the TG and TNC of Tac4 Gene-Deficient Mice

Mouse TG samples exhibited a relatively low value of *Tac4* expression levels, thus it could not be reliably detected and evaluated by RT-qPCR. We were unable to evaluate *Tac4* expression in TNC and PBMC samples either, similarly to rat TNC and PBMC samples.

We have previously described the gene activity profile of neuronal and glial activation markers in the rat TG and TNC, therefore we investigated the same markers in the mouse samples after orofacial inflammation. In wild-type (WT) mice, neuronal *FosB* gene expression was significantly upregulated by day 3 compared to intact samples (data not shown). However, not only CFA injection but also saline treatment caused an elevation of *FosB* in TG, therefore the differences between respective saline- and CFA-treated groups were not significant by days 3 and 7. A significant upregulation of the neuronal activation marker was only detected in *Tac4*$^{-/-}$ animals at a later time point, in day 7 samples. Comparison of matching WT and *Tac4*$^{-/-}$ animal groups showed that upregulation of the neuronal activation marker on days 3 and 7 was significantly lower in the TG of *Tac4*$^{-/-}$ mice (Figure 4a). In TNC only minor differences were seen (Figure 4b).

In both TG (relative fold change WT: 1.00 ± 0.03 vs. *Tac4*$^{-/-}$: 0.49 ± 0.03, $p < 0.0001$) and TNC (relative fold change WT: 1.00 ± 0.03 vs. *Tac4*$^{-/-}$: 0.82 ± 0.02, $p < 0.001$) samples of intact animals, the microglia/macrophage activation marker (*Iba1*) showed significantly lower expression levels in *Tac4*$^{-/-}$ mice compared to WTs. *Iba1* expression was slightly higher in both saline- and CFA-treated *Tac4*$^{-/-}$ mice compared to their corresponding WT groups, being significant on day 1 and 3 in the TG and day 7 in the TNC. However, these differences were probably too small to be biologically meaningful

(Figure 4c,d). The SGC/astrocyte activation marker *Gfap* was also expressed at a significantly lower level in the TG (relative fold change WT: 1.00 ± 0.16 vs. *Tac4*$^{-/-}$: 0.33 ± 0.06, $p < 0.01$) and TNC (relative fold change WT: 1.00 ± 0.03 vs. *Tac4*$^{-/-}$: 0.16 ± 0.05, $p < 0.0001$) of intact *Tac4*$^{-/-}$ compared to WT animals. After treatment, *Gfap* expression increased in all groups on all days compared to an intact group (data not shown). The effect of CFA on *Gfap* gene expression was a significant elevation in WT compared to the respective saline-treated group on day 1 and 3, but not in TNC samples. Moreover, *Gfap* levels were not altered due to CFA treatment in *Tac4*$^{-/-}$ mice. *Gfap* mRNA was decreased in all *Tac4*$^{-/-}$ groups compared to the WT group in most of the comparisons, both in TG and TNC (Figure 4e,f).

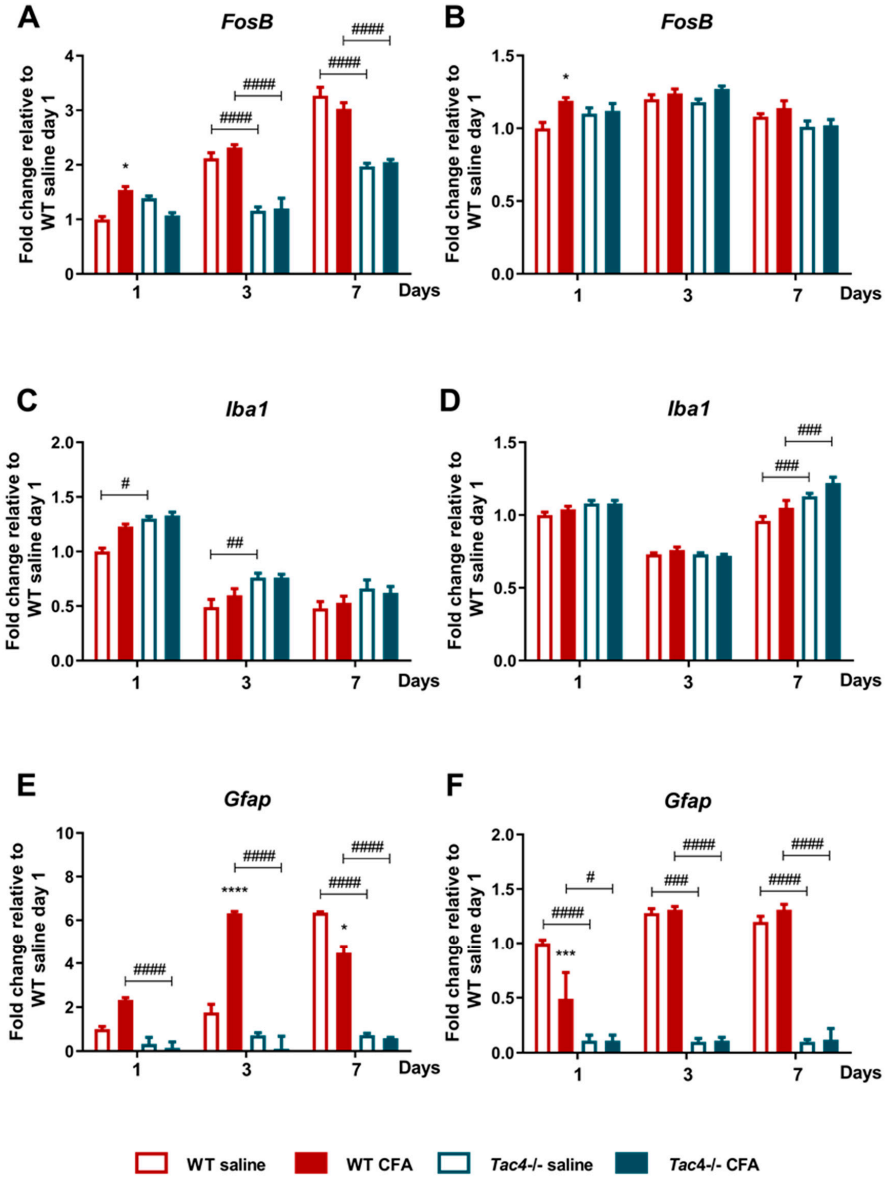

Figure 4. Time course of normalized fold changes in *FosB* (**A**,**B**), *Iba1* (**C**,**D**), *Gfap* (**E**,**F**) mRNA expression in the trigeminal ganglia (**A**,**C**,**D**) and trigeminal nucleus caudalis (**B**,**D**,**F**) of wild-type (WT) and *Tac4*$^{-/-}$ mice one, 3 and 7 days after saline/CFA injection. The mRNA levels were normalized to *Ppia* (TG) and *Ppia*, *Gapdh* (TNC), as detailed in Materials and methods. Data are means ± S.E.M. (WT CFA: n = 3–10, WT saline: n = 4–9, *Tac4*$^{-/-}$ CFA: n = 5–7, *Tac4*$^{-/-}$ saline: n = 5–10). Asterisks denote statistically significant differences between saline and CFA treated groups (* $p \leq 0.05$, *** $p \leq 0.001$), hash marks label statistically significant differences between WT and *Tac4*$^{-/-}$ groups (# $p \leq 0.05$, ## $p \leq 0.01$, ### $p \leq 0.001$, #### $p \leq 0.0001$), as analyzed by two-way ANOVA followed by Tukey's multiple comparison tests.

2.5. Neuroinflammation-Related Genes Are Differently Regulated between Saline-or CFA-Treated Tac4$^{-/-}$ and WT Mice

Nanostring results revealed differentially expressed genes, as well as statistically significant correlations of cell-type-specific gene expressions. In TG samples of saline-treated *Tac4*$^{-/-}$ mice, 15 genes were found to be differentially expressed with a *p*-value threshold of 0.05 when compared to saline-treated WT mice. Nine genes were upregulated, six were downregulated in the *Tac4*$^{-/-}$ TG samples (Figure 5). There were gene expression differences in saline-treated (non-inflamed control) animals in case of genetic lack of HK-1 in the KO mice in comparison with WTs. Changes in microglia/macrophage and cytotoxic cell-specific genes were significantly correlated when saline-treated *Tac4*$^{-/-}$ mice were compared to saline-treated WTs (Figure 6). In TG samples of CFA-treated *Tac4*$^{-/-}$ mice, 22 genes were found to be differentially expressed with a *p*-value threshold of 0.05 when compared to CFA-treated WT animals. Thirteen genes were upregulated, 9 were downregulated in the *Tac4*$^{-/-}$ TG samples (Figure 7). Changes in genes specific to neutrophil granulocytes were significantly correlated when CFA-treated *Tac4*$^{-/-}$ mice were compared to CFA-treated WTs (Figure 8). For a further description of other comparisons between groups, see Supplementary Material (Supplementary Figures S4–S7).

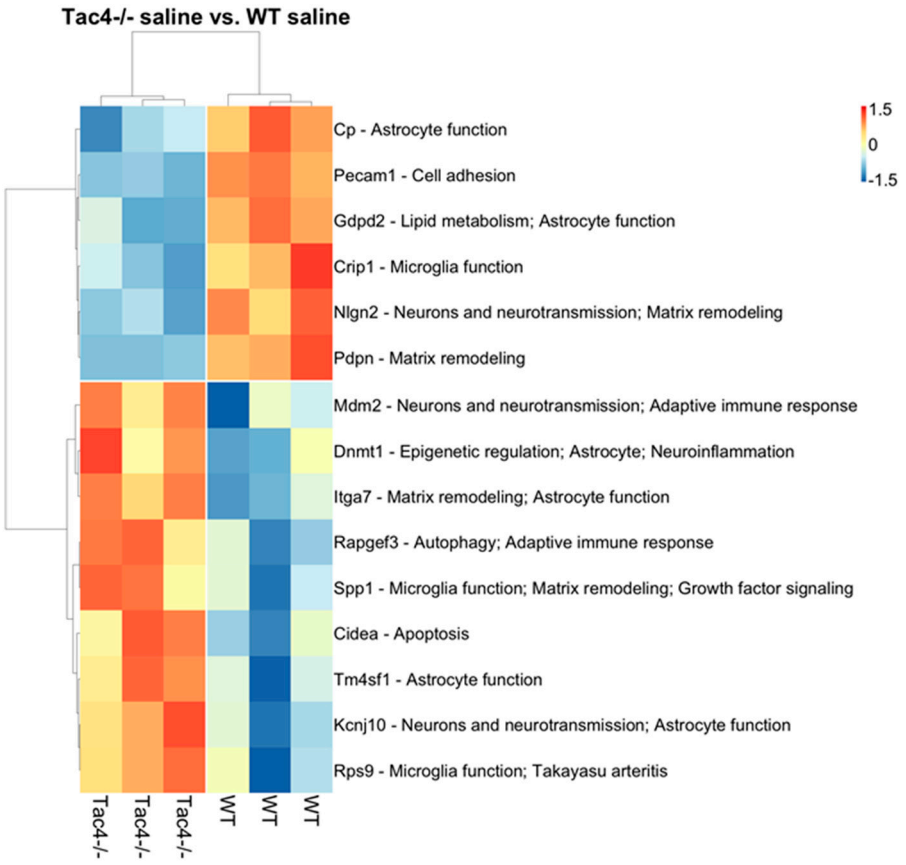

Figure 5. Heat map representation of the differentially expressed genes with annotations between TG samples of saline-treated *Tac4*$^{-/-}$ and WT mice. Rows represent genes and columns represent TG samples (n = 3 in each group). Normalized gene counts data are shown as row-wise z-scores (scale is shown on legend). Rows and columns were hierarchically clustered using Pearson correlation distance measure and average method. Distances are shown as dendrograms. References for the functional annotations: *Cp* [50] *Pecam1* [51] *Gdpd2* [52] *Crip1* [53] *Nlgn2* [54] *Pdpn* [55] *Mdm2* [56] *Dnmt1* [57] *Itga7* [58] *Rapgef3* [59] *Spp1* [60] *Cidea* [61] *Tm4sf1* [62] *Kcnj10* [63] *Rps9* [63].

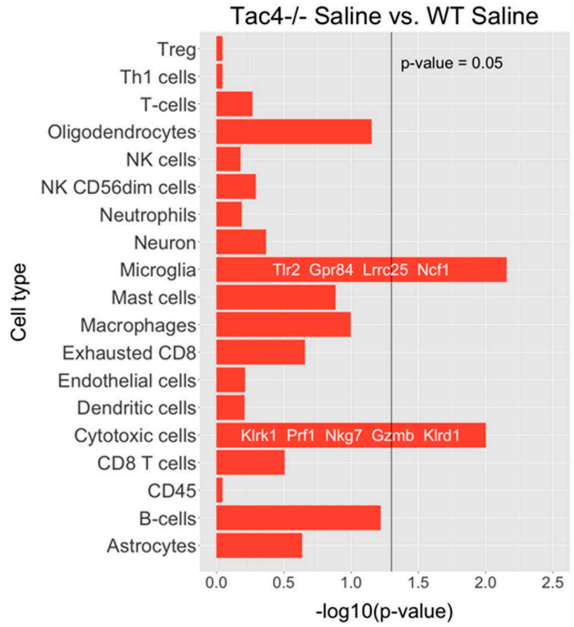

Figure 6. Barplots of *p*-values for correlation of cell-type-specific gene expressions as compared between saline-treated *Tac4*$^{-/-}$ and WT mice. *p*-values are -log$_{10}$ transformed.

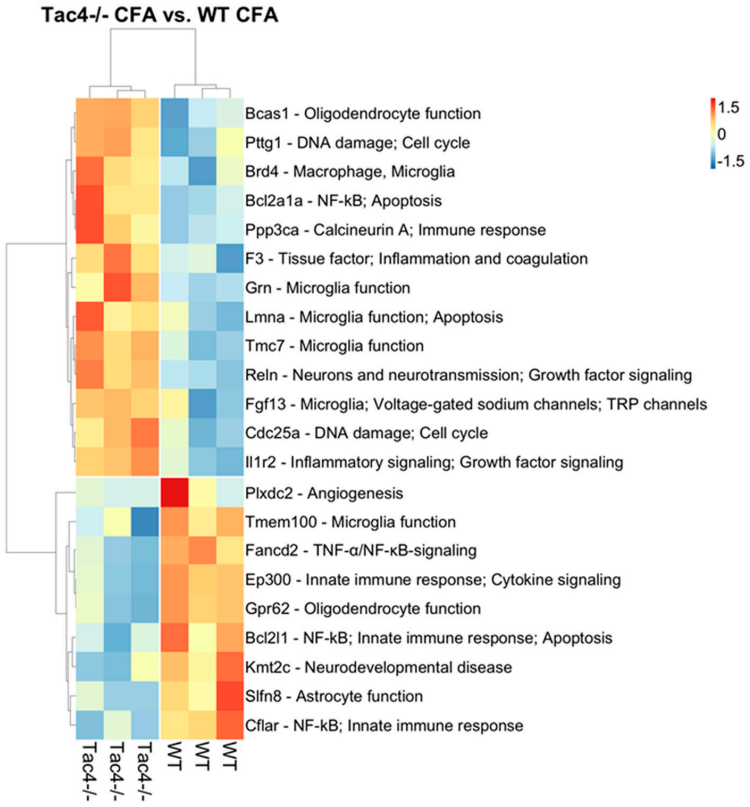

Figure 7. Heat map representation of the differentially expressed genes with annotations between TG samples of CFA-treated *Tac4*$^{-/-}$ and WT mice. Rows represent genes and columns represent TG samples (n = 3 in each group). Normalized gene counts data are shown as row-wise z-scores (scale is shown on legend). Rows and columns were hierarchically clustered using Pearson correlation distance measure and average method. Distances are shown as dendrograms. References for the functional annotations: *Bcas1* [64] *Pttg1* [65] *Brd4* [66,67] *Bcl2a1a* [68] *Ppp3ca* [69] *F3* [70,71] *Grn* [72,73] *Lmna* [74] *Tmc7* [75,76] *Reln* [77] *Fgf13* [78–81] *Cdc25a* [82] *Il1r2* [83] *Plxdc2* [84] *Tmem100* [85,86] *Fancd2* [87] *Gpr62* [88,89] *Bcl2l1* [90] *Kmt2c* [91] *Slfn8* [92,93] *Cflar* [94].

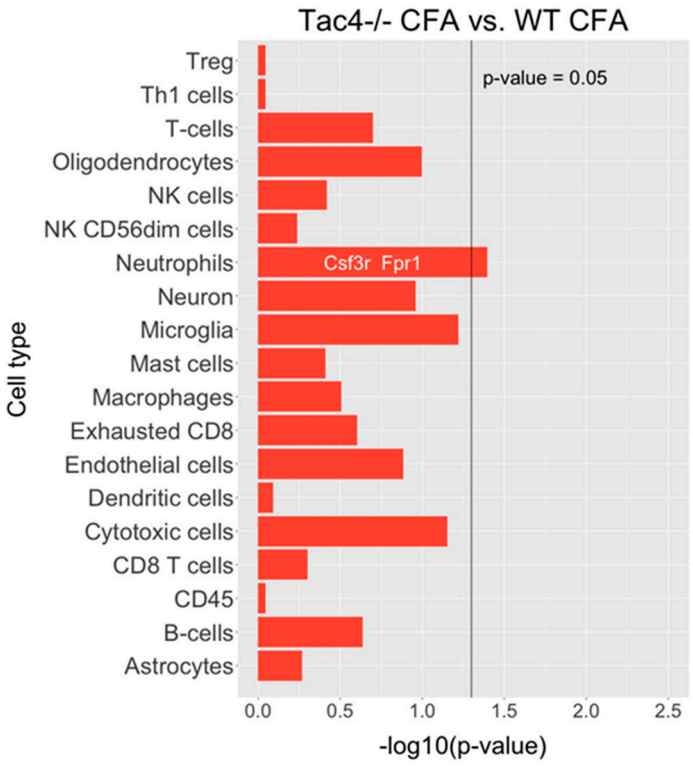

Figure 8. Barplots of *p*-values for correlation of cell-type-specific gene expressions as compared between CFA-treated *Tac4*$^{-/-}$ and WT mice. *p*-values are -log$_{10}$ transformed.

3. Discussion

In the present study, we confirmed the presence of *Tac4* mRNA in the TG and established its upregulation in response to orofacial inflammation. While it had been previously shown that HK-1 was expressed widely in the nervous system including the brain, spinal cord, dorsal root ganglia, brain stem and the TG [34,39], this is the first study to assess the changes of *Tac4* expression alterations under pathological conditions. HK-1 had only been detected in small and medium-size neurons by immunohistochemistry in the rat TG [39], but in the present study, we showed that besides the neuronal expression, *Tac4* mRNA was also expressed in satellite glial cells of the TG. More importantly, significant inflammation-related upregulation of *Tac4* was shown in both neurons and satellite glial cells. Based on our facial mechanonociceptive threshold measurements and the qPCR results in the rat, we showed that *Tac4* upregulation occurred parallel to the development of allodynia, which suggests its potential role in the sensitization process. Although we provide evidence for expression changes only at mRNA level, which is a clear limitation of the study, the concomitant behavioral alterations suggest that the protein products of the examined mRNAs were also affected. Without the availability of specific and sensitive antibody against HK-1, we cannot further confirm it experimentally. The concomitant upregulation of HK-1 in trigeminal sensory neurons and SGCs is of particular importance, since an increasing amount of evidence points to the importance of neuron-glia crosstalk in chronic pain conditions, including orofacial pain [2,6,95–98]. Other neuropeptides released from peptidergic sensory neurons have already been suggested to have a prominent role in glial cell activation during sensitization. Among these, CGRP, which has a clinically proven role in migraine headaches [99], appears to be a key mediator of the neuron-glia interactions in the TG [4,100,101]. HK-1 could be a neuropeptide participating in two-way communication between sensory neurons and satellite glial cells. Moreover, we have also provided evidence on a possible physiological role of HK-1 in the trigeminal system by showing that there is a baseline difference in the expression of genes associated with glial cell activity in both the TG and the TNC.

Previous studies by our and other groups have established that HK-1 contributes to the development of hyperalgesia in both acute and chronic pain models. HK-1 can elicit pain when injected intrathecally [34,43], and *Tac4*$^{-/-}$ mice have reduced nocifensive behavior in chemically-induced pain and suppressed hyperalgesia/allodynia in chronic inflammatory and neuropathic pain models [41,102]. In inflammatory pain and arthritis, a pro-inflammatory component is also likely to contribute to its action, since HK-1 expression was described in the immune system as well [30,33,103] and *Tac4* deficiency also alleviated experimental lung inflammation [42]. On the other hand, HK-1 was shown to have a direct role in central nociceptive sensitization, as spinal microglia and astrocyte activation was also attenuated in *Tac4*$^{-/-}$ mice after nerve injury [41]. HK-1 is a potent NK-1 receptor agonist [34], and most of its effects can be explained by NK-1 receptor activation. However, several lines of evidence point to a different mechanism of action compared to SP, and even a yet unknown target. This is supported by the observations that the phenotype of *Tac4*$^{-/-}$ deficient mice in chronic pain models is different from SP or NK-1 receptor-deficient mice and an opposite phenotype was also described in models of anxiety and depression as well [40].

We also investigated the contribution of HK-1 in trigeminal sensitization by adapting the CFA-induced orofacial pain model to mice to compare the allodynia and the changes of neuronal and glial activation markers between *Tac4*$^{-/-}$ and wild-type mice. In parallel, we confirmed the upregulation of *Tac4* in mice after inflammation by the ultrasensitive RNAscope technology [104]. However, RT-qPCR could detect neither basal nor upregulated *Tac4* in mice, probably owing to a low expression and the small tissue volume. Lamentably, we could not unequivocally show that orofacial allodynia was attenuated in *Tac4*$^{-/-}$ mice in the present study (Supplementary Figure S1a). The lack of clear behavioral functional data for the *Tac4*$^{-/-}$ phenotype in this model is another limitation of our study. This technical issue is likely the light restraint that had to be used to measure the von Frey threshold of the face, which appeared to be an important stress factor. In contrast with rats, mice do not adapt well to repeated handling [105], therefore we tried to limit the handling and the number of repeated measurements to the minimum. Despite this, the mice were probably too stressed during the experiment, which could be one of the reasons that the mechanical thresholds of both saline and CFA-treated animals decreased from the baseline. It is also worth mentioning that based on our unpublished observations already the baseline von Frey threshold values of C57Bl/6 mice were very low compared to the threshold of NMRI mice, which usually show lower anxiety level in our experience. Stress-induced hyperalgesia is a well-known phenomenon which is both detectable in humans and animal models [106]. Other researchers use special restrainers or cages to measure the orofacial thresholds in mice to overcome the challenges of handling-induced stress [107,108]. We have previously used the technique in NMRI mice [109], but in our experience C57Bl/6 mice tolerated this type of restraint less compared to the light manual handling. Changes in spontaneous behavior measured in the open field test corroborated previous results of our group regarding the possible role of HK-1 in mediating anxiolytic actions [40], but we could not detect any pain-induced reduction of spontaneous activity either (Supplementary Figure S1b).

Our previous results in the orofacial inflammation model showed that in rats the mRNA levels of neuronal and glial activation markers changed parallel with the mechanical hyperalgesia in the TG, TNC and PBMCs [49]. In contrast with rats, we could not unequivocally reproduce the results of the activation marker changes in the mice, either. As mentioned before, there was already a difference in the baseline expression of glial activation markers in intact mice between the two genotypes. In the intact TG and TNC of *Tac4*$^{-/-}$ mice, there was a lower expression of the microglia/macrophage marker *Iba1* and the SGC/astrocyte marker *Gfap* was also expressed at a significantly lower level in all the sampled tissues of *Tac4*$^{-/-}$ mice. The basal difference in activity is not entirely surprising since macrophages are known to express both HK-1 and the NK-1 receptor and the *Tac4* mRNA was also detected in cultured microglia [36]. Likewise, previous data also revealed that astrocytes and microglia in the brain express NK-1 receptors [110] and NK-1 receptor antagonist treatment could reverse opioid withdrawal-induced astrocyte and microglia activation [111]. All activation markers

increased significantly in both saline- and CFA-treated groups, which is most probably a consequence of the injection procedure and the previously mentioned restraint-induced stress during the von Frey threshold measurements. Both saline- and CFA-treated *Tac4*$^{-/-}$ mice had significantly lower levels of *FosB* and *Gfap* upregulation compared to their respective WT counterparts. The marked difference in *Gfap* between WT and *Tac4*$^{-/-}$ mice could also suggest that HK-1 plays a role in the activation of SGCs and astrocytes during stress. Similarly, NK-1 receptor upregulation in astrocytes was linked to stress-induced hyperalgesia and gastrointestinal motility disorders [112]. Nevertheless, compensatory changes secondary to *Tac4* deletion (e.g., expression changes of *Tac1*) cannot be excluded as factors responsible for the observed differences.

Analysis of the Nanostring neuroinflammation panel kit data also revealed that there were a number of differentially expressed genes between saline- or CFA-treated wild-type and *Tac4*$^{-/-}$ mice. To our knowledge, this is the first such analysis in the TG to investigate neuroinflammation in a pain model. The cell-type-specific profiling in the comparison of saline-treated wild-type and *Tac4*$^{-/-}$ animals showed that microglia and cytotoxic cell-related genes were regulated in a significantly different extent compared to other cell types involved in inflammatory processes. As we discussed before, the effect of HK-1 deficiency on expression levels of macrophage/microglia-related genes is expected due to the previously described distribution of both the peptide and the NK-1 receptor. However, looking at individual differentially regulated genes, the functions of SGCs are also likely to be affected. The most interesting finding among these genes is the downregulation of *Kcnj10*, encoding the inwardly rectifying potassium channel subunit $K_{ir}4.1$ in SGCs which has been linked to inflammatory sensitization [63] and pain modulation by $GABA_B$ receptors [113]. Comparison of the cell-type-specific profiling of differentially expressed genes between CFA-treated wild-type and *Tac4*$^{-/-}$ mice only yielded a significant result in neutrophils. However, in the list of differentially expressed genes, we have found various genes related to macrophage/microglia activity, neuronal transmission, as well as genes mediating immune cell activation, such as calcineurin A or members of the Bcl-2 protein family, regulating apoptosis. Further validation of selected genes should be performed to confirm their importance in the effects of HK-1 in the TG.

In summary, we conclude that HK-1 released from sensory neurons and satellite glial cells may contribute to inflammatory processes and nociceptive sensitization underlying orofacial pain. HK-1 is suggested to have a role in mediating neuron-glia interactions both under physiological and inflammatory conditions. These results open interesting novel perspectives to identify the role and mechanisms of action of HK-1 in neuroinflammation in other models of trigeminal sensitization and to determine its potential clinical relevance.

4. Materials and Methods

4.1. Animals

Experiments were performed on male Wistar rats (Toxi-Coop, Hungary) weighing between 200–300 g, as well as on male, 8–12 week-old C57Bl/6 and *Tac4*-deficient (*Tac4*$^{-/-}$) mice weighing between 20–25 g. The original breeding pairs of the *Tac4*$^{-/-}$ mice were generated as previously described [114]. Transgenic mice were generated on a C57Bl/6 background and backcrossed to homozygosity for >5 generations before using C57Bl/6 mice as controls, purchased from Charles River (Sulzfeld, Germany). Animals were kept under standard light-dark cycle (12-h light/dark cycle) and temperature (22 ± 2 °C) conditions. Food and water were provided ad libitum, in the Animal House of the Department of Pharmacology and Pharmacotherapy of the University of Pécs. All procedures were approved by the National Ethics Committee on Animal Research of Hungary on 1 Aug 2017 (license No.: BA02/2000-51/2017 issued on 22 Aug 2017 by the Government Office of Baranya County, Hungary) and were performed according to the European legislation (Directive 2010/63/EU) and Hungarian Government regulation (40/2013., II. 14.) on the protection of animals used for scientific purposes.

4.2. CFA Injection

Orofacial inflammation in mice was induced by bilateral s.c. injection of 10–10 µL complete Freund's adjuvant (CFA; Sigma-Aldrich, Saint Louis, MI, USA; killed Mycobacteria suspended in paraffin oil; 1 mg/mL) into the whisker pad under i.p. ketamine (100 mg/kg) and xylazine (5 mg/kg) anaesthesia. In the case of rats, unilateral injection of 50 µL CFA was used, as previously described [49]. Control groups received the same volume of saline injection in both cases. We randomized the treatment of animals within each cage, ensuring a similar sample size for each treatment group.

4.3. Orofacial Pain Sensitivity Tested with von Frey filaments

A set of calibrated nylon monofilaments (Stoelting, Wood Dale, Illinois, USA) was used to perform measurements before and after CFA/saline injection on all animals. Increasing strengths (rats: 0.8–12 g, mice: 0.0075–1 g) were used to measure facial mechanosensitivity. The mechanonociceptive threshold was defined as the lowest force evoking at least 2 withdrawal responses (face stroking with the forepaw or head shaking) out of 5 stimulations according to our previous paper [49]. The experimenter was not blinded for these measurements as the visible inflammatory oedema of the whisker pad cannot be hidden during the in vivo experiments.

4.4. Sample Collection

For RT-qPCR analysis, TG and TNC tissue and PBMC samples were collected from animals on day 1, 3, and 7 after receiving s.c. CFA injection and following behavioral tests. Animals were anaesthetized with pentobarbital (rats: 50 mg/kg and mice 70 mg/kg i.p.) and sacrificed by exsanguination. TGs and TNCs were excised and snap-frozen in liquid nitrogen.

For RNAscope, animals were transcardially perfused with 0.01 M phosphate-buffered saline (PBS; pH 7.6) followed by 4% paraformaldehyde solution on day 3 after CFA or saline injections. TGs were postfixed for 24 h at room temperature, rinsed in PBS, dehydrated, and embedded in paraffin using standard procedures. 5 µm sections were cut using a sliding microtome (HM 430 Thermo Fisher Scientific, Waltham, MA, USA).

TG samples for Nanostring analysis were snap-frozen on day 3 and stored at −80 °C until use. RNAscope and Nanostring analysis were performed on samples derived from animals not involved in behavioral studies. Samples were processed in a blinded manner.

4.5. RNAscope In Situ Hybridization (ISH)

RNAscope assay was performed on 5 µm thick longitudinal TG sections using RNAscope Multiplex Fluorescent Reagent Kit v2 (ACD, Hayward, CA, USA) according to the manufacturer's instructions. Briefly, tissue sections were baked, deparaffinized and H_2O_2-blocked, boiled, pretreated with Protease Plus and hybridized with mouse *Tac4*, *Kcnn3*, *Rbfox3*, mouse 3-plex positive and negative control probes. Signal amplification and channel development were applied sequentially. Nuclei were counterstained with 4',6-diamidino-2-phenylindole (DAPI) and mounted with ProLong Glass Antifade Mountant for confocal imaging. Probes, applied dilutions of fluorophores are listed in Supplementary Table S1. Fluorescent images were acquired using an Olympus Fluoview FV-1000 laser scanning confocal microscope (Olympus, Tokyo, Japan) and Fluo-View FV-1000S-IX81 image acquisition software system. The confocal aperture was set to 80 µm. The analogue sequential scanning was performed using a 40× objective lens (NA: 0.75). The optical thickness was set to 1 µm and the resolution was 1024 × 1024 pixel. The excitation time was set to 4 µs per pixel. Virtual colours were selected to depict fluorescent signals: blue for DAPI, green for fluorescein (*Polr2a*), red for Cyanine 3 (*Tac4* and *Ppib*) and white for Cyanine 5 (*Ubc*). Images of the respective four channels were stored both individually and superimposed to evaluate the co-localization of fluorescent signals. Basal and elevated *Tac4* expression levels were analyzed semi-quantitatively using ImageJ software according to the manufacturer's guideline in a blinded-manner. On rat TG, *Tac4* transcripts were quantified on *Tac4*-positive neurons and SGCs from

CFA (neuron, n = 120; SGC, n = 69)-and saline (neuron, n = 68 SGC, n = 52)-treated animals, n = 4–6 rats/group. Similarly, on mouse TG, *Tac4* transcripts were quantified on *Tac4*-positive neurons and SGCs from CFA (neuron, n = 119; SGC, n = 54)-and saline (neuron, n = 71; SGC, n = 38)-treated animals, n = 4–5 mice/group.

4.6. Mononuclear Cell Separation from Peripheral Blood

PBMCs were obtained by Ficoll-PaquePREMIUM (GE Healthcare, Budapest, Hungary) standard density gradient centrifugation method [49]. Briefly, the mixture of fresh anticoagulant-treated blood, pooled from 3 individual mice and an equal volume of balanced salt solution was carefully overlaid on Ficoll-PaquePREMIUM and centrifuged. The mononuclear layer was transferred into a new tube and washed twice with the salt solution. The supernatant was discarded, the cells were resuspended in TRI Reagent (Zymo Research, Irvine, CA, USA) and stored at −80 °C until use.

4.7. Quantitative Real-Time PCR (RT-qPCR)

Total RNA purification, transcription and RT-qPCR from rat samples were performed exactly as described previously [49]. In the case of samples from mice, the same protocol was used with minor modifications as follows. TRI Reagent manufacturer's (Zymo Research, Irvine, CA, USA) protocol was followed up to the step of acquiring the aqueous phase. Further RNA purification was made from the aqueous phase using the Direct-zol RNA MiniPrep kit (Zymo Research, Irvine, CA, USA) according to the manufacturer's protocol. Nanodrop ND-1000 Spectrophotometer V3.5 (Nano-Drop Technologies, Inc., Wilmington, DE, USA) was used to define the quantity and purity of the extracted RNA. Total RNA was reverse transcribed using Maxima First Strand cDNA Synthesis Kit (ThermoScientific, Santa Clara, CA, USA), PCR amplification was performed using SensiFast SYBR Lo-ROX Kit (Bioline, Taunton, MA, USA). From the enlisted reference genes: glyceraldehyde 3-phosphate dehydrogenase (*Gapdh*), hypoxanthine phosphoribosyltransferase 1 (*Hprt1*), beta-2-microglobulin (*β2m*) and Peptidyl-prolyl cis-trans isomerase (*Ppia*), after transcripts were detected in all samples, *Ppia* (TG) and *Ppia*, *Gapdh* (PBMCs, TNC) were chosen as internal controls. Primers of similar efficiencies were used and $2^{-\Delta\Delta Cq}$ fold change values were calculated. All the primers used for RT-qPCR are listed in Supplementary Table S2.

4.8. Nanostring

NanoString nCounter® technology (NanoString Technologies, Seattle, WA, USA) was used, for expression profiling of RNA isolated from TG, according to the manufacturer's instructions. Mouse Neuroinflammation Panel was composed of probes for 770 genes related to immunity and inflammation, neurobiology and neuropathology.

Total RNA isolation and purification from mouse TG samples were performed using TRI Reagent and Direct-zol RNA MiniPrep kit as previously described, performing column DNase treatment as well. The RNA quality and quantity were measured using Bioanalyzer 2100 (Agilent, Santa Clara, CA, USA), Qubit Fluorometer Fluorescence Qubit 3.0 (ThermoFisher Scientific, Waltham, MA, USA) and Nanodrop ND-1000 Spectrophotometer V3.5 (Nano-Drop Technologies, Inc., Wilmington, DE, USA). Only samples with an RNA integrity number RIN >8.1 and 260/280 ratios of ~2.0 were used for further analysis.

The RNA samples (25 ng of each) were processed using Mus musculus Neuroinflammation panel v1.0 according to the manufacturer instructions (user manual MAN-10023-11) on NanoString SPRINT Profiler instrument. Analysis of data was performed using nCounter® Advanced Analysis plugin v2.0.115 for the nSolver Analysis Software v4.0.70 with the ProbeAnnotations_NS_Mm_NeuroInflam_v1.0 file provided by NanoString, using default settings. Briefly, raw data with gene counts lower than 50 were removed, suitable reference genes were evaluated using geNorm pairwise variation statistic, gene count data were normalized, differentially expressed genes were determined and cell type profiling was performed for each comparison.

Differentially expressed genes were plotted on heat maps where rows represent genes and columns represent TG samples. Normalized gene counts data are shown as row-wise z-scores (scale is shown on legend). Rows and columns were hierarchically clustered using Pearson correlation distance measure and average method. Distances are shown as dendrograms. Clustering and heat map generation were performed using the R language version 3.6.1 and the pheatmap package v1.0.12.

4.9. Statistical Analysis

GraphPad Prism software (GraphPad Software, Inc., La Jolla, CA, USA) was used for the statistical analysis of behavioral data, RT-qPCR and RNAscope quantification. After testing datasets for normal distribution, two-way analysis of variance (ANOVA) with repeated measures followed by Tukey's multiple comparison tests was performed for time-matching samples (behavioral studies). One-way or two-way ANOVA followed by Tukey's multiple comparison tests was used for RT-qPCR data. Student's t-test for unpaired samples was preferred for RNAscope analysis to compare saline- and CFA-treated tissues. Sample numbers for each experiment are listed in Supplementary Table S3. Results are plotted as the mean ± standard error of the mean (SEM). Probability values $p \leq 0.05$ were accepted as significant in all tests.

Analysis of NanoString data was performed using nCounter® Advanced Analysis Software v2.0.115. Differentially expressed genes were determined by applying log-linear model (linear regression) with a *p*-value threshold of 0.05. Correlation of cell-type marker genes was determined with a threshold of $p < 0.05$ for each comparison.

Supplementary Materials: Supplementary Materials can be found at http://www.mdpi.com/1422-0067/21/8/2938/s1.

Author Contributions: Conceptualization, K.B. and Z.H.; methodology, T.A., A.K., B.G., P.U., K.S., F.B., S.S., K.B.; formal analysis, T.A., A.K., J.K., R.H. and G.A.; investigation, T.A., A.K., K.S., F.B., S.S., P.U., B.G., K.B.; writing—original draft preparation, T.A., A.K., J.K., K.S., K.B. writing—review and editing, T.A., A.K., J.K., K.S., F.B., S.S., R.H., P.U., A.G., B.G., Z.H., K.B.; supervision, Z.H., K.B.; funding acquisition, K.B. and Z.H. All authors have read and agreed to the published version of the manuscript.

Funding: This research was supported by National Brain Research Program 2017-1.2.1-NKP-2017-00002 (NAP-2; Chronic Pain Research Group), Gazdaságfejlesztési és Innovációs Operatív Program (Economy Development and Innovation Operative Programme) (GINOP)-2.3.2-15-2016-00050 (Peptidergic Signaling in Health and Disease; PEPSYS), Emberi Erőforrás Operatív Program (Human Resource Operative Programme) (EFOP) 3.6.2-16-2017-00008 (2017-2019) and EFOP-3.6.1-16-2016-00004, Programme of the Hungarian Ministry of Human Capacities NTP-NFTÖ-18-B-0455, OTKA FK132587, Higher Education Institutional Excellence Programme of the Ministry for Innovation and Technology in Hungary, within the framework of the 5. thematic programme of the University of Pécs to BG. Bioinformatics infrastructure was supported by ELIXIR Hungary (http://elixir-hungary.org/). János Bolyai Research Scholarship of the Hungarian Academy of Sciences to AK.

Acknowledgments: Confocal microscopy was performed in the facilities of the Department of Medical Biology and Central Electron Microscope Laboratory of the University of Pécs (Pécs, Hungary). We thank Dóra Ömböli and Anikó Perkecz for their expert technical assistance in the animal experiments and tissue preparation. We also thank Alexandra Berger (University of Toronto, Toronto, Canada) for providing the original breeding pair of *Tac4*$^{-/-}$ mice.

Conflicts of Interest: Kálmán Szenthe is the head of laboratory of Carlsbad Research Organization Ltd. The company participated in the study within the frame of a cooperation, there is no conflict of interest and financial relationship with the present work. Ferenc Bánáti is the head of laboratory of the RT-Europe Ltd. The company participated in the study within the frame of a cooperation, there is no conflict of interest and financial relationship with the present work. Susan Szathmary is the scientific director of the Galenbio Ltd. The company participated in the study within the frame of a cooperation, there is no conflict of interest and financial relationship with the present work. Zsuzsanna Helyes is the scientific director and shareholder of PharmInVivo, there is no conflict of interest and financial relationship with the present work; the company did not play any role in the paper.

Abbreviations

CFA	Complete Freund's Adjuvant
CGRP	Calcitonin gene-related peptide
GFAP	Glial fibrillary acid protein
HK-1	Hemokinin-1
IBA1	Ionized calcium-binding adaptor molecule 1
PBMCs	Peripheral blood mononuclear cells
SGC	Satellite glial cell
SP	Substance P
TG	Trigeminal Ganglion
TNC	Trigeminal Nucleus Caudalis

References

1. Harriott, A.M.; Strother, L.; Vila-Pueyo, M.; Holland, P.R. Animal models of migraine and experimental techniques used to examine trigeminal sensory processing. *J. Headache Pain* **2019**, *20*, 91. [CrossRef] [PubMed]
2. Iwata, K.; Takeda, M.; Oh, S.B.; Shinoda, M. Neurophysiology of orofacial pain. In *Contemporary Oral Medicine*; Farah, C.S., Balasubramaniam, R., McCullough, M.J., Eds.; Springer International Publishing: Cham, Switzerland, 2017; pp. 1–23. ISBN 978-3-319-28100-1.
3. Afroz, S.; Arakaki, R.; Iwasa, T.; Oshima, M.; Hosoki, M.; Inoue, M.; Baba, O.; Okayama, Y.; Matsuka, Y. CGRP induces differential regulation of cytokines from satellite glial cells in trigeminal ganglia and orofacial nociception. *Int. J. Mol. Sci.* **2019**, *20*, 711. [CrossRef] [PubMed]
4. Messlinger, K.; Balcziak, L.K.; Russo, A.F. Cross-talk signaling in the trigeminal ganglion: Role of neuropeptides and other mediators. *J. Neural Transm.* **2020**, *127*, 431–444. [CrossRef] [PubMed]
5. Dux, M.; Rosta, J.; Messlinger, K. TRP channels in the focus of trigeminal nociceptor sensitization contributing to primary headaches. *Int. J. Mol. Sci.* **2020**, *21*, 342. [CrossRef]
6. Gugliandolo, E.; D'Amico, R.; Cordaro, M.; Fusco, R.; Siracusa, R.; Crupi, R.; Impellizzeri, D.; Cuzzocrea, S.; Di Paola, R. Effect of PEA-OXA on neuropathic pain and functional recovery after sciatic nerve crush. *J. Neuroinflamm.* **2018**, *15*, 264. [CrossRef]
7. Lee, Y.; Kawai, Y.; Shiosaka, S.; Takami, K.; Kiyama, H.; Hillyard, C.; Girgis, S.; MacIntyre, I.; Emson, P.; Tohyama, M. Coexistence of calcitonin gene-related peptide and substance P-like peptide in single cells of the trigeminal ganglion of the rat: Immunohistochemical analysis. *Brain Res.* **1985**, *330*, 194–196. [CrossRef]
8. Ma, Q.-P.; Hill, R.; Sirinathsinghji, D. Colocalization of CGRP with 5-HT1B/1D receptors and substance P in trigeminal ganglion neurons in rats. *Eur. J. Neurosci.* **2001**, *13*, 2099–2104. [CrossRef]
9. Fernandes, E.S.; Schmidhuber, S.M.; Brain, S. Sensory-nerve-derived neuropeptides: Possible therapeutic targets. *Handb. Exp. Pharmacol.* **2009**, *194*, 393–416. [CrossRef]
10. Seybold, V.S. The role of peptides in central sensitization. *Handb. Exp. Pharmacol.* **2009**, *194*, 451–491. [CrossRef]
11. Brain, S.; Cox, H. Neuropeptides and their receptors: Innovative science providing novel therapeutic targets. *Br. J. Pharmacol.* **2006**, *147*, S202–S211. [CrossRef]
12. García-Recio, S.; Gascón, P. Biological and pharmacological aspects of the NK1-receptor. *BioMed Res. Int.* **2015**, *2015*, 1–14. [CrossRef] [PubMed]
13. Muñoz, M.; Coveñas, R. Involvement of substance P and the NK-1 receptor in human pathology. *Amino Acids* **2014**, *46*, 1727–1750. [CrossRef] [PubMed]
14. Rupniak, N.; Carlson, E.; Boyce, S.; Webb, J.K.; Hill, R.G. Enantioselective inhibition of the formalin paw late phase by the NK1 receptor antagonist L-733,060 in gerbils. *Pain* **1996**, *67*, 189–195. [CrossRef]
15. Jang, J.; Nam, T.S.; Paik, K.S.; Leem, J.W. Involvement of peripherally released substance P and calcitonin gene-related peptide in mediating mechanical hyperalgesia in a traumatic neuropathy model of the rat. *Neurosci. Lett.* **2004**, *360*, 129–132. [CrossRef]
16. Moskowitz, M.A. Neurogenic inflammation in the pathophysiology and treatment of migraine. *Neurology* **1993**, *43*, 16–20.
17. Pearson, J.C.; Jennes, L. Localization of serotonin- and substance P-like immunofluorescence in the caudal spinal trigeminal nucleus of the rat. *Neurosci. Lett.* **1988**, *88*, 151–156. [CrossRef]

18. Samsam, M.; Coveñas, R.; Csillik, B.; Ahangari, R.; Yajeya, J.; Riquelme, R.; Narváez, M.; Tramu, G. Depletion of substance P, neurokinin A and calcitonin gene-related peptide from the contralateral and ipsilateral caudal trigeminal nucleus following unilateral electrical stimulation of the trigeminal ganglion; a possible neurophysiological and neuroanatomical link to generalized head pain. *J. Chem. Neuroanat.* **2001**, *21*, 161–169. [CrossRef]
19. Teodoro, F.; Júnior, M.T.; Zampronio, A.R.; Martini, A.C.; Rae, G.A.; Chichorro, J.G. Peripheral substance P and neurokinin-1 receptors have a role in inflammatory and neuropathic orofacial pain models. *Neuropeptides* **2013**, *47*, 199–206. [CrossRef] [PubMed]
20. King, K.A.; Hu, C.; Rodriguez, M.M.; Romaguera, R.; Jiang, X.; Piedimonte, G. Exaggerated neurogenic inflammation and substance P receptor upregulation in RSV-infected weanling rats. *Am. J. Respir. Cell Mol. Boil.* **2001**, *24*, 101–107. [CrossRef]
21. Rittner, H.; Lux, C.; Labuz, D.; Mousa, S.A.; Schäfer, M.; Stein, C.; Brack, A. Neurokinin-1 receptor antagonists inhibit the recruitment of opioid-containing leukocytes and impair peripheral antinociception. *Anesthesiology* **2007**, *107*, 1009–1017. [CrossRef]
22. Diener, H.-C. RPR100893, a substance-P antagonist, is not effective in the treatment of migraine attacks. *Cephalalgia* **2003**, *23*, 183–185. [CrossRef] [PubMed]
23. Norman, B.; Panebianco, D.; Block, G.A. A placebo-controlled, in-clinic study to explore the preliminary safety and efficacy of intravenous L-758,298 (a prodrug of the NK-1 receptor antagonist L-754,030) in the acute treatment of migraine. *Cephalalgia* **1998**, *18*, 407.
24. Connor, H.E.; Bertin, L.; Gillies, S.; Beattie, D.T.; Ward, P. Clinical evaluation of a novel, potent, CNS penetrating NK-1 receptor antagonist in the acute treatment of migraine. *Cephalalgia* **1998**, *18*, 392.
25. Goldstein, D.J.; Wang, O.; Saper, J.R.; Stoltz, R.; Silberstein, S.D.; Mathew, N.T. Ineffectiveness of neurokinin-1 antagonist in acute migraine: A crossover study. *Cephalalgia* **1997**, *17*, 785–790. [CrossRef] [PubMed]
26. Reinhardt, R. Comparison of neurokinin-1 antagonist, L-745,030, to placebo, acetaminophen and ibuprofen in the dental pain model. *Clin. Pharmacol. Ther.* **1998**, *63*, 168.
27. Goldstein, D.J.; Wang, O.; Gitter, B.D.; Iyengar, S. Dose-response study of the analgesic effect of lanepitant in patients with painful diabetic neuropathy. *Clin. Neuropharmacol.* **2001**, *24*, 16–22. [CrossRef] [PubMed]
28. Borsook, D.; Upadhyay, J.; Klimas, M.; Schwarz, A.J.; Coimbra, A.; Baumgartner, R.; George, E.; Potter, W.Z.; Large, T.; Bleakman, D.; et al. Decision-making using fMRI in clinical drug development: Revisiting NK-1 receptor antagonists for pain. *Drug Discov. Today* **2012**, *17*, 964–973. [CrossRef]
29. Herbert, M.K.; Holzer, P. Warum versagen Substanz P (NK1)-Rezeptorantagonisten in der Schmerztherapie? *Der Anaesthesist* **2002**, *51*, 308–319. [CrossRef]
30. Zhang, Y.; Lu, L.; Furlonger, C.; Wu, G.E.; Paige, C.J. Hemokinin is a hematopoietic-specific tachykinin that regulates B lymphopoiesis. *Nat. Immunol.* **2000**, *1*, 392–397. [CrossRef]
31. Dai, L.; Perera, D.S.; King, D.W.; Southwell, B.R.; Burcher, E.; Liu, L. Hemokinin-1 stimulates prostaglandin E2 production in human colon through activation of cyclooxygenase-2 and inhibition of 15-hydroxyprostaglandin dehydrogenase. *J. Pharmacol. Exp. Ther.* **2011**, *340*, 27–36. [CrossRef]
32. Metwali, A.; Blum, A.M.; Elliott, D.; Setiawan, T.; Weinstock, J.V. Cutting edge: Hemokinin has substance P-like function and expression in inflammation. *J. Immunol.* **2004**, *172*, 6528–6532. [CrossRef] [PubMed]
33. Nelson, D.A.; Marriott, I.; Bost, K.L. Expression of hemokinin 1 mRNA by murine dendritic cells. *J. Neuroimmunol.* **2004**, *155*, 94–102. [CrossRef] [PubMed]
34. Duffy, R.A.; Hedrick, J.; Randolph, G.; Morgan, C.; Cohen-Williams, M.; Vassileva, G.; Lachowicz, J.; Laverty, M.; Maguire, M.; Shan, L.-S.; et al. Centrally administered hemokinin-1 (HK-1), a neurokinin NK1 receptor agonist, produces substance P-like behavioral effects in mice and gerbils. *Neuropharmacology* **2003**, *45*, 242–250. [CrossRef]
35. Morteau, O.; Lu, B.; Gerard, C.; Gerard, N.P. Hemokinin 1 is a full agonist at the substance P receptor. *Nat. Immunol.* **2001**, *2*, 1088. [CrossRef]
36. Borbély, É.; Zsuzsanna, H. Role of hemokinin-1 in health and disease. *Neuropeptides* **2017**, *64*, 9–17. [CrossRef] [PubMed]
37. Page, N. Hemokinins and endokinins. *Cell. Mol. Life Sci.* **2004**, *61*, 61. [CrossRef] [PubMed]
38. Jin, L.; Jin, B.; Song, C.-J.; Zhang, Y. Murine monoclonal antibodies generated against mouse/rat hemokinin-1. *Hybridoma* **2009**, *28*, 259–267. [CrossRef]

39. Igawa, K.; Funahashi, H.; Miyahara, Y.; Naono-Nakayama, R.; Matsuo, H.; Yamashita, Y.; Sakoda, S.; Nishimori, T.; Ishida, Y. Distribution of hemokinin-1 in the rat trigeminal ganglion and trigeminal sensory nuclear complex. *Arch. Oral Boil.* **2017**, *79*, 62–69. [CrossRef]
40. Borbély, É.; Hajna, Z.; Nabi, L.; Scheich, B.; Tékus, V.; László, K.; Ollmann, T.; Kormos, V.; Gaszner, B.; Karádi, Z.; et al. Hemokinin-1 mediates anxiolytic and anti-depressant-like actions in mice. *Brain Behav. Immun.* **2017**, *59*, 219–232. [CrossRef]
41. Hunyady, Á.; Hajna, Z.; Gubányi, T.; Scheich, B.; Kemény, Á.; Gaszner, B.; Borbély, É.; Zsuzsanna, H. Hemokinin-1 is an important mediator of pain in mouse models of neuropathic and inflammatory mechanisms. *Brain Res. Bull.* **2019**, *147*, 165–173. [CrossRef]
42. Hajna, Z.; Borbély, É.; Kemény, Á.; Botz, B.; Kereskai, L.; Szolcsányi, J.; Pintér, E.; Paige, C.J.; Berger, A.; Zsuzsanna, H. Hemokinin-1 is an important mediator of endotoxin-induced acute airway inflammation in the mouse. *Peptides* **2015**, *64*, 1–7. [CrossRef] [PubMed]
43. Endo, D.; Ikeda, T.; Ishida, Y.; Yoshioka, D.; Nishimori, T. Effect of intrathecal administration of hemokinin-1 on the withdrawal response to noxious thermal stimulation of the rat hind paw. *Neurosci. Lett.* **2006**, *392*, 114–117. [CrossRef] [PubMed]
44. Fu, C.-Y.; Xia, R.-L.; Zhang, T.-F.; Lu, Y.; Zhang, S.-F.; Yu, Z.; Jin, T.; Mou, X.-Z. Hemokinin-1(4-11)-induced analgesia selectively up-regulates δ-opioid receptor expression in mice. *PLoS ONE* **2014**, *9*, e90446. [CrossRef] [PubMed]
45. Fu, C.Y.; Zhao, Y.L.; Dong, L.; Chen, Q.; Ni, J.-M.; Wang, R. In vivo characterization of the effects of human hemokinin-1 and human hemokinin-1(4-11), mammalian tachykinin peptides, on the modulation of pain in mice. *Brain Behav. Immun.* **2008**, *22*, 850–860. [CrossRef]
46. Xia, R.-L.; Fu, C.-Y.; Zhang, S.-F.; Jin, Y.-T.; Zhao, F.-K. Study on the distribution sites and the molecular mechanism of analgesia after intracerebroventricular injection of rat/mouse hemokinin-1 in mice. *Peptides* **2013**, *43*, 113–120. [CrossRef] [PubMed]
47. Sakai, A.; Takasu, K.; Sawada, M.; Suzuki, H. Hemokinin-1 gene expression is upregulated in microglia activated by lipopolysaccharide through NF-κB and p38 MAPK signaling pathways. *PLoS ONE* **2012**, *7*, e32268. [CrossRef]
48. Ando, Y. Expression of hemokinin-1 in rat spinal cord after peripheral inflammation. *Kokubyo Gakkai Zasshi* **2009**, *76*, 81–90.
49. Aczél, T.; Kun, J.; Szőke, É.; Rauch, T.; Junttila, S.; Gyenesei, A.; Bölcskei, K.; Zsuzsanna, H. Transcriptional alterations in the trigeminal ganglia, nucleus and peripheral blood mononuclear cells in a rat orofacial pain model. *Front. Mol. Neurosci.* **2018**, *11*, 219. [CrossRef]
50. Wang, B.; Wang, X.-P. Does ceruloplasmin defend against neurodegenerative diseases? *Curr. Neuropharmacol.* **2019**, *17*, 539–549. [CrossRef]
51. Cheng, G.-Y.; Jiang, Q.; Deng, A.-P.; Wang, Y.; Liu, J.; Zhou, Q.; Zheng, X.-H.; Li, Y.-Y. CD31 induces inflammatory response by promoting hepatic inflammatory response and cell apoptosis. *Eur. Rev. Med. Pharmacol. Sci.* **2018**, *22*, 7543–7550.
52. Dobrowolski, M.; Cave, C.; Levy-Myers, R.; Lee, C.; Park, S.; Choi, B.-R.; Xiao, B.; Yang, W.; Sockanathan, S. GDE3 regulates oligodendrocyte precursor proliferation via release of soluble CNTFRα. *Development* **2020**, *147*, dev180695. [CrossRef] [PubMed]
53. Hallquist, N.A.; Khoo, C.; Cousins, R.J. Lipopolysaccharide regulates cysteine-rich intestinal protein, a zinc-finger protein, in immune cells and plasma. *J. Leukoc. Boil.* **1996**, *59*, 172–177. [CrossRef] [PubMed]
54. Kim, J.-Y.V.; Megat, S.; Moy, J.K.; Asiedu, M.N.; Mejia, G.L.; Vágner, J.; Price, T.J. Neuroligin 2 regulates spinal GABAergic plasticity in hyperalgesic priming, a model of the transition from acute to chronic pain. *Pain* **2016**, *157*, 1314–1324. [CrossRef] [PubMed]
55. Quintanilla, M.; Montero-Montero, L.; Renart, J.; Martin-Villar, E. Podoplanin in inflammation and cancer. *Int. J. Mol. Sci.* **2019**, *20*, 707. [CrossRef]
56. Heyne, K.; Winter, C.; Gerten, F.; Schmidt, C.; Roemer, K. A novel mechanism of crosstalk between the p53 and NFκB pathways. *Cell Cycle* **2013**, *12*, 2479–2492. [CrossRef]
57. Tang, R.-Z.; Zhu, J.-J.; Yang, F.-F.; Zhang, Y.-P.; Xie, S.-A.; Liu, Y.-F.; Yao, W.-J.; Pang, W.; Han, L.-L.; Kong, W.; et al. DNA methyltransferase 1 and Krüppel-like factor 4 axis regulates macrophage inflammation and atherosclerosis. *J. Mol. Cell. Cardiol.* **2019**, *128*, 11–24. [CrossRef]

58. Flanagan, L.A.; Rebaza, L.M.; Derzic, S.; Schwartz, P.H.; Monuki, E.S. Regulation of human neural precursor cells by laminin and integrins. *J. Neurosci. Res.* **2006**, *83*, 845–856. [CrossRef]
59. Robichaux, W.G.; Cheng, X. Intracellular cAMP sensor EPAC: Physiology, pathophysiology, and therapeutics development. *Physiol. Rev.* **2018**, *98*, 919–1053. [CrossRef]
60. Içer, M.A.; Gezmen-Karadag, M. The multiple functions and mechanisms of osteopontin. *Clin. Biochem.* **2018**, *59*, 17–24. [CrossRef]
61. Sans, A.; Bonnafous, S.; Rousseau, D.; Patouraux, S.; Canivet, C.M.; LeClere, P.S.; Tran-Van-Nhieu, J.; Luci, C.; Bailly-Maitre, B.; Xu, X.; et al. The differential expression of cide family members is associated with nafld progression from steatosis to steatohepatitis. *Sci. Rep.* **2019**, *9*, 7501. [CrossRef]
62. Zamanian, J.; Xu, L.; Foo, L.C.; Nouri, N.; Zhou, L.; Giffard, R.; Barres, B.A. Genomic analysis of reactive astrogliosis. *J. Neurosci.* **2012**, *32*, 6391–6410. [CrossRef] [PubMed]
63. Takeda, M.; Takahashi, M.; Nasu, M.; Matsumoto, S. Peripheral inflammation suppresses inward rectifying potassium currents of satellite glial cells in the trigeminal ganglia. *Pain* **2011**, *152*, 2147–2156. [CrossRef] [PubMed]
64. Ishimoto, T.; Ninomiya, K.; Inoue, R.; Koike, M.; Uchiyama, Y.; Mori, H. Mice lacking BCAS1, a novel myelin-associated protein, display hypomyelination, schizophrenia-like abnormal behaviors, and upregulation of inflammatory genes in the brain. *Glia* **2017**, *65*, 727–739. [CrossRef] [PubMed]
65. Vihervuori, H.; Autere, T.A.; Repo, H.; Kurki, S.; Kallio, L.; Lintunen, M.M.; Talvinen, K.; Kronqvist, P. Tumor-infiltrating lymphocytes and CD8+ T cells predict survival of triple-negative breast cancer. *J. Cancer Res. Clin. Oncol.* **2019**, *145*, 3105–3114. [CrossRef]
66. Dey, A.; Yang, W.; Gegonne, A.; Nishiyama, A.; Pan, R.; Yagi, R.; Grinberg, A.; Finkelman, F.D.; Pfeifer, K.; Zhu, J.; et al. BRD4 directs hematopoietic stem cell development and modulates macrophage inflammatory responses. *EMBO J.* **2019**, *38*, e100293. [CrossRef]
67. Hajmirza, A.; Emadali, A.; Gauthier, A.; Casasnovas, R.-O.; Gressin, R.; Callanan, M.B. BET family protein BRD4: An emerging actor in NFκB signaling in inflammation and cancer. *Biomedicines* **2018**, *6*, 16. [CrossRef]
68. Berberich, I.; Hildeman, D.A. The Bcl2a1 gene cluster finally knocked out: First clues to understanding the enigmatic role of the Bcl-2 protein A1. *Cell Death Differ.* **2017**, *24*, 572–574. [CrossRef]
69. Gaud, G.; Lesourne, R.; Love, P.E. Regulatory mechanisms in T cell receptor signalling. *Nat. Rev. Immunol.* **2018**, *18*, 485–497. [CrossRef]
70. Witkowski, M.; Landmesser, U.; Rauch, U. Tissue factor as a link between inflammation and coagulation. *Trends Cardiovasc. Med.* **2016**, *26*, 297–303. [CrossRef]
71. Zelaya, H.; Rothmeier, A.S.; Ruf, W. Tissue factor at the crossroad of coagulation and cell signaling. *J. Thromb. Haemost.* **2018**, *16*, 1941–1952. [CrossRef]
72. Horinokita, I.; Hayashi, H.; Oteki, R.; Mizumura, R.; Yamaguchi, T.; Usui, A.; Yuan, B.; Takagi, N. Involvement of progranulin and granulin expression in inflammatory responses after cerebral ischemia. *Int. J. Mol. Sci.* **2019**, *20*, 5210. [CrossRef] [PubMed]
73. Bateman, A.; Cheung, S.T.; Bennett, H.P.J. A brief overview of progranulin in health and disease. *Methods Mol. Biol.* **2018**, *1806*, 3–15. [PubMed]
74. Tran, J.R.; Chen, H.; Zheng, X.; Zheng, Y. Lamin in inflammation and aging. *Curr. Opin. Cell Boil.* **2016**, *40*, 124–130. [CrossRef] [PubMed]
75. Corey, D.P.; Holt, J.R. Are TMCs the mechanotransduction channels of vertebrate hair cells? *J. Neurosci.* **2016**, *36*, 10921–10926. [CrossRef]
76. Yue, X.; Sheng, Y.; Kang, L.; Xiao, R. Distinct functions of TMC channels: A comparative overview. *Cell. Mol. Life Sci.* **2019**, *76*, 4221–4232. [CrossRef]
77. Micera, A.; Balzamino, B.O.; Biamonte, F.; Esposito, G.; Marino, R.; Fanelli, F.; Keller, F. Current progress of reelin in development, inflammation and tissue remodeling: From nervous to visual systems. *Curr. Mol. Med.* **2016**, *16*, 620–630. [CrossRef]
78. Barbosa, C.; Xiao, Y.; Johnson, A.J.; Xie, W.; Strong, J.; Zhang, J.-M.; Cummins, T.R. FHF2 isoforms differentially regulate Nav1.6-mediated resurgent sodium currents in dorsal root ganglion neurons. *Pflugers Arch.* **2017**, *469*, 195–212. [CrossRef]
79. Yang, L.; Dong, F.; Yang, Q.; Yang, P.-F.; Wu, R.; Wu, Q.-F.; Wu, D.; Li, C.-L.; Zhong, Y.-Q.; Lu, Y.-J.; et al. FGF13 selectively regulates heat nociception by interacting with Nav1.7. *Neuron* **2017**, *93*, 806–821. [CrossRef]

80. Effraim, P.R.; Huang, J.; Lampert, A.; Stamboulian, S.; Zhao, P.; Black, J.A.; Dib-Hajj, S.D.; Waxman, S.G. Fibroblast growth factor homologous factor 2 (FGF-13) associates with Nav1.7 in DRG neurons and alters its current properties in an isoform-dependent manner. *Neurobiol. Pain* **2019**, *6*, 100029. [CrossRef]
81. Horta, K.C.; Weiss, S.G.; Miranda, K.; Sebastiani, A.M.; Da Costa, D.J.; Matsumoto, M.A.N.; Marañón-Vásquez, G.A.; Vieira, A.R.; Scariot, R.; Küchler, E.C. Polymorphisms in FGF3, FGF10, and FGF13 may contribute to the presence of temporomandibular disorders in patients who required orthognathic surgery. *J. Craniofacial Surg.* **2019**, *30*, 2082–2084. [CrossRef]
82. Boutros, R.; Lobjois, V.; Ducommun, B. CDC25 phosphatases in cancer cells: Key players? Good targets? *Nat. Rev. Cancer* **2007**, *7*, 495–507. [CrossRef] [PubMed]
83. Boraschi, D.; Italiani, P.; Weil, S.; Martin, M.U. The family of the interleukin-1 receptors. *Immunol. Rev.* **2017**, *281*, 197–232. [CrossRef] [PubMed]
84. Cheng, G.; Zhong, M.; Kawaguchi, R.; Kassai, M.; Al-Ubaidi, M.; Deng, J.; Ter-Stepanian, M.; Sun, H. Identification of PLXDC1 and PLXDC2 as the transmembrane receptors for the multifunctional factor PEDF. *eLife* **2014**, *3*, 05401. [CrossRef] [PubMed]
85. Weng, H.-J.; Patel, K.N.; Jeske, N.A.; Bierbower, S.M.; Zou, W.; Tiwari, V.; Zheng, Q.; Tang, Z.; Mo, G.C.; Wang, Y.; et al. Tmem100 is a regulator of TRPA1-TRPV1 complex and contributes to persistent pain. *Neuron* **2015**, *85*, 833–846. [CrossRef]
86. Yu, H.; Shin, S.M.; Wang, F.; Xu, H.; Xiang, H.; Cai, Y.; Itson-Zoske, B.; Hogan, Q.H. Transmembrane protein 100 is expressed in neurons and glia of dorsal root ganglia and is reduced after painful nerve injury. *PAIN Rep.* **2018**, *4*, e703. [CrossRef]
87. Ma, D.; Li, S.-J.; Wang, L.-S.; Dai, J.; Zhao, S.; Zeng, R. Temporal and spatial profiling of nuclei-associated proteins upon TNF-alpha/NF-kappaB signaling. *Cell Res.* **2009**, *19*, 651–664. [CrossRef]
88. Cahoy, J.D.; Emery, B.; Kaushal, A.; Foo, L.C.; Zamanian, J.; Christopherson, K.S.; Xing, Y.; Lubischer, J.L.; Krieg, P.A.; Krupenko, S.A.; et al. A Transcriptome database for astrocytes, neurons, and oligodendrocytes: A new resource for understanding brain development and function. *J. Neurosci.* **2008**, *28*, 264–278. [CrossRef]
89. Hay, C.M. Investigating the Role of Gpr62 in Oligodendrocyte Development and Central Nervous System Myelination. Ph.D. Thesis, University of Melbourne, Melbourne, Australia, 2015. Available online: http://hdl.handle.net/11343/58589 (accessed on 29 February 2020).
90. Kollek, M.; Müller, A.; Egle, A.; Erlacher, M. Bcl-2 proteins in development, health, and disease of the hematopoietic system. *FEBS J.* **2016**, *283*, 2779–2810. [CrossRef]
91. Shen, E.; Shulha, H.; Weng, Z.; Akbarian, S. Regulation of histone H3K4 methylation in brain development and disease. *Philos. Trans. R. Soc. B Boil. Sci.* **2014**, *369*, 20130514. [CrossRef]
92. Geserick, P.; Kaiser, F.; Klemm, U.; Kaufmann, S.H.; Zerrahn, J. Modulation of T cell development and activation by novel members of the Schlafen (slfn) gene family harbouring an RNA helicase-like motif. *Int. Immunol.* **2004**, *16*, 1535–1548. [CrossRef]
93. Nakagawa, K.; Matsuki, T.; Zhao, L.; Kuniyoshi, K.; Tanaka, H.; Ebina, I.; Yoshida, K.J.; Nabeshima, H.; Fukushima, K.; Kanemaru, H.; et al. Schlafen-8 is essential for lymphatic endothelial cell activation in experimental autoimmune encephalomyelitis. *Int. Immunol.* **2018**, *30*, 69–78. [CrossRef] [PubMed]
94. Silke, J.; Strasser, A. The FLIP side of life. *Sci. Signal.* **2013**, *6*, pe2. [CrossRef] [PubMed]
95. Hanani, M. Satellite glial cells in sensory ganglia: From form to function. *Brain Res. Rev.* **2005**, *48*, 457–476. [CrossRef] [PubMed]
96. Goto, T.; Oh, S.B.; Takeda, M.; Shinoda, M.; Sato, T.; Gunjikake, K.K.; Iwata, K. Recent advances in basic research on the trigeminal ganglion. *J. Physiol. Sci.* **2016**, *66*, 381–386. [CrossRef] [PubMed]
97. Iwata, K.; Katagiri, A.; Shinoda, M. Neuron-glia interaction is a key mechanism underlying persistent orofacial pain. *J. Oral Sci.* **2017**, *59*, 173–175. [CrossRef]
98. Shinoda, M.; Kubo, A.; Hayashi, Y.; Iwata, K. Peripheral and central mechanisms of persistent orofacial pain. *Front. Neurosci.* **2019**, *13*, 13. [CrossRef]
99. Edvinsson, L.; Haanes, K.A.; Warfvinge, K.; Krause, D.N. CGRP as the target of new migraine therapies—successful translation from bench to clinic. *Nat. Rev. Neurol.* **2018**, *14*, 338–350. [CrossRef]
100. Messlinger, K.; Fischer, M.J.M.; Lennerz, J.K. Neuropeptide effects in the trigeminal system: Pathophysiology and clinical relevance in migraine. *Keio J. Med.* **2011**, *60*, 82–89. [CrossRef]
101. Tajti, J.; Szok, D.; Majláth, Z.; Tuka, B.; Csáti, A.; Vécsei, L. Migraine and neuropeptides. *Neuropeptides* **2015**, *52*, 19–30. [CrossRef]

102. Borbély, É.; Hajna, Z.; Sándor, K.; Kereskai, L.; Toth, I.; Pintér, E.; Nagy, P.; Szolcsányi, J.; Quinn, J.P.; Zimmer, A.; et al. Role of tachykinin 1 and 4 gene-derived neuropeptides and the neurokinin 1 receptor in adjuvant-induced chronic arthritis of the mouse. *PLoS ONE* **2013**, *8*, e61684. [CrossRef]
103. Klassert, T.E.; Pinto, F.M.; Candenas, L.; Hernández, M.; Abreu, J.; Almeida, T.A. Differential expression of neurokinin B and hemokinin-1 in human immune cells. *J. Neuroimmunol.* **2008**, *196*, 27–34. [CrossRef] [PubMed]
104. Wang, F.; Flanagan, J.; Su, N.; Wang, L.-C.; Bui, S.; Nielson, A.; Wu, X.; Vo, H.-T.; Ma, X.-J.; Luo, Y. RNAscope. *J. Mol. Diagn.* **2012**, *14*, 22–29. [CrossRef] [PubMed]
105. Wilson, S.G.; Mogil, J.S. Measuring pain in the (knockout) mouse: Big challenges in a small mammal. *Behav. Brain Res.* **2001**, *125*, 65–73. [CrossRef]
106. Jennings, E.M.; Okine, B.N.; Roche, M.; Finn, D.P. Stress-induced hyperalgesia. *Prog. Neurobiol.* **2014**, *121*, 1–18. [CrossRef] [PubMed]
107. Krzyzanowska, A.; Pittolo, S.; Cabrerizo, M.; Sánchez-López, J.; Krishnasamy, S.; Venero, C.; Avendaño, C. Assessing nociceptive sensitivity in mouse models of inflammatory and neuropathic trigeminal pain. *J. Neurosci. Methods* **2011**, *201*, 46–54. [CrossRef]
108. Burgos-Vega, C.C.; Quigley, L.D.; Dos Santos, G.T.; Yan, F.; Asiedu, M.; Jacobs, B.; Motina, M.; Safdar, N.; Yousuf, H.; Avona, A.; et al. Non-invasive dural stimulation in mice: A novel preclinical model of migraine. *Cephalalgia* **2018**, *39*, 123–134. [CrossRef]
109. Farkas, S.; Bölcskei, K.; Markovics, A.; Varga, A.; Kis-Varga, Á.; Kormos, V.; Gaszner, B.; Horváth, C.; Tuka, B.; Tajti, J.; et al. Utility of different outcome measures for the nitroglycerin model of migraine in mice. *J. Pharmacol. Toxicol. Methods* **2016**, *77*, 33–44. [CrossRef]
110. Marriott, I. The role of tachykinins in central nervous system inflammatory responses. *Front. Biosci.* **2004**, *9*, 2153–2165. [CrossRef]
111. Tumati, S.; Largent-Milnes, T.; Keresztes, A.I.; Yamamoto, T.; Vanderah, T.W.; Roeske, W.R.; Hruby, V.J.; Varga, E.V. Tachykinin NK_1 receptor antagonist co-administration attenuates opioid withdrawal-mediated spinal microglia and astrocyte activation. *Eur. J. Pharmacol.* **2012**, *684*, 64–70. [CrossRef]
112. Steinhoff, M.; von Mentzer, B.; Geppetti, P.; Pothoulakis, C.; Bunnett, N.W. Tachykinins and their receptors: Contributions to physiological control and the mechanisms of disease. *Physiol. Rev.* **2014**, *94*, 265–301. [CrossRef]
113. Takeda, M.; Nasu, M.; Kanazawa, T.; Shimazu, Y. Activation of GABA(B) receptors potentiates inward rectifying potassium currents in satellite glial cells from rat trigeminal ganglia: In vivo patch-clamp analysis. *Neuroscience* **2015**, *288*, 51–58. [CrossRef] [PubMed]
114. Berger, A.; Benveniste, P.; Corfe, S.A.; Tran, A.H.; Barbara, M.; Wakeham, A.; Mak, T.W.; Iscove, N.N.; Paige, C.J. Targeted deletion of the tachykinin 4 gene (TAC4−/−) influences the early stages of B lymphocyte development. *Blood* **2010**, *116*, 3792–3801. [CrossRef] [PubMed]